## *Thin films of Cds and the CdS-Cu(_2)S hetherojunction*

Wilson, J. I. B.

# THIN FILMS OF CdS AND THE CdS-$Cu_2S$ HETEROJUNCTION

by

J.I.B. WILSON, B.Sc.

Presented in Candidature for the Degree of

Doctor of Philosophy in the University of Durham

November 1971

## Acknowledgements

The author wishes to express his appreciation for the guidance and encouragement given by his supervisor, Dr. J. Woods, and would like to thank Professor D.A. Wright for permitting the use of his laboratory facilities. The financial support granted by S.R.C. in the form of a C.A.P.S. research studentship is gratefully acknowledged. The expert knowledge and skill of the workshop staff headed by Mr. F. Spence have been invaluable. Members of the research group at Durham with whom the author has been associated are thanked for contributing their expertise, especially Dr. A.N. Rushby for taking the electron micrographs and Dr. K. Burr for growing the CdS crystals. This project was undertaken in co-operation with the research group headed by Dr. L. Clark at I.R.D. Co. Ltd., Newcastle-upon-Tyne, who are thanked for providing much useful information. Finally thanks go to Mrs. C.A. Pennington for her aid in drawing the diagrams, to Mrs. J. Henderson for her careful typing of this thesis, and to my wife, Sheila, for her constant support.

ABSTRACT

The thin film CdS-$Cu_2S$ solar cell is potentially a cheap and efficient device for converting sunlight into electrical energy, but there are various difficulties which present its ready fabrication. These centre on the CdS base layer and concern the uncertainties in the evaporation process. Moreover, the properties of the heterojunction itself are not well understood despite the profusion of theoretical models.

This thesis describes an investigation into the physical and electrical properties of vacuum evaporated CdS layers on a variety of substrates, as a function of the preparative conditions, i.e. evaporation rate, substrate temperature, film thickness, and source purity. The Hall mobility, resistivity and photo-sensitivity have been measured in both epitaxial and polycrystalline layers. X-ray studies revealed that a fibre-axis orientation existed in the thicker poly-crystalline films, and transmission electron microscopy enabled several defects in the epitaxial layers to be identified. It was essential to use a 'hot-wall' technique to deposit reproducible films. Since source purity affected the growth and subsequent electrical properties of the films, it was necessary to use re-crystallised CdS as the evaporant, and it was preferable to employ electron beam evaporation. Dopants such as indium were readily incorporated into the films. Much of the CdS film behaviour can be explained in terms of the evaporation and condensation

kinetics. An Appendix describes similar work on the properties of CdSe layers.

Investigations into the electrical properties of junctions prepared by chemi-plating $Cu_2S$ on boule CdS suggested that the best cells were made with copper-doped CdS. Open circuit voltage was highest if the base resistivity was a few hundred ohm cm. The existence of a photoconductive i-CdS region in heat-treated cells was demonstrated by the presence of long time constants and quenching effects. The importance of the CdS surface treatment was also shown.

CONTENTS

# CHAPTER 1 : THE PHOTOVOLTAIC EFFECT

## 1.1 HISTORY OF PHOTOELECTRICITY

1.1.1 Many of the classical "effects" of Physics and especially those phenomena discovered in the 19th century, bear the name of their discoverer or of a leading investigator. However, all but one of the photoelectric effects are known by a descriptive phrase, and it is not generally appreciated that they also were discovered over a century ago.

The photovoltaic effect (P.V.E.) or generation of electricity by absorption of photons, which is the main study of the present work was indeed known for many years as "the photoelectric effect" and was the most widely applied of the phenomena involving interactions between light and electricity. The inverse effect where an electric field produces light emission (electroluminescence) will not concern us, but similarities in the theory may be apparent.

At present the emphasis in research and development has shifted from P.V. to photoconductive and photoemissive devices, which effects were first observed after discovery of the P.V.E., and recent progress on P.V, devices is difficult to appraise since the majority of reports appear in private communications or obscure publications. (e.g. N.A.S.A. contract reports).

1.1.2 Although a P.V.E. was the first photoelectric effect to be observed (by E. Becquerel, 1839)

it required an inconvenient wet cell arrangement which consisted of two identical electrodes immersed in an electrolyte. When one electrode was illuminated with light of a suitable wavelength it caused a potential difference to be developed across the cell, or a current to flow in an external circuit. Any practical applications were not seriously considered until a similar effect had been reported in selenium (1876). Later the same effect was observed in a wide variety of semiconducting materials: $Cu/Cu_2O$ (1927), AgS, ZnS, PbS.

The present day interest in PV devices is based on the newer materials of Si, CdS, CdTe, InP, GaAs, which are more suited to the generation of electrical power from sunlight than $Cu/Cu_2O$ and Se which have been used mainly in light-meters.

The Becquerel-type PVE is one of the most difficult to explain fully, and as a result the earlier theories of PV action were necessarily sparse and were not developed until experiments on $Cu/Cu_2O$ "photocouples" had been performed. (For a recent examination of the Becquerel-type PVE using a CdS electrode, see Williams 1960). Early models were proposed by Frenkel (1933, 1935), Landau and Lifshitz (1936), Davydov (1938), Mott (1939), who came to the correct conclusion that the photo-emf arose from a non-equilibrium concentration of minority carriers. When Chapin et al discovered the PV action of p-n junctions in Si in 1954, much of the newly developed

p-n junction theory was invoked to explain the workings of the device. Attempts to apply this theory to the Cu or $Cu_2S$/CdS PV cell reported that year (Reynolds et al, 1954) were not so successful, and a single model for the particular device has yet to be universally accepted.

1.1.3 The second photoelectric effect to be discovered was the photoconductive effect (PCE) in selenium, by W. Smith (1873). A photoconductor changes its resistivity when illuminated with light of the correct wavelength, but no photo-emf is generated and its use in a device requires the addition of a power source.

Many of the group II - group VI compounds which include CdS, the material of particular interest in the present work, have been widely studied as photo-conductors. In practical applications a compromise has to be made between the two incompatible require-ments, the speed of response and the sensitivity, in a similar manner to the gain and bandwidth of an amplifier. (A. Rose 1963, R.H. Bube 1955,1960).

1.1.4 The third of the more important photoelectric effects is that of photo-emission (PEE), which H. Hertz observed during his experiments with electrical induction circuits (1887). He found that a spark in the secondary circuit passed across a gap with greater ease when that gap was illuminated by the primary circuit spark. Further experiments showed

this to be due to the u-v component of the spark falling on the negative terminal of the secondary gap. W. Hallwachs (1888) confirmed these results and concluded that negative electrical carriers, later identified as electrons, were emitted from the cathode under u.v. stimulation.

The foundations of all later practical applications of the PEE were laid by the work of Elster and Geitel on the much larger emission from the electrochemically positive metals, such as Na and K. Present day photocathodes are fabricated from such materials as Cs-O-Ag and $Cs_2Sb$ and are used as the first stages of photomultipliers, the most sensitive light detectors known.

1.1.5 Other photoelectrical phenomena should be mentioned. These are not of such practical use, but are extensively used in the determination of material parameters such as carrier mobility.

(a) The Dember voltage is produced in a sample in a direction parallel to that of illumination by incident photons, as a result of the different diffusion rates of electrons and holes, which do not possess the same mobility.

(b) A photopiezoelectric effect arises from the small local change in band-gap of a semiconductor when pressure is applied to a pair of opposing contacts. Illumination of the specimen during this compression produces a photovoltage.

(c) The photoelectromagnetic effect is analogous to the better known Hall effect. When a magnetic field is applied to a sample which is being illuminated in a direction at right angles to the applied field, a potential difference appears in the third orthogonal direction. This is due to the separation by the magnetic field of the electrons and holes created by the radiation.

These effects are all discussed phenomenologically in Tauc's book (1962), but the detailed theory must be treated with caution, in view of more recent experimental evidence.

1.1.6 A PVE can be produced in a number of different physical situations. For example:

(a) A "bulk" effect may be observed when a sample is illuminated non-uniformly, or if it has a non-uniform impurity distribution.

(b) A barrier effect arises whenever an electrostatic barrier exists within the sample. This will cause charge separation of optically-created electron-hole pairs. Illumination of the sample produces an emf perpendicular to the barrier. The barrier itself may be a diffusion potential between the p- and n-type regions of a semiconductor junction or between semiconductors with different energy gaps, or a surface potential barrier, or a junction between a metal and a semiconductor. The n-CdS/p-$Cu_2S$ heterojunction is a p-n junction with further

complications arising from an interposed, compensated layer of CdS.

(c) A transverse (or lateral) photovoltaic potential develops when the sample arrangement shown in Figure 1.1 is illuminated non-uniformly. Illumination perpendicular to the junction gives rise to a potential difference in a direction parallel to the junction (Wallmark 1957).

Since the p-type material has a high conductivity, it almost immediately attains a constant potential throughout, so that holes are re-emitted into the n-side over the whole junction area to balance the holes entering the p-side at the point of pair creation. This has the effect of charging the sample in the sense shown.

Since the polarity of this charge will change as the light spot passes the centre of the p-region, the device is extremely sensitive to the position of a small light spot near the centre.

(d) In thin films of most of the II-VI compounds and in certain single-crystal semiconductors, a photovoltage many times larger than the forbidden energy gap may arise. This voltage can be several hundred volts per cm. of sample length (Goldstein and Pensak, 1959, Brandhorst et al, 1968) and depends on the sample perfection, or on the method of production of the thin film. One of the most convincing models proposed to explain this anomalous effect suggested that the cubic phase/hexagonal phase stacking-faults which are present in these solids are the sources of

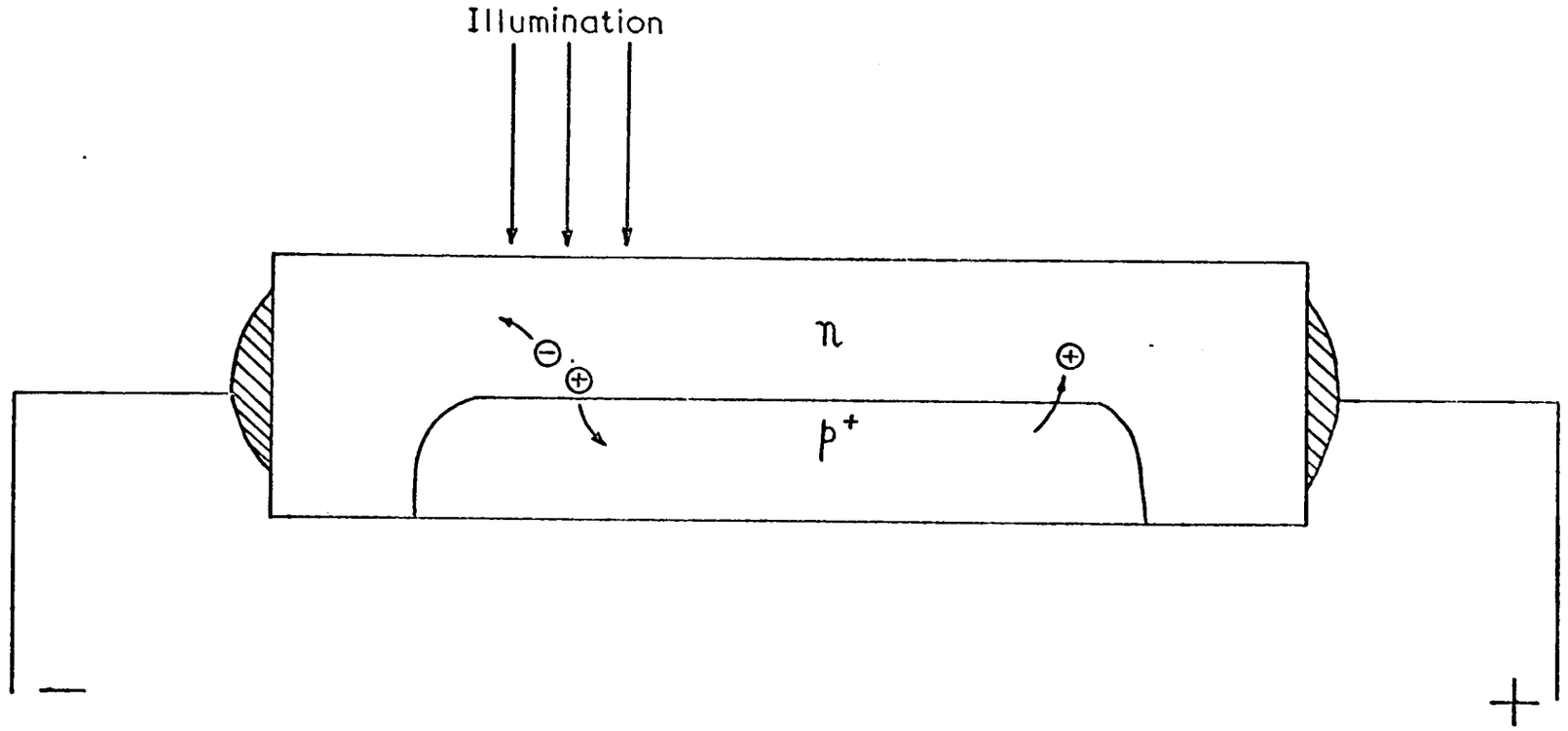


FIG. 1.1 THE TRANSVERSE P.V.E.

the barriers. The two phases have slightly different energy gaps and it is believed that the potential discontinuities are additive and can, therefore, give a total barrier of several hundred electron volts. (Ogawa et al. 1965, Gagliano et al. 1967). The high impedance of the materials involved (e.g. ZnS) has precluded any useful applications being made.

At this point it is useful to review some of the more common photoelectric devices. Most of these applications had occurred to the early researchers mentioned above, but had to await more advanced technologies before they could be realised.

## 1.2 PHOTOELECTRIC APPLICATIONS

1.2.1 Early applications of the photoconductive and photovoltaic effects were all variations of radiation detectors or flux-meters. (Zworykin and Ramberg, 1949). Photoconductivity can be used to detect most radiations from infra-red to atomic particles, but the higher energy emissions cause damage to the detector, which is not easily reversed. As light-detectors, photoresistors can be competitors to photomultiplier tubes when their small size and low cost are more important than sensitivity. Probably the most common application is as a light-operated switch for street lamps, lift doors, industrial control, or intruder alarms etc. A photoresistor can be used as an inexpensive feedback link between two electrical circuits at different potentials, eliminating expensive

high-voltage capacitors. More complex uses include electrophotography, image converters and image intensifiers, storage and display tubes, and the Vidicon television camera.

1.2.2 The photoemissive effect is most spectacularly used in photomultiplier tubes which can detect light invisible to the naked eye, or beyond its spectral range. Other light-measuring devices employing 'photocells' are refractometers, micro-densitometers, pyrometers, photometers. Some forms of film sound-recording use photocells, as do certain facsimile transmitters. A sensitive mirror galvanometer is given an expanded scale by employing two adjacent photocells in the light-beam path and using a differential output circuit. Photocells are used industrially in production line quality control, as smoke or flame detectors, and as intruder alarms.

1.2.3 On a cloudless summer day in latitude $55^{o}$N. we receive at sea level nearly 800 watts $m^{-2}$ of solar energy. It would seem more efficient to convert this radiation directly into electricity, rather than go through an intermediate thermal stage of burning fossil fuels, as at present. Even nuclear power would be converted directly to electrical power with more efficiency than by the heat transfer process used presently.

These were the hopes sustained for photovoltaic devices when the materials with theoretically low conversion losses were first recognised. A 20%

"limit conversion efficiency" was calculated for silicon p-n junctions, and even higher values for materials like GaAs, InP, AlSb. (Cummerow 1954, Pfann and Roosbroeck 1954, Rittner 1954, Prince 1955, Loferski 1956, Rappaport 1959, Wolf 1960).

The present work is concerned with some of the problems in achieving such high efficiencies. The major contribution in this field has been made on behalf of the huge U.S.A. space project which has supported most of the work on photovoltaic power supplies, since the available solar energy beyond the earth's atmosphere ("air mass zero". amO) is 1400 watts $m.^{-2}$ Even with low conversion efficiency an acceptable sized array of solar cells will provide adequate power for a communications satellite.

The PVE is also used in light-meters, light-actuated switches, pyrometers, and light-detectors with lower noise but slower response than photo-conductive detectors. The bulk effect mentioned above has been proposed as an analytical tool for determining the impurity distribution in a semi-conductor, and as has been suggested, the lateral effect can be used as a sensitive light spot position detector.

There are some applications then which are common to all three effects and the final choice of device will depend on the required sensitivity, speed of response, size and cost, (see also Larach 1965).

The photovoltaic device is the only one which can act as a detector and provide its own power source. A high efficiency PVE solar energy converter would be an excellent achievement, but is only likely to be realised if a fuller understanding of the photovoltaic mechanism can be obtained, together with a parallel development of suitable materials.

## 1.3 CHOICE OF PHOTOVOLTAIC MATERIALS

### 1.3.1 Silicon Cells

Owing to the advanced state of silicon technology in comparison to that of other photovoltaic materials, the silicon p-n junction was for long the unequalled photovoltaic converter. Theoreticians at first concentrated on predicting the possible efficiency of a Si solar cell since many of the parameters such as absorption coefficient and carrier mobility had been accurately measured on bulk material and did not have to be estimated.

However, as mentioned before, some then untested materials were thought to be capable of greater efficiency if certain problems of preparation were solved. These were well worth investigating because silicon cells have several disadvantages both as generators in Space and on the Earth's surface. For example:

(a) When an expensive Si single crystal p-n junction has been produced, it then has to be sliced, lapped, contacted and mounted, which produces waste at each stage and increases cost.

(b) Thin film Si cells are similarly expensive, and not easy to prepare.

(c) The absorption spectrum of Si cells does not match the sun's spectral output especially at the red end.

(d) Silicon cells have poor radiation resistance and cosmic ray or particle bombardment leads to a rapid deterioration in the operating characteristic unless periodic annealing of the damage can be effected. Doping with Cu or Li to provide a self-repairing facility has met with partial success, but at the cost of complexity in preparation (Loferski 1963, Usami 1970). (On the earth's surface the operating lifetime is virtually unlimited).

(e) The small area of such cells means that a large number of them must be connected in series-parallel arrangement, supported by a rigid frame, in order to provide useful current and voltage.

(f) The framework needed for support of an aerial array must be collapsible for launching but readily extendable for use without damaging the brittle silicon crystals.

(g) The power to weight ratio is low, which is a very undesirable feature in space vehicle economics.

### 1.3.2 Alternative cells

When the use of an alternative material is contemplated there are other factors to be considered

in addition to those listed above. Briefly these are:

(a) Reflection losses at the surface,

(b) Optimum use of the total energy of the photons absorbed to produce electron-hole pairs, with a minimum loss of excess energy to phonons,

(c) High carrier collection efficiency,

(d) High voltage factor, V.F., which is the ratio of open circuit voltage to energy gap,

(e) Low density of surface and interface states, especially on large area converters,

(f) High curve factor, C.F., which is the ratio of maximum power to the product of open circuit voltage and short circuit current,

(g) Low internal series resistance, (partly overcome by grid electrodes).

Some of these requirements can be achieved by improvements in the technology, but others have a theoretical limit which is controlled by the basic parameters of the material in question. Consideration of these factors gives rise to a curve of efficiency as a function of energy gap, which is favoured by theoreticians as a figure-of-merit-type curve. (Loferski 1956, Wolf 1960). This curve has a maximum around an energy gap of 1.6eV, for amO sunlight illumination. Silicon (1.1eV) is thus seen to be worse than gallium arsenide (1.34 eV) or aluminium

antimonide (1.52eV). CdS cells were usually assumed to be equally poor (2.4eV) but they have an effective energy gap of approximately 1.3eV, as will be discussed later. This should be borne in mind when early estimates of efficiencies for CdS cells are recalled.

This suggests that the CdS/$Cu_2S$ cell is in a strong position to challenge the supremacy of Si cells. Devices using CdTe (Vodakov et al 1960, Cusano 1963), AlSb (Rittner 1954), or InP are theoretically even better; however low carrier mobility, difficulties of growth, and high cost combine to make them economically unattractive.

GaAs is the only material other than Si and CdS to have made any impact in the field of PVE converters, (Jenny et al 1956), and this is even more difficult to produce in thin film, large area form than CdS. It should be noted that the preceding remarks about efficiency and energy gap apply to room temperature operation. If the temperature rises to about 200°C then GaAs is definitely the most promising material, because the increase in temperature leads to high leakage currents in low band gap materials (Wysocki and Rappaport 1960).

Some extremely complex structures have been proposed to ensure optimum conversion of solar energy to usable power. These include drift field junctions, graded energy gap materials (GaAs-P), and a layered structure comprising several superimposed materials

of increasing band gap (Wolf 1960, 1963). This last suggestion is difficult to realise in practice and any increase in the amount of useful energy absorbed would probably be cancelled by the increase in non-radiative recombination at the interface states. A simple method of contacting each stage would have to be devised, and the difficulty involved in ensuring the same impedance for each stage would seem to rule out layered structures.

It has been suggested (Wolf 1960) that the incorporation of defect levels into the energy gap by adding impurities to a semiconducting sample of, say, Si would increase the spectral absorption range and thus improve the efficiency of photovoltaic conversion. This was once believed to be the mechanism responsible for the wide response of CdS cells. Many workers have pointed out that a more probable result would be to increase the nonradiative recombination via these centres, and this has been shown to be the case, (Guttler and Queisser 1970).

Sakai and Milnes (1970) have suggested that heterojunctions of two of the following materials: ZnSe, GaAs, GaP, Si, Ge might provide suitable photovoltaic devices, though no work has been reported on the PVE in these.

Finally we return to CdS to mention briefly some research into junctions of CdS on Se (Kunioka and Sakai 1965), of CdS on Si (Okimura and Kondo 1970) and of CdS on ZnTe (Aven and Cook 1961), which produced

some interesting academic results but only confirmed the immense difficulties of growing good reproducible heterojunctions from these materials.

At present then, the conclusion is that the heterojunction of CdS and $Cu_2S$ is definitely in a position to compete with other photovoltaic devices, and it has these advantages:

(a) Easy and potentially cheap fabrication in thin film form;

(b) Good radiation resistance (Brucker et al 1966)

(c) High power to weight ratio in thin film form;

(d) Flexible and easy to handle or store, in thin film form;

(e) Long operating lifetime;

(f) Excellent matching to the solar spectrum;

(g) Large VF and CF.

The disadvantages of CdS/$Cu_2S$ cells provide the motivation for the present investigation. Apart from technological problems at the level of minimising contact resistance or improving encapsulation techniques, there are as yet several unanswered questions regarding the mechanism of electron-hole pair creation and separation. Since the thin film device is of the most importance, there are the usual problems associated with producing high quality, low resistivity thin films of a semiconductor. This forms the subject of a later chapter. There is an operating lifetime limitation at high voltage operating points, since electrolytic plating of copper from the

$Cu_2S$ and contacts occurs at cell weak spots. This is a reversible process, as is the lesser degradation due to moisture absorption, but neither of these was investigated in the present work.

There are also some interesting infra-red quenching effects, best observed with monochromatic illumination, which are similar to i-r quenching of photoconductivity in CdS, and merit some investigation. The response to low light levels, and at temperatures above and below room temperature are of interest and such studies are necessary before solar cells can be operated in 'deep' Space. (Ritchie and Sandstrom 1969).

Problems associated with the $Cu_2S$ layer are complicated by the fact that little is known about the chemistry and crystallography of the several possible compounds of copper and sulphur, and even less is known about their electrical properties. This thesis presents the results of an investigation into the structure and electrical properties of the CdS side of the junction only. Results of measurements on vacuum evaporated thin films of CdS are reported, followed by photovoltaic measurements, and their interpretation, which were obtained from hetero-junctions of $Cu_2S$ on thin film and single-crystal CdS. The effect of introducing impurities into the CdS is described from the view-point of cell processing and the final response.

REFERENCES

M. Aven and D.M. Cook (1961) J.A.P. 32, 960.

E. Becquerel (1839) Compt. Rend. 9, 145-149.

H.W. Brandhorst et al (1968) J.A.P. 39, 6071.

G.J. Brucker et al (1966) Proc. I.E.E.E. 54, 895.

R.H. Bube (1955) Proc. I.R.E. Dec., 1836.

R.H. Bube (1960) "Photoconductivity of Solids" (Wiley)

D.M. Chopin et al (1954) J.A.P. 25, 676.

R.L. Cummerow (1954) Phys. Rev. 95, 16-21.

D.A. Cusano (1963) Solid State Electron. 6, 217.

B.I. Davydov (1938) Zh. Tekh. Fiz. 5, 79.

J. Frenkel (1933) Nature 132, 312.

J. Frenkel (1935) Physik. Z. Sovietunion 8, 185.

A. Gagliano et al (1967) J. Phys. Chem. Solids 28, 737-740.

B. Goldstein and L. Pensak (1959) J.A.P. 30, 155.

G. Güttler and H.J. Queisser (1970) Energy Conversion 10, 51-55.

W. Hallwachs (1888) Ann. Physik. 33, 301-312.

H. Hertz (1887) Ann. Physik. 31, 421-448, 983-1000.

D.A. Jenny et al (1956) Phys. Rev. 101, 1208.

A. Kunioka and Y. Sakai (1965) Solid State Electron. 8, 961.

L.D. Landau and E.M. Lifshitz (1936) Physik. Z. Sovietunion 9, 477.

S. Larach (1965) "Photoelectronic Materials and Devices" (Editor) (Van Nostrand).

J.J. Loferski (1956) J.A.P. 27, 777-784.

J.J. Loferski (1963) Proc. I.E.E.E. 51, 667-674.

N.F. Mott (1939) Proc. Roy. Soc. A171, 281.

T. Ogawa et al (1965) Jap. J.A.P. 4, 948-957.

H. Okimura and R. Kondo (1970) Jap. J.A.P. 9, 274-280.

W.G. Pfann and W. van Roosbroeck (1954) J.A.P. 25, 1422-1434.

M.B. Prince (1955) J.A.P. 26, 534-540.

P. Rappaport (1959) R.C.A. Review 20, 373-396.

D.C. Reynolds et al (1954) Phys. Rev. 96, 533.

D.W. Ritchie and J.D. Sandstrom (1969) Energy Conversion 9, 83-90.

E.S. Rittner (1954) Phys. Rev. 96, 1708.

A. Rose (1963) "Theory of Photoconductivity."

R. Sahai and A.G. Milnes (1970) Solid State Electron. 13, 1289-1299.

W. Smith (1873) Am. J. Sci. 5, 301.

J. Tauc (1962) "Photo and Thermoelectric Effects in Semiconductors" (Pergamon).

A. Usami (1970) Solid State Electron. 13, 1202-1204.

Yu. A. Vodakov et al (1960) Sov. Phys. Sol. St. 2, 1-4.

J.T. Wallmark (1957) Proc. I.R.E. 45, 474.

R. Williams (1960) J. Chem. Phys. 32, 1505-1514.

M. Wolf (1960) Proc. I.R.E. 48, 1246-1263.

M. Wolf (1963) Proc. I.E.E.E. 51, 674.

J.J. Wysocki and P. Rappaport (1960) J.A.P. 31, 571.

V.K. Zworykin and E.G. Ramberg (1949) "Photoelectricity and its Application." (Wiley).

# CHAPTER 2 : THE CdS-$Cu_2S$ HETEROJUNCTION

Let us now turn to a description of the CdS/$Cu_2S$ heterojunction, and in particular to that structure known as the "CdS thin film solar cell," first prepared by Nadzhakov et al (1954) and the subject of intensive research, and many review articles published since. (Moss 1961, Shirland 1966, Perkins 1968).

## 2.1 PROPERTIES OF CADMIUM SULPHIDE

Cadmium sulphide is a group 2b-6b semi-insulating compound which normally crystallises in the hexagonal wurtzite structure, with a direct band gap of 2.4eV. Under certain growth conditions (e.g. at high pressures) a meta-stable, cubic sphalerite structure may dominate: a cubic thin film of CdS can be grown on a single crystal cubic substrate with nearly the same unit cell dimensions (Wilcox and Holt, 1969).

Since the energy gap is direct, the optical absorption coefficient changes as the square of the incident photon energy, and has high values for all energies greater than the band gap.

CdS starts to sublime at about 700°C and melts at above 1500°C only under several atmospheres pressure. This limits the available methods for producing single crystals to (a) vapour phase growth, or (b) high pressure liquid phase growth. It is the first of these methods which has been used to produce the CdS crystals for the present work.

Commercially produced CdS powder (B.D.H. "Optran" grade) was purified by resublimation in a flow of argon (Stanley, 1956) to give rods and platelets of light-yellow CdS. Mass spectrograph analyses were available for some of the CdS powders, and most impurities were present in quantities less than 0.1 p.p.m. after resublimation. These crystals were the source material for vacuum evaporation, and the charge in sealed silica growth tubes used in a modified Piper and Polich (1961) technique to grow large crystalline boules. Impurities such as Cu, Cl, In, were sometimes added to the charge, and in other runs either excess Cd or excess S was incorporated into the boule in order to change its stoichiometry and resistivity. (Clark and Woods 1966, 1968). Slices cut from the boules were either made into heterojunctions, or formed the charge for electron-beam evaporation when thin films were required.

Some mention must be made here of the composition of the vapour produced from subliming CdS. It is generally believed that CdS dissociates completely on heating according to: $CdS \longrightarrow Cd + \frac{1}{2}S_2$, with some higher aggregates of sulphur, and that no CdS molecules exist in the vapour. This belief originates from the work of a number of investigators on the vapour pressures and dissociation coefficients of the 2-6 compounds (Pogorelyi 1948, Hsaio and Schlechten 1952, Somorjai 1961, Goldfinger and Jeunehomme 1963). Recently however, Caveney (1970)

has asserted that a recognisable proportion of the vapour is in the form of CdS molecules, and he maintains that CdS crystals grow only from these CdS molecules. This has yet to be corroborated.

Unlike the Group IV or III-V semiconductors, most of the II-VI compounds are not amphoteric, and do not show intrinsic behaviour at room temperatures. CdS can only be made n-type and any attempt to diffuse in acceptor impurities results in self compensation by vacancies, to maintain charge neutrality. (p-CdS has been reported, following experiments with Bi and P ion implantation (Anderson and Mitchell, 1968, Chernow et al 1968) but the omission of a post-bombardment annealing process suggests that radiation damage, not chemical impurity, is the source of the p-type conductivity (Tell and Gibson, 1969). This is the reason for using p-$Cu_2S$ as one side of the p-n junction, since $Cu_2S$ forms epitaxially on CdS by a substitution reaction which will be described later.

The high resistivity of pure crystals makes the measurement of the transport properties of CdS rather difficult. The resistivity may be as high as $10^{12}$ Ohm cm, but can of course be reduced by optical irradiation. However the Hall mobility is dependent on the intensity of the light. The room temperature value of the Hall mobility of electrons is about 300 $cm^2.V^{-1}.S^{-1}$ in good quality single crystals. Hole mobilities are much lower (about 10 $cm^2.V^{-1}.S^{-1}$) and have been measured in transit time and acoustoelectric

experiments. In single crystals the possible contributory carrier scattering mechanisms are ionised impurity scattering, acoustic mode scattering, polar optical mode scattering, and piezoelectric scattering, with additional geometrical scattering effects in thin film specimens.

CdS exhibits many interesting phenomena, some of which have been mentioned already. A list of the more important properties will suffice for present purposes, but more information and references to original work may be obtained from Aven and Prener (1967), or Ray (1969). The important physical properties displayed by CdS are:-

(a) High photoconductivity;

(b) A large piezoelectric effect;

(c) Acoustoelectric amplification;

(d) Luminescence (thermo-, photo-, tribo-, cathodo-, electro-luminescence);

(e) Laser emission;

(f) Electrical conductivity storage (Wright et al 1968).

## 2.2 PROPERTIES OF COPPER SULPHIDE

The copper sulphide which forms half of the heterojunction of the title has several different crystalline structures and chemical formulae. "$Cu_2S$" in this context should be taken as a generic term for all of the sulphides of monovalent copper.

The layer formed epitaxially on CdS by dipping a crystal into a hot solution of $Cu^+$ ions is chalcocite, $Cu_2S$, formed according to the substitution reaction:

$$CdS + 2Cu^+ \longrightarrow Cu_2S + Cd^{++}$$

When the junction is subsequently heated in air, some of this is converted to djurleite, $Cu_{1.96}S$. Both chalcocite and djurleite have two temperature modifications which can be converted further to such compounds as $Cu_{1.92}S$ and $Cu_xS$, where x is between 1.8 (digenite) and 1.96. A fuller discussion of the Cu-S phase diagram appears in a report by Shiozawa et al (1969).

It is possible to convert completely a single crystal of CdS into a cracked, but single, crystal of $Cu_2S$ by the chemi-plating process. The cracks are the result of tension in the $Cu_2S$ layer, produced by the mismatch in volume of the two sulphides, although the sulphur ions probably have the same arrangement in both compounds (Singer and Faeth 1967, Cook et al 1970).

$Cu_2S$ has an indirect band gap of 1.2 eV. with an indicated second threshold for direct transitions at 1.8 eV. The optical absorption coefficient changes slowly with increasing photon energy below the direct transition energy, then more rapidly. High energy photons are thus easily absorbed close to the surface of the $Cu_2S$ for the

commonly used 'frontwall' cell configuration, in which light is incident on the $Cu_2S$ first. Unfortunately this leads to a poor conversion efficiency for short wavelength illumination since the electrons and holes are created adjacent to surface recombination centres, and in addition constitute a high non-equilibrium concentration of carriers with consequent high recombination rates. Some light of energy between 1.2 eV and 2.4 eV will pass through the $Cu_2S$ and be absorbed in the i-CdS (Cu compensated) layer.

The 1.2 eV band gap agrees well with the experimentally observed long wavelength threshold for the PVE in these cells. The existence of such a threshold below the direct band gap of CdS was the basis for the early arguments in favour of an active impurity level in the CdS, before the important role of the $Cu_2S$ layer was appreciated.

$Cu_2S$ is a p-type degenerate semiconductor, with a measured hole mobility at room temperature of only about 10 $cm^2.V.^{-1}S.^{-1}$, which may be improved by advances in the technology. There is appreciable ionic mobility even at room temperature due to the high diffusion rate of $Cu^+$ in $Cu_2S$, which increases rapidly with temperature, (Hirahara 1951).

The effect of high temperatures on $Cu_2S$ is to produce a loss of copper by chemical and structural changes (Cook et al 1970). In a vacuum, copper whiskers grow on the surface of heated $Cu_2S$.

This process is reversible. In air however an irreversible oxidation of surface-migrated copper results. The surface then becomes coated with $Cu_2O$ or CuO, and the interior changes progressively, according to the sequence:

$$Cu_2S \text{ ------ } Cu_{1.96}S \text{ ------ } Cu_{1.8}S$$

This is a known cause of degradation in unencapsulated cells since the various phases have different absorption coefficients and reflectivities. In contrast, a beneficial effect of a short heat treatment in air is to reduce the resistivity of $Cu_2S$ by 50%, so reducing the cell internal series resistance.

Nodules of copper have even been produced on the surface of encapsulated cells during operation for long periods at voltages about 400 mV. This appears to be the threshold for an electrolytic action, which either may be avoided by ensuring that the voltage across a cell remains below 400 mV., or may be reversed by periodically applying reverse bias (Shiozaea et al, 1969).

It is possible that the high radiation resistance of CdS solar cells can also be attributed to the high mobility of the $Cu^+$ ions which permits the rapid annealing of 'knock-on' damage.

The region of the CdS solar cell between the underlying n-type CdS and the p-type $Cu_2S$ has

yet to be mentioned. This is the intermediate, 1 micron thick, layer of copper-compensated CdS known as the i-CdS region. It is formed when a $Cu_2S$-plated sample is heated briefly at temperatures above 200°C.

Diffusion rates of copper in CdS have usually been obtained from tracer experiments with crystals on which metallic copper was first evaporated onto the surface (Clarke 1959, Woodbury 1965, Szeto and Somorjai 1966). From this work it is known that copper diffuses more rapidly perpendicular to the c-axis than parallel to it. However a lower value of the diffusion coefficient of copper in CdS has been obtained by using $Cu_2S$ as the copper source (Purohit et al 1969). These facts suggest that only a prolonged heat treatment can cause the copper to penetrate to the substrate and so affect the cell shunt resistance, as has been observed.

The effects of successive periods of heat treatment on several solar cells will be described in this thesis, but the actual $Cu_2S$ plating process was kept invariant for all cells. A full investigation of the properties of $Cu_2S$ is obviously desirable, but promises to be extremely time consuming judging from the few crystal structure experiments so far reported.

## 2.3 ELECTRICAL CONTACTS

A brief discussion of the metals which form ohmic contacts to high resistivity CdS is clearly of importance. The most commonly used contact is indium (Smith 1955, Schulman 1955) but other metals of suitable work function are silver/zinc, aluminium, and chromium (Learn et al 1966, Bujatti 1968). These metals are usually vacuum evaporated onto a polished and etched sample. Sometimes the crystal is cleaned prior to an evaporation by passing a discharge in hydrogen. Aluminium unfortunately oxidises on exposure to the atmosphere, and a protective layer is necessary to prevent this. Böer and Hall (1966) have described a method whereby the oxygen can be gettered by titanium which is co-evaporated with the aluminium. The contact is finally covered with a layer of platinum without breaking the vacuum.

Theoretically gold has such a high work function that a blocking contact would be expected. However, if CdS thin films are evaporated on top of gold layers, an Ohmic contact is formed. This is attributed to the formation of an Au/Cd intermetallic compound below the CdS, although etching studies by Vecht et al (1965) suggest that a sulphur face is in contact with the substrate normally.

Gold contacts are more durable, have less tendency to oxidise and do not diffuse into the CdS as readily as indium, but the sticking coefficient of CdS (or CdSe) is higher on gold than on glass and so a non-uniform CdS film is deposited.

On the other hand, $Cu_2S$ requires a high work function metal for an Ohmic contact, and gold is usually chosen for this, although copper can also be used.

## 2.4 FORMATION OF THE HETEROJUNCTION

The first CdS photovoltaic devices were constructed from a metal contact on a CdS crystal (Reynolds et al 1954) or thin film (Nadzhakov et al 1954). It was discovered that copper was the best metal for this purpose. A thin copper layer was deposited onto the CdS, usually followed by a heat treatment to "form" the junction. Early explanations of the origin of the photo-emf invoked photoemission from the metal into the CdS, and impurity band conduction in the CdS due to the high concentration of copper impurities. It was not until later that it was realised that a thin layer of $Cu_2S$ probably formed at all such junctions. This meant that the models for cells which had been formed from $Cu_2S$ on CdS were relevant to the studies of copper on CdS cells, and the possibility of an <u>active</u> $Cu_2S$ layer was admitted.

$Cu_2S$/CdS cells were found to have a larger spectral response and better characteristics than the early cells, but the cell configuration was limited to the "frontwall" type, in which the "barrier layer" (or junction) was adjacent to the illuminated surface. The active role of the $Cu_2S$ layer was suggested by spectral response measurements,

in which it was noticed that in "backwall" cells most of the light with wavelength greater than 5200 Å was wasted, as it was absorbed by the CdS layer close to the substrate.

The structure of present thin film CdS solar cells is shown in Figure (2.1). Light passes through a grid electrode onto the $Cu_2S$, which has been chemiplated onto a vacuum-evaporated layer of CdS on a metallised plastic substrate. Low resistivity CdS is employed to reduce the cell series resistance. Further reductions in this parameter can be achieved by using a thinner layer, at the cost of a higher probability of pinholes being formed through the film.

The plating solution used to form the p-layer in the junctions constructed for the present work was prepared as follows:-

(a) 750 ml. of distilled water was heated and stirred in a closed reaction vessel whilst oxygen-free nitrogen was continuously bubbled through the liquid to displace oxygen.

(b) 100 ml. of hydrazine hydrate solution was added.

(c) A pH meter (E.I.L. model 23A) with calomel reference electrode in a salt-bridge container, and a general purpose glass electrode, was used to bring the pH to a value of 2.5 by adding approximately 120 ml. of conc. hydrochloric acid.

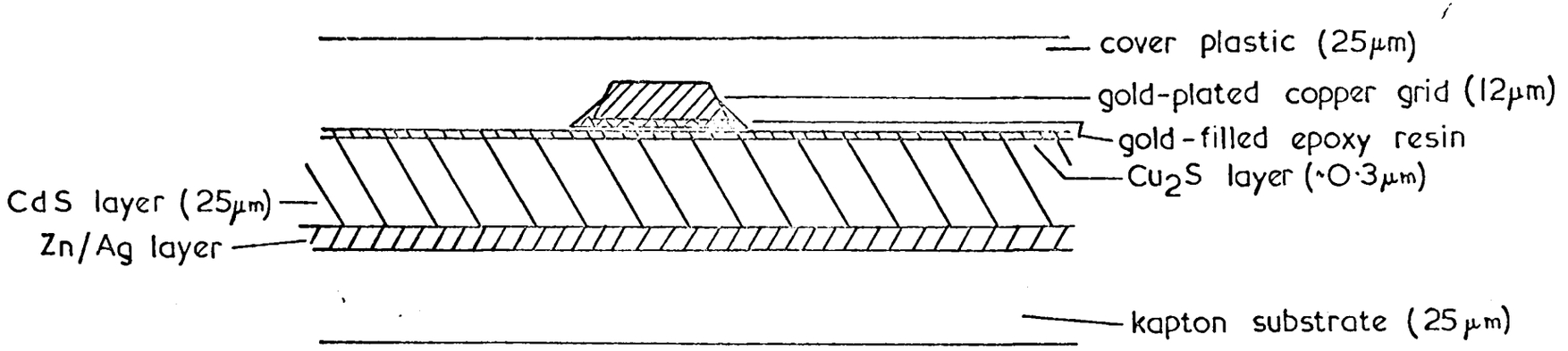


FIG. 2.1 SCHEMATIC CROSS-SECTION OF CdS THIN FILM SOLAR CELL.

(d) 10 gm. of CuCl chloride powder was added, and the liquid volume was made up to 1 litre by adding distilled water.

(e) When the solution reached 90°C., the pH was accurately adjusted to 2.5 by adding drops of hydrochloric acid or hydrazine hydrate. The plating of $Cu_2S$ was begun by dipping polished and etched CdS into the bath for a measured period.

During this time oxygen-free nitrogen was continuously bubbled through the liquid, while a magnetic stirrer kept the solution agitated. The combined effect of the hydrazine and the nitrogen was to prevent the formation of $Cu^{++}$ ions. A deep blue copper complex did precipitate from the cold solution, but was readily redissolved in excess acid when the bath was heated again.

The same strength plating solution was used to prepare all the junctions investigated in the present work. Crystals of CdS were etched in cold 40% HCl for five seconds before plating for ten seconds in 2.5 pH at 90°C. After this they were washed, and then dried in a jet of dry nitrogen. At this stage either preliminary measurements were made, or heat treatment at 200°C. in air was carried out.

Boule slices were coated on one face with evaporated indium before plating. Evaporated CdS films and crystals with indium contacts were masked

with wax or varnish to prevent $Cu_2S$ from forming a short circuit to the ohmic contact. Crystals were fastened to pieces of copper sheet after plating, with a thin layer of silver paste (JMM FSP 43, or FSP 51) between the indium and the copper.

Other recipes for making a $Cu_2S$/CdS junction are summarised below:

(a) Evaporate copper onto CdS crystals or films (Grimmeis and Memming 1962);

(b) Electroplate copper onto CdS crystals (Williams and Bube 1960, Shitaya and Sato 1968);

(c) Electroplate copper onto ceramic plates of CdS (Nakayama 1969);

(d) Evaporate $Cu_2S$ onto CdS (Keating 1963);

(e) Chemically spray $Cu_{1.8}S$ onto chemically sprayed CdS films (Chamberlain and Skarman 1966 a, 1966 b);

(f) Diffuse copper into CdS by mixing CuS with the $C_dS$ crystal growth charge (Woods and Champion 1959).

The use of such a wide range of methods has given rise to a variety of explanations of the conflicting behaviour of the cells produced. It is most likely that many of the experiments were misinterpreted either because it was supposed that no $Cu_2S$ was formed, or due to a reluctance to ascribe an active role to the $Cu_2S$ layer. The small amount of $Cu_2S$ formed by some techniques would be undetectable by conventional means, but was probably present even in unheated cells.

## 2.5 MODELS AND PROPERTIES OF THE PHOTOVOLTAIC JUNCTION

The diversity of approaches to the development of a high efficiency CdS solar energy converter inhibited the development of a single model which would explain all of the features of the junction. Early models supported various types of junction according to the exact construction technique employed, and it is possible that some were correct in certain details for that device alone. Some of the models suggested were:-

(a) Photoemission of electrons from plated copper into n-CdS (Williams and Bube 1960, for their unheated junctions);

(b) Two junctions in series: metal/$n^+$-CdS/n-CdS (Bockemuehl et al 1961, for cells formed by diffusing copper into high resistivity CdS);

(c) n-CdS/p-CdS homojunction, with a copper impurity band giving the p-type conduction (Reynolds and Czyzak 1954, Woods and Champion 1959, Grimmeis and Memming 1962a, b, Fabricius 1962);

(d) p-$Cu_2Te$/n-CdTe heterojunction, with the theory extended to $Cu_2S$/CdS cells, with the p-layer playing only a minor role in the light absorption and energy conversion (Cusano 1963);

(e) Heterojunction in $Cu_2Te$/CdTe and $Cu_2S$/CdS cells, deduced from theoretical calculations (Keating 1965);

(f) Severely localised PVE at interface states between p-$Cu_2S$ and n-CdS, causing electrons to be emitted from these states into the CdS. In this model the long wavelength response is attributed to absorption by impurities in the CdS (Balkanski and Chone 1966);

(g) Impurity PVE at copper centres in the CdS (Duc Cuong and Blair 1966);

(h) Impurity PVE at copper centres in the CdS, plus a surface barrier created by a copper contact (Shitaya and Sato 1968);

(i) Impurity PVE, plus a $p^+$-$Cu_2S$/n-CdS heterojunction with light absorption in the $Cu_2S$ layer for a Mott-barrier type cell. This is the structure which includes an i-layer, although this is formed only after a heat treatment. There is also some intrinsic absorption in the n-CdS (Nakayama 1969);

(j) Impurity PVE (1.8 eV. response) and photoemission from the $Cu_2S$ (1.2 eV. response) (Gill et al 1968);

(k) p-n heterojunction (Chamberlain and Skarman 1966, Pavelets and Fedorus 1966);

(l) Keating (1963) has reported electroluminescence in $Cu_2S$/CdS diodes, which he attributed to hole injection from the $Cu_2S$ into the CdS.

More complex models by Potter and Schalla 1967 ("Lewis" model), Hill and Keramidas 1966 ("Harshaw" model), Shiozawa et al, 1966 ("Clevite" model), van Aerschot et al, 1968 ("E.S.R.O." model) contain

some details common to all, but differ in their interpretations of the energy band at the $Cu_2S$/CdS contact. We shall discuss the 1969 Clevite model (Shiozawa et al 1969) in more detail since this model has been amended to conform with data from other sources, and explains most of the experimental observations.

The observations to be explained by any model are:

(a) The reduction in barrier height produced by illumination, shown by a cross-over of the dark and light I(V) curves, (see Figure (2.2));

(b) The enhancement and quenching effects of certain wavelength illumination when superimposed on steady white illumination;

(c) The wide spectral response with a low energy threshold at 1.2 eV.;

(d) The slow response time at certain wavelengths. (This is observed with heated cells only);

(e) The slow drift of cell characteristics under forward bias in the dark;

(f) The sharp dip in the photocurrent spectral response at the band gap of CdS when the $Cu_2S$ layer is thin;

(g) The reduction in junction capacitance after heating a cell;

(h) The improved squareness of the I(V) curve after heating a cell;

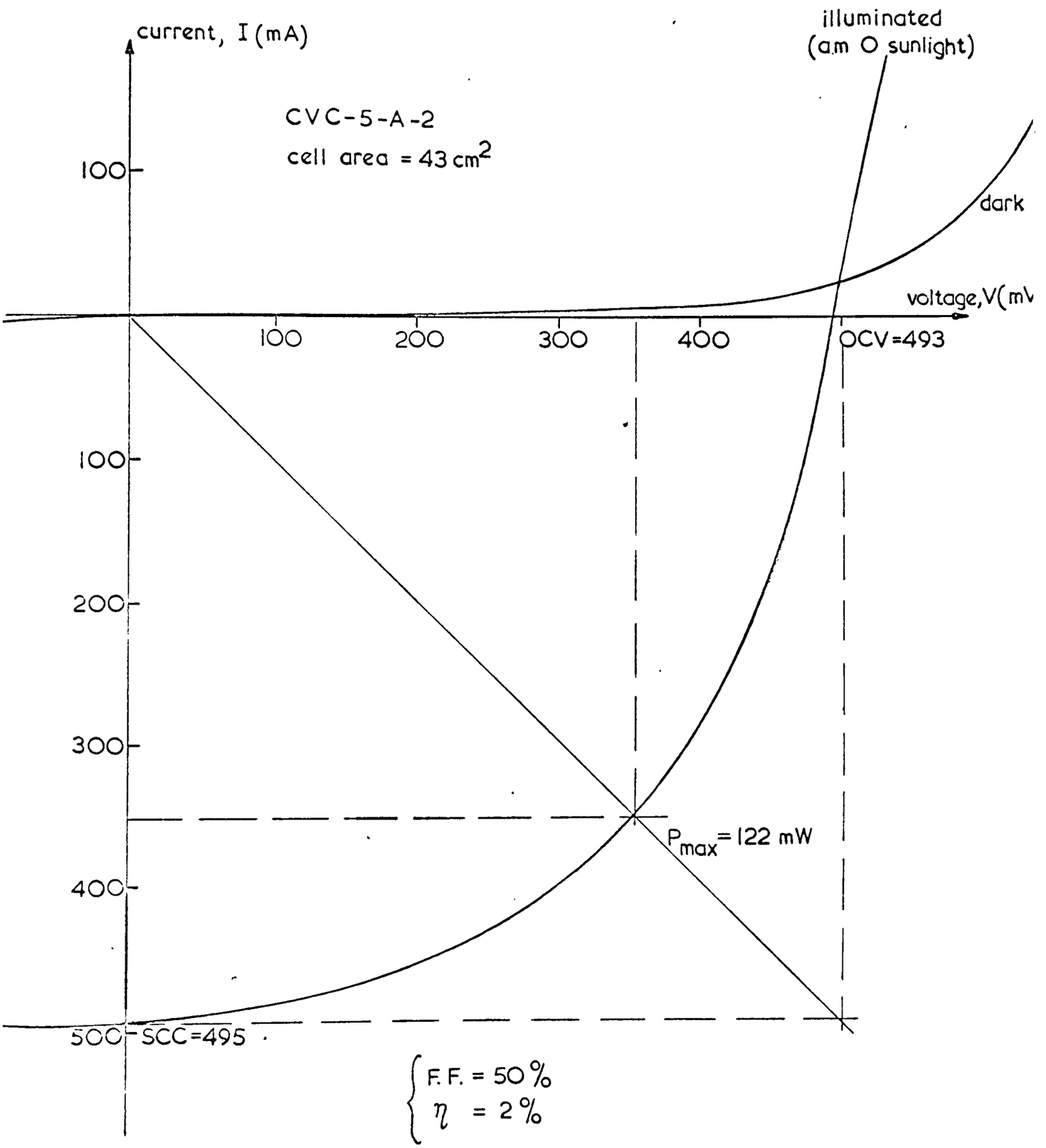


FIG. 2.2. I(V) FOR LARGE AREA CdS SOLAR CELL.

(i) Highest observed open circuit voltage (OCV) is 800 mV., at 4°K with the equivalent of five suns illumination;

(j) The effects of donor doping the CdS, (e.g. the enhancement spectrum moves to longer wavelengths when indium is introduced);

(k) Radiation resistance, nodule growth, and other effects already ascribed to the high $Cu^+$ mobility;

(l) Degradation after heating for several minutes, connected with the change in composition of the $Cu_2S$ layer.

## 2.6 THE CLEVITE CdS SOLAR CELL MODEL

Reference should be made to the energy band diagram shown in Figure (2.3), in conjunction with this section.

This model has the following features:-

(a) Gold forms an ohmic contact to p-$Cu_2S$, and silver/zinc forms an ohmic contact to n-CdS.

(b) When the cell is illuminated, the principle photo-junction is at the p-$Cu_2S$/i-CdS interface, with a barrier height of 0.85 eV.

(c) When the cell is in darkness, the principal junction is at the i-CdS/n-CdS interface, with a barrier height of 1.2 eV. There is also a small reverse-biased junction between the p-$Cu_2S$ and the i-CdS, with a barrier height of 0.35 eV.

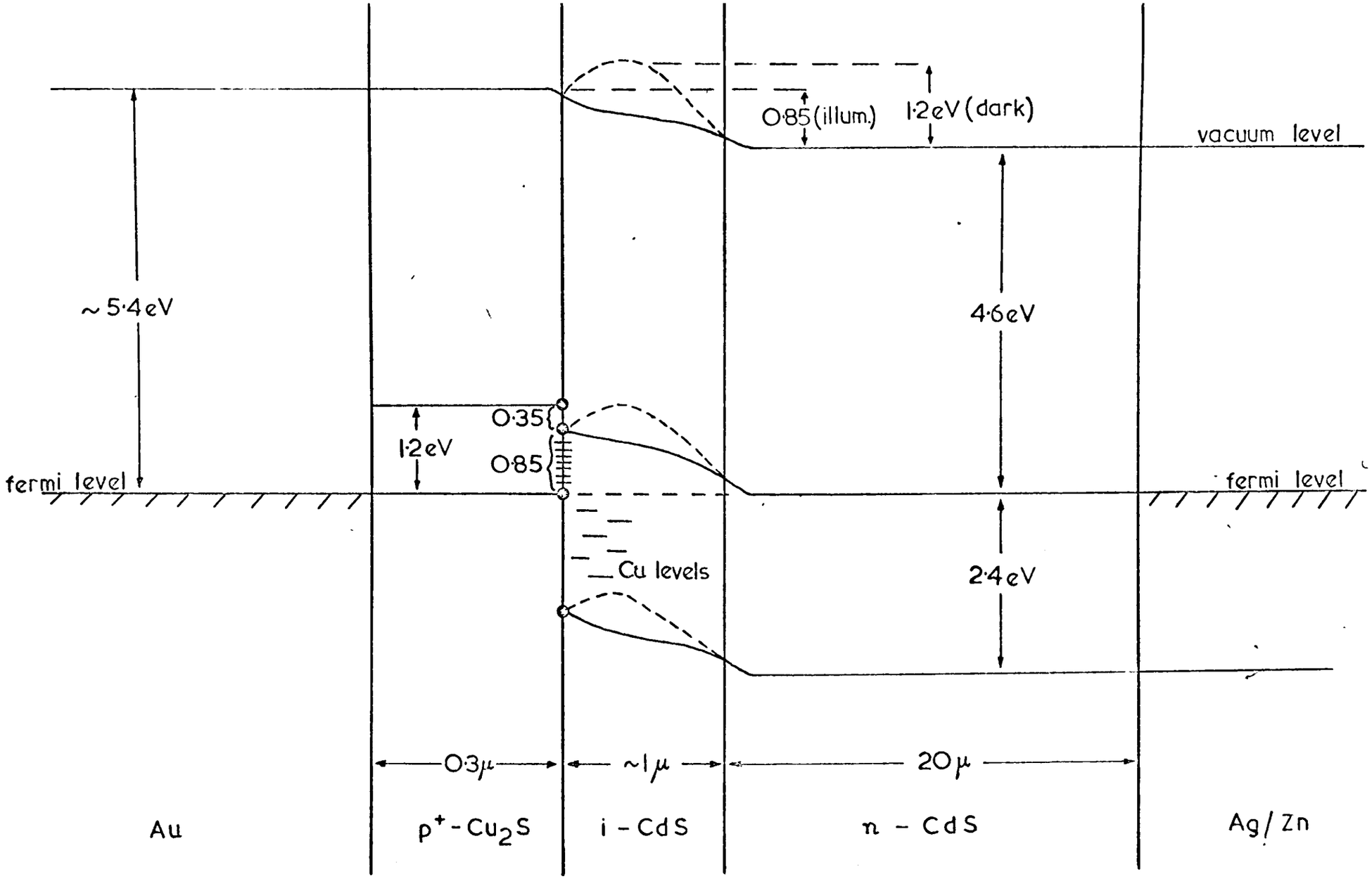


FIG. 2.3 'CLEVITE' CdS SOLAR CELL MODEL. (ILLUMINATED SHORT CIRCUIT CONDITIONS.)

(d) The electron affinity difference of 0.35 eV. is a step, with no electric field associated with it.

(e) Most of the light is absorbed in the p-$Cu_2S$ layer, aided by the non-planar topology of the cell surface.

(f) The copper-compensated i-CdS region is photoconductive and behaves as weakly n-type CdS when illuminated through the $Cu_2S$.

(g) The cell spectral response agrees with the intrinsic absorption spectrum of $Cu_2S$ modified by the photoconductive properties of CdS.

(h) Under forward bias (n-CdS negative) there is recombination via the $Cu_2S$/CdS interface states, plus bulk and surface recombination.

(i) $Cu_2S$ has appreciable ionic mobility at room temperature, increasing with temperature, and changes its stoichiometry and structure in air, so that its electrical and optical properties change.

The electrons and holes are optically created, and are subsequently collected by the Ag/Zn and Au electrodes respectively. Photons with energies below 1.2 eV. are not absorbed by the semiconductors and are lost in the substrate or are reflected. Photons with energies between 1.2 eV. and 2.4 eV. are mostly absorbed in the $Cu_2S$ to produce electrons and holes, but a fraction is transmitted and absorbed in the i-CdS region to give the observed photoconductive effects. Photons with higher energies are absorbed

near the outer face of the $Cu_2S$ layer to produce electrons and holes, which rapidly recombine by the mechanisms mentioned previously.

Electrons produced in the $Cu_2S$ layer diffuse towards the $Cu_2S$/CdS interface. From here they fall into the i-CdS region and drift into the n-CdS under the influence of the built-in field. Holes are the majority carriers in p-$Cu_2S$ and are easily collected by the gold grid. At the same time the electrons are collected by the substrate electrode.

Bube et al of Stanford University propose a slightly different energy band scheme at the $Cu_2S$/i-CdS junction. Their model places the conduction band of CdS 0.1 eV. above the bottom of the conduction band of $Cu_2S$, instead of 0.35 eV. below. This gives rise to a narrow energy spike which allows electrons to tunnel through it. With this model the electrostatic barrier would be 1.2 eV.; far greater than the maximum observed OCV. The arguments for and against this model hinge on the width of the spike, which itself depends on the net donor concentration adjacent to the $Cu_2S$. The Stanford group's assumed value of $10^{17}$ $cm.^{-3}$ is too high for heat-treated cells, but may be reasonable for unheated cells, where tunnelling is in fact a likely cause of the unstable and poorly shaped I(V) curves.

## 2.7 CONCLUSION

It must be understood that in normal operation the photovoltaic junction is working in the reverse direction: since the minority carriers constitute the photocurrent, the photojunction aids their movement. The diffusion potential is only a barrier for the dark current which flows under forward bias. The current which is delivered by an illuminated solar cell is therefore given by the photovoltaic diode equation:

$$I = I_O (\exp(eV/AkT) - 1) - I_L$$

where: $I_L$ = light-generated current,

$I_O$ = reverse (leakage) current,

V = potential across the junction,

A = diode factor,

T = operating temperature.

The cell has the equivalent circuit shown in Figure (2.4) when the shunt and series resistances are included.

Although only a very brief survey of the fabrication and operation of the CdS solar cell has been given, various features of the device can be seen to require further investigation. Some of these form the subjects of the following chapters.

The work of this thesis concerns the effect of varying the resistivity and dopant concentration of the CdS on the cell characteristics, and in particular on the OCV. From the foregoing discussion,

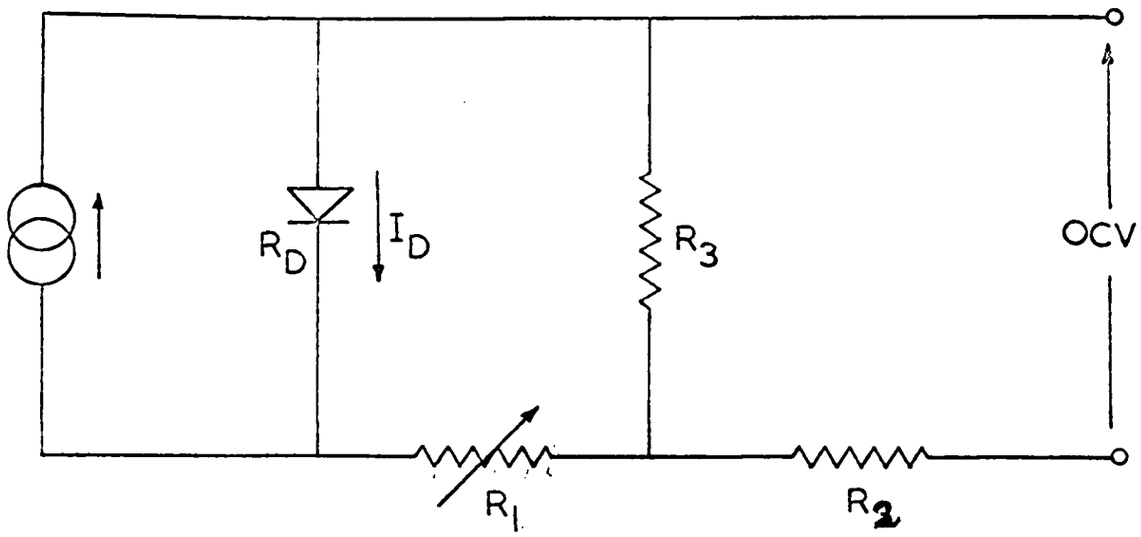


$I_D$ = Recombination Current.

$R_D$ = Diode effective resistance (voltage dependent).

$R_1$ = i – CdS resistance.

$R_2$ = Lumped series resistance.

$R_3$ = Shunt resistance.

FIG. 2.4. CdS SOLAR CELL EQUIVALENT CIRCUIT.

these parameters would be expected to have an effect on the series resistance of the cell, and on the rate of growth of the i-layer.

Quenching and enhancement of the photovoltage, with the associated response time effects, have also been investigated to confirm the existence of a photoconducting CdS layer.

A polished and plated CdS surface would be expected to give a lower short circuit current (SCC) than a roughened surface, since the topology affects the optical absorption. We shall present results showing a correlation between OCV and surface finish.

Further experiments have been carried out in vacuum to determine in what way an increase or decrease in operating temperature would affect the OCV.

Preliminary T.S.C. measurements were made on unilluminated biased cells to ascertain the feasibility of determining the concentration of interface states and their energy distribution by this technique.

It was hoped that if a low concentration of interface states could be achieved, infra-red electro-luminescence would be detected when the cell was operated under reverse bias.

This led naturally to a structural study of thin film CdS using X-rays and electron microscopy. Since CdS is the base layer of the $Cu_2S$/CdS cell, it would seem that a major part of the research effort should be concentrated on its properties if the physics of the CdS solar cell is to be fully understood.

REFERENCES

W. Anderson and J.T. Mitchell (1968) Appl. Phys. Lett. 12, 334.

M. Aven and J.A. Prener (1967) "Physics and Chemistry of II-VI Compounds" (Editors)(North Holland).

M. Balkanski and B. Chone (1966) Rev. de Phys. Appl. 1, 179.

R.J. Bockemuehl et al (1961) J.A.P. 32, 1324.

K.W. Boer and R.B. Hall (1966) J.A.P. 37, 4739.

M. Bujatti (1968) B.J.A.P. 1, 581.

R.J. Caveney (1970) J. Cryst. Growth, 7, 102-106.

R.R. Chamberlain and J.S. Skarman (1966) (a) Solid State Electrons, 9, 819.

R.R. Chamberlain and J.S. Skarman (1966) (b) J. Electrochem. Soc. 113, 86.

F. Chernow et al (1968) Appl. Phys. Lett. 12, 339.

L. Clark and J. Woods (1968) J. Cryst. Growth, 3, 126-130.

L. Clark and J. Woods (1966) B.J.A.P. 17, 319-325.

R.L. Clarke (1959) J.A.P. 30, 957.

W.R. Cook et al (1970) J.A.P. 41, 3058-3063.

D.A. Cusano (1963) Solid State Electron. 6, 217.

N. Duc Cuong and J. Blair (1966) J.A.P. 37, 1660.

E.D. Fabricius (1962) J.A.P. 33, 1597.

W.D. Gill et al (1968) "Proc. of Seventh Photovoltaic Specialists' Conference" 47-53.

P. Goldfinger and M. Jeunehomme (1963) Trans. Faraday Soc. 59, 2851.

H.G. Grimmeis and R. Memming (1962) (a) J.A.P. 33, 2217.

H.G. Grimmeis and R. Memming (1962) (b) J.A.P. 33, 3596.

E.R. Hill and B.G. Keramidas (1966) Rev. de Phys. Appl. 1, 189.

E. Hirahara (1951) J. Phys. Soc. Japan, 6, 422-427.

C.M. Hsaio and A.W. Schlechten (1952) J. Metals, 4, 65-69.

P.N. Keating (1963) J. Phys. Chem. Solids, 24, 1101.

P.N. Keating (1965) J.A.P. 36, 564.

A.J. Learn et al (1966) App. Phys. Lett. 8, 144.

H.I. Moss (1961) R.C.A. Review, 22, 29.

G. Nadzhakov et al (1954) Izv. bulg. Akad. Nank. 4, 4.

N. Nakayama (1969) Jap. J.A.P. 8, 450-462.

S. Yu Pavelets and G.A. Fedorus (1966) Ukrayinski Fiz. Zhurnal, 11, 686-688.

Perkins (1968) Advanced Energy Conversion, 7, 265.

W.W. Piper and S.J. Polich (1961) J.A.P. 32, 1278-1279.

A.D. Pogorelyi (1948) J. Phys. Chem. (U.S.S.R.), 22, 731-745.

A.E. Potter and R.L. Schalla (1967) NASA TND - 3849.

R.K. Purohit et al (1969) J.A.P. 40, 4677-4678.

B. Ray (1969) "II-VI Compounds" (Pergamon).

D.C. Reynolds et al (1954) Phys. Rev. 96, 533.

D.C. Reynolds and S.J. Czyzak (1954) Phys. Rev. 96, 1705.

C.I. Schulman (1955) Phys. Rev. 98, 384.

L.R. Shiozzawa et al (1966) Contract AF 33(615)-5224, Second Q.P.R.

L.R. Shiozawa et al (1969) Aerospace Research Labs. ARL 69-0155.

F.A. Shirland (1966) Advanced Energy Conversion, 6, 201.

T. Shitaya and H. Sato (1968) Jap. J.A.P. 7, 1348-1353.

J. Singer and P.A. Faeth (1967) App. Phys. Letters, 11, 130.

R.W. Smith (1955) Phys. Rev. 97, 1525.

G.A. Somorjai (1961) J. Phys. Chem. 65, 1059-1061.

J.M. Stanley (1956) J. Chem. Phys. 24, 1279.

W. Szeto and G.A. Somorjai (1966) J. Chem. Phys. 44, 3490-3495.

B. Tell and W.M. Gibson (1969) J.A.P. 40, 5320-5323.

A.E. van Aerschot et al (1968) "Proc. Seventh Photovoltaic Specialists' Conf."

A. Vecht et al (1965) J.A.P. 36, 2935.

D.M. Wilcox and D.B. Holt (1969) J. Mat. Sci. 4, 672-680.

R. Williams and R.H. Bube (1960) J.A.P. 31, 968-978.

H.H. Woodbury (1965) J.A.P. 36, 2287.

J. Woods and J.A. Champion (1959) J. Electronics and Control, 7, 243-253.

H.C. Wright et al (1968) B.J.A.P. 1, 1593.

# CHAPTER 3 : CdS THIN FILMS

The broad subject known as 'thin films' embraces several disciplines and has a vast literature associated with it, including several specialist journals. In this chapter it is proposed to indicate a number of available methods which have been used to prepare thin films of semiconducting II-VI compounds, with special reference to CdS. The reasons for the choice of method used to make thin films of CdS and CdSe in the present work should then become apparent.

Since some initial work was carried out on thin films of CdSe in preparation for the subsequent studies of CdS thin films, the results of these earlier studies have been presented as an appendix to this thesis.

## 3.1 II-VI THIN FILM PREPARATION

The exact technique employed in fabricating a semiconducting thin film can have a strong influence on the properties of the film, and so different devices may require different fabrication methods. It is possible that a comparatively crude technology will suffice for certain applications in which a polycrystalline structure is acceptable, whereas an elaborate and expensive method may be imperative if a single crystal film is necessary. Discussions of the many methods available for producing thin films of a wide range of materials are to be found in books by Holland (1963), Anderson (1966), and Chopra (1969). Shallcross (1967) has reviewed those methods of film deposition which have been used specifically for II-VI compounds.

Below we give a summary of those techniques which have been reported to produce CdS thin films, with an indication of the use to which each type of film has been put by previous researchers.

(a) Sintered layers of CdS powder were prepared by Thomsen and Bube (1955), Kitamura (1960), Micheletti and Mark (1968). Dopants such as Cu and Cl were sometimes added to increase the photosensitivity of the layers, and the effects of oxygen on the photosensitive response were studied after heat treatment of the layers in various ambients. Nakayama (1969) has reported a 6-9% efficient CdS solar cell based on a ceramic plate of CdS, thus the method, although crude, can produce a cheap but heavy device.

(b) By spraying two solutions, one of $CdCl_2$ and one of thiourea, onto a heated substrate and then thermally decomposing the resulting layer by a further bake, it is possible to form a polycrystalline CdS film. The other constituents escape as vapours, but there is the possibility of some chlorine contamination of the film. Micheletti and Mark (1967) have studied photo-conducting CdS layers made in this way, and Chamberlain and Skarman (1966 a, b) have made CdS solar cells from such layers. The process appears to yield adherent stoichiometric CdS if the ratios of the two solutions are correct. Lawrance (1959) studied similar layers made by spraying $CdCl_2$ onto a substrate and then heating the film in $H_2S$, but the problems of contamination are even higher with this technique.

(c) A second chemical deposition method, of limited application, is to deposit CdS onto a substrate from a heated solution of cadmium tetra-ammonium sulphate and thiourea (B.I.O.S. final report 530, Nagao and Watanabe 1968). This is similar to a technique used to prepare PbS dielectric mirrors, and has similar difficulties. It is reported that the films are polycrystalline, cubic, tenacious and have high resistivity. The photosensitivity is unaffected by oxygen or water vapour. Unfortunately it is very difficult to increase the thickness above about two microns. (Pavaskar and Menezes 1968, 1970).

(d) Vapour phase epitaxy, as used for Si and III-V compound devices has been used to produce epitaxial ZnS on single-crystal Si substrates (Lilley et al 1970), and a variant of the technique was used by Cusano (1963) to make CdTe layers for solar cells. This produced high quality films, but is not practical for large area devices on amorphous substrates.

(e) Thick film technology based on 'silk-screened' layers is mainly concerned with the deposition of conductors and insulators. Some experiments on semiconducting 'inks' have been carried out, if not reported. Witt et al (1966) have used silk-screened CdS layers in insulated-gate thin film transistors (TFT). The main problem with this technology is that the composition of the existing conductor inks is an industrial secret, and the problems of the conduction mechanism in glassy solids have not been solved.

(f) Vacuum evaporation is an established process for producing both thick and thin layers of most materials, and as a result a large industry had evolved which manufactures specialised evaporators for many branches of science and technology. The major problem is to choose the optimum method for supplying energy to the source, such that a vapour beam is produced which will condense on a substrate to form the film. (For some suggestions for evaporating a wide range of solids see the Sloan 'notebook').

Sputtering methods utilise several alternative electrode and source arrangements, although some configurations are limited to conductors alone. In all of these it is the positive ions which bombard the source and eject pieces of it towards the substrate.

R.F. sputtering has been used to produce layers of CdS, as has argon ion sputtering (Comas and Cooper, 1966), and reactive sputtering of Cd in $H_2S$ (Lakshmanan and Mitchell, 1963) or CdO in air plus a bake in $H_2S$ (Lawrance, 1959).

Some sputtering rigs require an expensive pure CdS cathode plate, and most use pressures of greater than $10^{-4}$ torr which encourages the inclusion of impurities. In addition, the process is not easy to control, and the film structure can be affected by the electric fields present.

Thermal evaporation in one of its guises, of either CdS or a mixture of CdS and an excess of one component has been the most popular technique.

Flash evaporation has been used for the III-V compounds, where the problems of maintaining stoichiometry are tackled by evaporating the compound a particle at a time, to ensure complete vapourisation. The source is complex, and difficult to control in order to avoid spattering of the charge.

Co-evaporation of CdS and S was used by Pizzarello (1964), and of Cd and S by de Klerk and Kelly (1965), Llewellyn et al (1969), and King (1969), to ensure that stoichiometric proportions of the constituents arrived at the substrate. This seems to be an excessively complex way of controlling the film properties, since it is possible to change the stoichiometry of CdS films by varying the evaporation rate of CdS and the substrate temperature. However, it is possible to attain very high resistivities, of the order of $10^{12}$ ohm cm., in co-evaporated CdS films.

In order to reduce the number of controllable parameters in a CdS evaporation, it is advisable to evaporate the compound by supplying energy in one of the following forms: laser beam, r.f. field, electron beam, thermal radiation or conduction from a resistively-heated filament.

Most workers, in common with ourselves, have used resistively-heated or electron-beam-heated sources in a vacuum of about $10^{-6}$ torr, so that their results can be compared directly with ours. With other methods there are additional parameters, perhaps unrecognised, which should be stated before a complete comparison can be made with confidence.

From an academic point of view, U.H.V. of less than $10^{-8}$ torr is the only environment in which to prepare and study a thin film in order to ensure a low impurity content. This is commercially impractical owing to the expense, sophistication and long duty cycle of U.H.V. rigs. It would be more useful (i.e. commercially practicable) if reproducible devices could be prepared in a high vacuum of $10^{-6}$ torr.

## 3.2 APPLICATIONS AND PROPERTIES OF CdS THIN FILMS

Early researchers did not realise the importance of controlling, or at least knowing the magnitude of all the parameters involved in making a thin CdS film. In essence their procedure was to prepare a film, then spend the greater part of their research effort measuring its properties. Often the source material was of dubious quality, and a post-deposition treatment was necessary to 'activate' the film. It is perhaps not surprising that many conflicting reports were published.

The results of three early researchers, Veith (1950), Aitchison (1951) and Bramley (1955), who investigated the photosensitivity of evaporated CdS layers, emphasised the importance of controlling the pressure, substrate temperature, and impurity content. It is now realised that equally important variables are the evaporation rate and source temperature, the film thickness, the composition of the residual gas, the nature of the substrate and

surface morphology. Post-evaporation treatment of a film may override the importance of some of these by altering the structure of the film.

In addition to photovoltaic heterojunctions, evaporated CdS films have been used as:

(a) ultrasonic transducers (de Klerk and Kelly 1965, Sliker and Roberts 1967, Foster 1967, Duncan et al 1968, 1969, Curtis 1969);

(b) photoresistors;

(c) phosphors;

(d) electroluminescent layers (Andrews and Haden, 1969);

(e) S.C.L. triodes and diodes (Dresner and Shallcross 1962, Zuleeg 1963, Zuleeg and Muller 1964, Brojdo et al 1965, Learn and Scott-Monck 1968, Srivastava and Sinha 1970);

(f) heterojunction diodes (Aven and Cook 1961, Aven and Garwacki 1963, Muller and Zuleeg 1964, Dutton and Muller 1968);

(g) insulated gate T.F.T.s (Haering 1964, Miksic et al 1964, Weimer 1964, O'Hanlon and Haering 1969).

Structural, electrical, and optical studies of CdS thin films have been performed in a number of laboratories, often with a particular application in mind.

When deposited normally onto a heated substrate, CdS takes the hexagonal, wurtzite structure, with a fibre axis orientation of microcrystallites. The film is polycrystalline with the individual c-axes roughly

aligned perpendicular to the substrate surface (Andrushko 1962, Shalimova et al 1964, Rozgonyi and Foster 1967, Shallcross 1967). By evaporating at an angle to the substrate surface, the c-axes of a thick film may become aligned at an angle to the substrate surface, parallel to the incident vapour beam (Foster 1967, Fukunishi and Niizeki 1969). The size of the microcrystallites depends on both the film thickness and the substrate temperature. Crystallites may be several microns across for a film 20 microns thick. (Addiss 1963, Shallcross 1966, Berger et al 1968).

The substrate temperature is of major importance, for at low temperatures (i.e. less than 150°C) more of the cubic, sphalerite structure is present. A film deposited on a room temperature substrate contains so much excess cadmium that it is black. At substrate temperatures above 150°C the film is orange, changing to a pale yellow colour and the hexagonal phase above 200°C. Above 400°C the substrate is hot enough to cause appreciable re-evaporation and it becomes increasingly difficult to form a deposit. (Wendland 1962, Shalimova et al 1964, Shallcross 1966, Bujatti 1968).

Substrate texture and cleanliness are always important if reproducible results are to be obtained, but especially so when single-crystal substrates are used. Under these conditions it is possible to grow epitaxial cubic or hexagonal CdS layers if the correct evaporation conditions and substrate are employed

(Holloway and Wilkes 1968, Wilcox and Holt 1969). The cleaner the system, the less stringent are the epitaxial limits, and the lower is the defect content. Differently orientated cubic and hexagonal CdS evaporated films have been prepared on different faces of cleaved and polished NaCl crystals, by controlling the evaporation rate and substrate temperature (Aggarwal and Goswami 1963, Chopra and Khan 1967). Chopra (1969a) has reviewed the formation of metastable structures by epitaxial processes, and Holt (1966) has reviewed the crystallography of defects in epitaxial films with the sphalerite structure.

The dark resistivity of polycrystalline CdS films changes with the deposition conditions, but there have been conflicting reports about the effects of substrate temperature and evaporation rate. The majority view is that the resistivity increases with increasing substrate temperatures, but decreases with increasing evaporation rates.

The photosensitivity changes in the expected manner: the higher the resistivity, the higher the photosensitivity (Shalimova et al 1961).

The electron Hall mobility, $\mu_H$, is also affected by the deposition conditions and crystalline structure. It is lower in polycrystalline films than in single crystal films, and much lower than in bulk CdS. Typical values of about 10 cm. $^2$V.$^{-1}$S.$^{-1}$ for polycrystalline CdS films can be interpreted using the Petritz (1956) model for polycrystalline films of PbS, PbSe, and PbTe.

According to this theory the carriers are scattered and trapped by intercrystallite barriers, which leads to an exponential dependence of mobility on temperature and barrier height:

$$\mu_H = \mu_o \exp -(E/kT) \qquad \text{(Berger 1961)}$$

Unfortunately, ionised impurity scattering leads to a dependence of $\mu_H$ as $T^{3/2}$ and the two mechanisms are difficult to distinguish experimentally (Shallcross 1967, Neugebauer 1969). However most workers have favoured the Petritz barrier model (Karpovich and Zvonkov 1965, Shallcross 1966, Neugebauer 1968). A study of the drift mobility, $\mu_D$, in CdS thin films has been made by Waxman (1965, 1966) and Neugebauer (1968) using a field-effect configuration of contacts to examine the surface states. The conclusion that inter-crystallite barriers exist was supported by this work.

Measurements of various optical properties, such as visible reflectivity, infra-red reflectivity, and photoluminescence have been made by Gottesman and Ferguson (1954), Proix and Balkanski (1969), Bleha and Peacock (1970), respectively.

It has been reported that post-deposition baking in vacuum, air, $H_2S$, or a non-reactive gas such as argon increases both the photosensitivity and the carrier mobility of CdS thin films (Boesman and Avis 1963, Berger et al 1964, Sakai and Okimura 1964). The dark resistivity has been shown to increase or decrease after such treatment. This depends on the

substrate temperature used during the initial preparation (Wendland 1962). These effects have been explained by (i) the substantial recrystallisation which occurs, and (ii) by the fact that a reaction with oxygen can occur. Oxygen is known to be an active constituent which promotes changes in the photosensitivity. (Kuwabara 1954, Esbitt 1965).

Many workers have investigated the recrystallisation phenomena which can be observed when a CdS film is heated in contact with a thin metal layer. Gilles and Van Cakenberghe (1958) used a thin evaporated layer of Ag, Cu, Pb, In, Al, B, or Zn followed by baking in an inert atmosphere at 500° - 600°C. This increased the crystallite size and photosensitivity of the evaporated layers of CdS. Using this technique, Addiss (1963) increased the mobility of his films from 1 to 50 $cm.^{2}V.^{-1}S.^{-1}$, and Dresner and Shallcross achieved mobilities equal to that in bulk CdS.

More complicated methods in which several of the above treatments were employed jointly have been reported by Böer et al (1966). Vecht and Apling (1963) used a variant of the Gilles and Van Cakenberghe method. In their technique the CdS film was immersed in a suspension of an organometallic compound in a hot inert organic fluid (such as Silicone 704).

Previous to this, Nelson (1955) had studied the early forming processes and had suggested that excess cadmium was oxidised during the air bake, with varying effects according to the purity of the CdS charge.

Vecht has also studied the effects of a hot bake in the absence of a metal, and concluded that the recrystallisation was initiated by dust and scratches, whereas the metal aided recrystallisation by the formation of an intermediate compound. The activation and recrystallisation of II-VI compound layers is reviewed in an article by Vecht (1966).

## 3.3 CONCLUSION

The large amount of published work on CdS thin films is indicative of the wide range of possible applications of such structures. However, much of the early work produced conflicting results and should be treated with caution wherever the preparation technique has not been fully described. The cleanliness both of the system and of the material is very important, although a forming process has been known to override this consideration. The following chapter will be devoted to a description of the apparatus which was used to produce the thin films used in the present study.

REFERENCES

R.R. Addiss (1963) Trans. 10th Nat. Vac. Symp., 354-363 (MacMillan).

P.S. Aggarwal and A. Goswami (1963) Indian J. Pure Appl. Phys. 1, 366.

R.F. Aitchison (1951) Nature, 167, 812-813.

J.G. Anderson (1966) "The Use of Thin Films in Physical Investigations" (Academic Press).

A.M. Andrews and C.R. Haden (1969) Proc. I.E.E.E., 57, 99-100.

H.F. Andrushko (1962) Sov. Phys. Crystallog. 7, 172.

M. Aven and D.M. Cook (1961) J.A.P. 32, 960.

M. Aven and Garwacki (1963) J. Electrochem. Soc. 110, 401.

H. Berger (1961) Phys. Stat. Sol. 1, 739.

H. Berger et al (1968) Phys. Stat. Sol. 28, K97.

H. Berger et al (1964) Phys. Stat. Sol. 7, 679.

B.I.O.S. final report 530 "Production of CdS Mirrors."

W.P. Bleha and R.N. Peacock (1970) J.A.P., 41, 4992-5003.

K.W. Böer et al (1966) J.A.P. 37, 2664.

W.C. Boesman and G.G. Avis (1963) Trans. 10th Nat. Vac. Symp. 364-367.

A. Bramley (1955) Phys. Rev. 98, 246.

S. Brojdo et al (1965) B.J.A.P. 16, 133.

M. Bujatti (1968) B.J.A.P. 1, 983.

R.R. Chamberlain and J.S. Skarman (1966) (a) Solid State Electron. 9, 819-823.

R.R. Chamberlain and J.S. Skarman (1966) (b) J. Electrochem. Soc. 113, 86-89.

K.L. Chopra (1969) "Thin Film Phenomena" (McGraw-Hill).

K.L. Chopra (1969) (a) Phys. Stat. Sol. 32, 489.

K.L. Chopra and I.H. Khan (1967) Surf. Sci. 6, 33.

J. Comas and C.B. Cooper (1966) J.A.P. 37, 2820.

B.J. Curtis (1969) J.A.P. 40, 433.

D.A. Cusano (1963) Solid State Electron. 6, 217-232.

J. de Klerk and E.F. Kelly (1965) Rev. Sci. Instrum. 36, 506.

J. Dresner and F.V. Shallcross (1962) Solid-State Electron. 5, 205-210.

J. Dresner and F.V. Shallcross (1963) J.A.P. 34, 2390.

W. Duncan et al (1968) J.A.P. 39, 5987.

W. Duncan et al (1969) J. Vac. Sci. Technol, 6, 555-558.

R.W. Dutton and R.S. Muller (1968) Solid-State Electron 11, 749.

A.S. Esbitt (1965) Phys. Stat. Sol. 12, K35-K37.

N.F. Foster (1967) J.A.P. 38, 149-159.

S. Fukunishi and N. Niiezeki (1969) Jap. J.A.P. 8, 1274-1275.

J.M. Gilles and J. Van Cakenberghe (1958) Nature 182, 862.

J. Gottesman and W.F.C. Ferguson (1954) J. Opt. Soc. Amer. 44, 368-370.

R.R. Haering (1964) Solid-State Electron. 7, 31.

L. Holland (1963) "Vacuum Deposition of Thin Films" (Chapman and Hall).

H. Holloway and E. Wilkes (1968) J.A.P. 39, 5807.

D.B. Holt (1966) J. Mat. Sci. 1, 280-295.

I.A. Karpovich and B.N. Zvonvov (1965) Sov. Phys. Sol. St. 6, 2714.

P.J. King (1969) B.J.A.P. 2, 1349-1352.

S. Kitamura (1960) J. Phys. Soc. Japan 15, 2343.

G. Kuwabara (1954) J. Phys. Soc. Japan 9, 97-102.

T.K. Lakshmanan and J.M. Mitchell (1963) Trans. 10th Nat. Vac. Symp. 335-338.

R. Lawrance (1959) B.J.A.P. 10, 298-300.

A.J. Learn and J.A. Scott-Monck (1968) J.A.P. 39, 2480-2481.

P. Lilley et al (1970) J. Mat. Sci. 5, 891-897.

J.D. Llewellyn et al (1969) J. Sci. Instrum. 2, 535-536.

F.B. Micheletti and P. Mark (1967) App. Phys. Letters 10, 136.

F.B. Micheletti and P. Mark (1968) J.A.P. 39, 5274.

M.G. Miksic et al (1964) Solid-State Electron. 7, 39-48.

R.S. Muller and R. Zuleeg (1964) J.A.P. 35, 1550.

M. Nagao and S. Watanabe (1968) Jap. J.A.P. 7, 684.

N. Nakayama (1969) Jap. J.A.P. 8, 450-462.

R.C. Nelson (1955) J. Opt. Soc. Amer. 45, 774-775.

C.A. Neugebauer (1968) J.A.P. 39, 3177-3186.

C.A. Neugebauer (1969) J. Vac. Sci. Technol. 6, 454-460.

J.F. O'Hanlon and R.R. Haering (1969) Solid-State Electron. 12, 363.

N. Pavaskar and C. Menezes (1968) Jap. J.A.P. 7, 743.

N. Pavaskar and C. Menezes (1970) Jap. J.A.P. 9, 212-216.

R.L. Petritz (1956) Phys. Rev. 104, 1508.

F.A. Pizzarello (1964) J.A.P. 35, 2730.

F. Proix and M. Balkanski (1969) Phys. Stat. Sol. 32, 119.

G.A. Rozgongi and N.F. Foster (1967) J.A.P. 38, 5172.

Y. Sakai and H. Okimura (1964) Jap. J.A.P. 3, 144.

K.V. Shalimova et al (1961) Sov. Phys. Doklady, 6, 404.

K.V. Shalimova et al (1964) Sov. Phys. Crystallog. 8, 618.

F.V. Shallcross (1966) Trans. Met. Soc. of A.I.M.E., 236, 309-313.

F.V. Shallcross (1967) R.C.A. Rev. 28, 569.

T.R. Sliker and D.A. Roberts (1967) J.A.P. 38, 2350.

S.K. Srivastava and A.P.B. Sinha (1970) Solid-State Electron. 13, 57-60.

S.M. Thomsen and R.H. Bube (1955) Rev. Sci. Instrum. 26, 664-665.

A. Vecht (1966) in "Physics of Thin Films" 3. (Academic Press).

A. Vecht and A. Apling (1963) Phys. Stat. Sol. 3, 1238-1246.

W. Veith (1950) Comptes Rend. Acad. Sci. 230, 947-949.

A. Waxman et al (1965) J.A.P. 36, 168-175.

A. Waxman (1966) Solid-State Electron. 9, 303.

P.K. Weimer (1964) in "Physics of Thin Films" 2, (Academic Press).

P.H. Wendland (1962) J. Opt. Soc. Amer. 52, 581-582.

D.M. Wilcox and D.B. Holt (1969) J. Mat. Sci. 4, 672-680.

W. Witt et al (1966) Proc. I.E.E.E. 54, 897-898.

R. Zuleeg (1963) Solid-State Electron. 6, 193.

# CHAPTER 4 : PREPARATION OF THE CdS FILM

## 4.1 THE VACUUM SYSTEMS

Figure (4.1) is a schematic diagram of the valves and pumps on the evaporation system which was used to produce most of the films to be discussed. Two gauges were employed to measure the pressure in the work chamber: a thermocouple gauge (A.E.I. VC 12) for pressures above $10^{-2}$ torr, and an ion gauge (A.E.I. VC 10/VH9) for pressures below $10^{-3}$ torr. The lowest attainable pressure was $1.0 \times 10^{-6}$ torr, with Silicone 705 pump fluid in the 3" diffusion pump, and liquid nitrogen in the cold trap. Most evaporations were carried out at pressures below $10^{-5}$ torr.

A larger system with similar components (made by Edwards High Vacuum Ltd.) was built around a 4" oil diffusion pump, to enable the electron gun to be used at higher powers, where the speed of the smaller diffusion pump was insufficient to handle the outgassing of the source.

A third system was used at I.R.D. Co. Ltd. This consisted of a C.V.C. 18" bell jar (CV-164) with oil diffusion pump and cold trap, operated by automatic switching. A pressure of $10^{-7}$ torr could be achieved within 30 minutes. A 'Sloan' deposit control master (OMNI II) was installed to monitor film thickness and evaporation rate. A complete evaporation cycle could be controlled using its oscillating quartz crystal detector and relays.

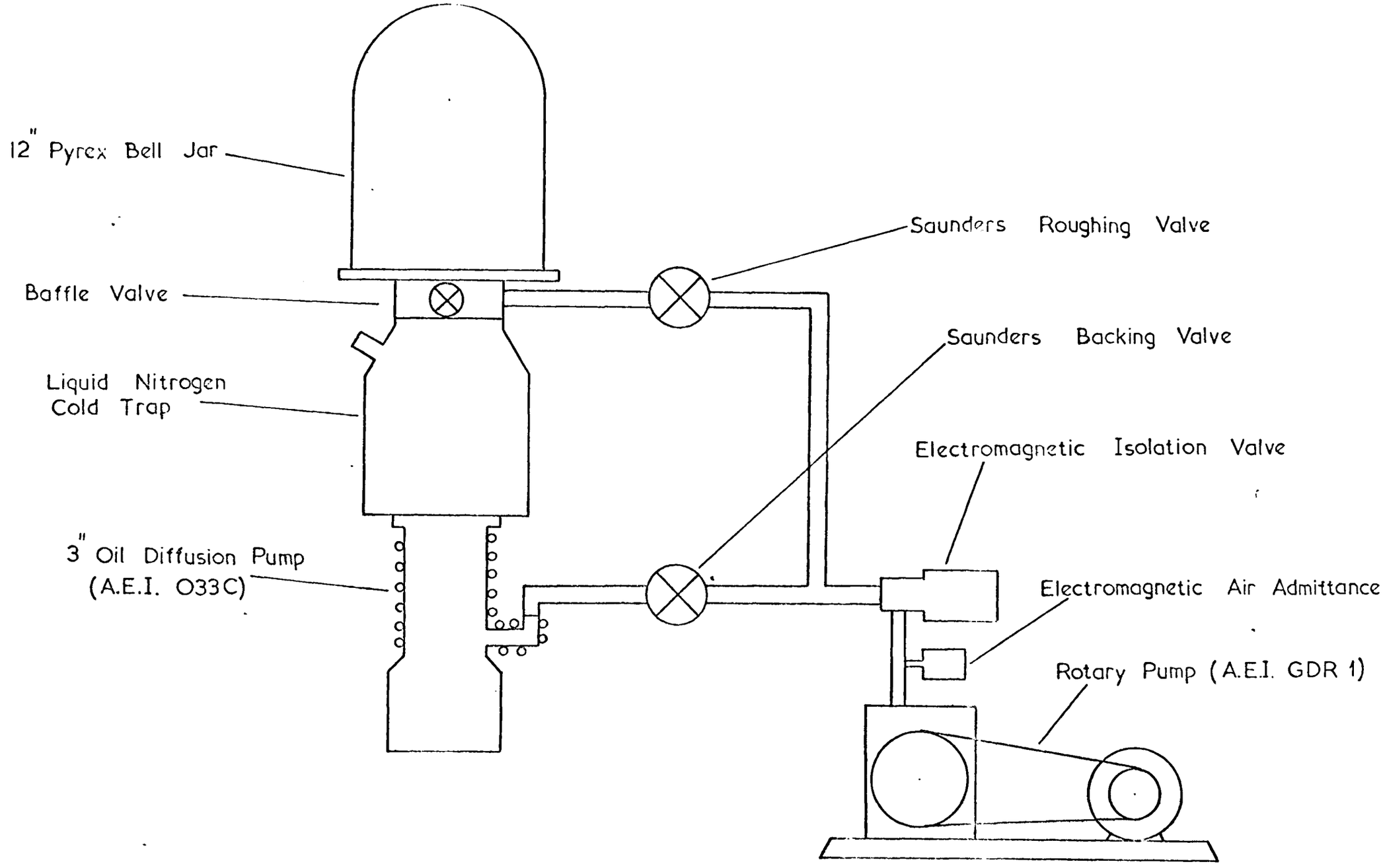


FIG. 4.1 12" EVAPORATOR : SCHEMATIC OF PUMPS and VALVES

## 4.2 VACUUM CHAMBER FIXTURES

Reference should be made first to Fig. (4.2) which depicts the arrangement used with the resistively-heated source in the 3" pump system.

Several sizes of silica crucible wound with tungsten or molybdenum wire were used successfully, and the diagram shows the largest of these. This heating element was matched to the L.T. transformer, enabling the full 30 A., 30V. to be drawn if required. A thin quartz wool baffle in the mouth of this crucible was essential to prevent spattering of the CdS at high evaporation rates. A deposition rate of several thousand Ångstroms per minute was easily attainable with CdS.

The substrates and their masks were clamped to a stainless steel block containing an insulated tungsten heating element. The temperature was controlled by an Ether "mini" controller with a NiCr/NiAl thermocouple in contact with the substrate surface.

The volume between substrate and source was encircled by a 9 cm. diameter silica cylinder, which was radiation-heated by the source, in an effort to retain both components of the vapour within the vicinity of the substrate. This enhanced stoichiometric growth by preventing the preferential condensation of one element on the relatively cold walls of the bell-jar. Reproducible results from films deposited at low evaporation rates could only be obtained when this "hot wall" was in position.

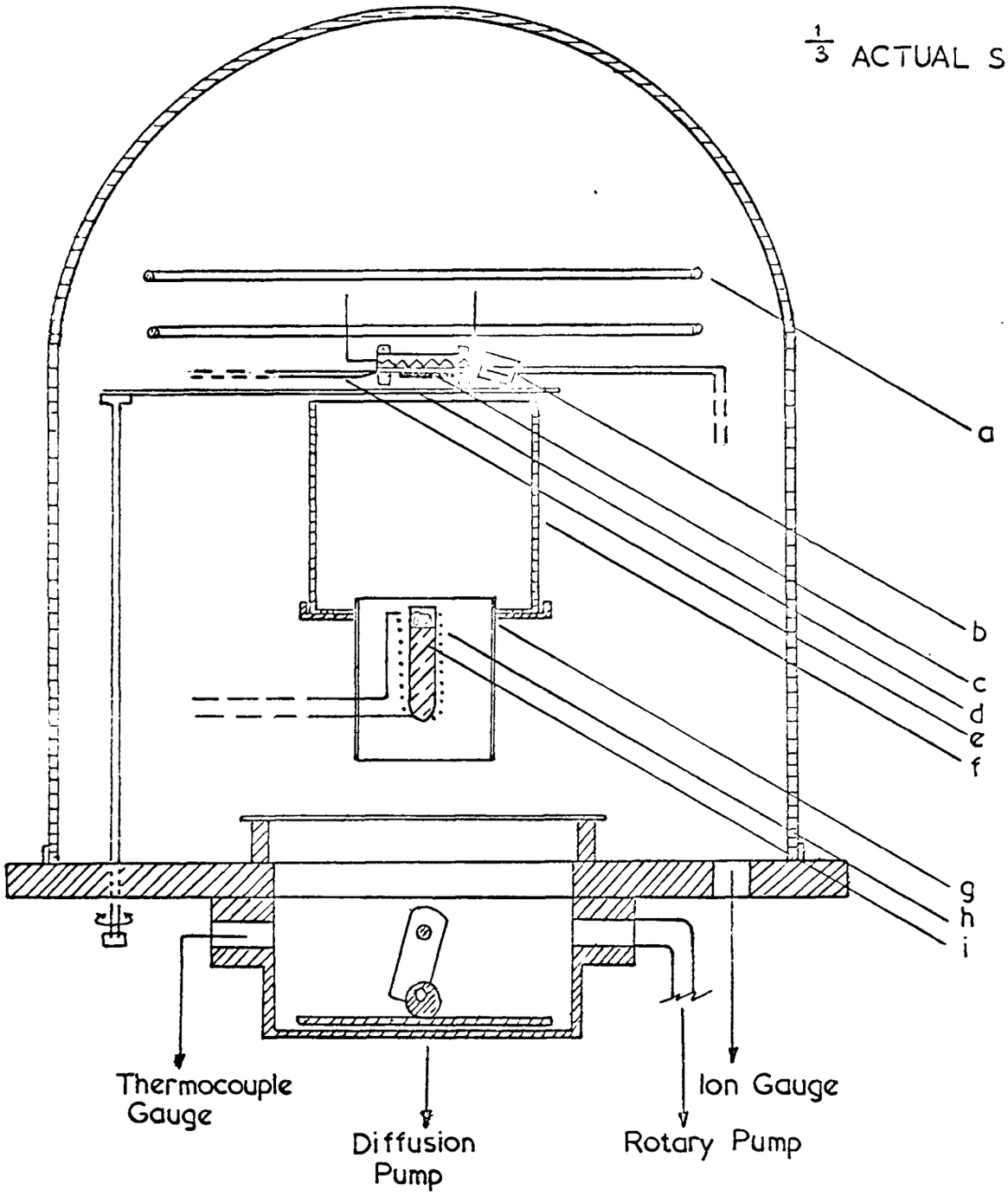


a) Ion Bombardment Rings

b) Deposit Thickness Monitor

c) Substrate Heater, Substrate, and Copper Mask.

d) Shutter

e) Thermocouple

f) Silica Cylinder

g) Mo Radiation Shield

h) Silica Crucible and Tungsten Heater

i) Charge and Quartz Wool Baffle.

FIG. 4.2 BELL JAR FIXTURES

A deposit thickness monitor of the oscillating quartz crystal type (Genevac DTM 1) was positioned close to the substrate. The instrument was calibrated against post-evaporation optical determinations of film thicknesses. Not only could film growth be followed in situ, but in addition the evaporation could be stopped when the desired thickness had been laid down.

A stainless steel shutter, operated through a rotary seal, was positioned immediately below the substrate and the crystal of the DTM 1. CdS vapour could then be exposed to each or neither during a cycle, and the substrate could be masked until outgassing had been completed and the evaporation rate had attained a constant value.

The Genevac EBU 1 electron beam evaporator is shown in Fig. (4.3). It will be seen that the hot molybdenum filament was optically screened from both source and substrate by the negatively biased focussing cage and washer. The electrons were focussed on to the surface of the evaporant which was either contained in one of the four molybdenum crucibles in the water-cooled hearth, or, when boule slices were the evaporant, was placed directly on the hearth. Each crucible could be positioned below the emitter by a lateral movement of the bellows seal, through a stainless steel collar between bell-jar and baseplate.

A 10 kV., 20 A. at 7 V., variable power supply was constructed to provide both the filament power and

FULL SIZE

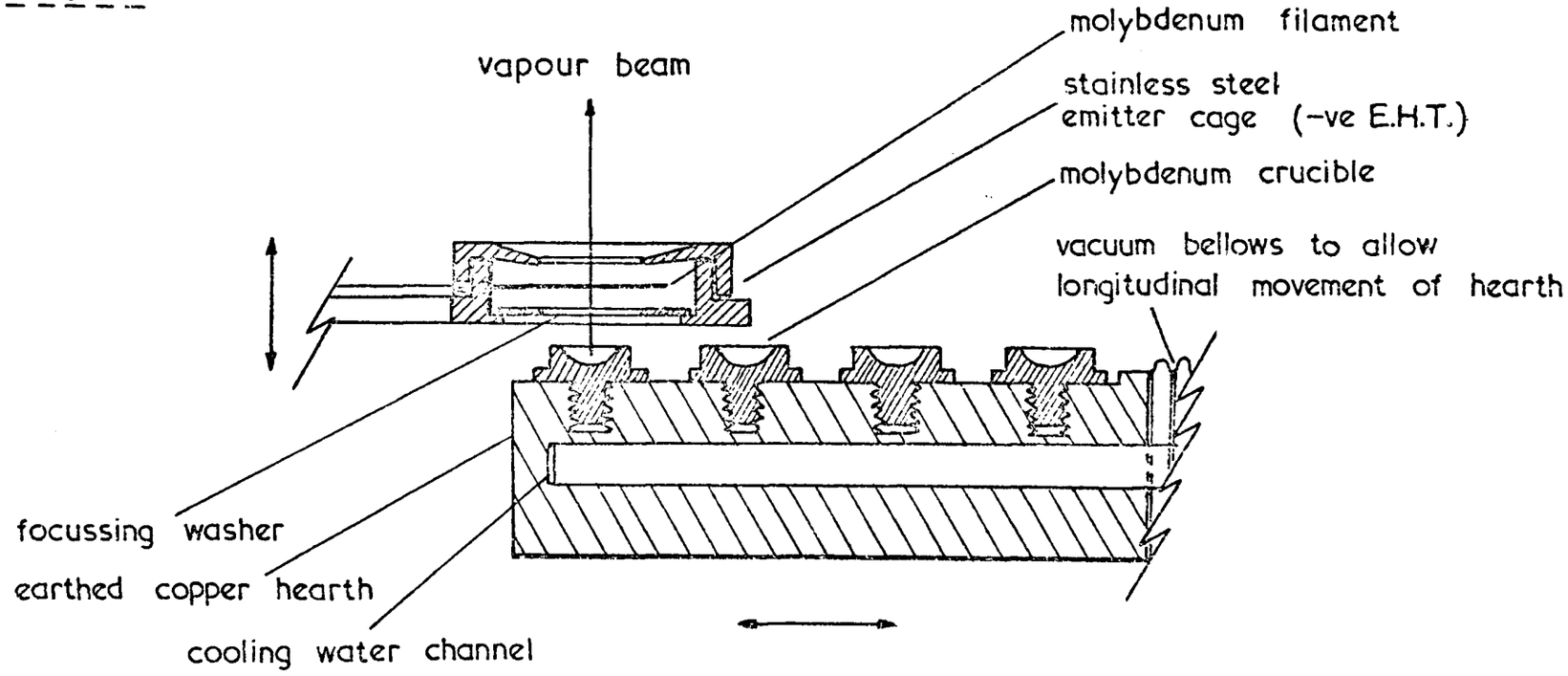


FIG. 4.3 'GENEVAC' EBU 1 ELECTRON BEAM EVAPORATOR.

accelerating potential. This equipment followed a design of Martin (1970). Safety interlocks were provided to protect both the supply and the operator. A stabilised, maximum beam power of 150 mA., 10 kV. was available. Both the current and the E.H.T. were independently variable within these limits.

The I.R.D. Co. Ltd. source which was placed in the 18" system is shown in Fig. (4.4). This was a directly-heated tantalum crucible containing 40 gm. of powdered CdS when full. Evaporation rates of more than a micron a minute were attained, and six 3" by 3" substrates could be coated simultaneously with 20 microns of CdS. Source and substrates were 36 cm. apart, and no 'hot wall' was used.

The six substrates were held against a radiation-heated block and covered by a shutter until the source had been outgassed and the evaporation rate was steady. On completion of the evaporation the substrates were lowered away from the substrate heater and so allowed to cool more rapidly. The substrate temperature was controlled by an Ether "mini" and thermocouple.

A few photovoltaic cells were made at I.R.D. Co. Ltd. from films prepared in the 18" system by evaporating CdS from a small tantalum crucible on to a single substrate, employing the hot wall technique. This alternative arrangement had a source to substrate distance of 15 cm.

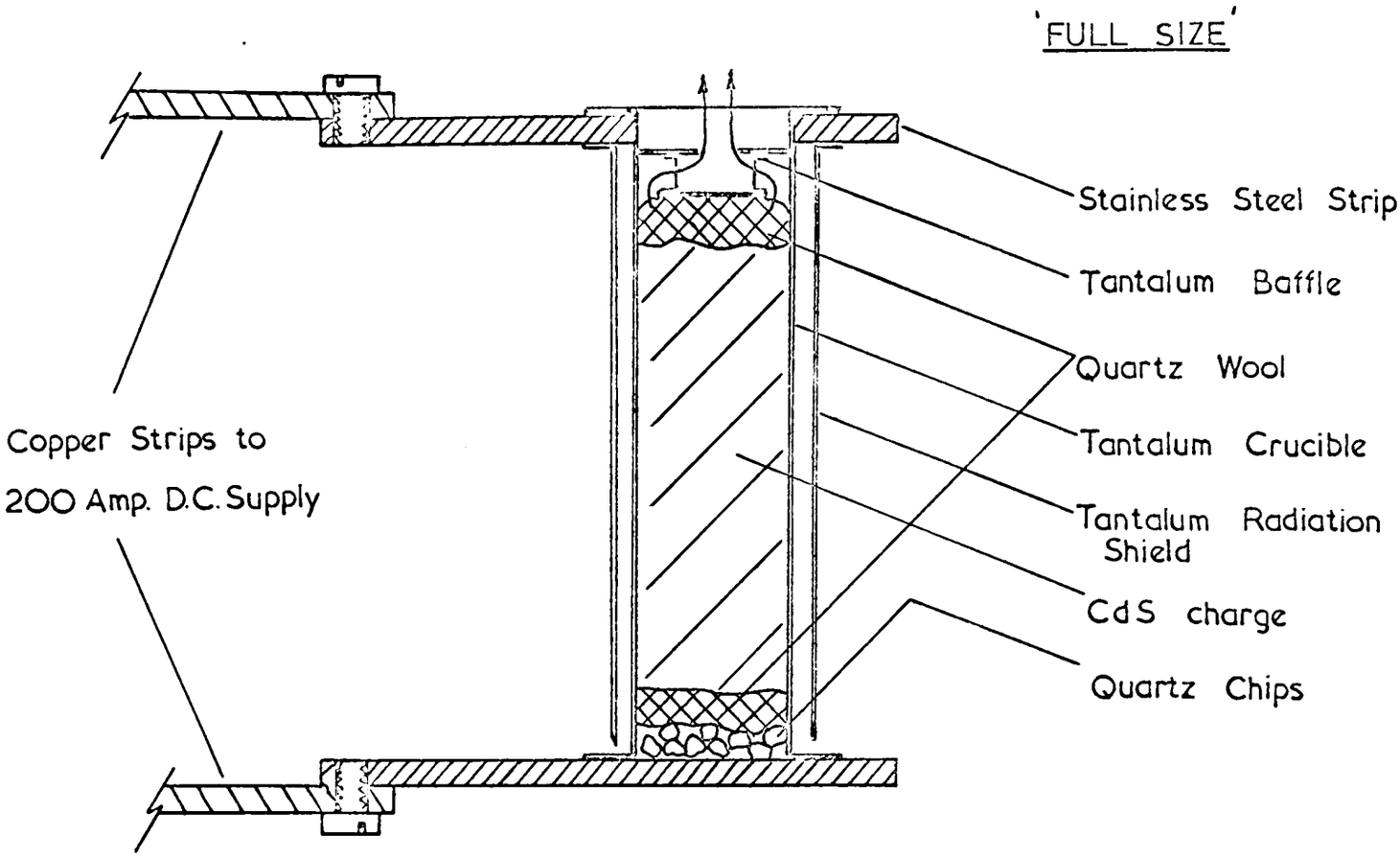


(Tantalum is spot welded to stainless steel)

FIG. 4.4 I.R.D. TANTALUM CRUCIBLE

## 4.3 MASKS AND SUBSTRATES

Evaporation masks for delineating electrical contacts and samples on which the Hall coefficient could be measured were manufactured from 0.005" thick copper sheet by photochemical etching. Less complex patterns were machined from copper or Duralumin sheet. The copper masks were cleaned in chromic acid before placing them in the work chamber.

There are many suitable substrate materials, with contrasting properties. Those which were actually employed included various glasses (pyrex, Corning 0211, Corning 7059), mica, MgO, $BaF_2$, NaCl, GaAs, and metallised Kapton (a polyimide plastic). These obviously required different cleaning and handling techniques before a film could be deposited.

Much work had been done to discover the best way of cleaning glass substrates when metal films became commercially important. The most commonly used methods were a series of chemical rinses, or glow discharge cleaning (Holland, 1958), or alcohol vapour degreasing (Putner, 1959). In his book on glasses, Holland (1966) came to the conclusion that a thorough chemical wash was at least as good as ion bombardment cleaning. The best technique is to remove gross contamination in a detergent-type solvent by ultrasonic agitation, followed by degreasing in propan-2-ol vapour.

Although glow discharge cleaning was later discontinued without any adverse effects on film structure or tenacity, some of our early films were

deposited on to glass which had been subjected to ion bombardment after chemical washing with trichloroethylene and then with propan-2-ol.

To produce the ion bombardment a rectified E.H.T. supply of 0-2.5 kV. was connected to the two isolated, pure aluminium ring electrodes positioned around the substrate as shown in Fig.(4.2). Since the faster electrons will coat surfaces with decomposed hydrocarbons, only the positive ions will give any beneficial effect. It follows therefore that the substrate must be immersed in the anode glow. This was accomplished by suitable positioning of the rings, and increasing the pressure to about $10^{-2}$ torr by admitting dry air through a needle valve. It has been shown by Bateson (1952) that a fast reversible absorption of gas commenced as soon as the discharge stopped, but the absorbed layer can be displaced by the vapour beam (Ellis, 1968).

The single-crystal substrates were cleaved or polished before deposition of the films. Cleavage took place either in air before loading the work chamber, using a cleaver of the type described by Harris (1969), or in situ in the vapour beam by sharply rotating a ground edge of the shutter against the crystal. Oxygen contamination will be greater for a surface which has been cleaved before loading than for a similar surface cleaved in the vapour beam, although it should be noted that the time taken to form a monolayer of oxygen on a clean surface at $10^{-6}$ torr (assuming a sticking probability of 0.2) is only about 10 S.

## 4.4 THE EVAPORATION CYCLE

This section is devoted to a description of the sequence of steps in a typical evaporation of CdS on to glass, using the 3" pump system previously described.

(i) The substrate was cleaned by ultrasonic agitation in a solution of teepol or "quadralene," US/7 instrument cleaner, rinsed in distilled water, washed in propan-2-ol, and finally suspended in propan-2-ol vapour for several minutes to ensure that no stains would persist on the dry surface.

(ii) The substrate and a mask were clamped on to the substrate heater, and the crucible was filled with crushed CdS flow crystals. If the CdS was to be evaporated from a boule slice by the electron gun, it was cut by a diamond wheel or the wire saw described by Rushby and Woods (1970), and placed directly on the copper hearth.

(iii) The system was evacuated to less than $10^{-5}$ torr, and the substrate was heated to at least 50°C above the required substrate temperature for one hour.

(iv) The CdS was outgassed by gradually increasing the source power.

(v) (The hot substrate was ion bombarded at a pressure of $10^{-2}$ torr for a few minutes, before pumping down again).

(vi) The evaporation rate and substrate temperature were set to the required value and the shutter was opened after a steady state condition had been attained.

(vii) The evaporation rate was monitored by the DTM 1 until the film had grown to the desired thickness,

at which point the shutter was closed and the source and substrate heaters were switched off.

(vii) The substrate was allowed to cool to room temperature before breaking the vacuum.

(ix) Electrical contacts, when desired, were evaporated from a molybdenum boat in a separate glass vacuum system pumped by a small mercury diffusion pump and cold trap.

## 4.5 DETERMINATION OF FILM THICKNESS

When the film thickness was required to be known accurately, it was measured optically with a Watson interference objective. A reflecting metallised layer over an edge of the film was desirable, and the indium electrical contacts proved ideal for this purpose, provided that they were deposited at a pressure of less than $10^{-5}$ torr and at a high rate.

This optical technique of measuring film thickness employs double beam interferometry with monochromatic illumination, to produce Fizeau interference fringes from both the metallised film and the metallised substrate. The purpose of the metallic layer was to increase fringe contrast, and to eliminate the different and unknown phase changes which occur on reflection from dielectrics. The film thickness could be calculated from the fringe displacement across the step, which arose from the difference in path lengths of the reflected beams, since the separation of like-intensity fringes is equal to half the wavelength of the illuminating light (See Fig.4.5).

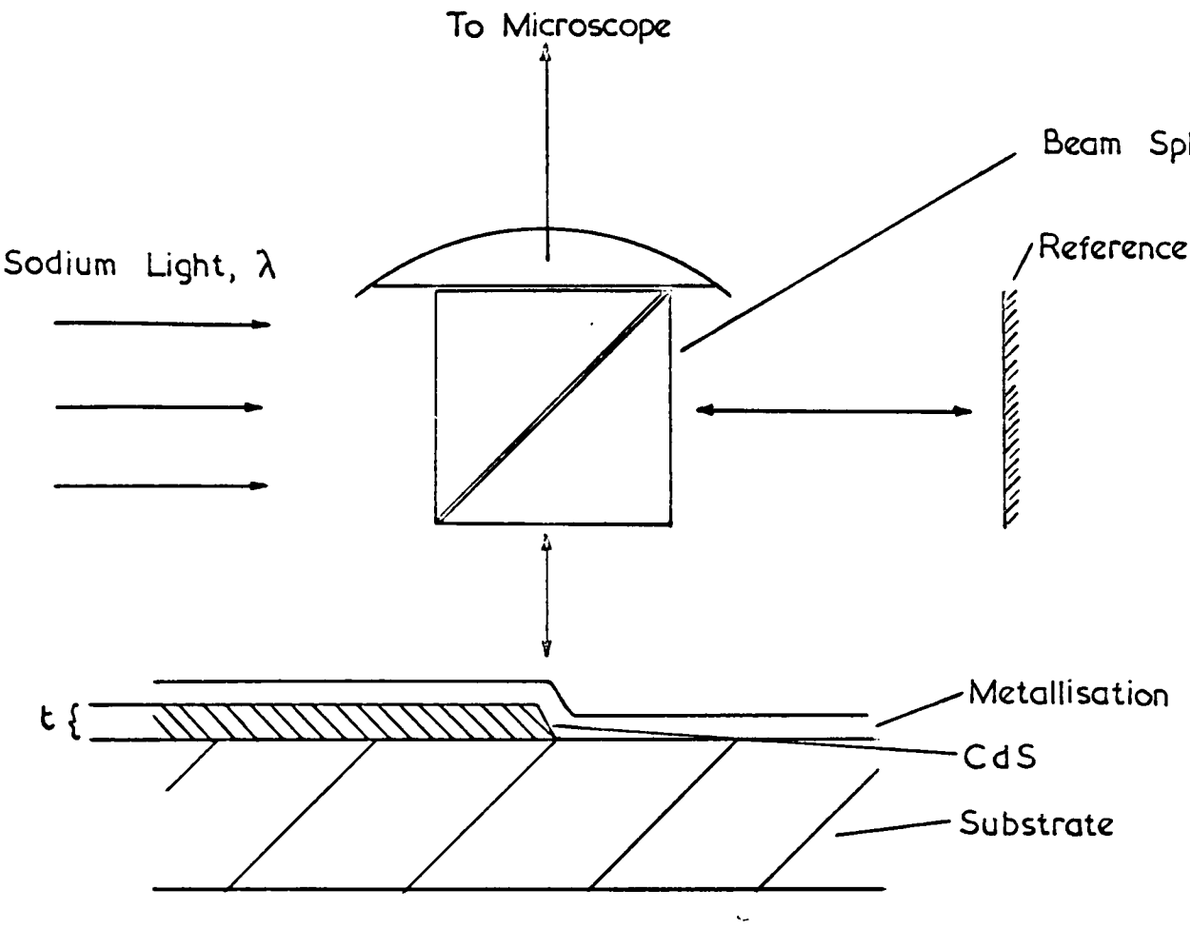


a) Formation of the Fringes.

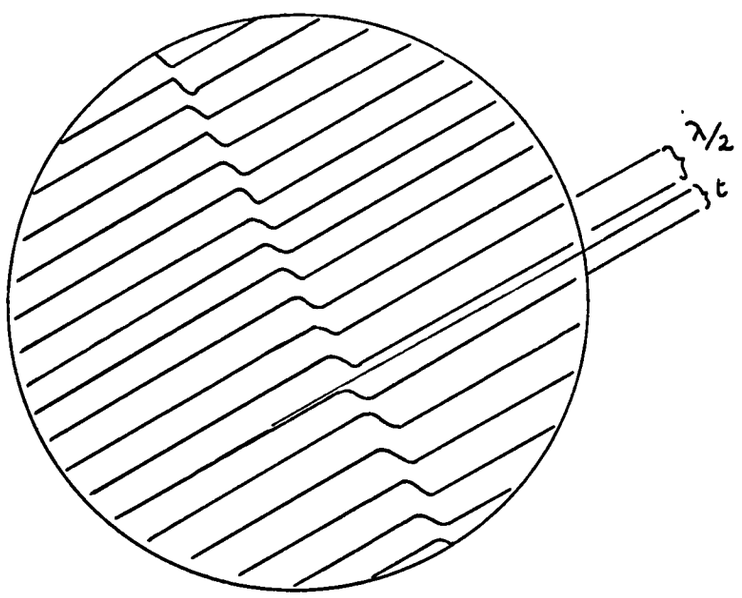


b) Appearance of the Fringes

FIG. 4.5 USE OF THE WATSON INTERFERENCE OBJECTIVE

The thicker films (about 20 microns) prepared at I.R.D. Co. Ltd. could be measured directly using a calibrated microscope stage. This was done by focussing successively on the film and on the adjacent substrate. These values of thickness were checked for some films on glass by optical transmission in the near infra-red, which gave intensity oscillations with wavelength scan. From the separation of these peaks, the film thickness was calculated and found to agree with the previous values.

Chopra (1969) reviews the available methods for film thickness measurement, including those used here.

## 4.6 CONCLUSION

A number of samples were prepared as described above, to characterise the system with respect to film resistivity as a function of deposition parameters. We were especially interested in the conditions required to produce low resistivity films, for use in photovoltaic junctions. The results, together with those obtained from other electrical measurements, will be presented in a later chapter. The importance of a clean system and pure source material will be appreciated from the results of the structural studies made on both CdS and CdSe epitaxial films on single-crystal substrates.

REFERENCES

S. Bateson (1952) Vacuum 2, 365.

K.L. Chopra (1969) "Thin Film Phenomena" (McGraw-Hill).

S.G. Ellis (1968) J. Phys. Chem. Solids 29, 1139-1142.

L.B. Harris (1969) J. Phys. E, 2, 432-433.

L. Holland (1958) B.J.A.P. 9, 410.

L. Holland (1966) "The Properties of Glass Surfaces" (Chapman and Hall).

P.G. Martin (1970) Thesis, University of Durham.

T. Putner (1959) B.J.A.P. 10, 332.

A.N. Rushby and J. Woods (1970) J. Phys. E, 3, 726.

# CHAPTER 5 : STRUCTURAL PROPERTIES OF THE CdS FILMS

## 5.1 POLYCRYSTALLINE LAYERS

5.1.1 Reflection electron microscopy (using a JEOL JEM 120 microscope, AD3 attachment and charge neutraliser), and Laue back-reflection X-ray photographs (using a Philips PW 1003 X-ray generator and PW 1030 flat-plate camera), of CdS films in situ on amorphous substrates have shown that they were polycrystalline and hexagonal structured regardless of substrate temperature, deposition rate, or film thickness. However, all films of more than a certain thickness tended towards one degree of preferential orientation, in which the individual microcrystallite c-axes were nearly aligned perpendicular to the substrate surface. This critical thickness was found to be dependent on the growth conditions of the film.

Values for the spread in angle between the c-axes and the normal to the CdS film, the misorientation angle, were obtained by measuring the angular length of the dense arcs on glancing angle X-ray photographs, obtained as shown in Figure 5.1. The optical density of such arcs gradually decreased towards each end, indicating that the distribution of c-axes within this angle was not uniform but 'bell-shaped'.

In addition to the arcs, the diffraction patterns contained radial streaks originating from the white radiation of the X-ray source which was not completely removed by the Ni filter in the type of monochromator installed. (Since these streaks showed the same preferential orientation as the arcs, some difficulty was experienced in measuring the radial line width whenever overlapping occurred).

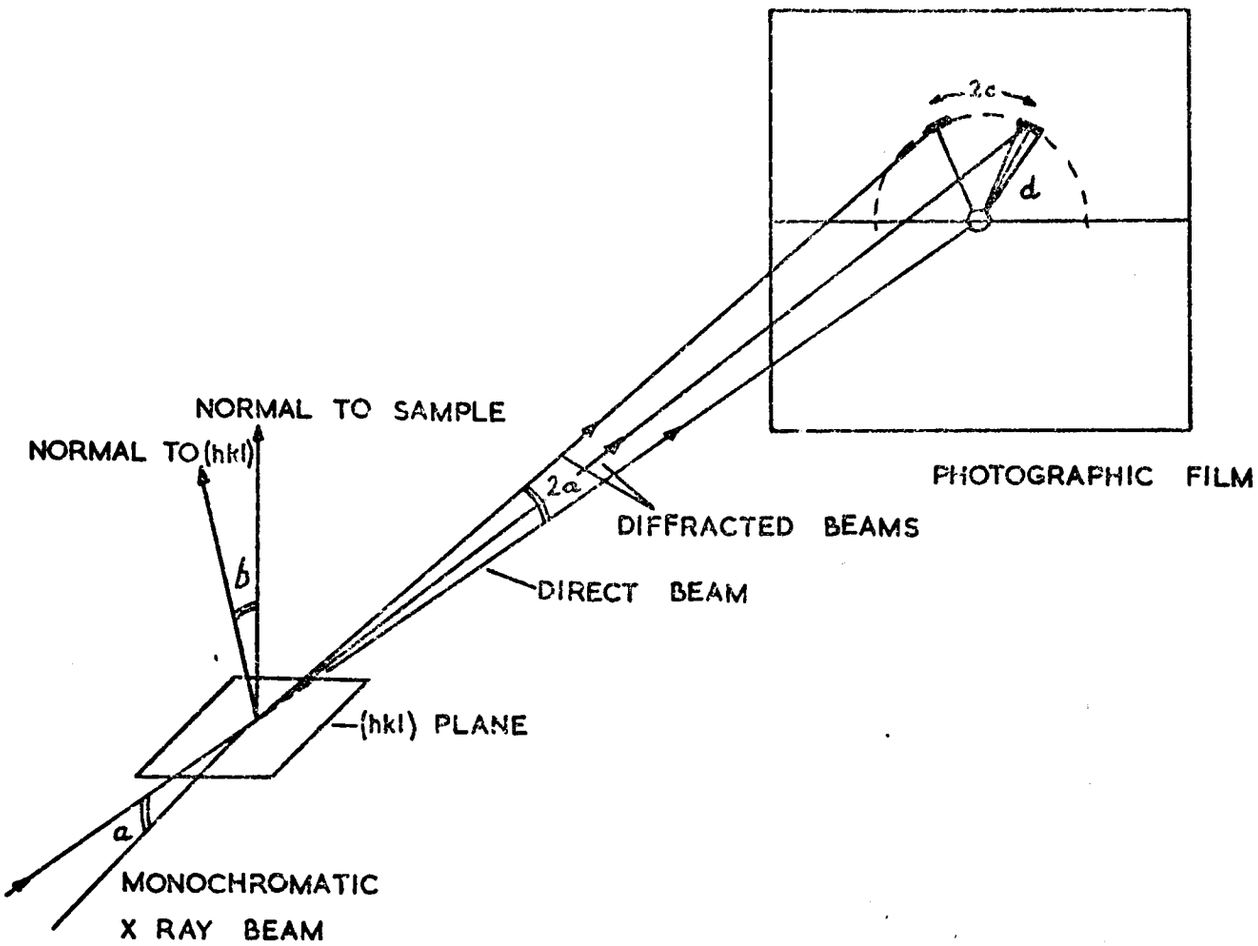


$\angle a$ = BEAM INCIDENT ANGLE ON (hkl)

$\angle d$ = ANGLE OF DEVIATION OF PLANE NORMALS

$$\cos c \approx \frac{\cos b}{\cos a}$$

$\therefore \angle c = \angle b$ for small $\angle a$

FIG. 5·1 PRODUCTION OF GLANCING-ANGLE X-RAY PATTERNS.

The misorientation angle was measured for a number of films deposited on glass substrates at 220°C at three different rates, covering the range of thickness from 1000 to 40,000 Å. The resulting plots of angle against film thickness are shown in Figure 5.2. From these curves it can be seen that for the thicknesses of CdS commonly employed in the solar cell device (i.e. about 20 microns), the c-axes will be closely aligned with the substrate normal. Measurements on 20 micron thick CdS layers on metallised Kapton, and examination of cross-sections of devices, confirm that columnar crystallites extend across the CdS layers. At the other extreme, thin films a few hundred angstroms thick are seen to be nearly randomly orientated, irrespective of the conditions of preparation. This confirms the earlier report by Addiss (1963).

Slow deposition rates, obtained by using lower source temperatures, yield better orientated films than fast rates. From the few measurements made on films deposited on substrates held at low temperatures it can be concluded that the preferential alignment increases with decreasing substrate temperature to at least 150°C. The early saturation of the 350-400 Å/minute curve in Figure 5.2 is a consequence of the substrate temperature increasing with time as the evaporation cycle became longer: for example the temperature of the 2.5 micron film grown at this rate had risen by 40°C to 260°C by the end of the evaporation.

In the next chapter we shall describe somewhat similar variations with thickness of the Hall mobility, electrical resistivity, and photosensitivity. For the present it should

FIG. 5·2 C-AXIS MISORIENTATION OF CdS POLYCRYSTALLINE FILMS ON GLASS

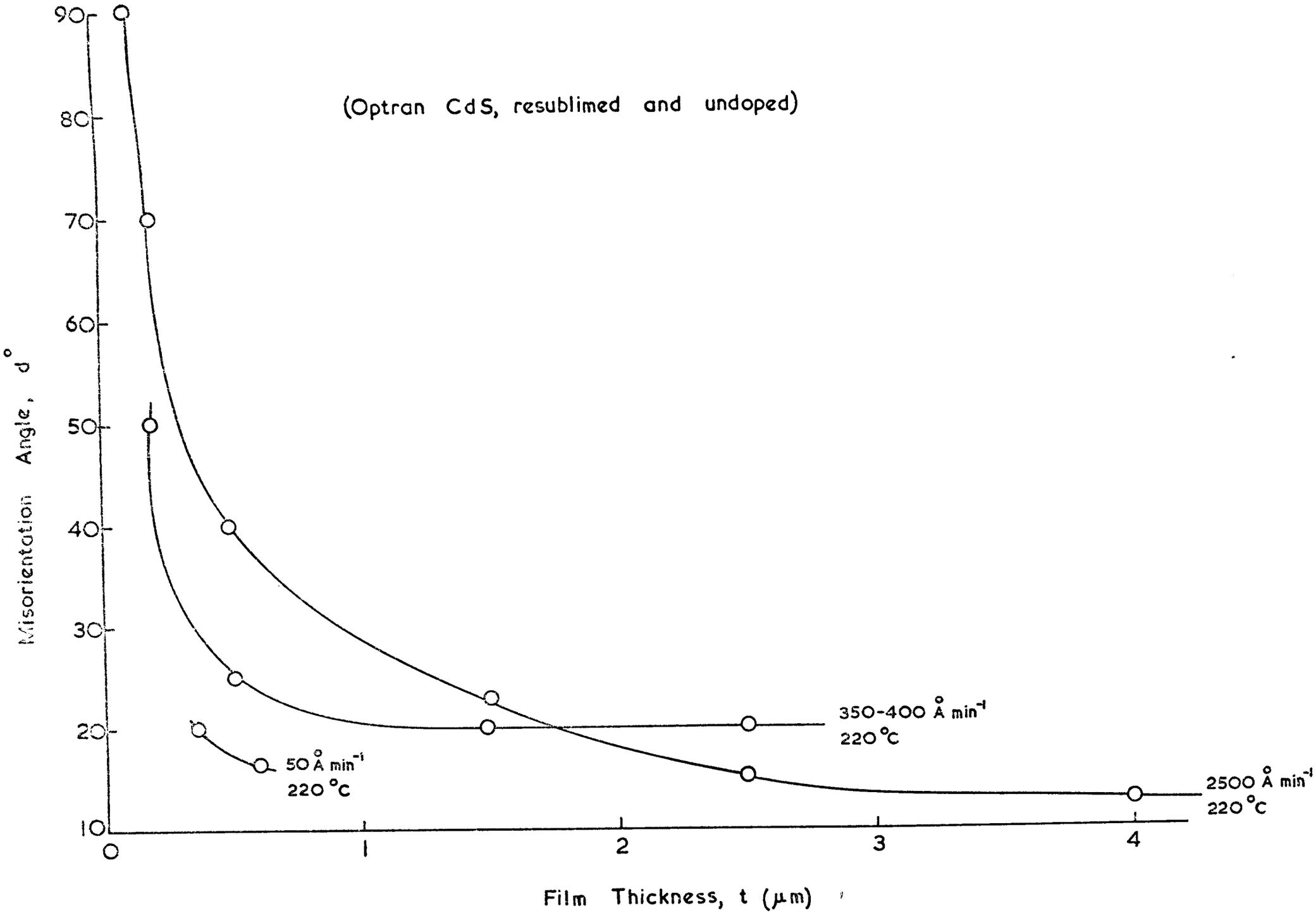

be noted that the thickness of the CdS film is an important parameter unless the film is several microns thick.

5.1.2 The films which have been described so far were all evaporated on glass substrates, and their crystallite size was such that Laue back-reflection photographs consisted of continuous rings with no "spottiness". The following line-width formula, with a structure factor of unity, has been applied to the (002) arcs on both X-ray and reflection electron diffractograms, to obtain an apparent crystallite size for each sample, i.e.

$$d = \lambda / D \cos\theta$$

where $\lambda$ is the X-ray or electron wavelength, D is the angular line-width at half maximum line intensity, and $\theta$ is the Bragg angle.

The crystallite dimension, d, was found to increase ~~almost exponentially~~ with film thickness (Figure 5.3). Although an accurate determination of the actual crystallite size required many corrections to be made to this simple formula, some idea of the magnitudes involved can be obtained from its direct application. The apparent electron grain size is smaller than the X-ray grain size because incident beam-width effects are greater, and it is necessary to subtract the beam-width from the measured line-width. This correction has not been made to the results shown in Figure 5.3. Elastic strain effects in the sample may also be more important in the electron microscopy technique. (See for example Rymer, 1970, pages 71-74).

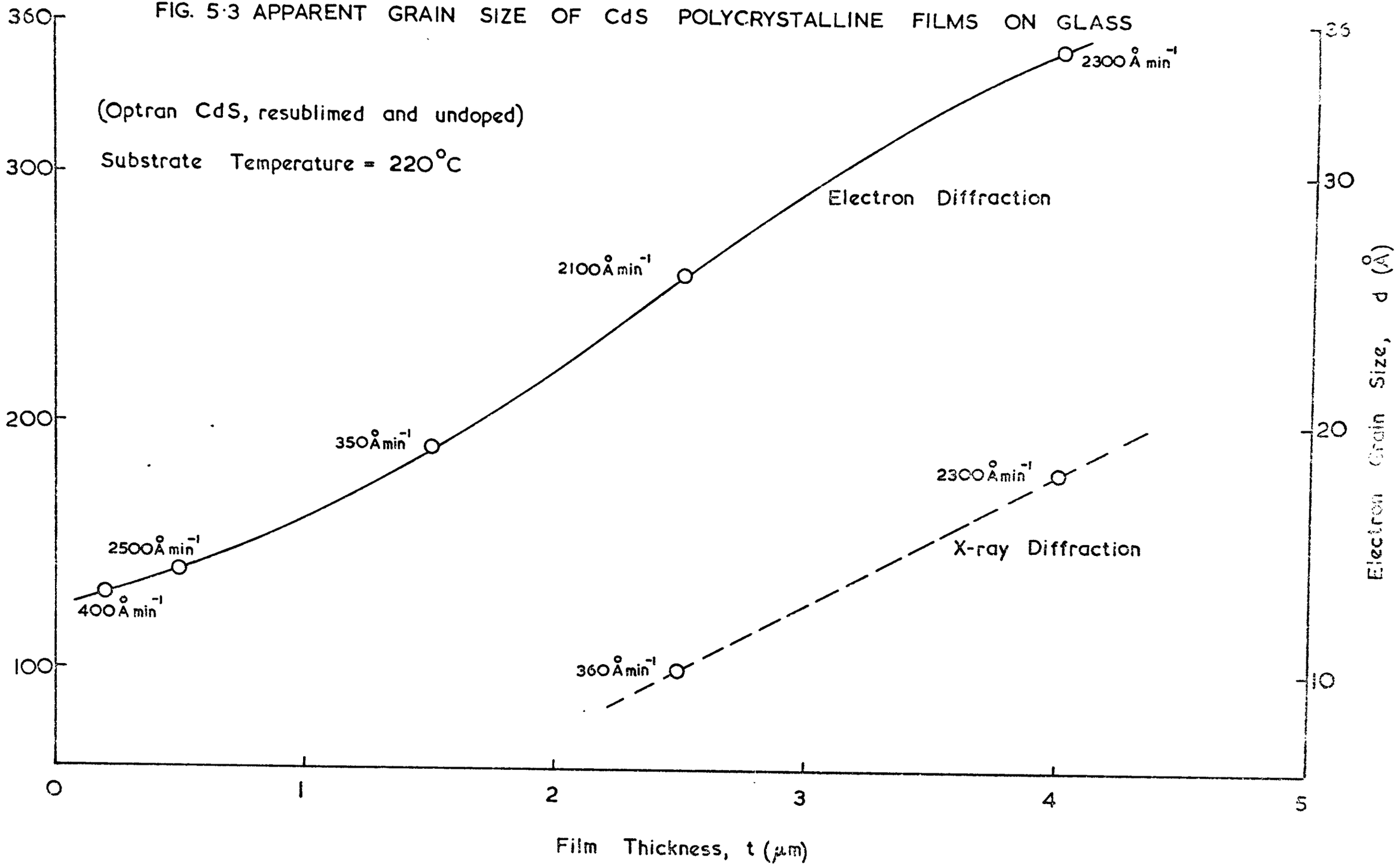
FIG. 5·3 APPARENT GRAIN SIZE OF CdS POLYCRYSTALLINE FILMS ON GLASS
(Optran CdS, resublimed and undoped)
Substrate Temperature = 220°C
Electron Diffraction
X-ray Diffraction
2300 Å min⁻¹
2100 Å min⁻¹
350 Å min⁻¹
2500 Å min⁻¹
400 Å min⁻¹
2300 Å min⁻¹
360 Å min⁻¹
360
300
200
100
0
1
2
3
4
5
40
30
20
10
Film Thickness, t (μm)
Electron Grain Size, d (Å)

More importantly it appears that the crystallite size is not primarily a function of the deposition rate since points obtained from two series of films deposited at widely different rates lie on the same curve.

The absence of information for the thinner films on the X-ray size curve is due directly to the difficulty of obtaining a clear arc in the radial direction from such thin samples. The general blackening, and streaks already mentioned, towards the centre of the photographic film made microphotometer traces very difficult to obtain, even when a CdS photocell was installed on the Hilger and Watts L 450 instrument.

A selection of the reflection electron diffraction patterns is shown in Figure 5.4. These indicate the increasing orientation of the fibre axis of these films as the thickness was increased.

In summary it can be said that these results confirm and extend those produced by Shallcross (1966).

## 5.2 EPITAXIAL LAYERS

5.2.1 Films deposited under the correct conditions on (111) faces of $BaF_2$, and on (110) or (100) NaCl cleaved faces, were found to be epitaxial when stripped from their substrates in water and examined by transmission electron microscopy. The films on (100) or (110) NaCl substrates possessed the cubic (sphalerite) structure, whilst those on (111) $BaF_2$ were hexagonal (wurtzite). Most of the work to be reported was performed on (100) cubic layers.

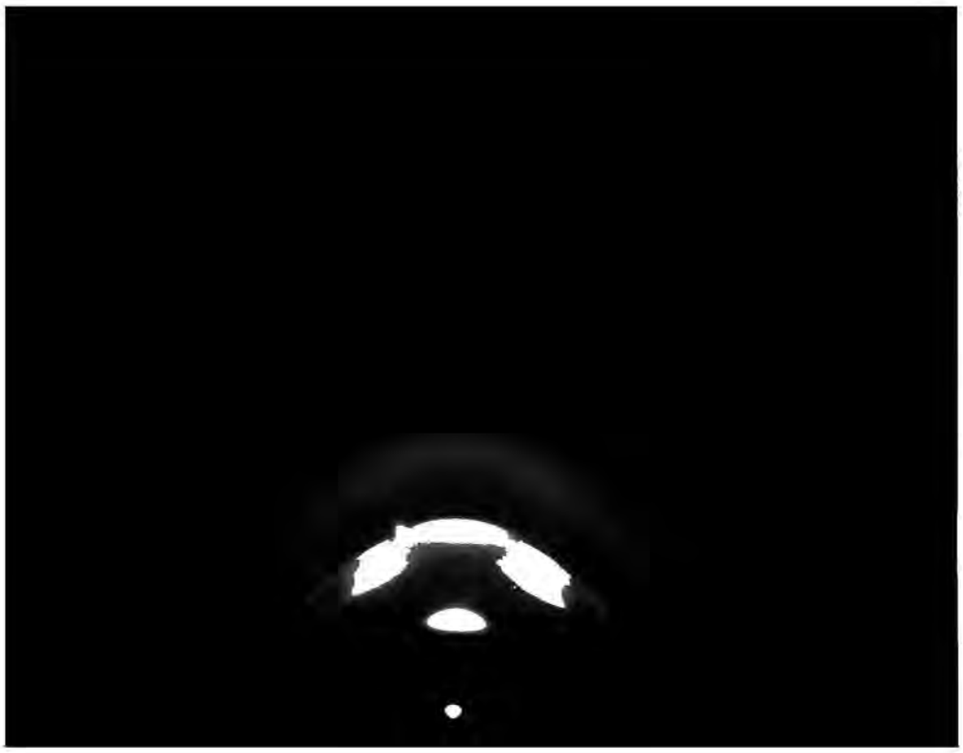

Fig.5.4(a) Film Thickness = 2,000Å

Fig.5.4(b) Film Thickness = 15,000Å

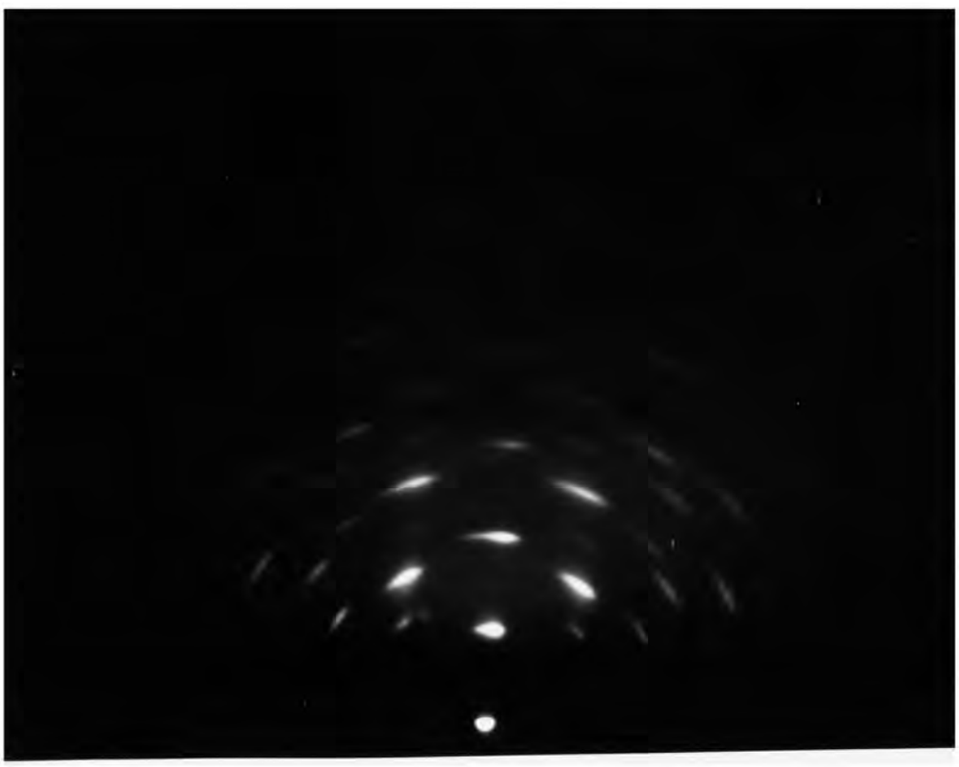

Fig.5.4(c) Film Thickness = 40,000Å

In order to eliminate the complications and unknown factors introduced by the use of a thinning technique to obtain adequate electron transmission, the samples were all less than 2000 Å thick, which was well within the poorly-orientated region for films grown on amorphous substrates.

A few of the films on NaCl tended to wrinkle on the substrate when removed from the vacuum chamber. This is thought to be due to the formation of a moisture-sensitive layer of cadmium chloride between substrate and CdS by the preferential evaporation of contaminating chlorine compounds from the source. (See Chapter 6 for some comments on the source purity). Relaxation initiated by misfit dislocations would have occurred during the cooling period before exposure to the atmosphere and may therefore be excluded as a cause of this phenomenon.

5.2.2 It was difficult but possible to grow good epitaxial films on (100) NaCl substrates cleaved in air, by the evaporation of CdS from the resistively-heated crucible. Success was achieved by employing deposition rates as low as 5 Å/minute on substrates at temperatures of more than 180°C. Higher rates, of up to 180 Å/minute, produced increasingly poorer films. Transmission electron diffraction patterns from these films began to show polycrystalline regions between adjacent (100) regions which were rotated with respect to one another.

By raising the substrate temperature to over 200°C, large epitaxial layers could be obtained with deposition rates of up to 70 Å/minute. If the substrate temperature was below 180°C, then regardless of the deposition rate

the films were ~~equally or~~ predominantly polycrystalline according to the exact temperature.

The electron-beam technique was more successful, allowing a deposition rate of up to 300 Å/minute on a substrate at more than 200°C to produce single-crystal (100) epitaxial films over at least one microscope support-grid spacing (200 x 200 micron$^2$).

There were indications that for films produced by either technique the maximum useful value of the substrate temperature lay at about 300°C. Above this temperature polycrystalline diffraction rings became of equal or greater intensity than the superimposed spot-array characteristic of a single crystal.

When substrates were cleaved in situ in the vapour beam no appreciable improvement in epitaxial quality was apparent. To extract any advantage from this technique, the higher evaporation rates which can be used with the electron-beam method are preferable because the possibility of contamination of the clean surface is then reduced.

5.2.3 Selected-area transmission electron diffraction patterns from the good quality epitaxial films were arrays of spots, uniform over at least one support-grid spacing, even when the high resolution diffraction stage was employed (see Figure 5.5). Other films gave patterns containing features extraneous to the appropriate pure diffractogram. For instance, the less perfect (100) sphalerite structure films (those prepared near the upper end of the epitaxial conditions stated previously) contained split spots.

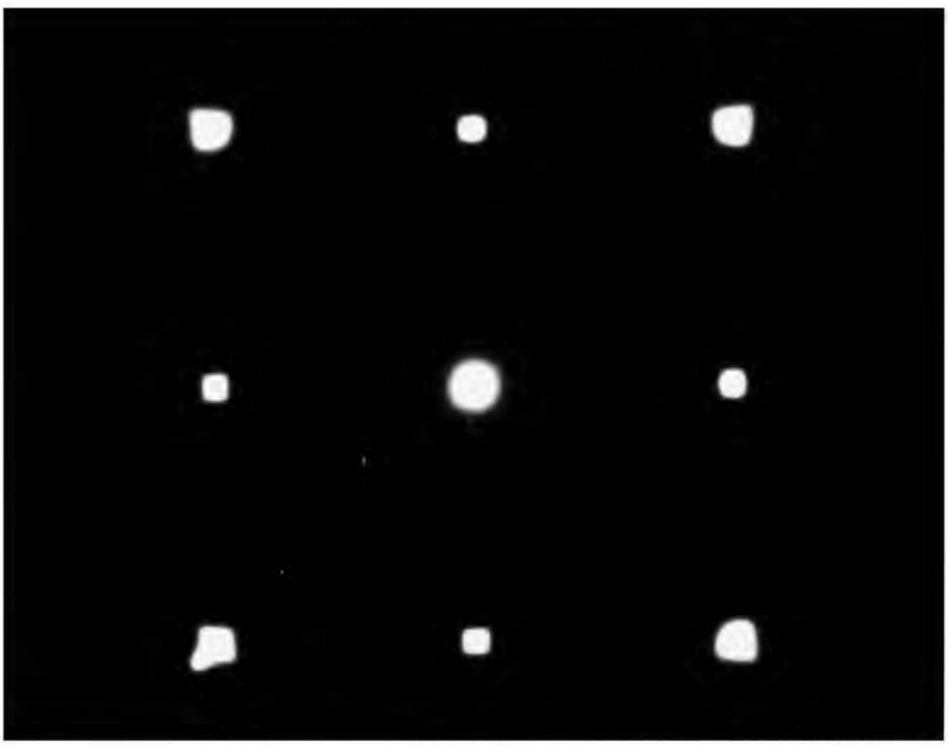

Fig.5.5 (100) Epitaxial CdS

The exact appearance of these patterns is of interest since the presence of extra spots, split spots, and streaking allows deductions to be made concerning the nature of some of the defects in the films. Electron diffraction is not a very sensitive tool for this purpose since two areas will have different contrast on a micrograph if they differ in orientation by a fraction of a degree, whereas a misorientation of several degrees is necessary to produce two resolved diffraction spots. Therefore one must also employ the techniques of bright-field (BF) and dark-field (DF) microscopy, whilst tilting the specimen to new orientations, if a complete identification of the structural defects is to be made.

The defects expected in a II-VI compound film include those listed below:

(a) point defects, e.g. vacancies, interstitials, impurities, and aggregatesof these;

(b) dislocation lines and networks;

(c) grain boundaries and twins;

(d) planar defects such as stacking faults, polytypes, and microtwins;

(e) phase transformations.

The last two groups are started by stacking disorders in which the usual sequence of atomic planes is interrupted in various ways. Since they are so similar, these defects have caused much controversy as to the effect they each have on the electron diffraction patterns, and recognition of them from diffractograms is not straightforward.

The split spots observed on some sphalerite (100) electron diffraction patterns from II-VI films have their origin in twinning, or in included grains of wurtzite structure material, or in planar defects. Holt and coworkers (Woodcock and Holt 1969, Wilcox and Holt 1969, Holt and Wilcox 1971) strongly support the presence of included wurtzite grains in thin films of sphalerite ZnS and CdS, whereas Rawlins (1970) stated that the extra feature in his electron diffraction patterns from ZnS on Si could be totally explained by twinning and double diffraction. The two theoretical (100) diffraction patterns for sphalerite structure compounds with either twinning or included hexagonal phase material are the same as those published by Pashley and Stowell (1963) for fcc (100) epitaxial gold films. (In fact they supported the existence of twinning in their samples).

Planar defects, if present in large numbers, may give rise to streaks between the principal diffraction spots. Such streaks have been observed in the present study of (110) cubic films of CdS and CdSe. Unfortunately, streaking can also be produced by thermal lattice disorder or by strain, and once again the specimen must be tilted to eliminate two of these possibilities. Planar defects may also give rise to pseudo-splitting or diffraction spots, but tilting the specimen in the microscope enables one to distinguish between this and the two other causes of spot-splitting, for diffraction from planar defects is strongly orientation-dependent.

Finally, the remaining types of defects such as dislocation lines and loops may be directly visible at high magnification on a micrograph.

5.2.4 We shall now describe the results of the present investigation of the defects in epitaxial CdS layers, on the basis of the discussion in the preceding section.

The best of the (100) films deposited from the resistance-heated source contained partial streaks in the (110) directions between the principal diffraction spots from some areas. These short streaks, or pseudo-split-spots, moved away from one spot to merge with next in the row as the sample was tilted, the appropriate direction of movement being selected by the direction of tilt (see Figure 5.6). This indicates that there were planar defects present, which produced diffraction spikes perpendicular to their plane. These spikes were then intersected at various points by the Ewald sphere according to the specimen orientation. Continuous streaks between the principal spots in the (111) direction were observed for cubic (110) - orientated films, and these vanished together with the principal spots when the specimen was tilted, without showing intensity maxima at any point along the streaks. It is deduced that the planar defects must lie on the (111) planes. (See also the appendix on CdSe layers).

The films deposited at the higher rates of around 90 Å/minute from the resistance-heated source gave (100) diffraction patterns with extra spots. The appearance of these patterns was similar to that of the pseudo-split-spot

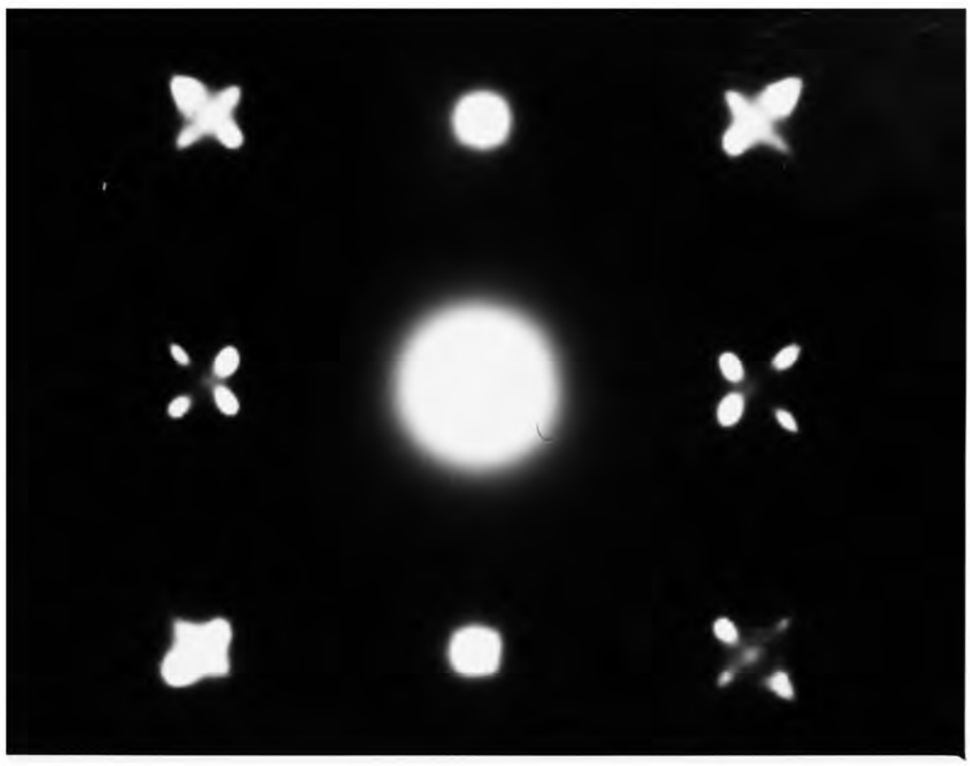

Fig.5.6(a) Splitting due to Planar Defects

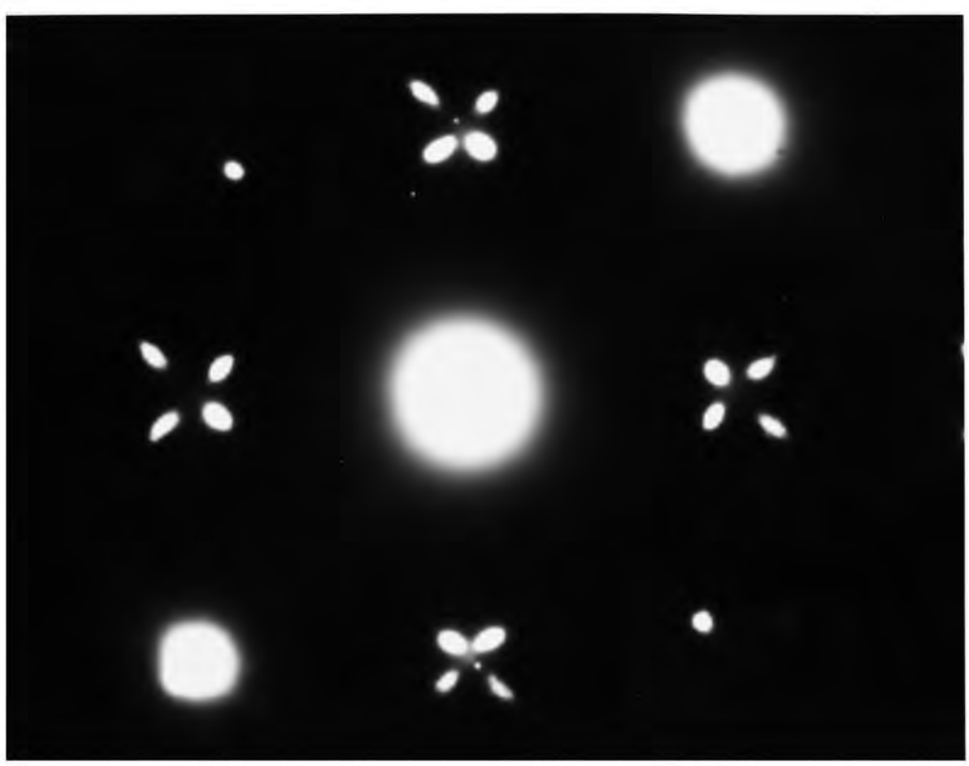

Fig.5.6(b) Splitting due to Planar Defects

patterns just described, but on tilting the specimen the extra spots did not merge with the principal spots. Sample F-13 (deposited at 87 Å/minute on (100) NaCl at 220°C) was one of these films. Both the diffraction pattern and a micrograph of the selected area used to form the pattern are shown in Figure 5.7.

The central ring of twelve spots is seen to be composed of two equal sets of six spots, with a 30° rotation between the two sets. These may be indexed as due to two sets of hexagonal structure planes as shown. Close examination of the micrograph (5,7a) reveals the existence of hexagonal-shaped grains (150-450 Å A.F.) orientated in two positions with respect to the cubic matrix and rotated by 30° from one another. By D.F. imaging each of the extra diffraction spots in turn, the two orientated types of grains were imaged alternately. Thus these cubic films prepared on (100) NaCl faces using a high deposition rate with the resistance-heated source have been observed to contain doubly-positioned grains of hexagonal material with their basal planes parallel to the (100) sphalerite structure planes. Woodcock and Holt (1969) reported a similar diffraction pattern for their ZnS films, but the hexagonal structure grains were shapeless and they deduced that their basal planes were parallel to the (100) cubic surface. Wilcox and Holt (1969) and Holt and Wilcox (1971) also reported that their (100) CdS layers had included hexagonal grains with (0001) planes parallel to the (111) surface.

Woodcock and Holt (1969) have also reported that excess Zn and S in the evaporation source enhanced the

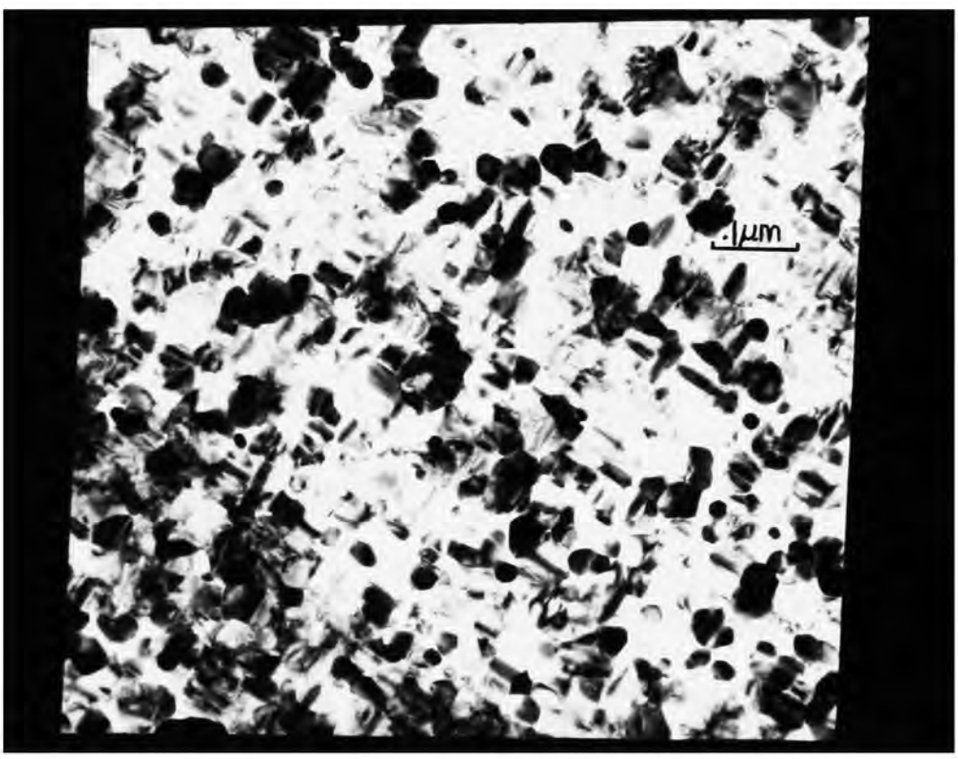


Fig.5.7(a) Selected Area for Diffraction

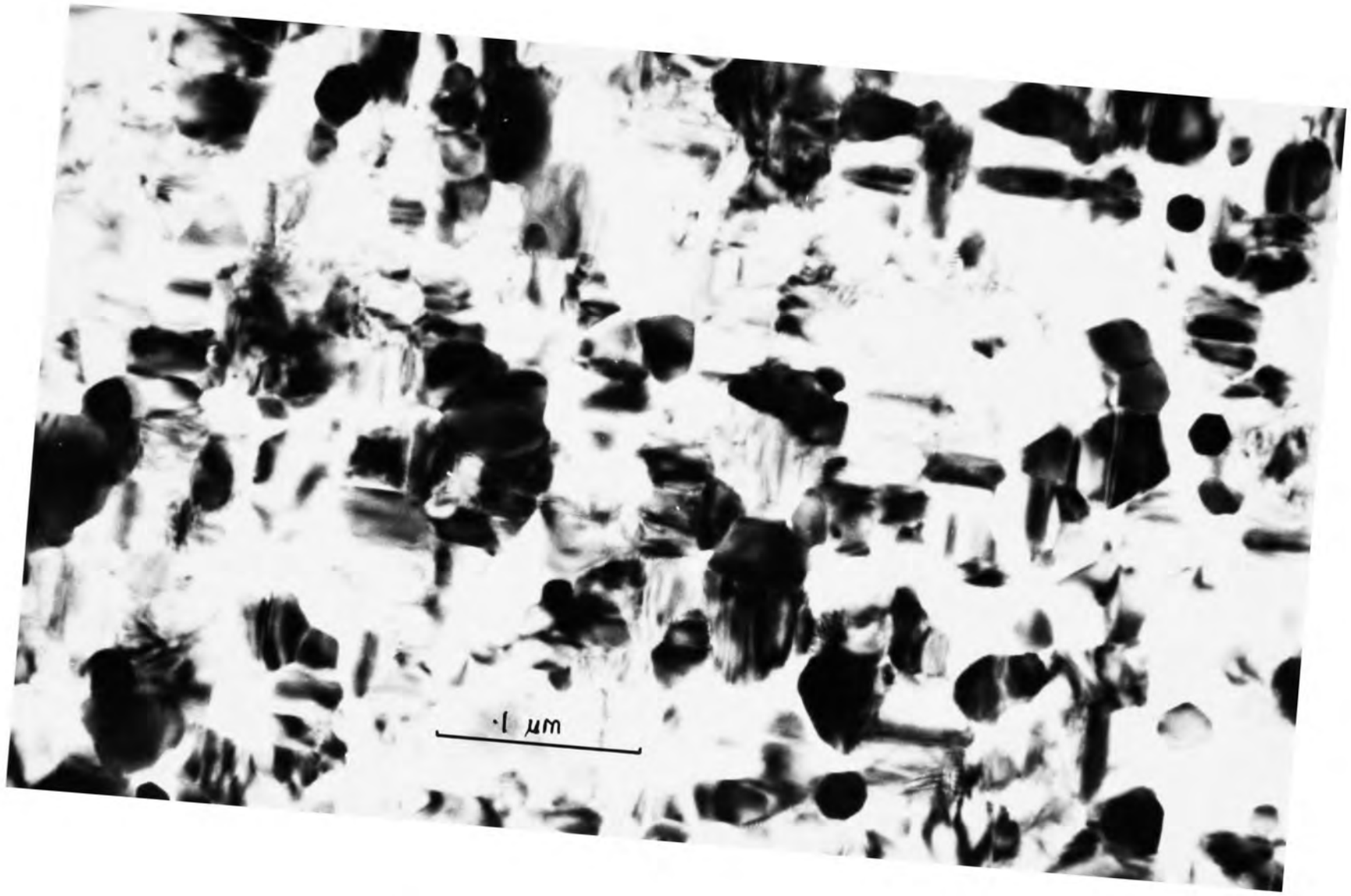


Fig.5.7(a) Detail of Micrograph

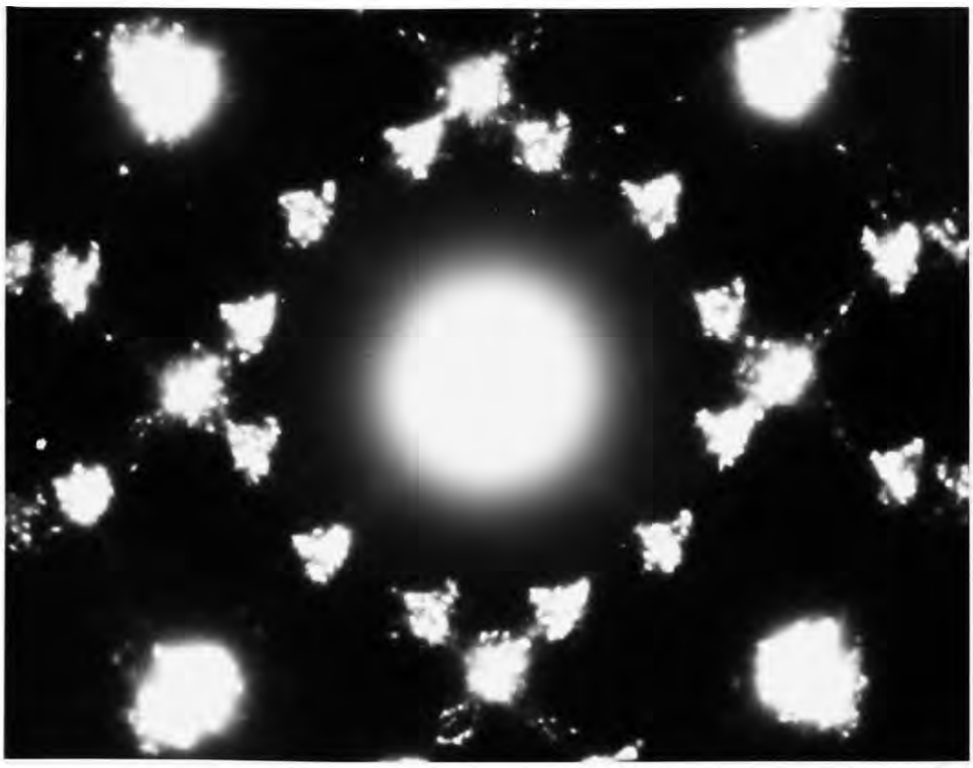

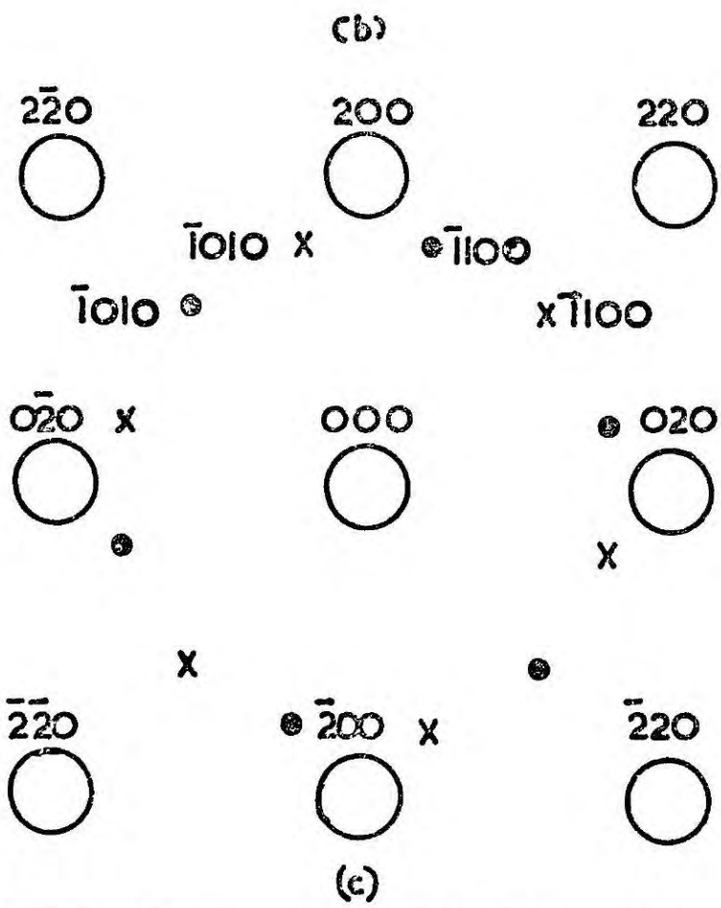


FIG.5.7 DIFFRACTION PATTERN FROM AREA IN (a)

production of included wurtzite grains in their (100) ZnS layers. From the results of the present investigation it is suggested that metal evaporating from the hot filament has contaminated the growing films and has had a similar effect of enhancing hexagonal growth.

The (100) cubic films deposited by electron-beam evaporation were of higher quality than those just discussed, and no evidence of included wurtzite grains or twinning was observed. Pseudo-split-spots were seen from some of these films evaporated at the highest rates (over 300 Å/minute) but were identified as due to planar defects. The exact nature of these defects is difficult to determine and may be either microtwinning or stacking faults. The widespread spot and fringe contrast seen in micrographs with a high density of planar defects is characteristic of such structure, and arises mainly from interference effects between the imaged beams (Holt and Woodcock, 1970). Only some of this contrast is due directly to stacking faults or microtwins or dislocations.

Further examination of many micrographs (for example, those from sample F-13) reveals the existence of stacking faults or microtwins, approximately 60 Å across, within the grains. There are also small arrays of fringes with a separation of about 20 Å, which may be Moire patterns. In the case of these fringes on Figure 5.7(a) the Moire pattern could be formed by overlapping (100) cubic and (0001) hexagonal areas. The Moire separation, M, for no relative rotation between the overlapping areas is given by the following formula:

$$M = \frac{d_1 d_2}{/d_1 - d_2/}$$

where $d_1$ and $d_2$ are the two plane spacings, in this case 5.818 Å and 4.136 Å. This gives a value for M of 14 Å, in close agreement with the measured fringe spacing. If rotation exists between the overlapping grains then a large number of possible d values are available, but the feasibility of Moire fringes being the explanation of this feature has been demonstrated.

Dislocation loops were readily observed from cubic (110) CdSe layers (see Appendix), and from some cubic (110) CdS layers, but were not apparent on (100) layers. Any loops present are therefore likely to be on (110) or (111) planes.

One further type of defect observed in cubic (100) CdS films was that seen in Figure 5.8. This appears on the B.F. micrographs as a dark spot, 300 Å long, surrounded by a grey ring. It has the characteristic appearance of a small precipitate or inclusion parallel to the plane of the film, surrounded by a possible dislocation or strain field (Ashby and Brown, 1963).

Finally, a brief word on the few CdS layers prepared on (111) $BaF_2$ surfaces. These were evaporated from the resistance-heated crucible at a variety of rates up to 200 Å/minute on substrates at 200-300°C. All of the diffraction patterns contained only spots indexed as (0001) wurtzite structure, with no streaking (see Figure 5.9). Neither planar defects nor dislocation loops were observed on the micrographs.

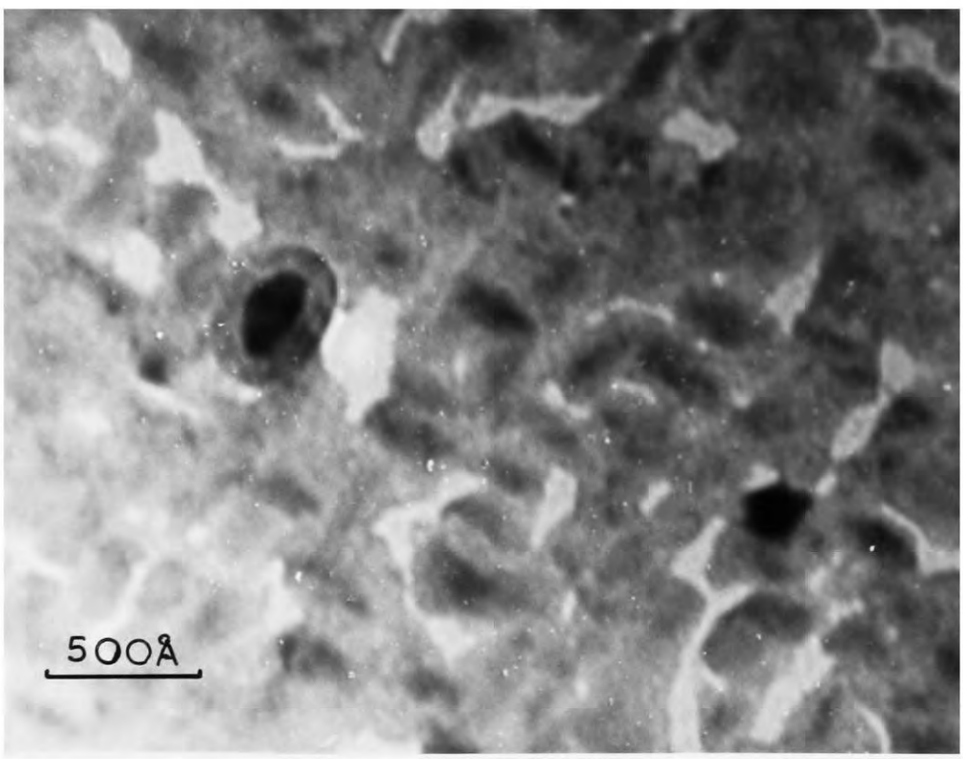


Fig.5.8 Defect in (100) CdS Film

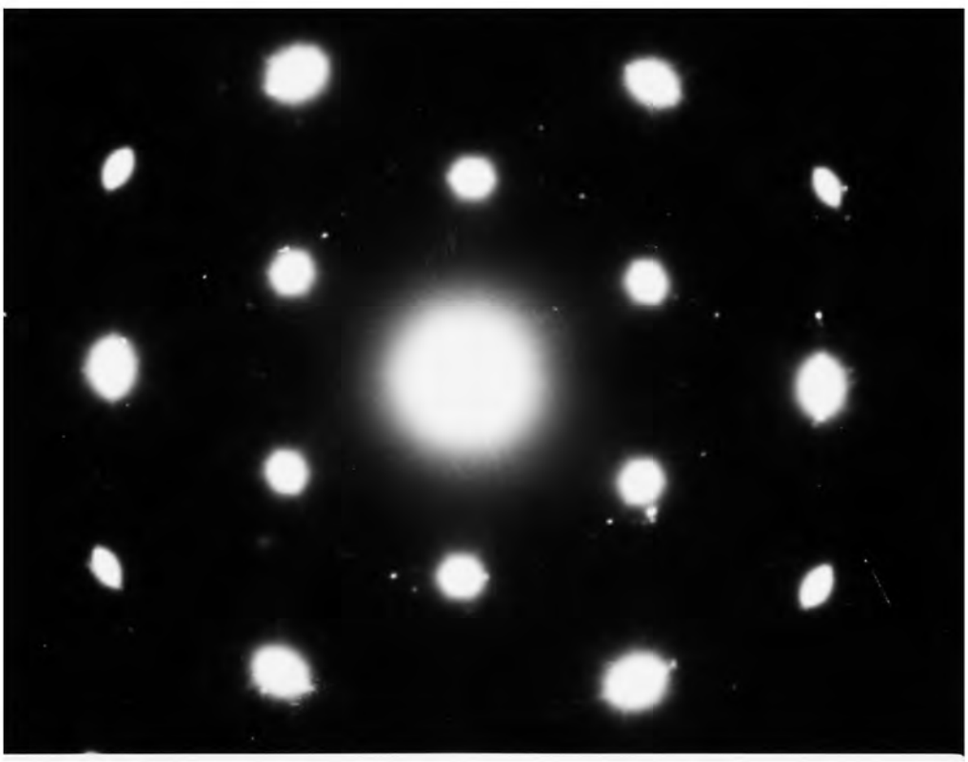

Fig.5.9 (0001) Epitaxial CdS

5.2.5 One electron-beam evaporated film (EG-F-24, 130 Å/minute on (100) NaCl at 225°C) upon re-examination by transmission electron microscopy after storage on a support grid in air for several days was found to have drastically changed its structure. Instead of a nearly featureless micrograph at low magnifications there were bend extinction contours, and much diffraction contrast, including a large number of stacking faults or microtwins, at high magnifications (see Figure 5.10). It was possible to examine the same areas of the specimen as had previously been investigated since shadowing of the NaCl surface features existed at one edge (see Figure 5.11) and acted as a reference mark. Tilting the specimen failed to restore the diffraction pattern to its original (100) orientation, and some regions now gave hexagonal patterns whilst others were polycrystalline. It is suggested that this film was relaxing to the more stable hexagonal (wurtzite) structure because the constraints imposed by the substrate had been removed. This change should be hastened by artificially ageing a film, after removal from its substrate, by annealing at temperatures above 300°C, and this appears to be the case from initial experiments along these lines.

5.2.6 The electrical properties of these epitaxial films were not studied in detail, and so these results will be presented separately here and not in the following chapter. In general the resistivity and photosensitive behaviour were similar to those of the polycrystalline films with respect to the deposition conditions. The dark resistivity was slightly lower than for the corresponding

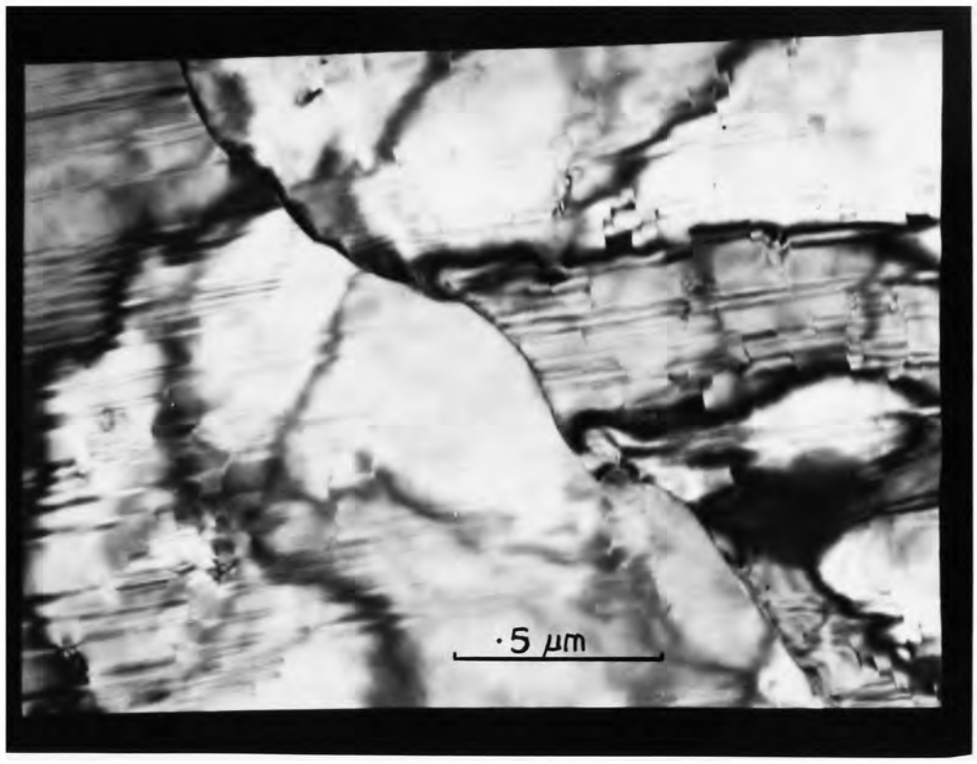


Fig.5.10(a) Selected area for Diffraction

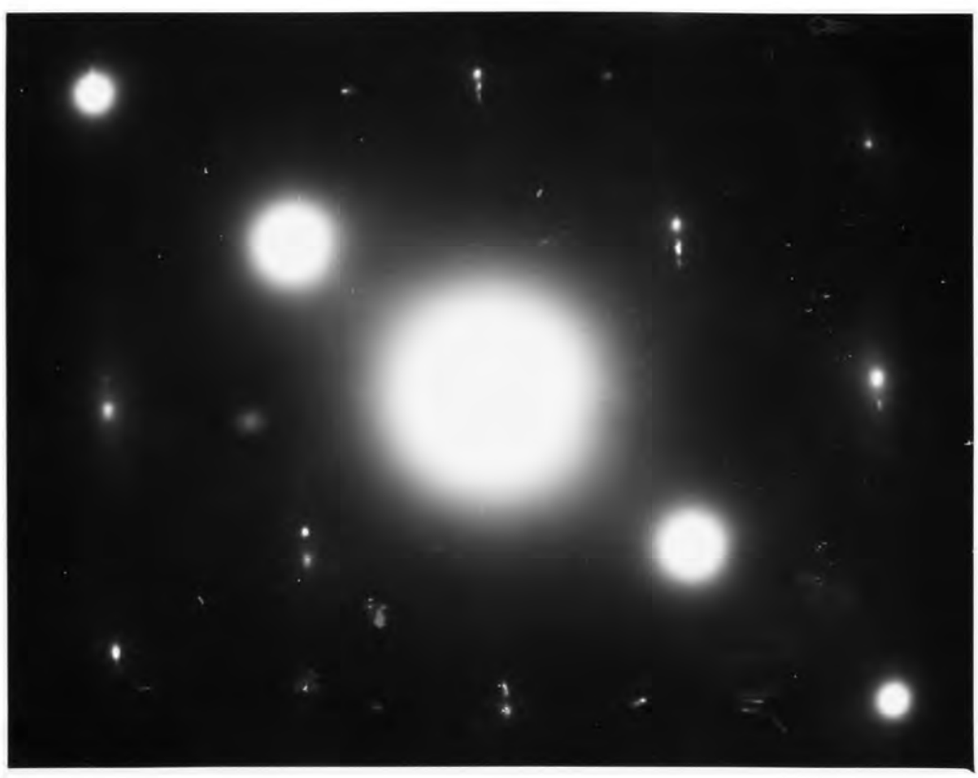

Fig.5.10(b) Diffraction Pattern from (a)

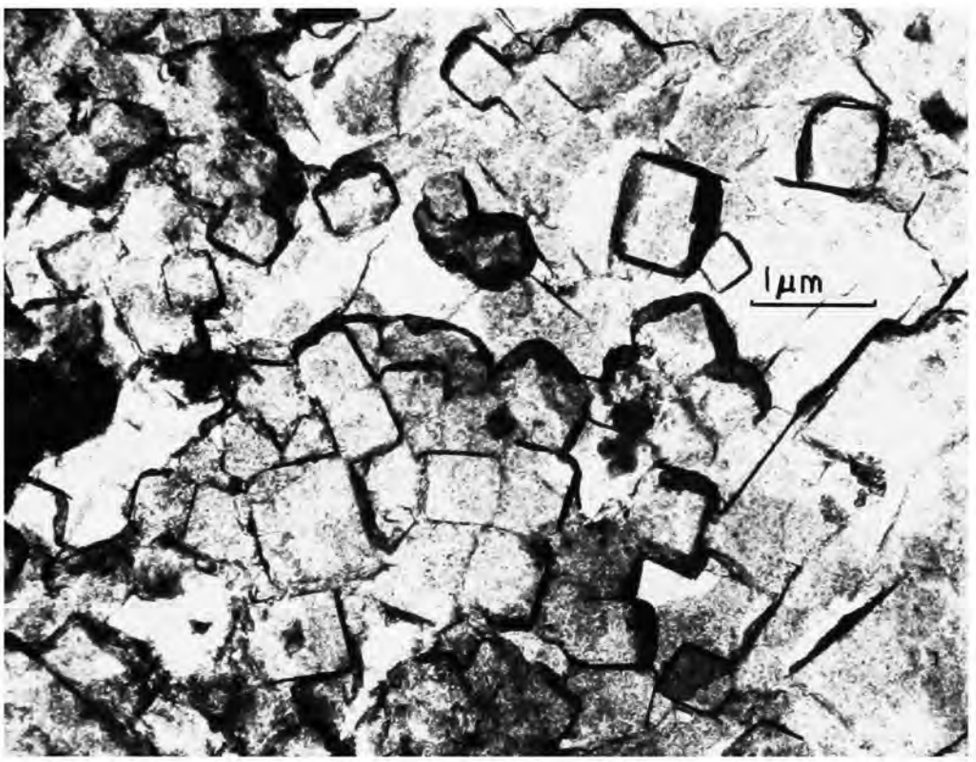


Fig.5.11 Substrate Shadowing by CdS

polycrystalline films, and the photosensitivity and Hall mobility were somewhat higher. (For example a 1000 Å film deposited on to (100) NaCl at 225°C and 290 Å/minute had a Hall mobility of 4 $cm^2V^{-1}S^{-1}$ compared with a value of about 1 $cm^2V^{-1}S^{-1}$ for the equivalent polycrystalline film on glass). This behaviour would be expected from the greater crystalline perfection of these layers.

It is difficult to distinguish between the effects of impurities, defects, and non-stoichiometry on the transport properties, but a few remarks on the relative importance of these can be made in the light of the present results. As will be seen in the next chapter on the electrical properties of the polycrystalline films, an improvement in the cleanliness of the fabrication technique led to higher values of resistivity and photosensitivity; and the purer the source, the better the mobility and reproducibility. The results obtained from the (100) CdSe layers (see Appendix) show that the resistivity is affected by some unrecognised aspect of the structure. The problems of non-stoichiometry will be dealt with after a description of the variation in resistivity produced by varying the film growth conditions.

It should also be stated that none of the epitaxial layers was found to be photoluminescent when excited by a low pressure mercury lamp, even at liquid nitrogen temperatures.

## 5.3 DISCUSSION OF EPITAXIAL LAYERS

Whilst these films are two orders of magnitude thinner than the layers used in the solar cell device,

they are not only intrinsically interesting but also serve as a useful check on the source material purity and process cleanliness. When attempts were made to prepare epitaxial films using untreated Optran CdS no success was achieved: the films were polycrystalline and varied greatly in colour. Chlorine impurity was suspected in some lots of source material from the propensity to wrinkle exhibited by some films on exposure to the atmosphere. The resistance-heated source was shown to be significantly less clean than the electron-beam technique, and indeed, metal contamination from the hot filament was believed to enhance the growth of hexagonal structure material in an otherwise cubic film. The use of a quartz halogen strip lamp in place of a hot tungsten filament for heating the substrates was also found to be cleaner.

Some of the defects in the epitaxial layers were identified and the presence of twinning was not supported. Instead, direct observation of hexagonal-shaped grains was achieved. 'Spot-splitting' was generally found to be due to planar defects, but these were substantially eliminated from the resistance-heated source films by using low evaporation rates and substrate temperatures above 220$^{o}$C. The electron-beam evaporator always gave a low density of planar defects (less than 4 x $10^{10}$ $cm^{-2}$). We have also observed dislocation loops, stacking faults or microtwin contrast, and small inclusions. A possible transition from cubic to hexagonal phase material has been observed in an aged film, and appears to be hastened by an annealing process.

This concludes the structural analysis of the CdS layers, but some further relevant results are given in an Appendix on CdSe films. We shall now turn to a discussion on the electrical properties of the CdS polycrystalline films on glass substrates.

REFERENCES

R.R. Addiss (1963), Trans. Tenth Nat. Vac. Symp. 354-363.

M.F. Ashby and L.M. Brown (1963), Phil. Mag. 8, 1083-1103 and 1649-1676.

D.B. Holt and D.M. Wilcox (1971), J. Cryst. Growth, 9, 193-208.

D.B. Holt and J.M. Woodcock (1970), J. Mat. Sci. 5, 275.

D.W. Pashley and M.J. Stowell (1963), Phil. Mag. 8, 1605-1632.

T.G.R. Rawlins (1970), J. Mat. Sci. 5, 881-890.

T.B. Rymer (1970), "Electron Diffraction" (Methuen and Co. Ltd.)

F.V. Shallcross (1966), Trans. Met. Soc. AIME, 236, 309-313.

D.M. Wilcox and D.B. Holt (1969), J. Mat. Sci. 4, 672-680.

J.M. Woodcock and D.B. Holt (1969), J. Phys. D: Appl. Phys. 2, 775-786.

# CHAPTER 6 : ELECTRICAL PROPERTIES OF THE CdS FILMS

## 6.1 INTRODUCTION

We have observed in Chapter 2 that the electrical resistivity of the CdS layer is an important parameter for the subsequent formation of an efficient photovoltaic junction. It follows that an examination of the conditions required to produce CdS films of suitable resistivity is obviously of major importance. A low resistivity is essential, as has already been described, so that the series resistance of the device is low enough to ensure maximum power extraction, but this must be achieved without departing far from the optimum composition at which a p-n junction can be formed.

In what follows the effects of film thickness, deposition rate, substrate temperature and source purity on the dark resistivity of CdS films on glass substrates are described. The associated photosensitivity and Hall mobility have also been investigated. It will be appreciated that a very large number of samples would be necessary to cover the available wide ranges of parameters (substrate temperature: $20^{\circ}$-$350^{\circ}$C., deposition rate: 10-10,000Å/minute, thickness: up to several microns), so that from practical considerations it was necessary to impose artificial limits on these. This explains the unequal distribution of results, concentrated around a substrate temperature of $220^{\circ}$C., i.e. that most widely used for device fabrication. (One of the few reported large-scale investigations of semiconductor thin film properties was that of Davey et al (1963) into polycrystalline Ge films in which twelve hundred samples were prepared).

## 6.2 APPARATUS

The electrical circuit used for these measurements is shown in Figure 6.1, and a scale drawing of the thin film sample and contacts is shown in Figure 6.2.

The current flowing along the sample was derived from a dry battery and was monitored by a sensitive mirror galvanometer (2400 mm/microamp). An electromagnet produced a field of 5 kG., uniform over the sample area, across a gap of 2 cm. in which the light-tight sample holder was supported. A removable blank in the side of this container enabled the sample to be illuminated if required during the Hall measurements. Non-microphonic coaxial screen cable was used between the sample, meters, and power supplies, since the high resistance of a large number of the samples made the use of an E.I.L. Vibron 33B electrometer essential for the Hall voltage determinations.

In order to off-set the voltage across the Hall probes, which was present in zero magnetic field because of slight contact misalignment, a variable 'backing-off' battery supply was inserted into the Hall voltage circuit.

Since the length to width ratio of the thin films was greater than three, no 'end effect' corrections to the Hall voltage were necessary to compensate for the possible short-circuiting effect of large current contacts observed by Isenberg et al (1948).

For the standard photosensitivity measurements, the illumination was provided by 75 $mW.cm^{-2}$ of unfiltered tungsten lamp radiation, as determined by a calibrated Si photovoltaic cell.

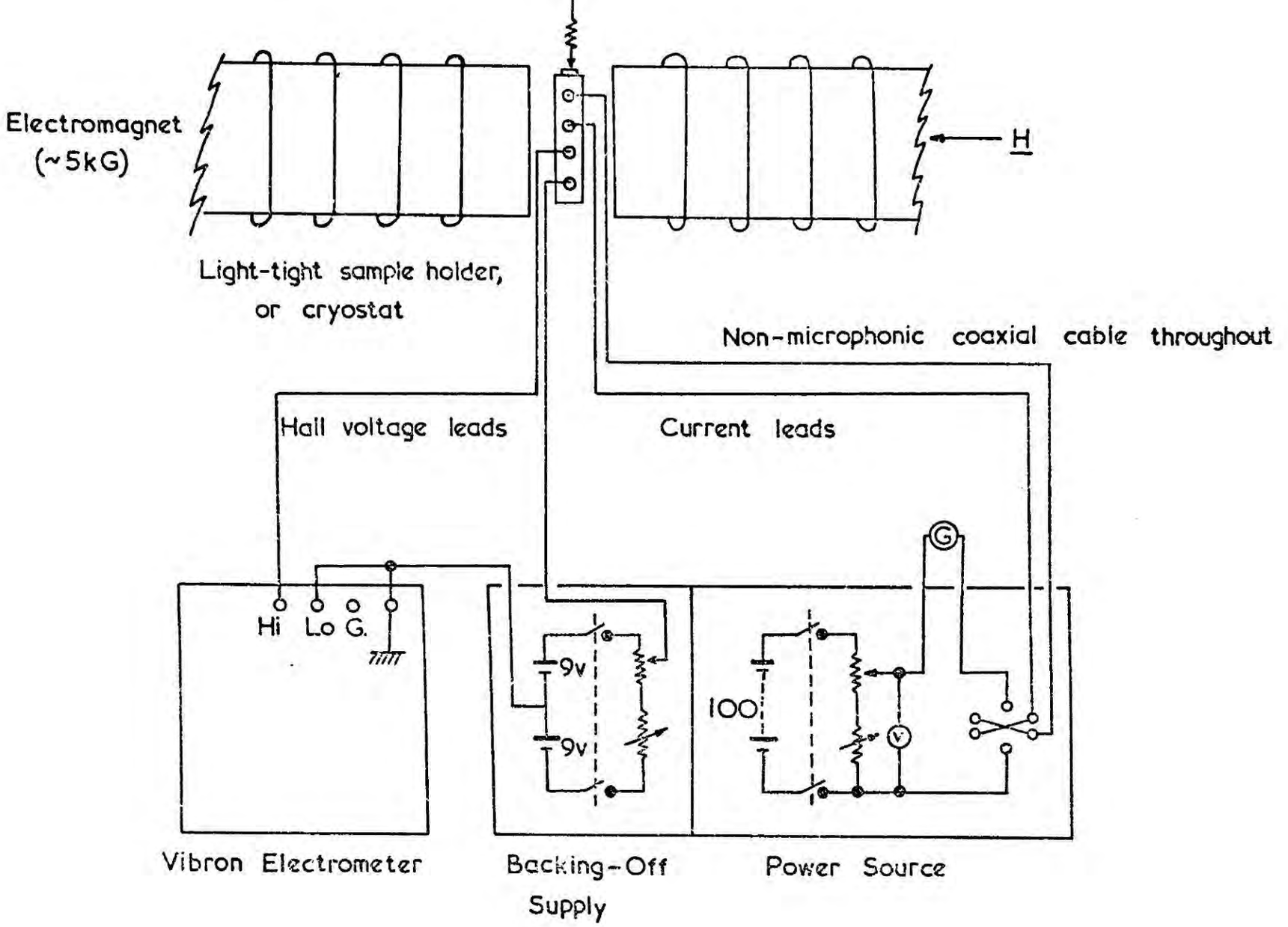


FIG. 6·1 CIRCUIT FOR ELECTRICAL MEASUREMENTS ON THIN FILMS.

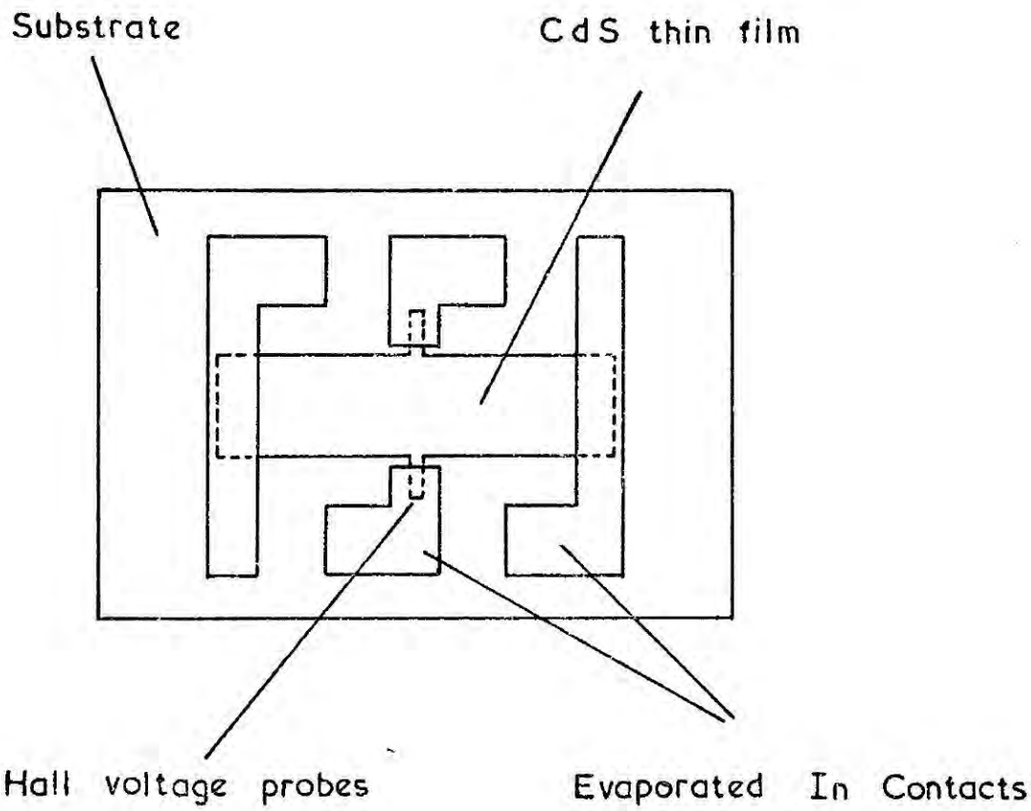


FIG. 6·2 THIN FILM SAMPLE AND ELECTRICAL CONTACTS

## 6.3 CURRENT CHARACTERISTICS

6.3.1 In order to check that the evaporated In contacts were ohmic, a series of I(V) curves with 'forward' and 'reverse' voltages of up to 100 V. were obtained for CdS films prepared under a wide variety of evaporation conditions. These variations in substrate temperature, deposition rate and thickness produced films with resistivities ranging from $6.3 \times 10^{1}$ to $4.5 \times 10^{5}$ ohm cm., as shown in Figure 6.3.

The sample numbers with the prefix EG refer to films produced by electron-beam evaporation. The remaining films were evaporated from the resistively-heated source. Prefix G denotes 7059 glass substrates and J denotes microscope slide substrates. These conventions were used throughout the present work.

It will be seen from the curves of Figure 6.3 that the higher resistivity samples were slightly non-ohmic because In has a less suitable work function for such samples. No differences were discovered on reversing the polarity in any sample. In the lower range of resistivities of present interest the samples were ohmic, but in what follows, values of resistance quoted are those measured at 50 V. This is a suitable voltage to provide a measurable current through the samples without introducing high-field effects.

6.3.2 The effect of illuminating the sample and changing the intensity of the white light with neutral density filters was to produce a non-linear variation of the photocurrent with intensity (see Figure 6.4). In this series of measurements 100% illumination was approximately

FIG. 6·3 Dark I (V) characteristics of polycrystalline CdS films on glass

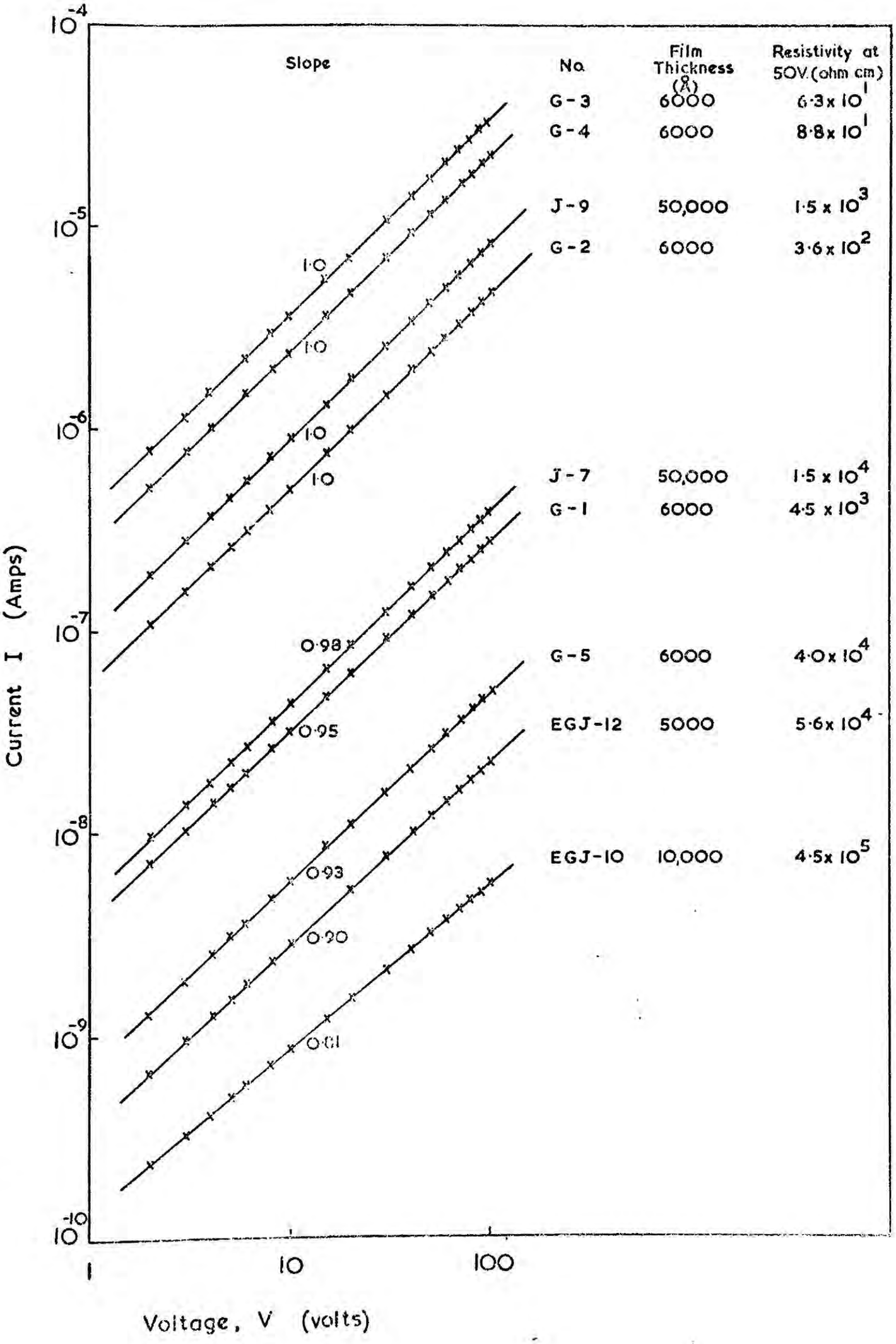

G. 6·4 Photocurrent versus white light intensity for CdS polycrystalline films on (100 % L x am O sunlight)

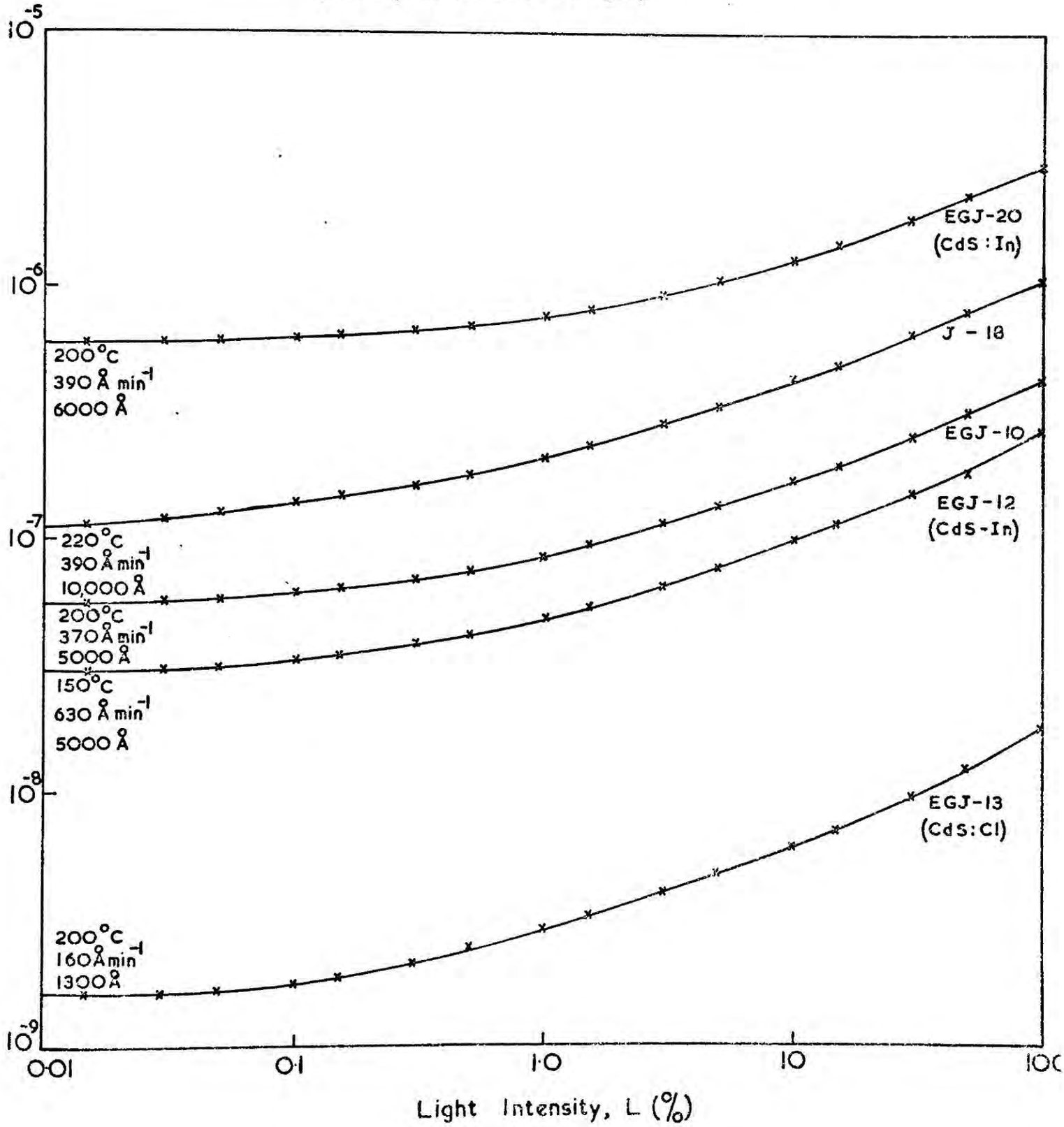

equal to am0 sunlight, and the samples were mounted on a copper heat-sink to maintain isothermal conditions. Three of the samples were produced by evaporating CdS doped with In or Cl, but they behaved in a similar manner to the undoped films.

6.3.3 Figures 6.5 and 6.6 depict the results obtained from a determination of the temperature dependence of the dark current at 50 V. These samples were again prepared under a variety of conditions, and cover the thicknesses 5000 to 50,000 Å. The results are presented in the form of resistivity versus temperature curves, for a range of temperatures limited by the melting point of In and by the temperature of liquid nitrogen. Measurements were performed with the samples in a metal cryostat pumped by a rotary pump to about $10^{-2}$ torr. The temperature was determined using a copper/constantan thermocouple and potentiometer, and a resistance heater coil was used to raise the temperature above ambient. Readings were taken for every 0.5 mV increase in the thermocouple reading. The experimental points are shown only in Figure 6.5, but a similar close fit to smooth curves was obtained for the samples of Figure 6.6.

If the variation of the resistivity with temperature is taken to be of the form:

$$\rho = \rho_o e^{E/kT}$$

(according to the Petritz, 1956, intercrystallite barrier model), then an activation energy of about 0.5 eV can be obtained from the high temperature end of these curves.

6.5 Temperature dependence of dark resistivity for CdS polycrystalline films on 7059 glass.

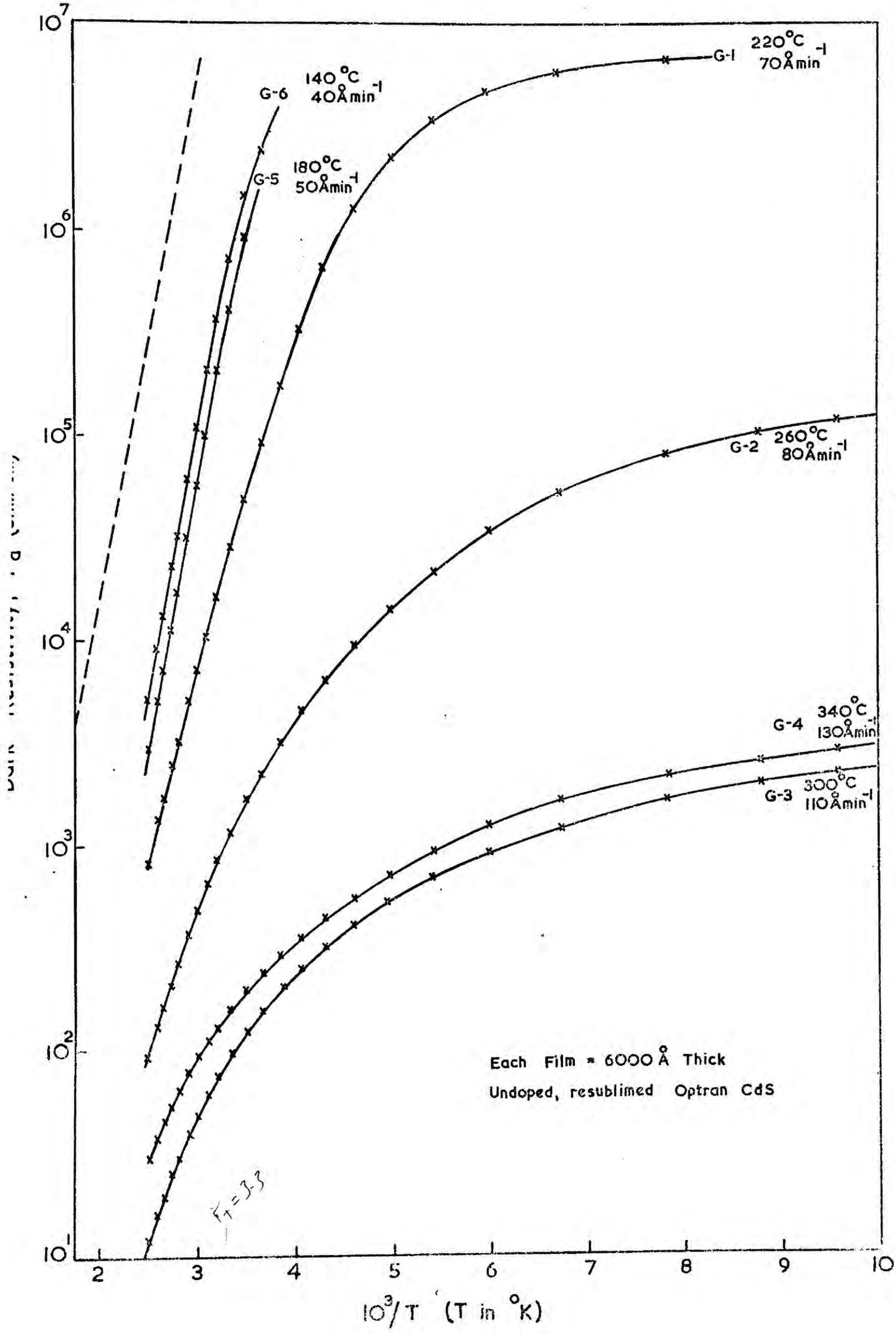

5. 6 Temperature dependence of dark resistivity for CdS polycrystalline films on Pyrex glass.

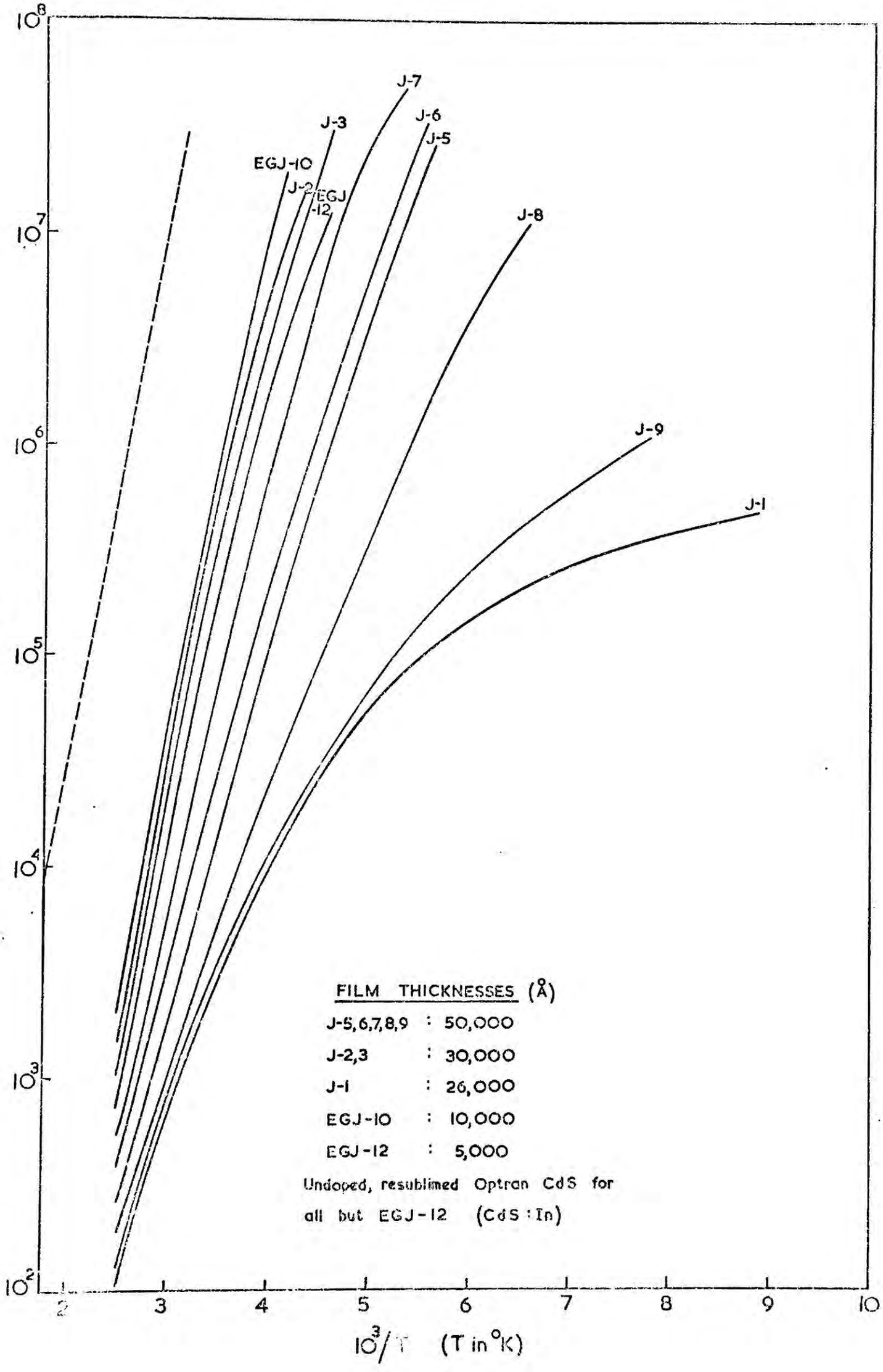

(The broken line on each graph has a slope with this activation energy).

This activation energy is in fact a combination of the exponents involved in the variation of both the carrier density and the mobility with temperature. To this degree of approximation we have:

$$\rho = 1/ne\mu$$

$$\rho = e^{E/kT}/n_o e\mu_o$$

Figure 6.6

| Sample number | Activation energy |
|---|---|
| EG-J-10, J-2, J-3, EG-J-12 (CdS:In), J-7 | 0.50 eV |
| J-6, J-5 | 0.36 eV |
| J-8, J-9, J-1 | 0.29 eV |

Figure 6.5

| Sample number | Activation energy |
|---|---|
| G-6, G-5 | 0.50 eV |
| G-1 | 0.36 eV |
| G-2 | 0.28 eV |
| G-4, G-3 | 0.2 eV |

The experimental values given above for the activation energies of conduction are within the range of those obtained by Shallcross (1966) of 0.22 to 0.66 eV. He found that the major contribution to the activation energy was due to the variation in carrier concentration and that the activation energy of the mobility was only about 0.1 eV.

Both series of films examined here behaved in a similar manner, indicating that films on microscope slides were not significantly worse than those on Corning 7059, barium alumino-silicate alkali-free glass, as far as electrical conduction was concerned.

## 6.4 EFFECTS OF FILM THICKNESS ON ELECTRICAL PARAMETERS

It has been affirmed earlier that the thickness of a film is an important parameter in determining its structure, even for thicknesses up to several microns. There is a parallel and similar dependence of the resistivity, Hall mobility and photosensitivity on film thickness.

6.4.1 Shallcross (1966) indicated that the resistivity of his films might have been dependent on the thickness, but did not pursue this suggestion. Figure 6.7 shows the results obtained from the present investigation, for the two series of films described in Chapter 5. (In both series the films were evaporated on glass at 220°C.; in one series the rate was 2500 Å/minute and in the other 350-400 Å/minute). The sharp initial drop in the curves reflects the increasing degree of preferential orientation which occurs at thicknesses up to 5000 Å, but a further and slower decrease in resistivity then occurs.

Fig. 6·7 Dark Resistivity size effect of CdS polycrystalline films on glass.

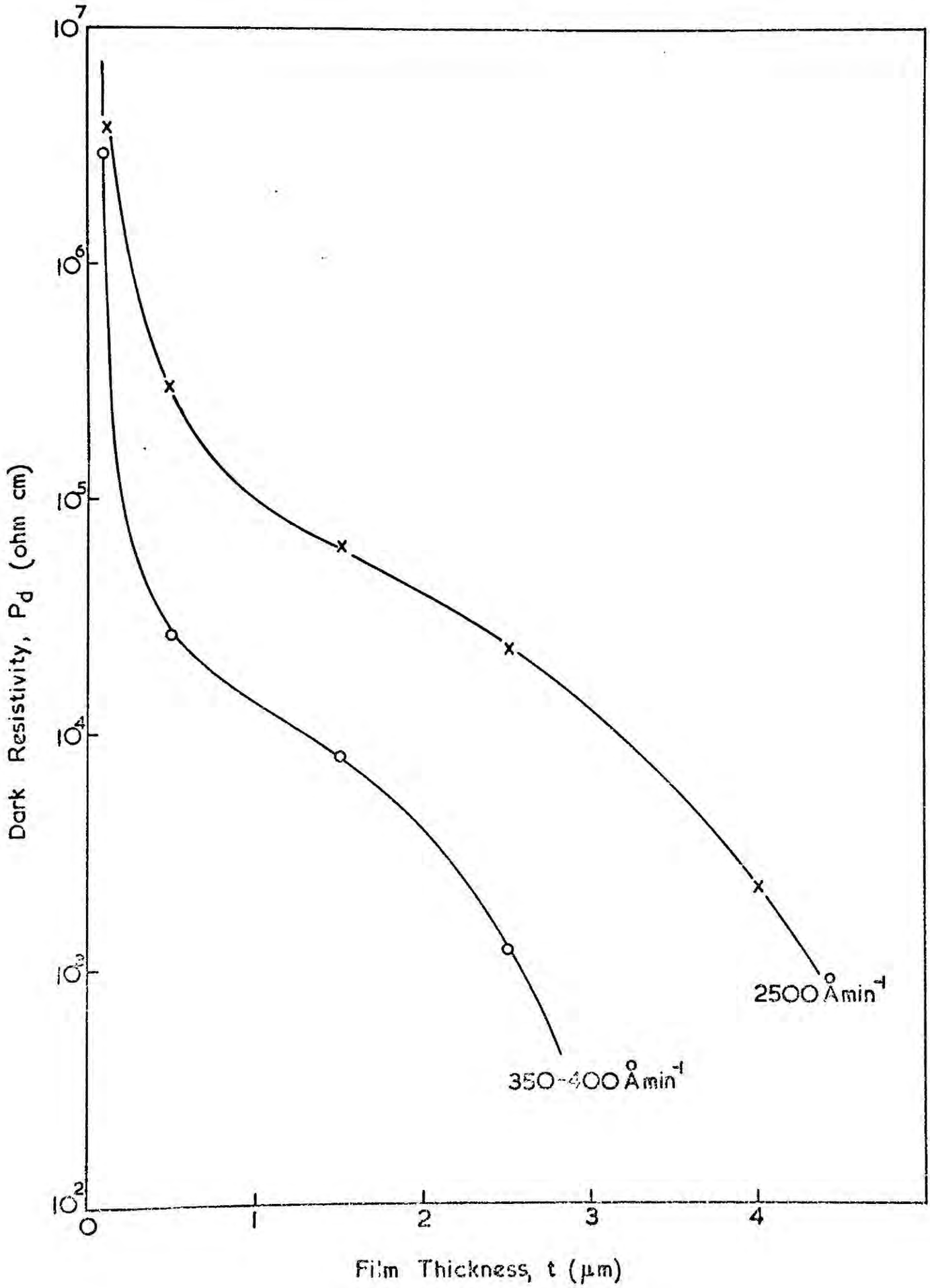

6.4.2 We require to distinguish between changes in mobility and changes in carrier concentration before a model for the conduction processes can be constructed, but first let us examine the change in photosensitivity with thickness, Figure 6.8. Here the photosensitivity is defined as the ratio of the current through the illuminated sample to the current in the dark, with both currents measured at 50 V. There is a close similarity between the curves of Figure 6.8 and those of Figure 5.2, which show the fibre axis orientation, but it appears that at large thicknesses the photosensitivity continued to fall towards unity as the concentration of photoexcited-carriers becomes comparable to the thermal equilibrium concentration. A calculation of the number of carriers created by the light would help to check whether the photosensitivity is associated with photovoltaic effects at the intercrystallite barriers or with bulk excitation of carriers. (See Chapter 8 for some further comments). It was also noticed that the Hall voltage was unaffected by illuminating the sample.

6.4.3. A study of the Hall mobility in these films did not reveal the same dependence on film thickness as that shown by the dark resistivity. In fact the variation observed, see Figure 6.9, can be closely explained by a simple model of diffuse scattering at the surfaces, using a flat band approximation, according to which:

$$\mu = \mu_K (1 - 2\lambda/t) \quad \text{(Fleitner, 1961)}$$

Here $\mu_K$ is the bulk mobility, including the effects of grain boundary and impurity scattering, t is the film

FIG. 6·8 Photosensitivity size effect of CdS polycrystalline films on glass.

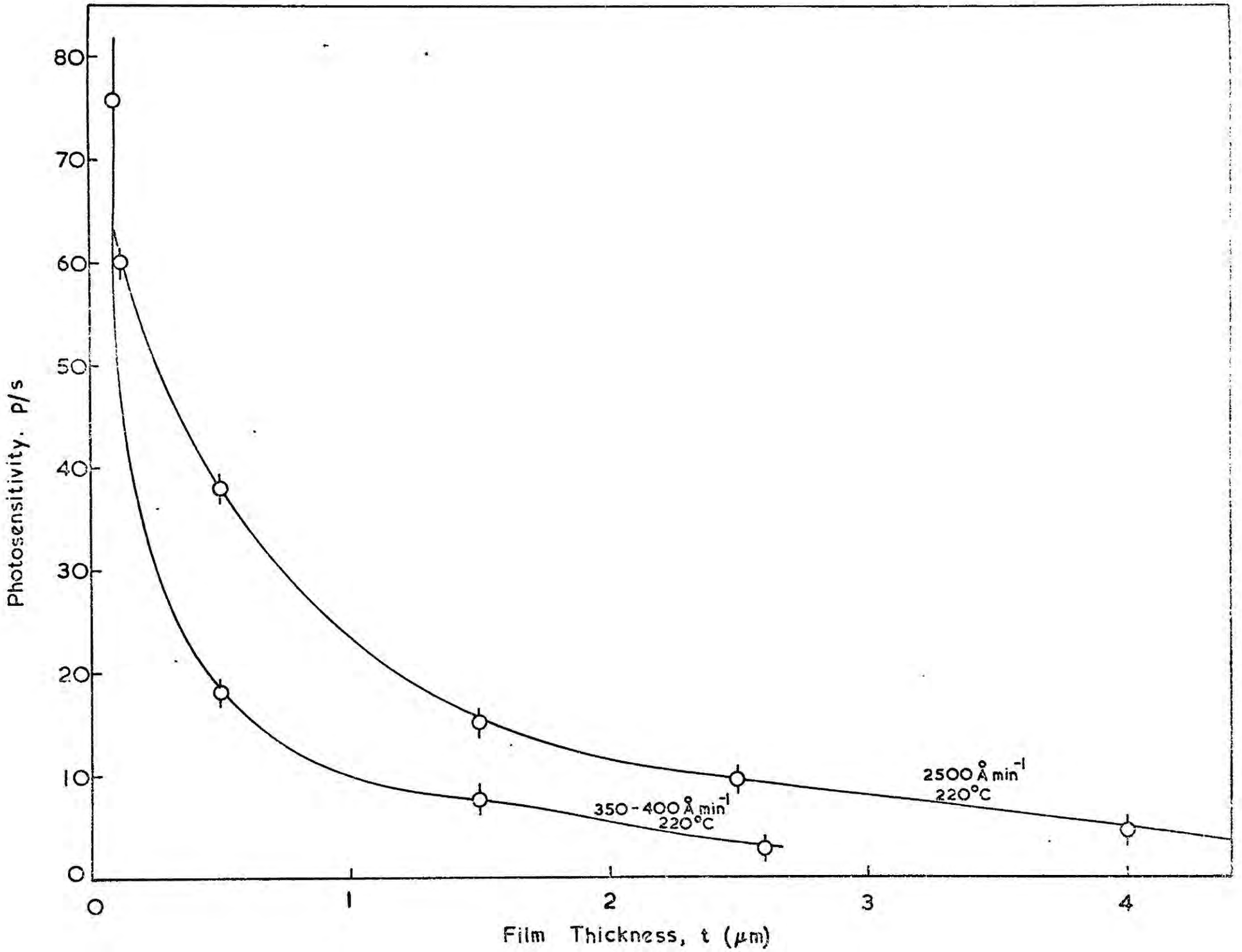

FIG. 6·9 Hall mobility size effect of CdS polycrystalline films on glass.

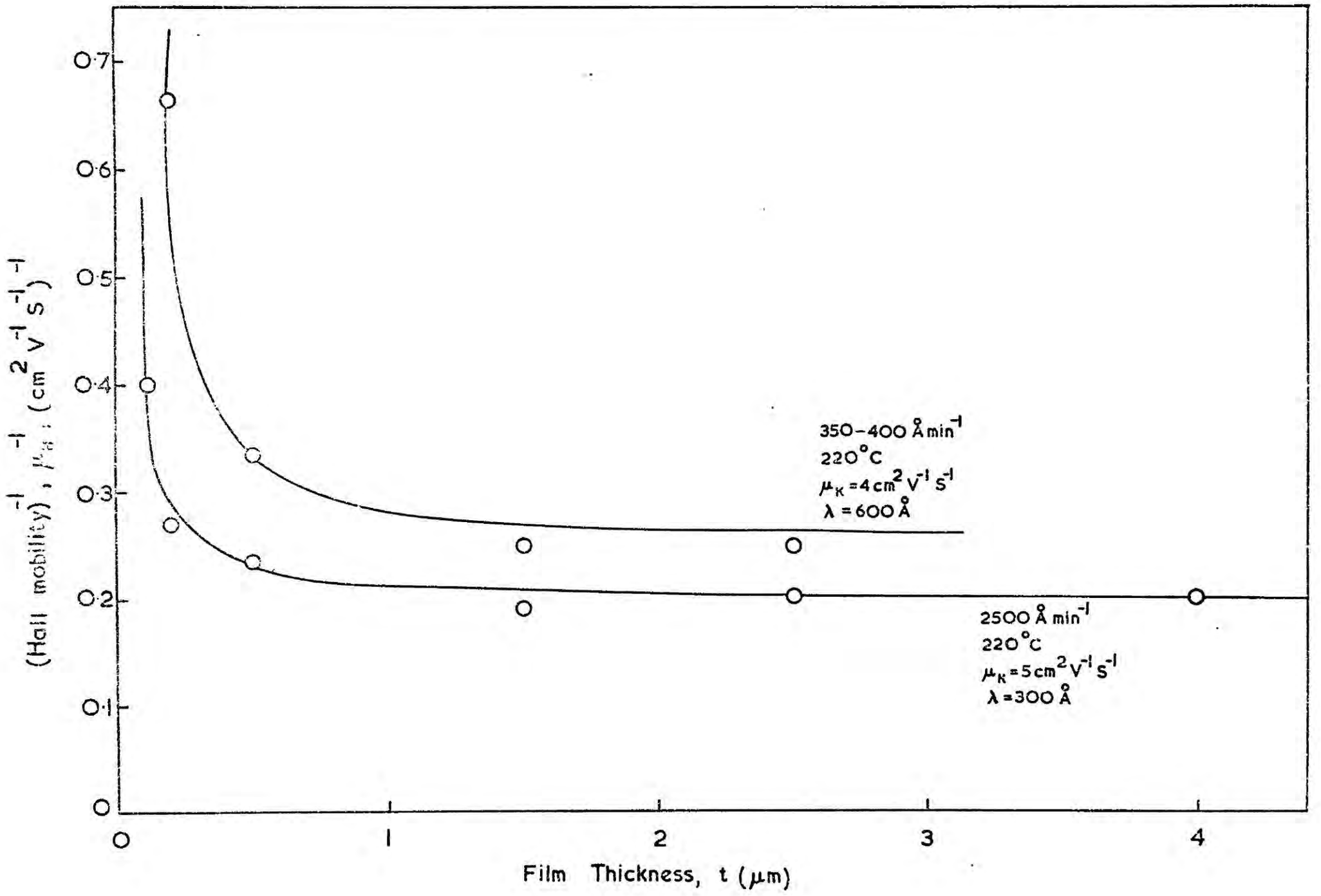

thickness, and $\lambda$ is the effective mean free path between surface collisions.

By using the values of $\lambda$ and $\mu_K$ shown on the figure, a very close fit was obtained between the pair of continuous lines, and the experimental points. Kazmerski et al (1970) have shown a similar good fit for a series of CdS films grown at 400 Å/minute on substrates at 180°C. In that series the values for $\mu_K$ and $\lambda$ were 16 $cm^2V^{-1}S^{-1}$ and 1100 Å, for films with resistivities of about one ohm cm. and a grain size of about 1000 Å.

Earlier it was explained that it is difficult to distinguish experimentally between ionised impurity scattering and grain boundary scattering, but the results described in chapter five for the grain sizes of our films indicate that the effects of microcrystallites must be included in any model of the transport properties, since $\lambda$ has a value of the same order as this grain size.

Now if the Petritz (1956) grain boundary barrier model is applicable, the mobility will be given by:

$$\mu = \mu_B e^{-A/kT}$$

where: $\mu_B$ = the mobility in the crystallites;

$A$ = the grain boundary barrier height.

In a discussion of this model, Neugebauer (1969) showed that the mobility ($\mu$) was approximately equal to the measured Hall mobility in thick films ($\mu_K$).

Assuming a single crystal mobility of 200 $cm^2V^{-1}S^{-1}$ for $\mu_B$, the present results lead to values of 0.092 eV and 0.098 eV for the barrier heights in the two series of films

at 2500 Å/minute and 350-400 Å/minute. These compare favourably with the values of 0.11 eV reported by Mankarious (1964), and 0.06 eV reported by Neugebauer (1968), for their CdS layers. However if impurity scattering is active in the crystallites, $\mu_B$ will be less than the bulk mobility used and the activation energies will be larger than those calculated above.

6.4.4 The variation in mobility indicated in Figure 6.9 shows that the resistivity versus thickness relation cannot be due solely to variations in the mobility for samples thicker than 5000 Å. However a plot of the Hall coefficient, $R_H$, against thickness, Figure 6.10, does have the same shape as the resistivity curve and this indicates that the carrier concentration increased from $3 \times 10^{11}$ $cm^{-3}$ to $3 \times 10^{14}$ $cm^{-3}$ as the film approached a thickness of 4 microns (2500 Å/minute) or 2.5 microns (300-400 Å/minute). The carrier density was higher in the series of films which were grown more slowly. It is clear, therefore, that it was the carrier density rather than the mobility which was responsible for the resistivity-thickness phenomena. This leaves the problem of discovering the source of the extra carriers.

## 6.5 EFFECT OF PREPARATIVE CONDITIONS ON THE ELECTRICAL PARAMETERS°

6.5.1 So far we have not discussed the conditions which are required to produce a film with a given resistivity and photosensitivity, apart from stating that a variety of films with different properties can be reproduced by

Fig.6·10 Hall coefficient size effect of CdS polycrystalline films on glass.

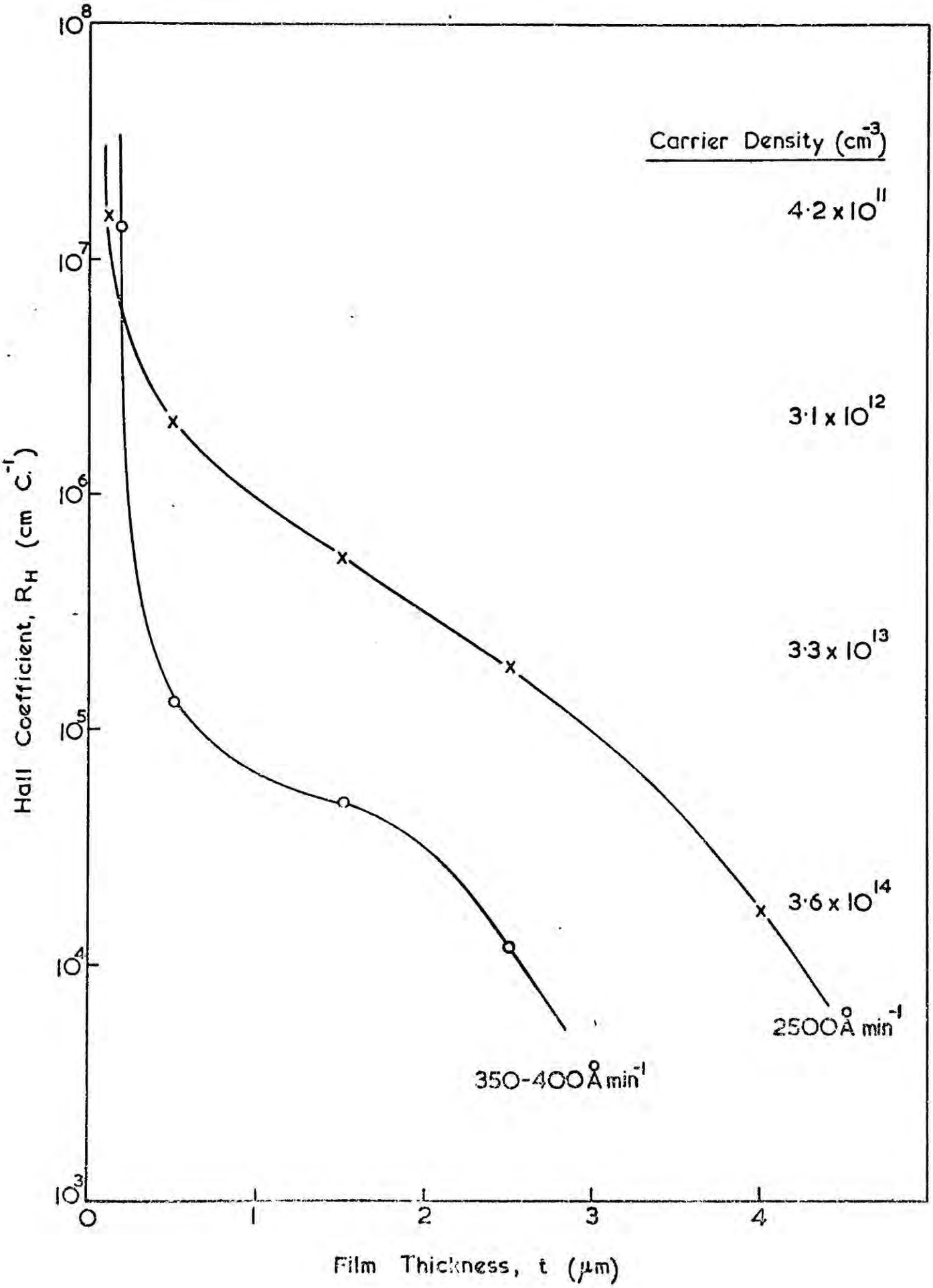

varying the substrate temperature and deposition rate.

In this investigation over 60 films on glass, prepared from undoped resublimed Optran (BDH) CdS have been studied, together with a smaller number prepared from either doped CdS or untreated CdS as received from the suppliers.

The black films which were fabricated by using a cold substrate were of no interest for photovoltaic purposes because they were very rich in cadmium and consequently highly conducting, and not photosensitive. This set a lower limit to the substrate temperature of around 50$^{o}$C. At the other extreme, great difficulty was experienced in condensing CdS on a substrate at more than 350$^{0}$C. Near this temperature a thin, pale yellow film resulted. The possible rate had limits imposed by the length of the evaporation cycle, and by the maximum power available.

Most previous workers have reported that the resistivity increased with increasing substrate temperature and decreased with increasing deposition rate, although some dissenting voices have been raised, as mentioned in Chapter 3. It appears from our results that many workers continue to pay insufficient attention both to the thickness of the CdS layers, and to the purity of the source material. Moreover we believe that the relationships between deposition rate, substrate temperature and resistivity are more complex than the statement above would lead one to suppose. Indeed a reversal of the effect of any one parameter may well be possible.

6.5.2 It is convenient here to describe the connection between resistivity and photosensitivity (still defined as the ratio of illuminated current to dark current at 50 V.) in order that both parameters may be discussed together with respect to the preparative conditions. Figure 6.11 shows this connection for several batches of Optran CdS, before and after resublimation, and also for a Leuchstoffwerk CdS powder used by I.R.D. Co. Ltd. in their solar cell work. It should be noted that the crucible was refilled for each run so that no distillation effects would alter the composition of the source from run to run. The points on each line refer to films of the same batch deposited at different rates and substrate temperatures.

Slight differences are apparent between different lots of starting material, but each series of films gives a straight line plot of log resistivity against log photosensitivity, even when values of photosensitivity close to unity are approached. Both of the untreated lots of material have a steeper characteristic than the flow-purified CdS, but small differences also exist from one flow run to another. For this reason the variations of film parameters with thickness which have just been reported were investigated on the same lot of CdS.

It is most likely that the differences between the various lots were due to varying amounts of impurities in the starting material. For instance, a spark mass spectrographic analysis performed at the Fulmer Research Institute on Optran batch 7 CdS before and after resublimation revealed that the Cl content had been increased by the

FIG. 6·11 Relation between Dark Resistivity and Photosensitivity of polycrystalline CdS films on glass.

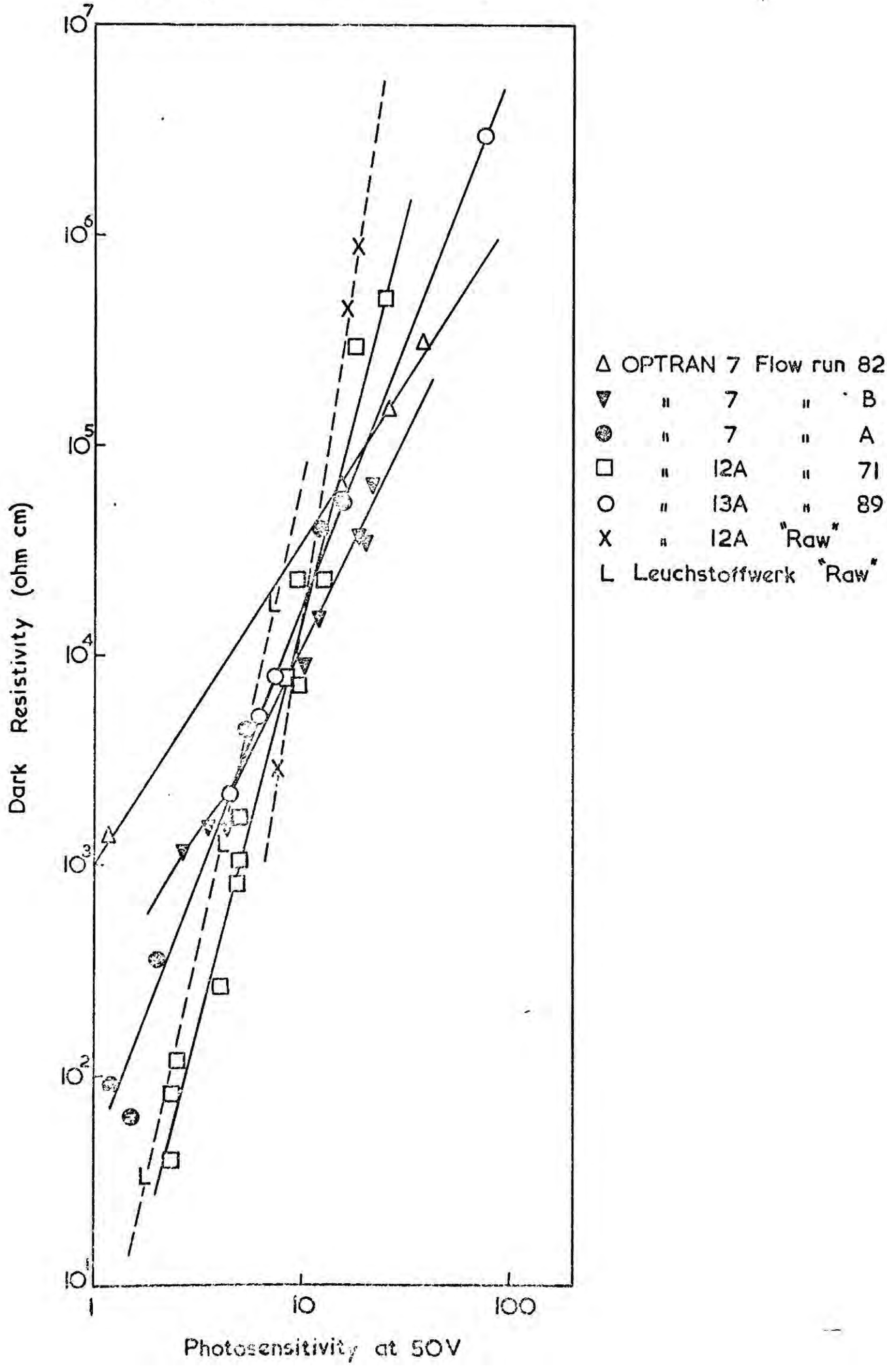

flow process from 0.08 to 1 ppm. Certain metals were also present in increased ppm (Na: 0.4 increased to 1; Ag: less than 0.04 to less than 0.1; Li: less than 0.02 to 0.04; Cr: less than 0.02 to 0.06), as was P (less than 0.02 to 0.06), but most elements were either unaffected or reduced in concentration by the process. The effect of Cl impurity in the source would be to decrease the photosensitivity of the evaporated film, as well as to reduce its adhesion as suggested earlier.

6.5.3 In Figure 6.12 the resistivity of some of the films already discussed has been replotted as a function of deposition rate. All these films had substrate temperatures of 220°C., and the film thicknesses in angstroms are marked on the graph. The lines indicate the effect of increasing the deposition rate whilst maintaining constant thickness. It is clear that at constant thickness an increase in rate produces an increase in film resistivity.

Figure 6.13 shows the results obtained for some depositions carried out at similar rates but with lower substrate temperatures. Once again, resublimed, undoped Optran CdS was the source material. In this case the parameter marked on the graph is substrate temperature, and different symbols are used for the four film thicknesses employed. Broken lines indicate the effect of a change in rate or in substrate temperature for constant film thickness.

First consider the series of points for thickness values of 1500 Å. As the substrate temperature was

FIG. 6·12 Resistivity versus Deposition Rate of CdS polycrystalline films on glass at 220°C.

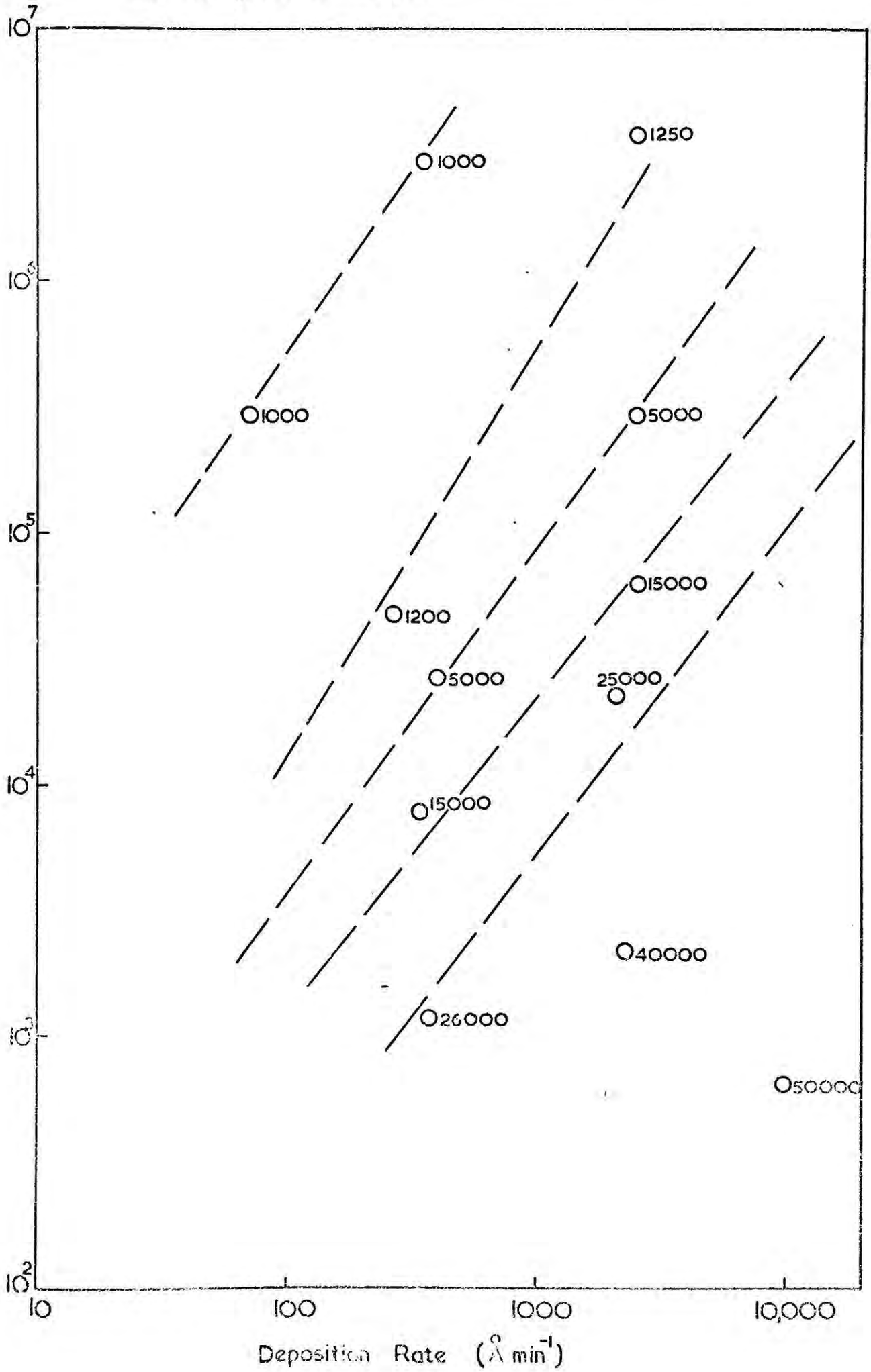

FIG. 6·13 Resistivity versus Deposition Conditions of CdS polycrystalline films on glass.

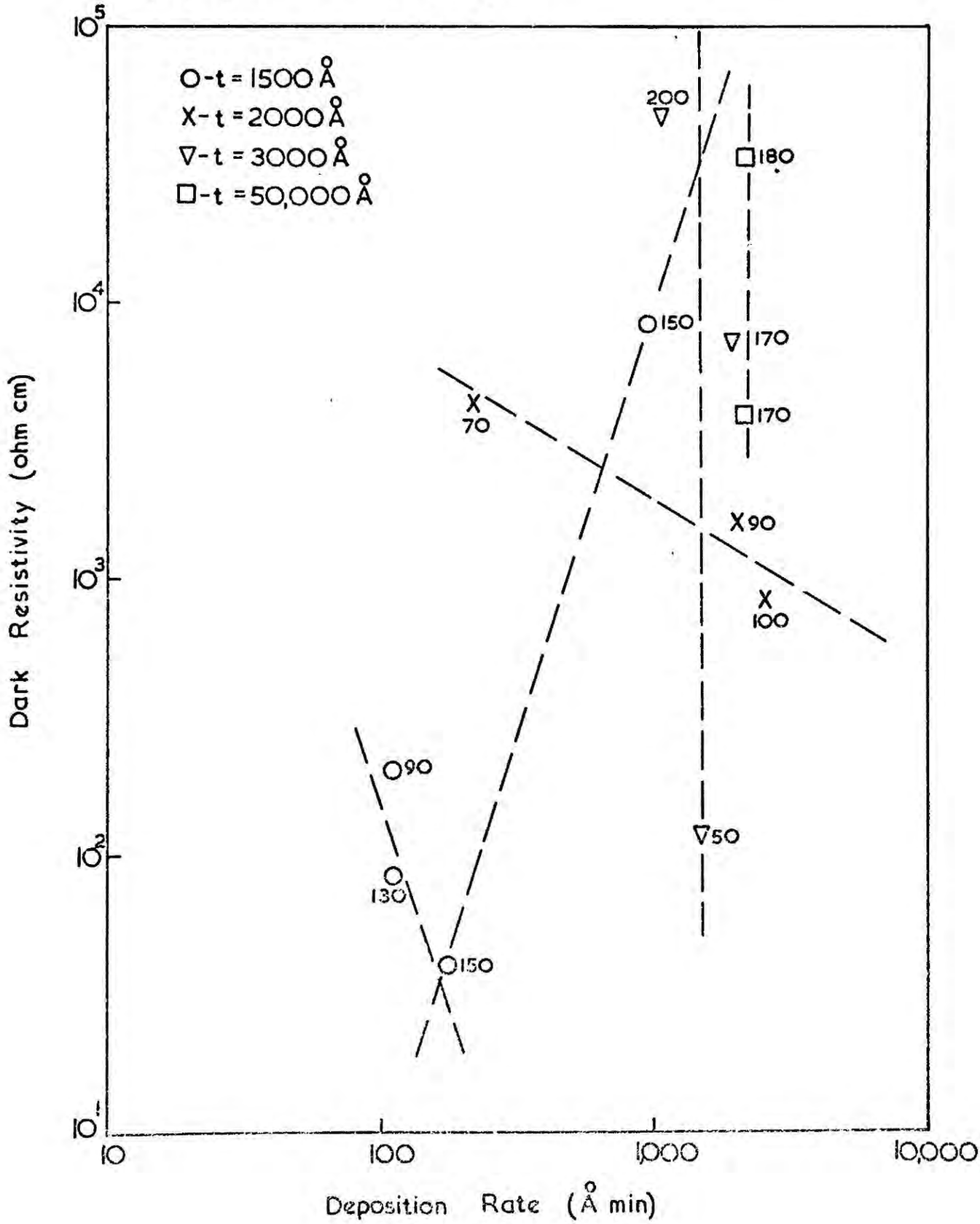

increased from 90° to 150° C, with the deposition rate remaining essentially constant at 150 Å/minute, the dark resistivity decreased by nearly an order of magnitude. This appears to be an effect caused by the substrate temperature and not by the rate. When the substrate temperature was kept constant at 150°C and the rate was increased, then a large increase in resistivity occurred, as already observed with a substrate temperature of 220°C. Therefore the resistivity decreases with any increase in substrate temperature below 150°C, and increases with deposition rate.

This conclusion is supported by the points for the 2000Å films, with the additional observation that the substrate temperature is dominant. For despite an increase in deposition rate from 200 to 2000 Å/minute, the resistivity fell due to the influence of the 30°C increase in substrate temperature over the range covered by this set of films.

The 3000 Å points are for films all deposited at the rate of 1500 Å/minute, and the resistivity is seen to increase with substrate temperature, which has now risen above 150°C.

The 50,000 Å points are also for films deposited at a fixed rate (2200Å/minute), but at different substrate temperatures, and support the conclusion of the preceding paragraph: i.e. the resistivity increases with any increase in substrate temperature above 150°C.

For films grown above 220°C. variable results were obtained as the sticking coefficient was low, but the resistivity was found to continue increasing with substrate

temperature. There were also indications that the resistivity began to fall with increasing deposition rate.

Throughout this series of measurements, the substrate temperature was more important than the evaporation rate, but the film thickness was at least as important. The combination of these conflicting variables complicates the prediction of the resultant resistivity of a growing film, but the conclusions reached so far are grouped below for convenience:

(i) the resistivity increases as the film thickness decreases;

(ii) with substrate temperatures <u>below</u> about 150°C, the resistivity <u>decreases</u> as the substrate temperature increases;

(iii) with substrate temperatures <u>above</u> about 150°C, the resistivity <u>increases</u> as the substrate temperature increases;

(iv) the resistivity increases as the deposition rate increases, except for high values of substrate temperature;

(v) the substrate temperature is more important than the deposition rate.

<u>6.5.4</u> Electron beam evaporation persistently gave layers with dark resistivities one to one and a half orders higher than those evaporated from the tungsten-wound crucible. This is thought to be due to the superiority of the electron-beam method, where no hot metal filament is exposed to the substrate, in contrast with the simple resistive filament technique. With the

latter method some filament atoms would inevitably be carried on to the substrate and be incorporated into the film. In addition, because of the geometry of the electron gun, the source vapour passes through the electron beam and becomes charged, which may have a beneficial effect on the alignment of the first few monolayers deposited.

6.5.5 The dependence of the Hall mobility on deposition rate and substrate temperature was more difficult to quantify since similarly produced films, with similar resistivities and photosensitivities, exhibited a spread in mobility. This difference was occasionally very large (e.g. $5 cm^2V^{-1}S^{-1}$ and $8 cm^2V^{-1}S^{-1}$). In particular, the dependence of mobility on the substrate temperature was difficult to determine, but in general lower substrate temperatures led to higher mobilities. For example, for films 1500 Å thick grown at a rate of 100 Å/minute, the following values were obtained:

$6 cm^2V^{-1}S^{-1}$ on $90^oC$. substrate,

$3 cm^2V^{-1}S^{-1}$ on $135^oC$. substrate,

$1 cm^2V^{-1}S^{-1}$ on $340^oC$. substrate.

Higher rates gave higher mobilities, as already noted for the two series of films used in the thickness investigations. A further example of this is provided by the following result: 1500 Å thick films grown at $135^oC$. had a mobility of $3 cm^2V^{-1}S^{-1}$ for 100 Å/minute, and $6 cm^2V^{-1}S^{-1}$ for 130 Å/minute.

As with the resistivity versus photosensitivity measurements, the film thickness was clearly the most

evident of the parameters, and we can also conclude that the intercrystallite barrier heights and crystallite sizes are extremely important in the scattering processes. Impurity scattering may also be prominent. An investigation of the temperature dependence of the mobility would be most desirable, but the high resistance of the samples, and the temperature coefficient of resistance require a cryostat with a very long warm-up period if a stable Hall voltage is to be measured at each temperature.

6.5.6 Measurements made on layers evaporated from CdS:In crystals showed that In was successfully incorporated into the film in that it had the effect of reducing the resistivity and photosensitivity, but of increasing the Hall mobility to a value as high as 21 $cm^2V^{-1}S^{-1}$. The structural characteristics of these films were similar to those of the undoped films, with the same crystallite size and orientation effects.

Evaporation of low resistivity CdS:Cl crystals produced high resistivity layers. It would appear that the more volatile Cl component was preferentially evaporated from the source and not incorporated into the films. However, the resistivity of these films was much higher than similarly evaporated undoped layers, which suggests that the stoichiometry of the vapour was affected by the presence of Cl.

6.5.7 A few remarks will now be made on the purity of the CdS starting material since it is obvious that this must also be included as a parameter in the preparative conditions.

The Leuchstoffwerk CdS powder was used as received, without resublimation or crystallisation, as this was the procedure followed by the I.R.D. team, and it was desired to examine their source material. It was found that the films produced from this material had unpredictable electrical properties. The resistivity/photosensitivity curve has already been mentioned as being similar to the 'raw' Optran 7 curve, but the individual values which make up this plot did not fit into the pattern of the preparative conditions listed earlier. Moreover, the values of Hall mobility were exceptionally low and even impossible to determine on some samples. The film appearance was non-uniform and very pale, with a rough surface not attributable to spattering.

The untreated Optran CdS also produced films with uneven texture and thickness, but the properties were nearly the same as those of films produced from resublimed Optran CdS. Although the resistivity changed with the preparative conditions in the prescribed manner, the Hall mobilities were very low, and a value of 2 $cm^2V^{-1}S^{-1}$ was the highest value recorded.

With both these types of starting material frequent adjustments were necessary to the source input power to ensure a constant evaporation rate, owing to the uneven texture of the CdS, which caused bursts of vapour to be evolved.

The sum of these facts indicates that undesirable additional impurities were present in these materials, especially in the Leuchstoffwerk CdS, together with an unevenness in composition and texture of the powders before

recrystallisation. All starting material should therefore be purified by a recrystallisation technique.

## 6.6 SUMMARY

The need to control both the substrate temperature and the evaporation rate, and of using a pure source of CdS, plus a means of monitoring the film thickness, has been clearly demonstrated if semiconducting thin films of CdS are to be prepared reproducibly. The advantages of focussed electron beam evaporation have been indicated, but many such sources have a limited capacity and can only produce very thin layers.

It is proposed to discuss the problems raised by some of the measurements reported in this chapter in a later section. Such difficulties include the origin of the photosensitivity of these layers, and the origin of the extra carriers possessed by the thicker films. The reasons for the higher carrier mobility of the doped layers need to be examined. Further, some discussion of the mechanism which allows the production of a range of resistivities from the same source by altering the growth conditions is required.

REFERENCES

J.E. Davey et al (1963), Solid State Electron. 6, 205-216

H. Fleitner (1961), Phys. Stat Sol. 1, 483-488

I. Isenberg et al (1948), Rev. Sci. Instrum. 19, 685

L.L. Kazmarski et al (1970), 8th IEEE Photovoltaic Specialists' Conference.

R.G. Mankarious (1964), Solid State Electron. 7, 702-704

C.A. Neugebauer (1968), J.A.P. 39, 3177-3186

C.A. Neugebauer (1969), J. Vac. Science Technol. 6, 454-460, (Proc. of Int. Conf. on Thin Films, 1969)

R.L. Petritz (1956), Phys. Rev. 104, 1508

F.V. Shallcross (1966), Trans. Met. Soc. AIME, 236, 309-313

# CHAPTER 7 :

# THE PHOTOVOLTAIC EFFECT IN CdS-$Cu_2S$ HETEROJUNCTIONS

## 7.1 INTRODUCTION

The work reported so far demonstrates that it is possible to grow CdS films with a range of resistivities, and that indium doping of the source readily leads to a low resistivity film. However one of our aims was to determine whether efficient CdS photovoltaic devices can be fabricated from doped CdS, and further, to determine how critical the resistivity of the CdS is for maximum open circuit voltage (OCV). (The bulk of this chapter will be concerned with OCV, but complete I(V) curves of the junctions were also determined at various stages in their development).

Polycrystalline slices of CdS boules, instead of evaporated films, were used to provide the n-type layers. In this way it was possible to study the effects of introducing a variety of dopants into the growth charge, and at the same time produce a large amount of material with the same dopant concentration. Over 30 photovoltaic cells were manufactured from 1 mm thick slices cut from more than 16 CdS crystals, but some of these were too inefficient to investigate in detail. In many cases it was possible to ascribe the failures to a poor $Cu_2S$ layer or a short-circuited junction. When high resistivity slices were plated with $Cu_2S$ they yielded very poor cells which were impossible to characterise fully.

After preparing the $Cu_2S$ layer by chemiplating in the solution described earlier (Chapter 2), electrical contact

was made to the $Cu_2S$ layer by a spring-loaded contact. The bottom of the CdS slice was bonded to a copper plate with indium.

## 7.2 CIRCUIT ARRANGEMENT

The electrical circuit and apparatus used to determine the (I)V characteristics under equivalent amO sunlight illumination are shown in Figure 7.1. A 1500W quartz halogen strip lamp with a parabolic reflector housing was mounted above a 1cm deep water filter under which the sample and its heat-sink were placed. The intensity of illumination at the surface of the sample was set to 140mW $cm^{-2}$ by adjusting the height of the heat-sink table whilst monitoring the short circuit current (SCC) of a calibrated silicon photovoltaic cell. This intensity of illumination was used throughout the present series of experiments.unless otherwise stated.

The OCV of each cell was measured by a Philips GM6020 VVM with leads attached to the cell contacts. Separate leads were taken from the cell to a bias supply which was continuously variable from -1.5 to +1.5 volts and consisted of a multi-turn 'helipot' connected as a potential divider. Connections were made from this to a Bryans 21001 X-Y plotter. The current through the cell was measured by recording the potential drop across a one ohm resistor.

## 7.3 MAXIMUM OPEN CIRCUIT VOLTAGE

Details of the growth and doping conditions of the

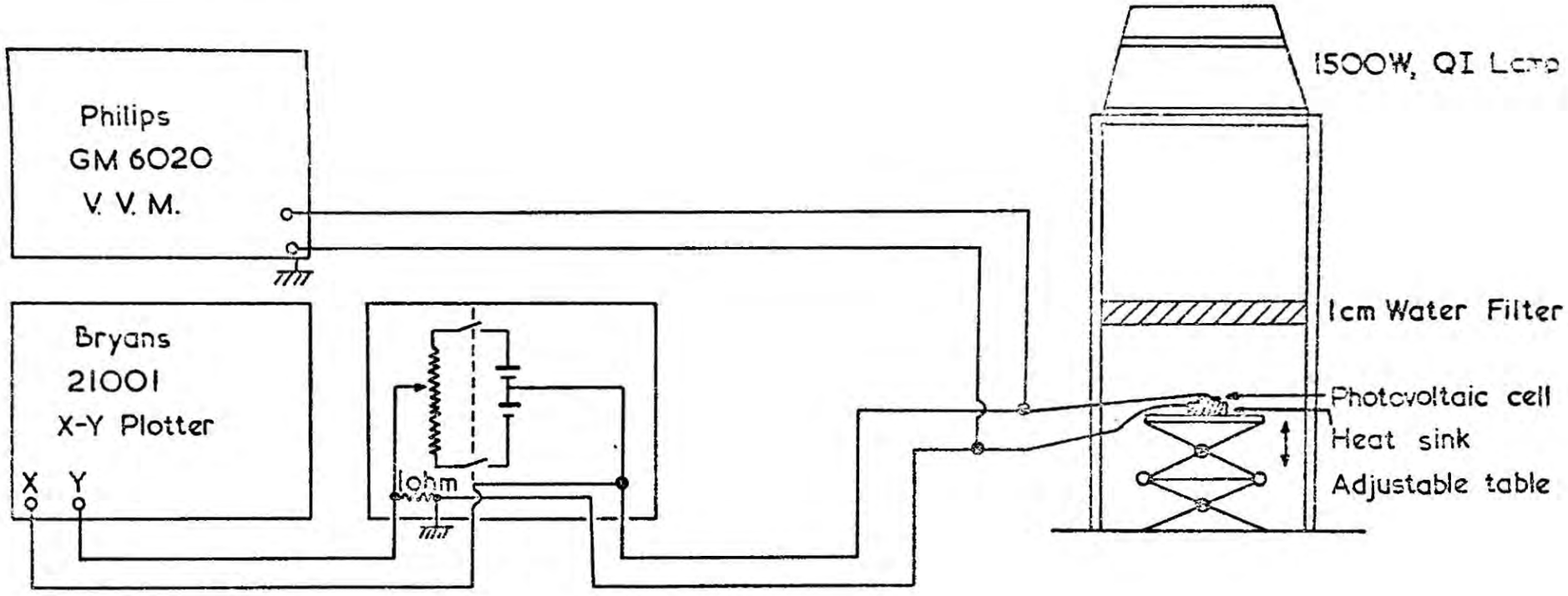


FIG. 7.1 CIRCUIT FOR DETERMINING I (V) CHARACTERISTICS OF PHOTOVOLTAIC DEVICES

CdS boules used to make heterojunctions are summarised in Table I. The d.c. resistivities of the boules and the maximum OCVs obtained from the finished cells under 140mW $cm^{-2}$ illumination intensity are also recorded in this table. The maximum OCV was reproducible from slice to slice of the same boule, provided that care was taken in the plating and contacting processes.

It appears that for the maximum OCV the optimum resistivity of the CdS is between $10^2$ and $10^3$ ohm cm (see Figure 7.2). The samples produced from CdS:In which were grown with the dopant in the reservoir furnace lie on a different curve of maximum OCV versus CdS resistivity (Figure 7.2) but show the same trend of increasing OCV with resistivity in the range 10 to $10^2$ ohm cm. The best choice for the value of the CdS resistivity would appear to be a few hundred ohm cm, which is well within the range obtainable by thin film techniques either with or without dopants added to the source. It will be noted that the lower values of OCV were obtained from devices made from boules containing either excess sulphur alone, or a high percentage of indium.

In order to obtain the maximum photovoltage it was necessary to heat the cells in air at 200°C to form the intrinsic CdS layer. The usual length of time for this process was 30-60 seconds but the effects of more prolonged heating have been examined in successive stages.

The best cells, with maximum OCVs of more than 400mV, all possessed an initial OCV of up to 480mV before

TABLE I

| Boule No. | Dopant | Tail Furance | Growth Temp. (°C) | Resistivity (ohm cm) | OCV max (mV) |
|---|---|---|---|---|---|
| 194 | Excess S added to charge | | 1160 | $>10^7$ | 5 |
| 208 | none | S @ 300°C | 1150 | 0.50 | 430 |
| 209 | none | S @ 300°C | 1150 | 0.60 | 390 |
| 218 | 100ppm Cu | S @ 300°C | 1150 | $10^2$ | 550 |
| 245 | none | Cd @ 550°C | 1100 | $10^4$ | 480 |
| 246 | 50ppm Cl | Cd @ 550°C | 1080 | 10 | 460 |
| 247 | 50ppm Cl | S @ 300°C | 1080 | 25 | 500 |
| 274 | 1000ppm In | S @ 290°C | 1080 | 1.4 | 360 |
| 275 | 1000ppm In | Cd @ 550°C | 1080 | 0.52 | 160 |
| 276 | 100ppm In | Cd @ 520°C | 1080 | 0.33 | 420 |
| 278 | 1000ppm In | S @ 150°C | 1080 | 0.094 | 390 |
| 282 | 10ppm In | S @ 150°C | 1080 | 3.4 | 460 |
| 283 | 1000ppm In in tail @ 850°C | | 1080 | 22 | 240 |
| 285 | 1000ppm In in tail @ 650°C | | 1080 | 50 | 340 |
| AEI 558 | — | — | ∿1170 | $4x10^8$ | 32 |
| AEI 594 | — | — | ∿1170 | 160 | 460 |

FIG. 7.2 MAXIMUM OCV AT am O SUNLIGHT FOR VARIOUS CdS RESISTIVITIES

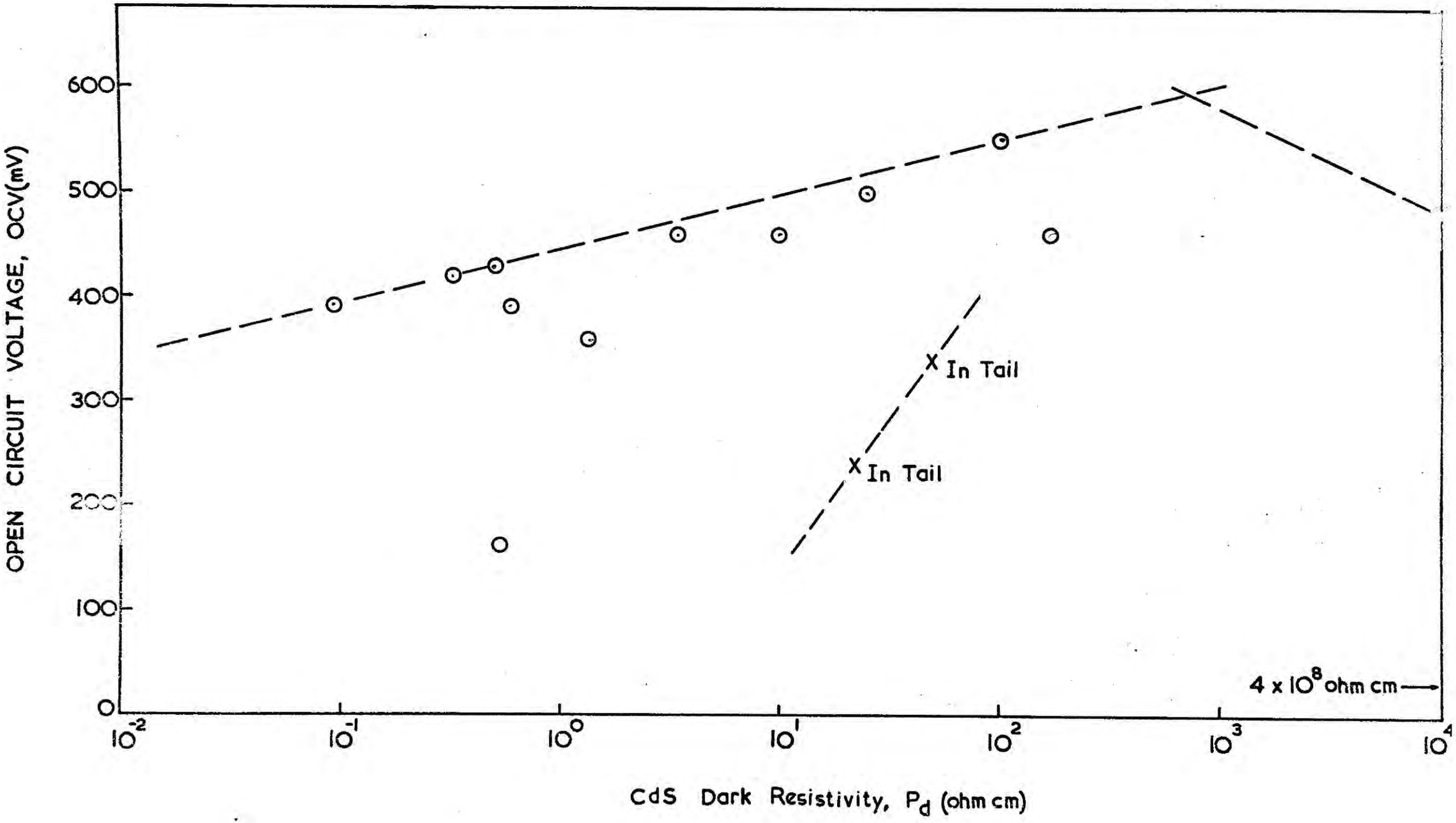

any heat-treatment. Those cells which had no OCV immediately after plating improve after heating at 200°C but the OCV then obtained never exceeded 400mV. The OCVs of all of the cells examined are shown at various stages of the heat-treatment at 200°C in Figure 7.3. The curves demonstrate that the maximum value was not always sustained, and that the highest 'saturation' value was obtained from cells prepared on CdS with a resistivity of $10^2$ ohm cm.

## 7.4 SHORT CIRCUIT CURRENT

Although only a small area contact to the $Cu_2S$ surface was used, with the result that current collection was inefficient, the SCC was also monitored as a function of the 'bake' time. It will be appreciated that a gridded contact suitably applied would have allowed larger currents to be drawn. The SCC as a function of bake time for a number of devices is plotted in Figure 7.4. The curves are similar in shape to those of Figure 7.3. With most devices the current decreased from a maximum after continued baking and only one device, 247-B, gave an appreciable current which did not decrease on prolonged heating at 200°C. The reasons for this behaviour are not known.

This cell, although having the best SCC of all the boule cells, still possessed a poor FF and low efficiency because of the inefficient current collection. (See the I(V) curve after 12 minutes at 200°C in Figure 7.5). The SCC density of this boule cell should be compared with that of the 2% efficient thin film cell, the characteristics

FIG. 7.3 OCV VERSUS BAKE TIME

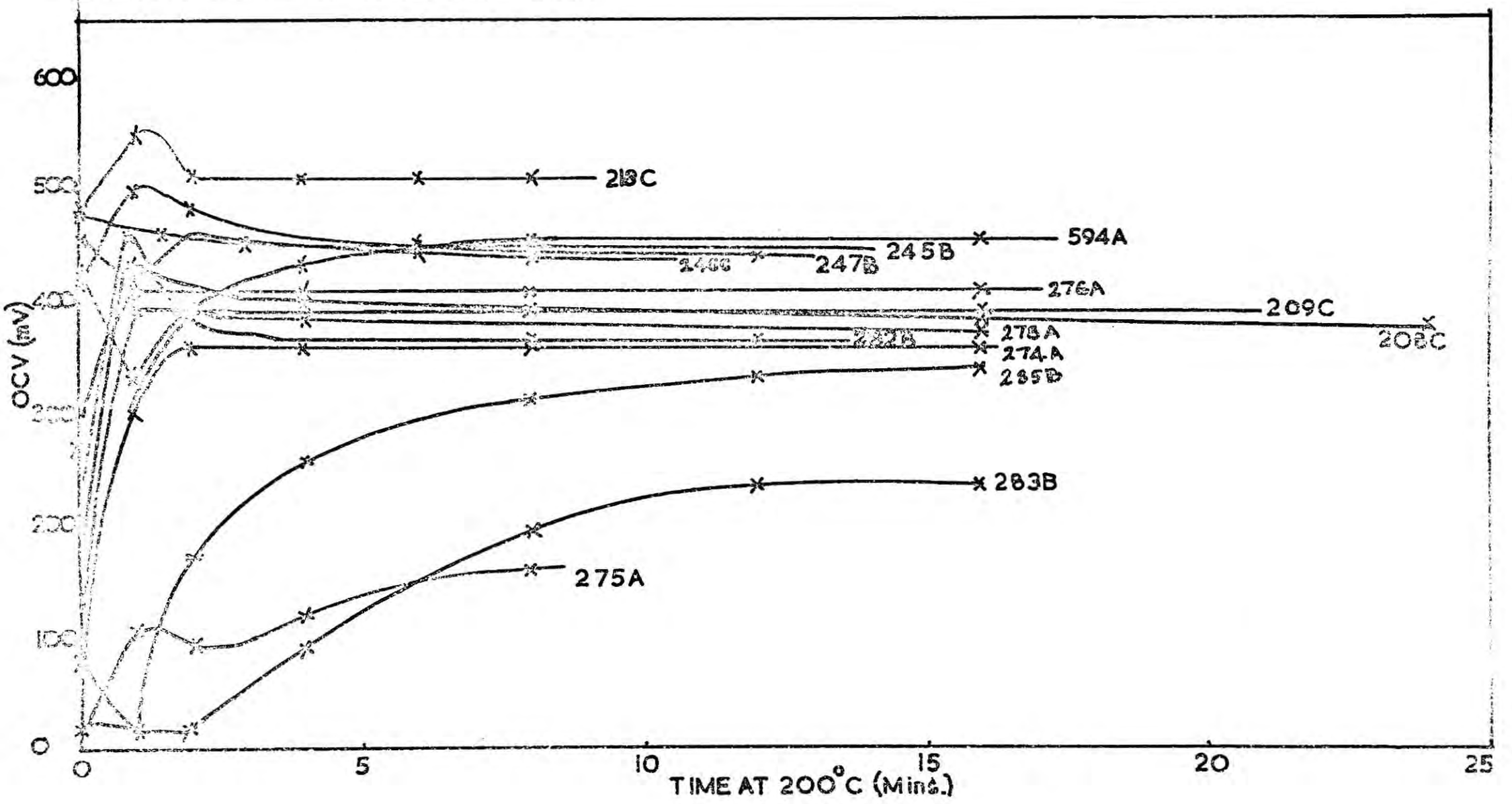

FIG. 7.4 SCC VERSUS BAKE TIME

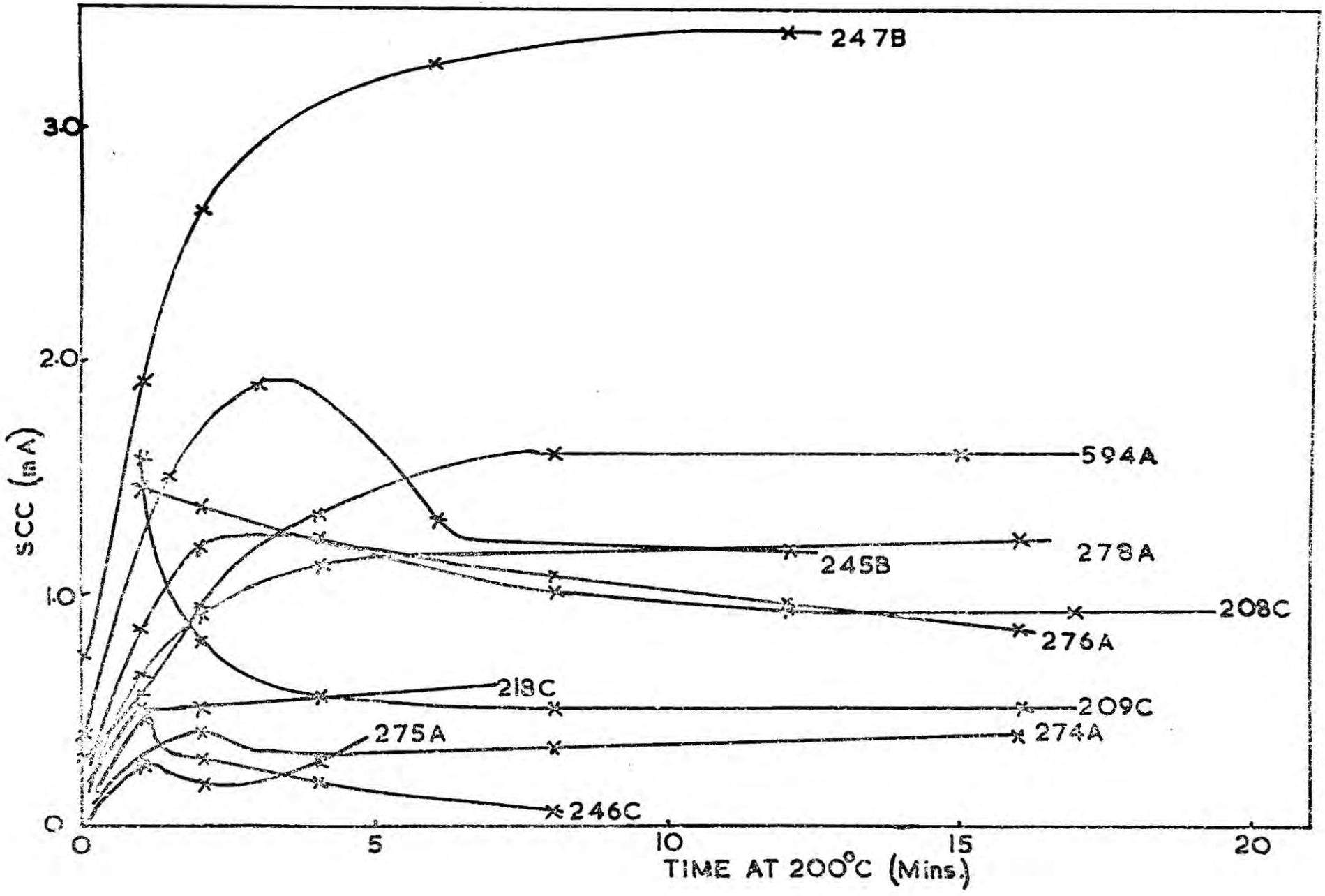

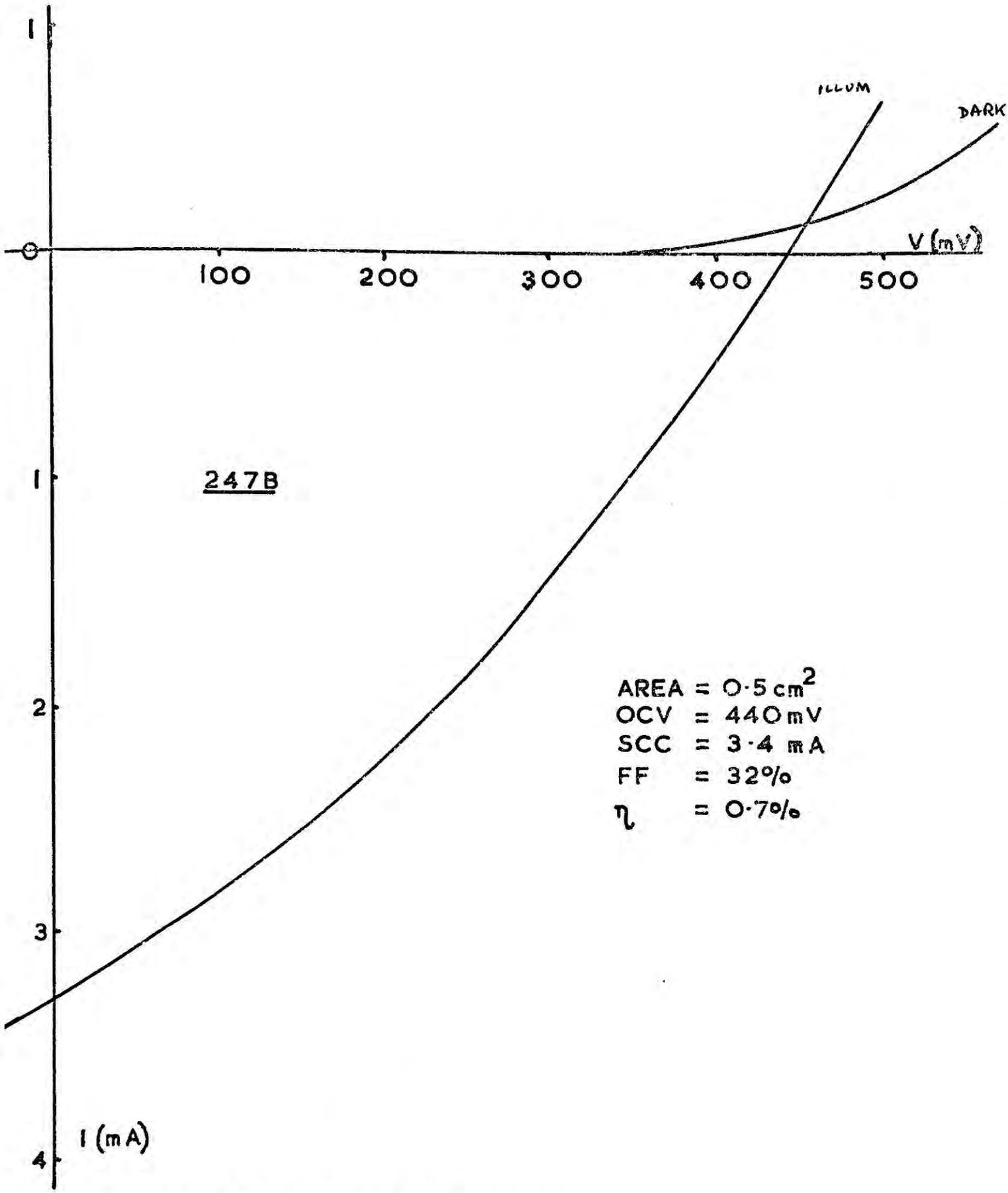


FIG. 7.5 I(V) FOR BOULE CdS CELL

of which are illustrated in Figure 7.6. This latter cell, CVC-90-C, had a gridded top electrode.

In general it was observed with boule cells that the FF deteriorated after long heat-treatment, whereas the OCV usually stabilised after the initial changes.

For completion it would be useful to compare the I(V) characteristics of boule cells with the I(V) characteristics obtained from the poorer of the thin film junctions with a gridded top electrode. Some results from a small selection of thin film cells are shown in Figure 7.7, where the length of the heat-treatment is marked on each graph. These cells had poor shunt resistances and low FFs, which are attributable in thin film cells to pinhole short-circuits in the CdS layer. Some improvement in these characteristics was achieved by removing the short-circuited areas, which had been identified as local hot-spots on the display from an 'Aga' thermovision i-r camera. Such defects were observed only in the CdS thin film cells and are the most common cause of poor thin film device yield, necessitating the use of a thicker film than the operating mechanism requires.

## 7.5 CdS SURFACE QUALITY

Pinhole defects were not present in cells formed from CdS boule slices, but care had to be taken to use the same surface treatment for each slice. This was especially important when several cells were manufactured from the same boule. The standard process consisted of removing the cutting marks by polishing with 600 grade

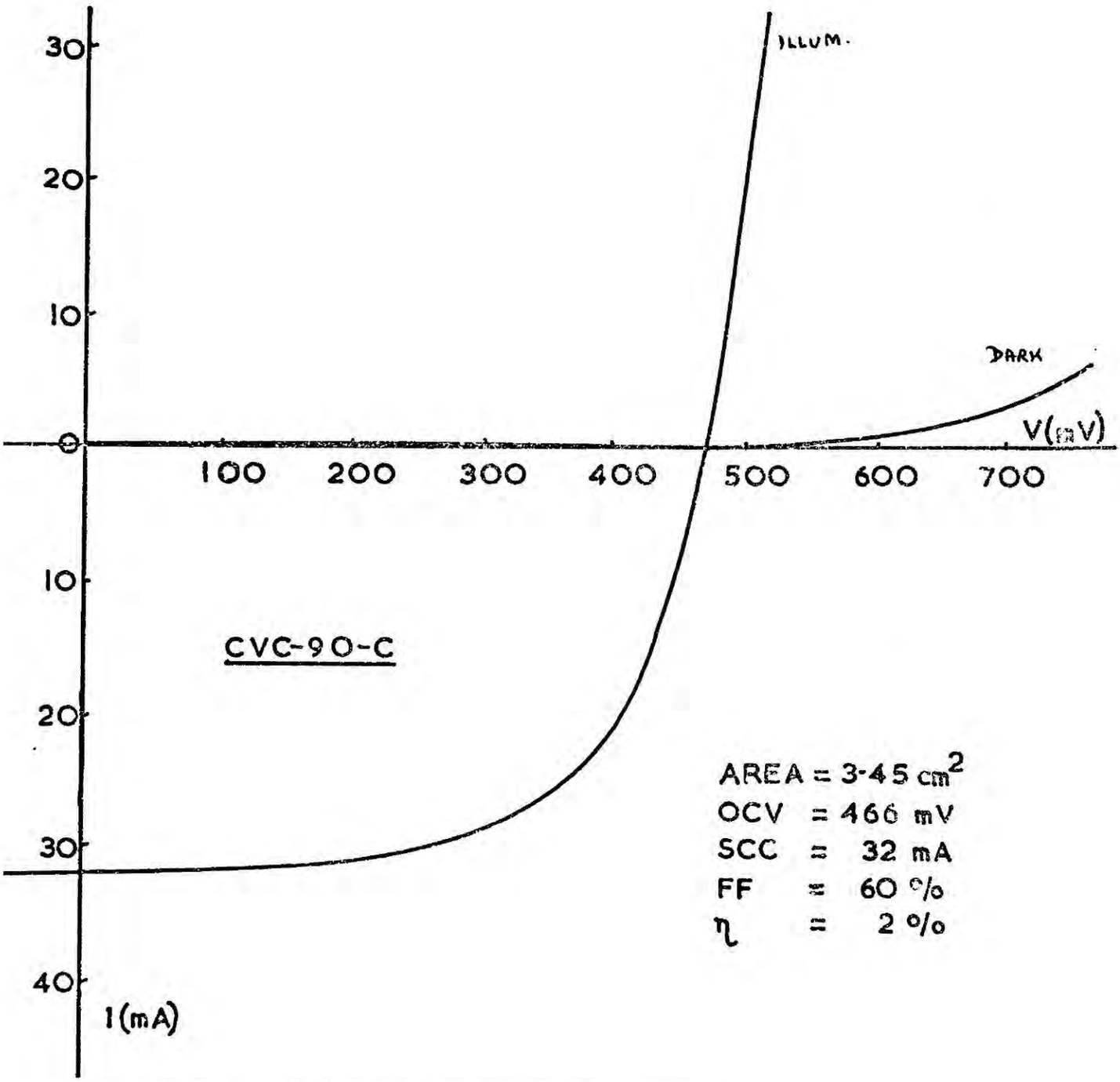


FIG. 7.6 I(V) FOR THIN FILM CELL

FIG. 7.7 I(V) FOR POOR THIN FILM CELLS

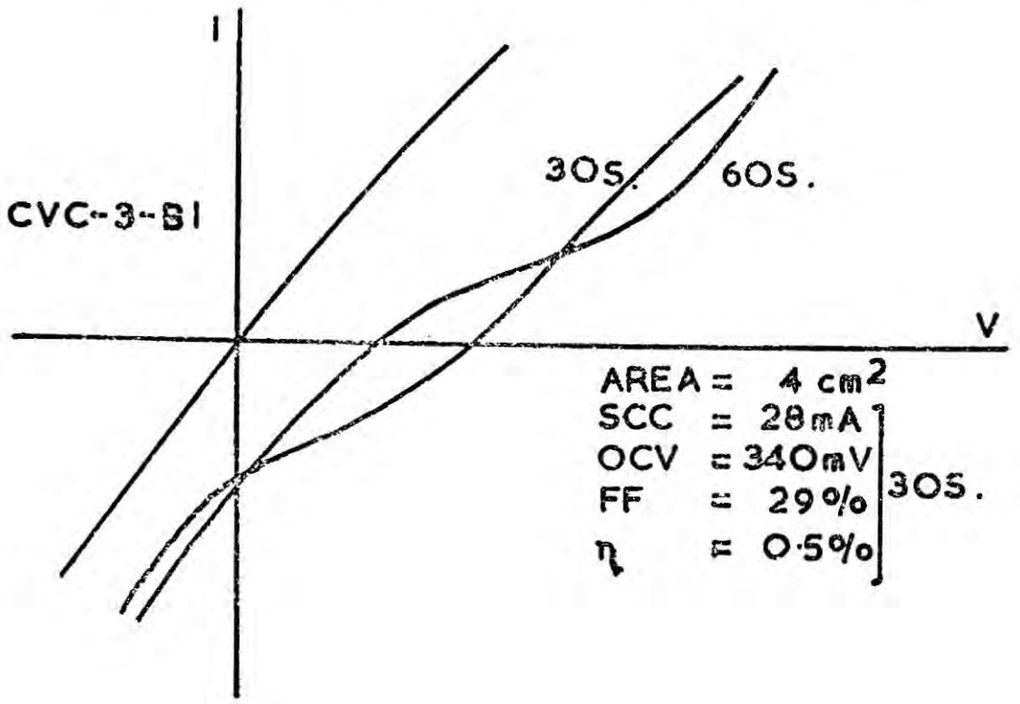


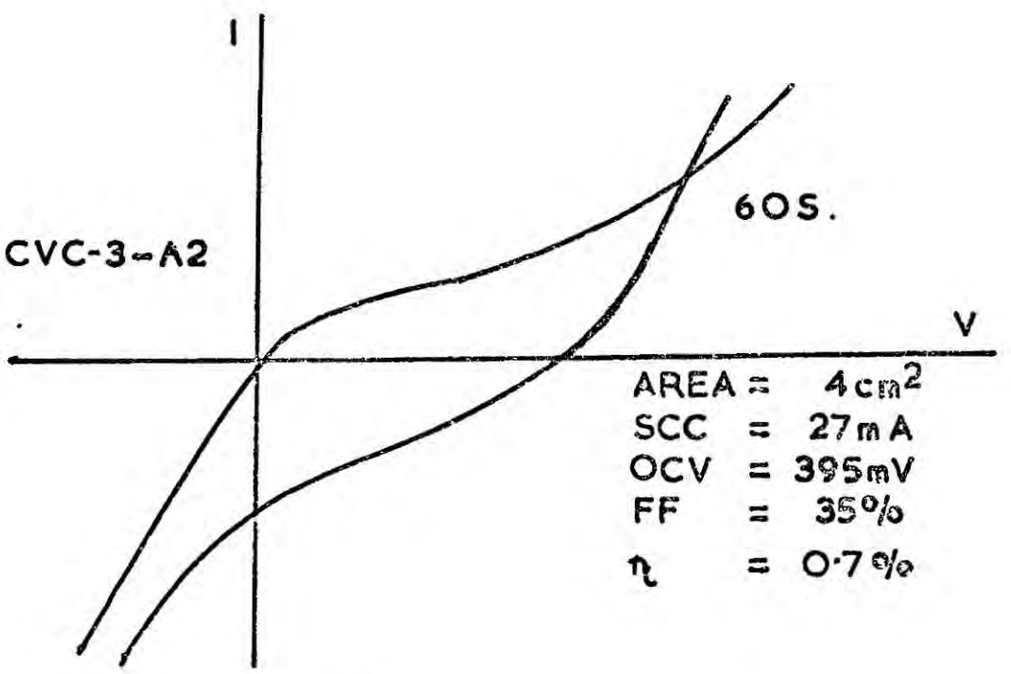


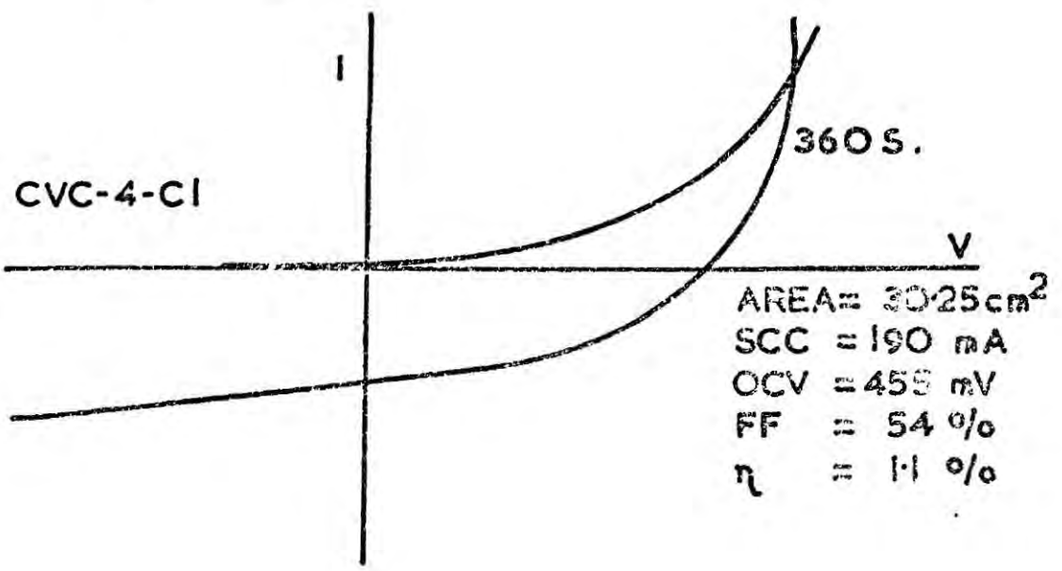

carborundum followed by a ten minute etch in hot (110°C) orthophosphoric acid. If instead the surface was roughened by abrasion before chemi-plating a lower OCV was the result, together with a higher SCC. Alternatively the OCV was improved slightly by polishing the CdS surface with 3 micron diamond powder before etching and chemi-plating.

It is obvious that a rough surface forms a larger area junction with more efficient light absorption than a polished surface, but against this, more surface damage is created together with the associated traps and recombination centres.

It would be interesting to extend this study to discover the optimum surface treatment for high FF and maximum power point, but in the present investigation the standard polishing and etching treatment was used each time.

Although a brief etch in cold HCl was used immediately before the chemiplating stage to extend the grain boundaries, this etch was under review at IRD Co. Ltd. during this period and was subsequently replaced by a cold KI etch. This was found to be milder and etched less preferentially, so roughening the whole surface slightly, but it was decided not to change any parameter of the plating process at Durham to avoid the introduction of too many variables.

## 7.6 PHOTOVOLTAGE UNDER LOW LEVEL ILLUMINATION

Until now we have only described results for high

intensity illumination of the junction, but for Earth's surface or outer planet use it would be necessary to utilise a lower intensity of illumination than 140mW $cm^{-2}$. Therefore the steady-state OCV white light response of the boule cells was investigated over four orders of intensity by inserting neutral density filters between the cell and the 140mW $cm^{-2}$ source.

The CdS:In devices, including 276-A which possessed a high OCV under 140mW $cm^{-2}$ illumination, were the most insensitive to low light levels, even after lengthy heat-treatment at 200°C. Their response to intensity changes was slow and several tens of seconds were needed under microwatts $cm^{-2}$ illumination before the maximum OCV was reached. The variation of OCV with intensity of illumination was linear. (See Figure 7.8, in which the parameter is the length of the bake at 200°C in minutes).

The other cells showed various degrees of saturation of the OCV with increasing light intensity after prolonged baking at 200°C. The OCV saturated at progressively lower light intensities until eventually no further improvement in response was possible by heating at 200°C. The response time of the cells (including those prepared from CdS:Cl boules and from CdS grown with excess cadmium) also became longer after several minutes at 200°C.

The devices made from CdS grown with a sulphur tail furnace had a very good low intensity response

FIG. 7.8 OCV VERSUS WHITE LIGHT INTENSITY

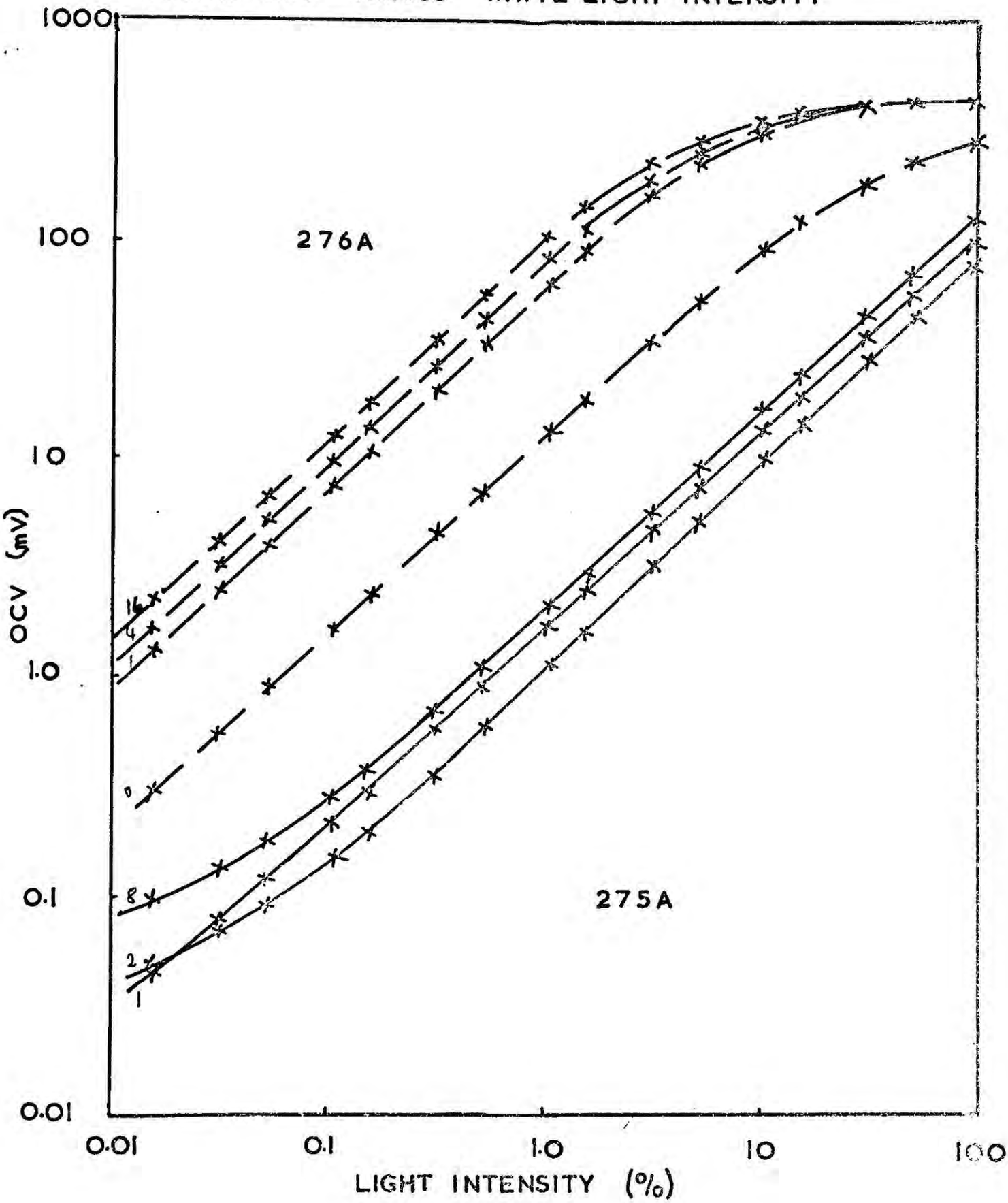

before any heating, and rapidly attained the maximum OCV response curve after a very short bake (Figure 7.9). Cells made on CdS:Cu slices were even better at low light intensities, for example device 218:C, gave saturated characteristics after only one minute at 200$^{o}$C(Figure 7.9).

Cells made from boules 282, 283, 285 were not investigated fully, but even the 10ppm indium doped boule, 282, failed to give a high OCV at low light levels.

From this part of the work therefore, it appears that to achieve a high OCV under weak white illumination it is necessary to use CdS doped with copper or grown in excess sulphur.

## 7.7 SPECTRAL RESPONSE OF THE PHOTOVOLTAIC CELLS

To measure the spectral response a Barr and Stroud VL2 double prism monochromator was used, with a 500W tungsten lamp source run from a stabilised mains supply. The output energy distribution of the lamp was measured with a Hilger and Watts FT 16.301 Schwartz compensated linear vacuum thermopile with a KBr window and a sensitivity of 27 microvolts/microwatt. The illumination at the entrance slits of the VL2 was mechanically chopped at 20 Hz, and the resulting thermopile output was fed to a Barr and Stroud 7921 tuned amplifier. This calibration enabled the OCV spectral response of the cells to be corrected for equal incident energy if required. For the present purposes the differences between one cell and another are more readily

FIG.7.9 OCV VERSUS WHITE LIGHT INTENSITY

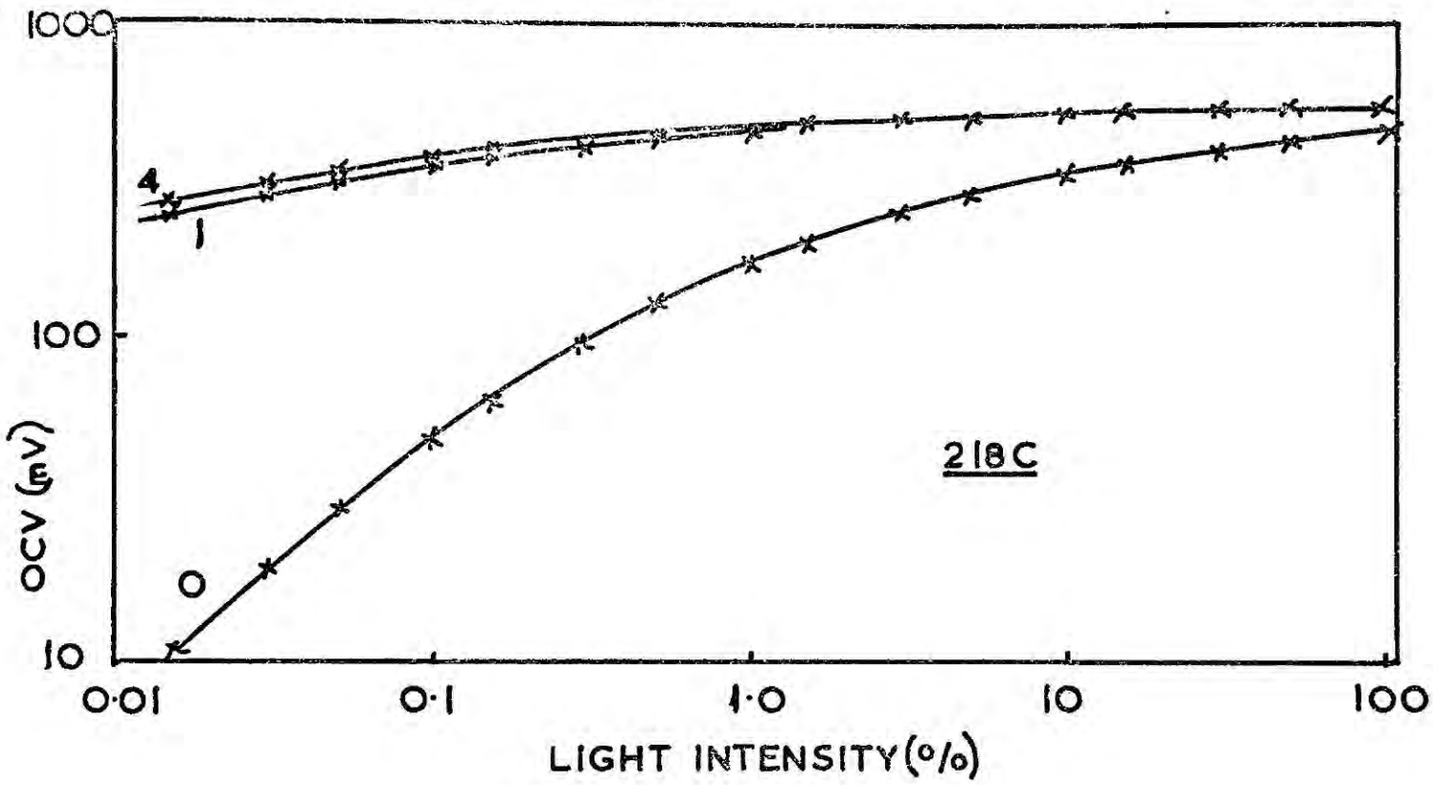


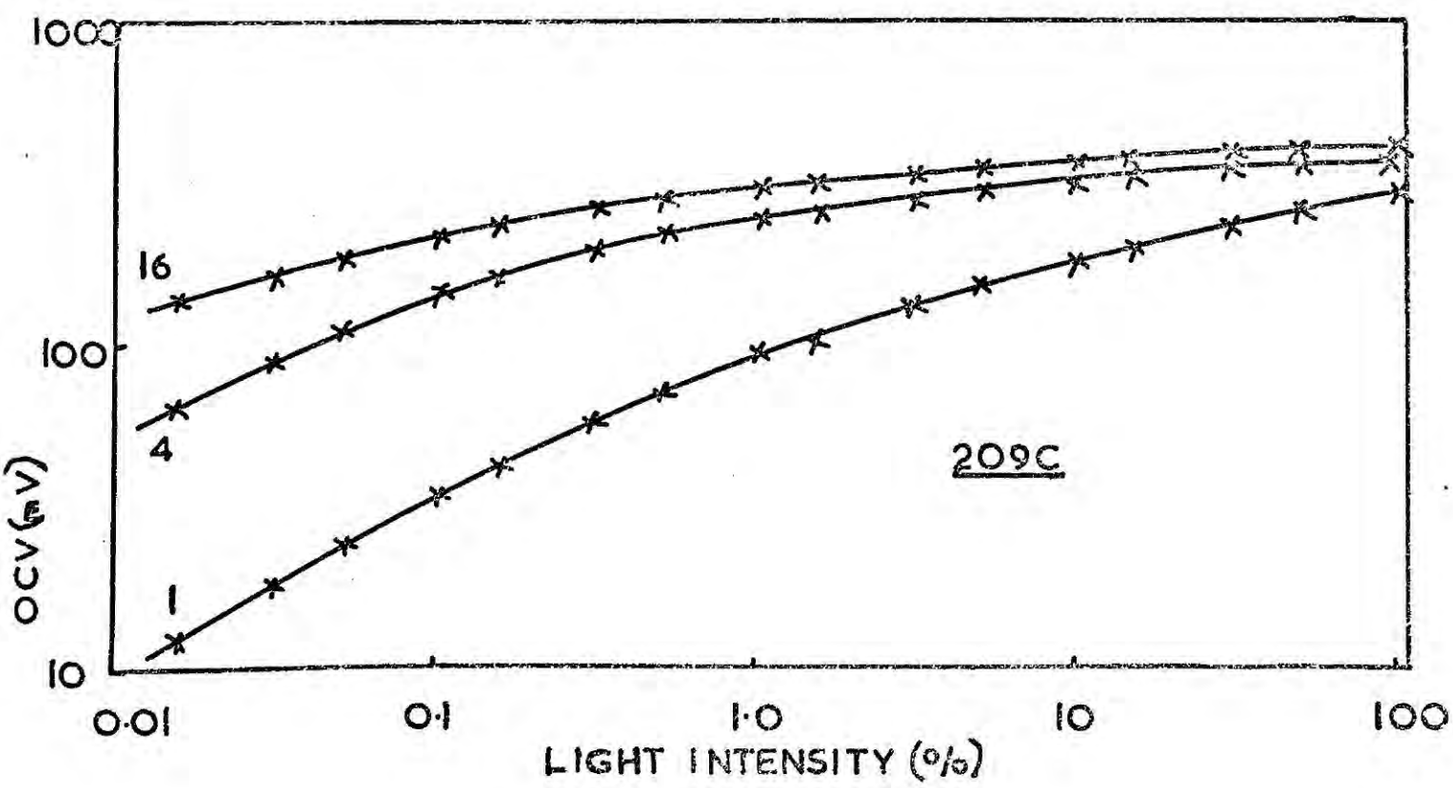

FIG.7.9 OCV VERSUS WHITE LIGHT INTENSITY

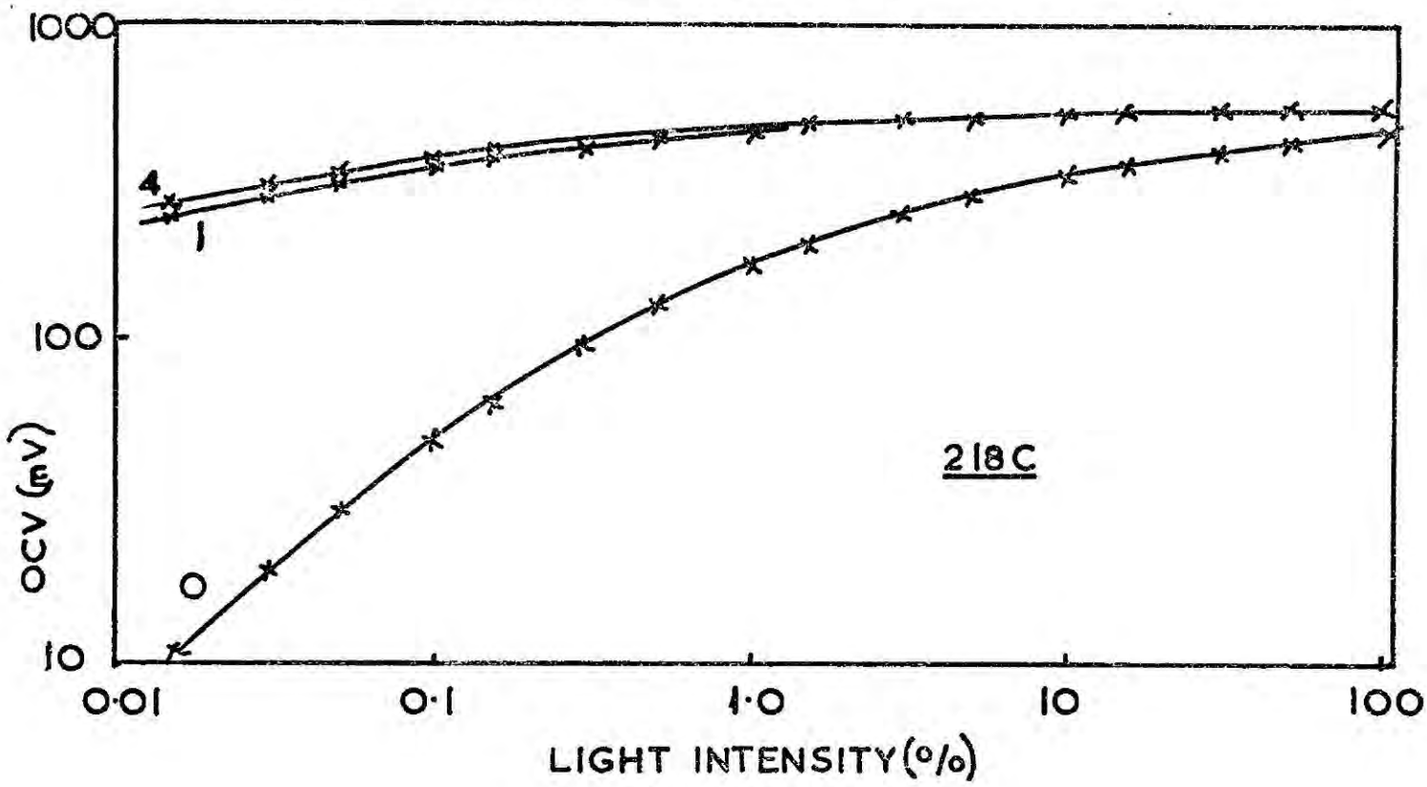


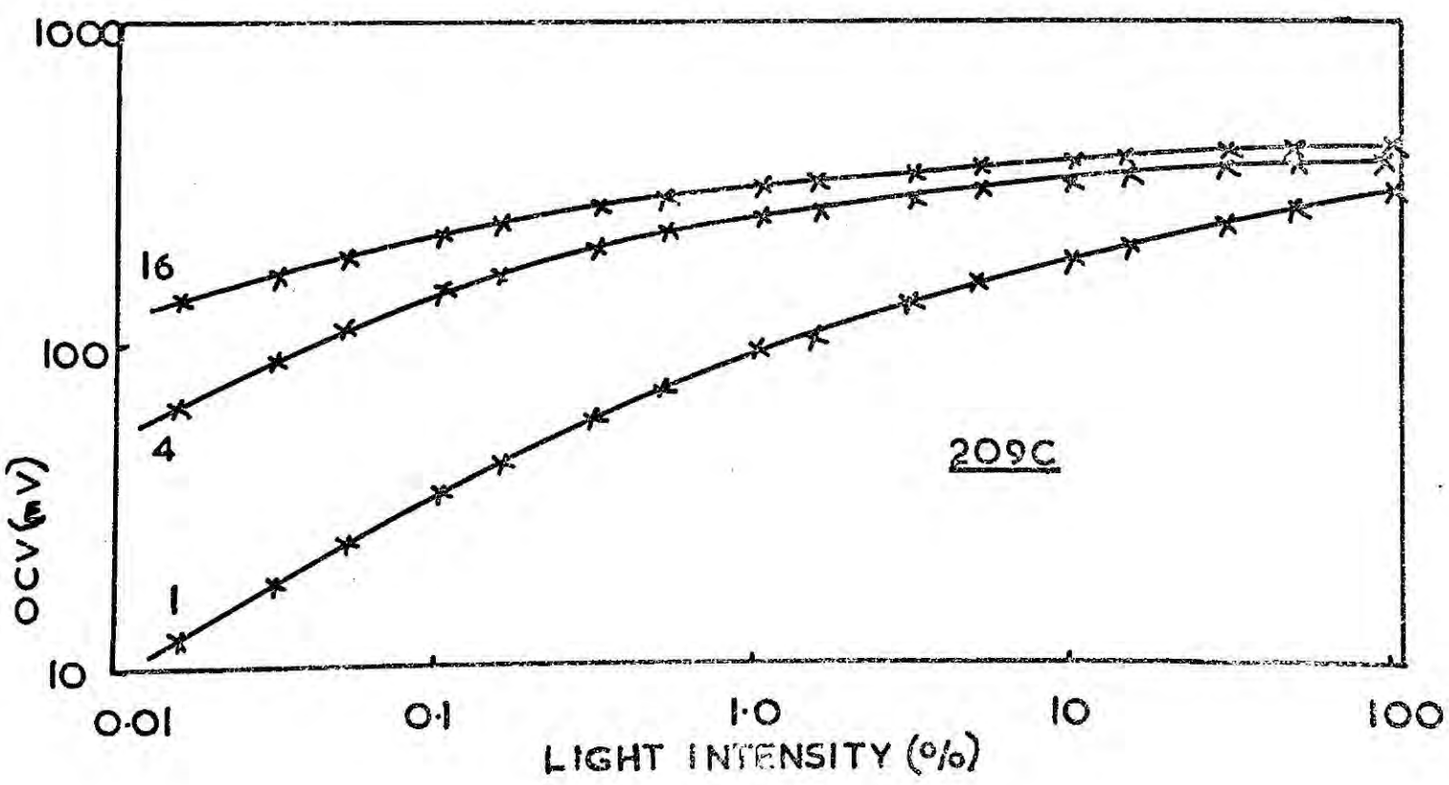

discussed if no such corrections are made, and the absolute values of the OCV are then more readily compared.

The intensity of monochromatic light on the photovoltaic junction through the VL2 was about one microwatt $cm^{-2}$ at the peak of the response. Both entrance and exit slits of the monochromator were held at the same aperture throughout, giving a bandwidth varying monotonically from 380Å at 1.5 microns to 72Å at 0.5 microns.

Only the OCV was monitored (with the GM6020 VVM) since the SCC of all the cells was too low to determine accurately over the whole wavelength band.

The photovoltaic cells were mounted in the metal cryostat described previously, and their temperature was monitored with a copper/constantan thermocouple. Some samples possessed a small thermoelectric emf which was subtracted from the measured voltage to give the OCV. It was established that this emf arose from the CdS part of the junction alone.

No extra structure in the OCV spectral response was observed on cooling the cells to liquid nitrogen temperatures, so that it is only necessary to discuss the room temperature spectral response for a number of cells. Unless otherwise stated the response given is the steady-state value of the OCV reached after several tens of seconds, not the initial voltage. Following heat-treatment all cells were slow to respond to changes

in illumination, although this was not true for cells in the 'as-prepared' condition.

The spectral response of the OCV for both steady-state and initial values is given in Figure 7.10 for a typical cell, 594-A, after baking for a total period of sixteen minutes at 200°C. The differences between the initial and steady-state values became apparent after such treatment. The slow component of the steady-state response enhanced or quenched the initial fast response depending on whether the incident wavelength was shorter or longer than 8000Å. Gill and Bube (1970) have reported a similar phenomenon for the SCC spectral response of their CdS/$Cu_2S$ devices which were prepared under somewhat different conditions.

Figure 7.10 should be compared with Figure 7.11 which shows the steady-state OCV response of cell 594-A after successive periods of heat-treatment (in minutes). The broken curve is an example of the shape of the equal energy spectral response after correction for the spectral distribution of the lamp. Increasing structure appeared on the curves as the heating proceeded, and the relative heights of the two major peaks at 6400Å and 9000Å was reversed after four minutes at 200°C. These two peaks are due either to impurities in the CdS or to the $Cu_2S$. The peak at about 4900Å, the band gap of CdS, was not very evident before heating. Most of the cells had spectral responses with this shape and behaviour.

Differences arose with the two CdS:Cl cells,

FIG. 7.10 SPECTRAL RESPONSE OF OCV

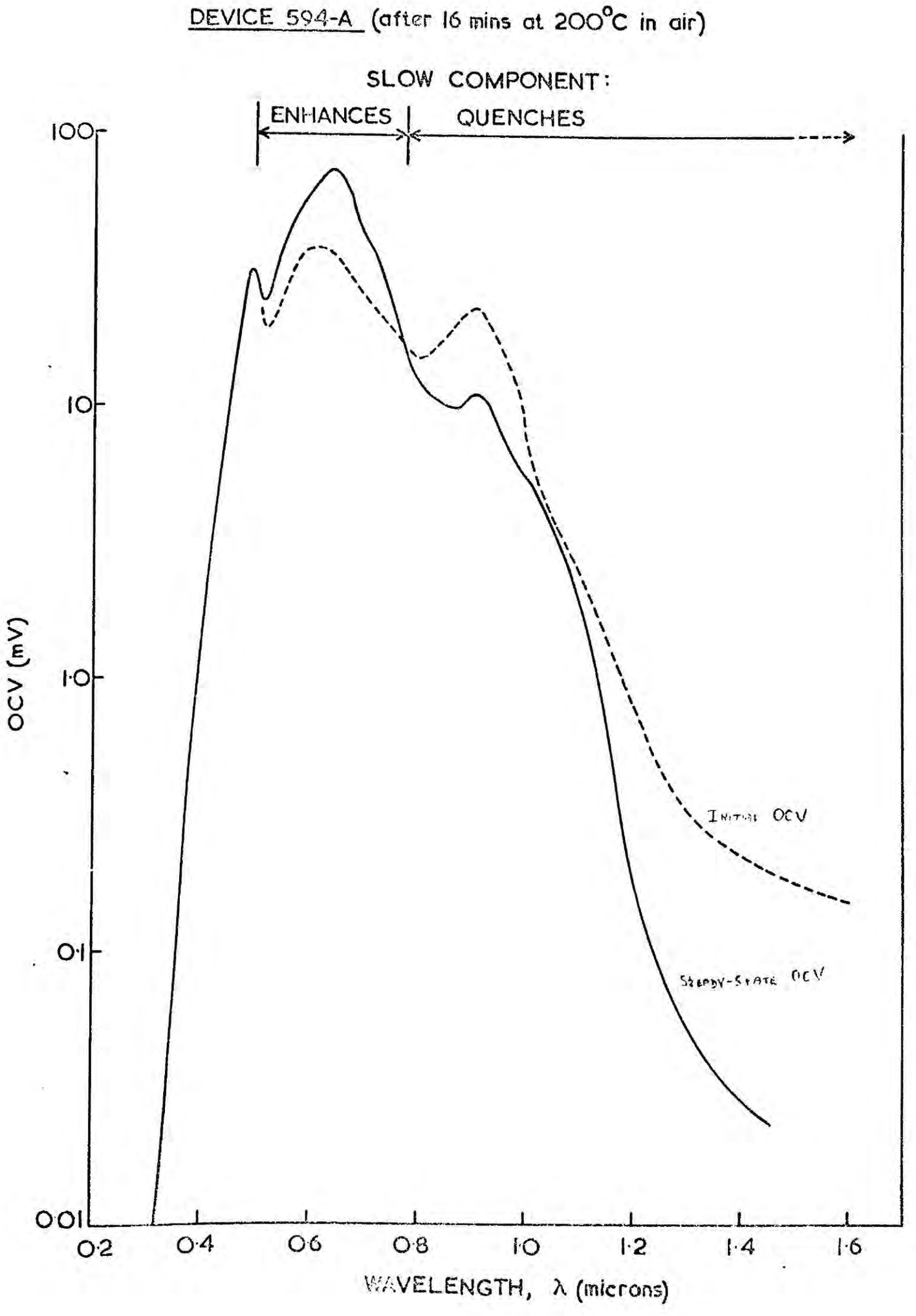

FIG. 7.11 OCV SPECTRAL RESPONSE

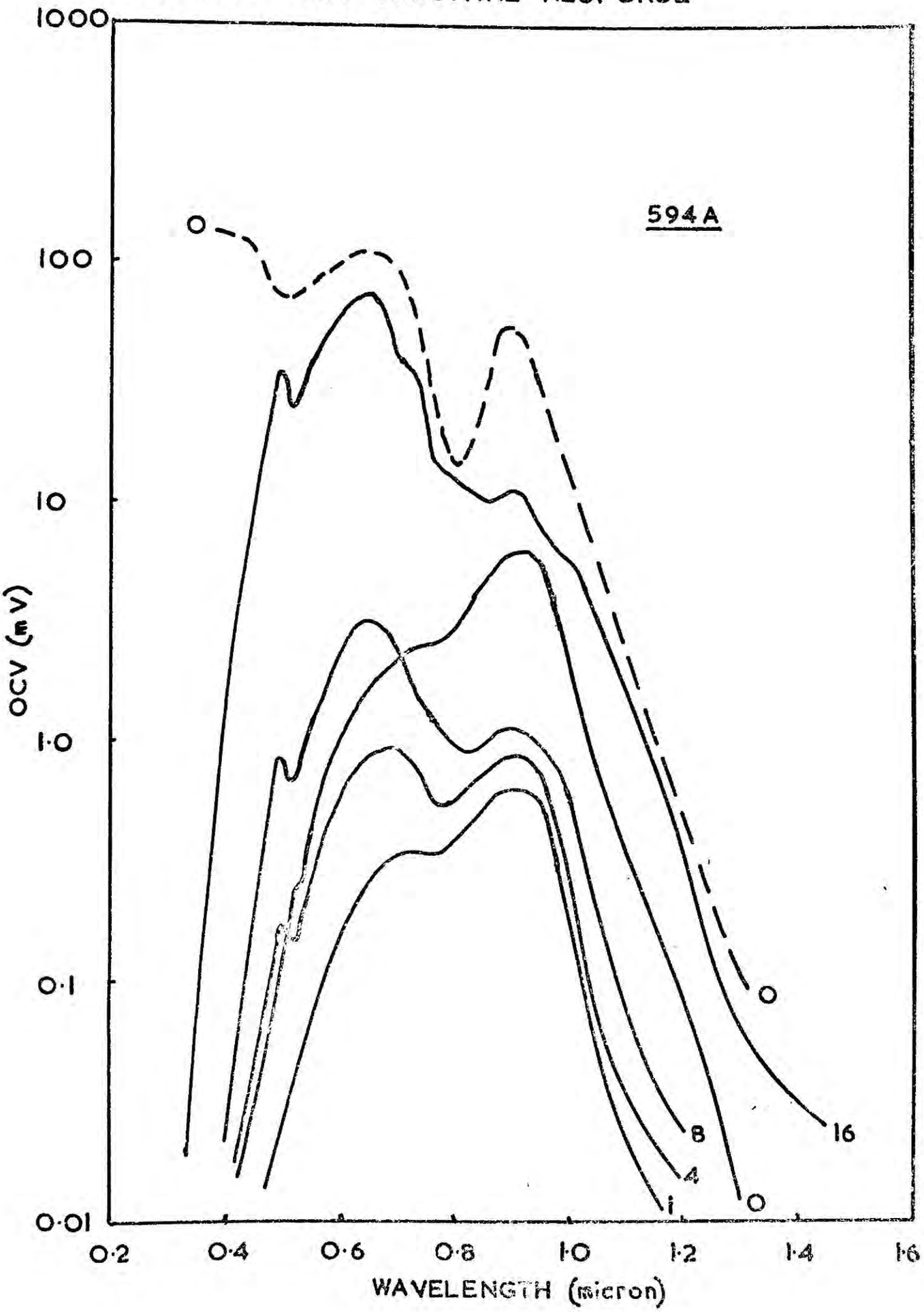

246-C and 247-B, which were similar in having a peak at 0.90 microns which persisted in dominating the response until after the cells had been baked for twelve minutes at 200°C. In addition the peak at 0.49 micron was very small (Figure 7.12). The CdS:In cell, 274-A, also had a small 0.49 micron peak, and did not show the extended long wavelength response which had been reported by the Clevite group. Cells 245-B (excess cadmium) and 218-C (CdS:Cu) were very similar to each other, but again the dopant had no effect on the bandwidth of the response (Figure 7.13).

It is perhaps surprising that the presence of dopants in the CdS had such a small effect on the spectral response, for if the CdS layer had been active in the pair-production process then some extension to the red end of the spectral response would be expected by the presence of, say, indium.

## 7.8 PHOTOVOLTAIC PROPERTIES AS A FUNCTION OF TEMPERATURE

The various dopants do affect some of the other properties of the cells, for example differences in the temperature variation of the OCV can be observed. Before the cells were subjected to any form of heat-treatment they were sensitive to small increases in temperature, even in a vacuum, and irreversible changes took place exactly similar to those brought about by the 200°C treatment. Although with many cells the response to 140mW $cm^{-2}$ white light was not very temperature dependent, a few exhibited large variations in OCV as the temperature

FIG. 7.12 OCV SPECTRAL RESPONSE

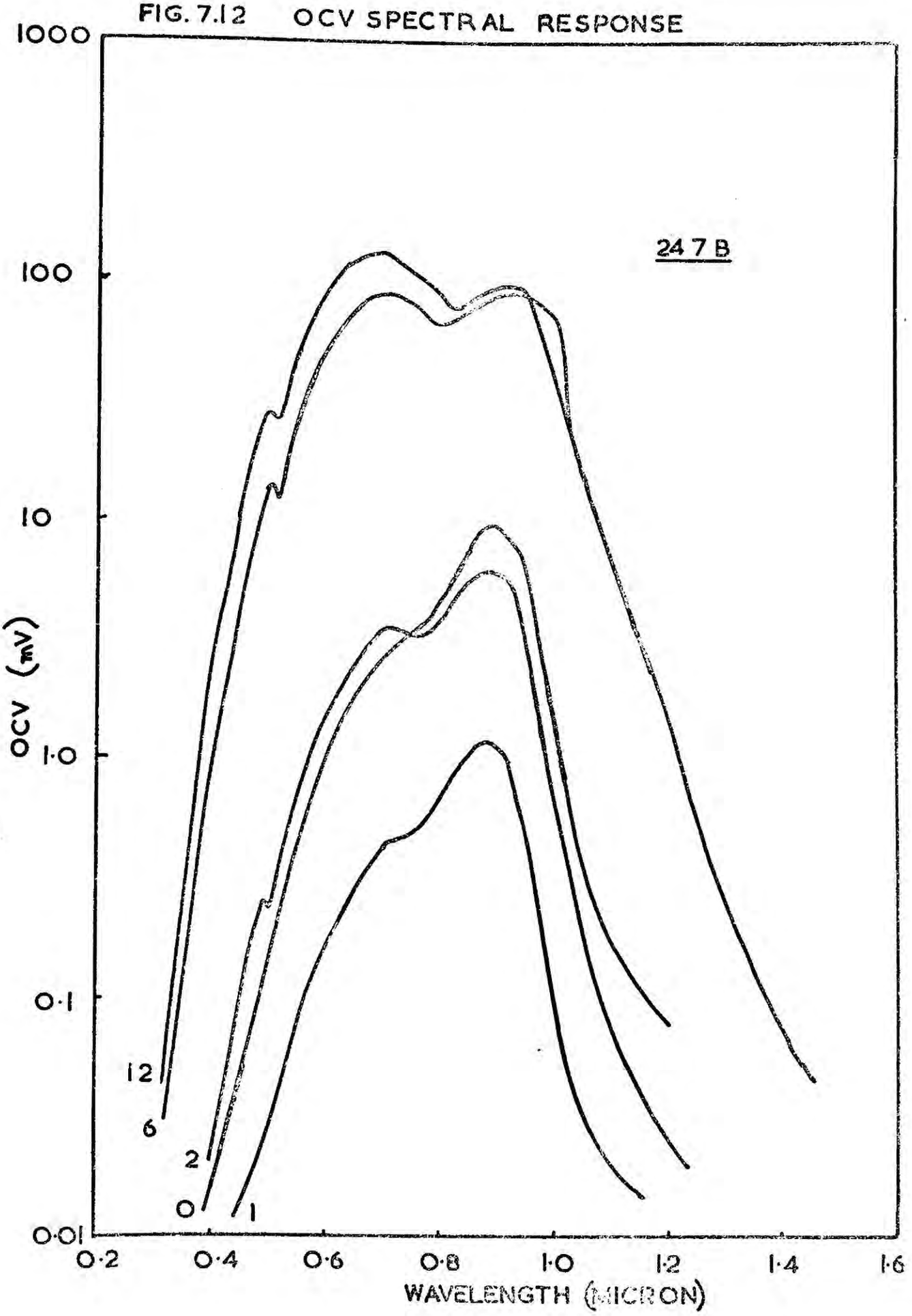

FIG. 7.13 OCV SPECTRAL RESPONSE

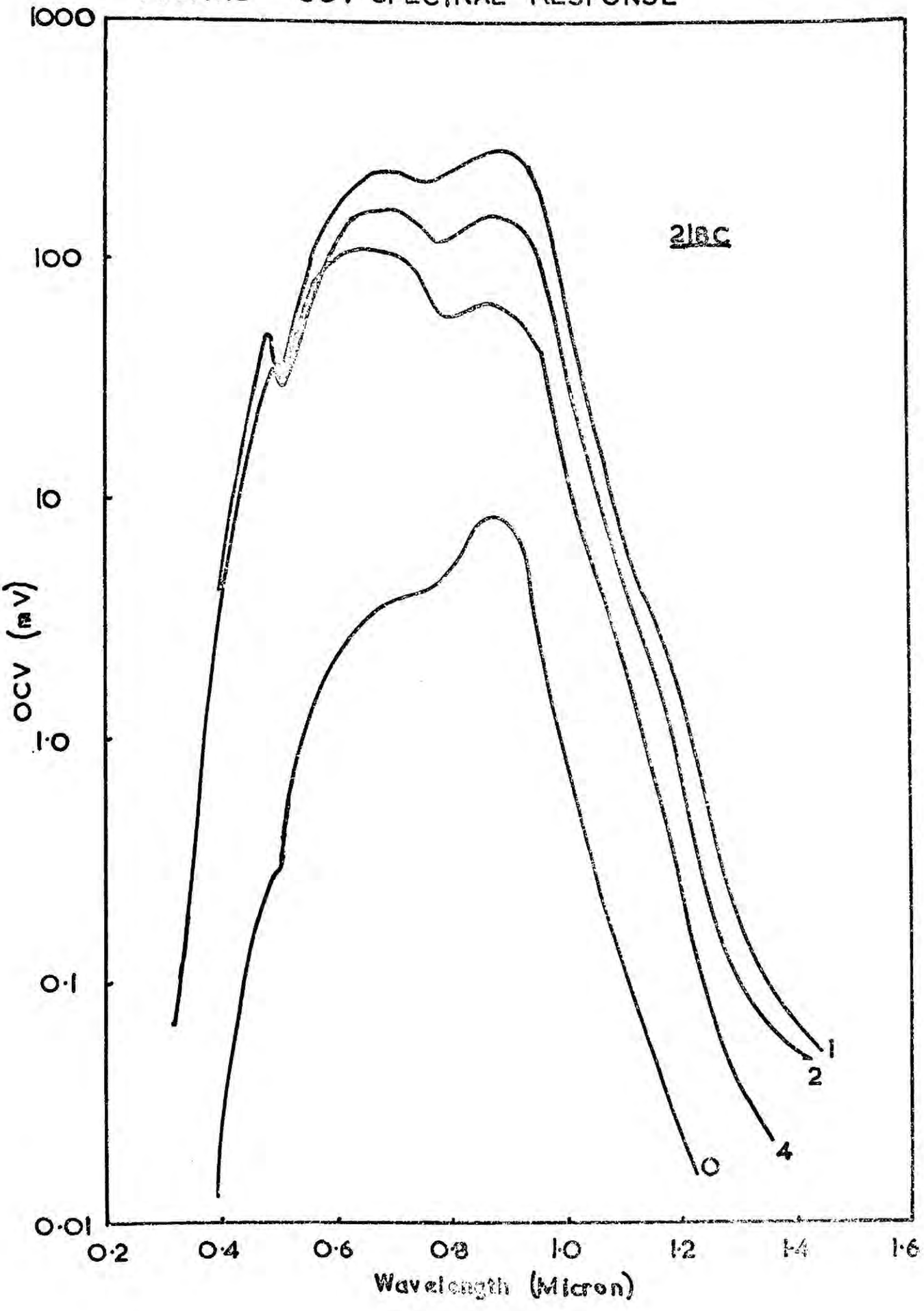

was raised from 100° to 420°K (see Figure 7.14 and 7.15).

The undoped CdS samples behaved very much alike: the structure present after an initial one minute at 200°C gradually vanished after further periods of heating, to give a smooth curve from which the OCV is seen to decrease with increasing ambient temperature.

The CdS:Cu cell, 218-C, in an 'as-prepared' condition behaved as though it had already been subjected to a lengthy heating at 200°C, and in fact heating at 200°C made very little difference. No structure existed on the curve of OCV versus temperature, which was similar to those of the undoped cells after they had been heated. Device 246-C had the most unusual of all the temperature characteristics. A poor low temperature OCV was further degraded by heating at 200°C. 247-B, also doped with chlorine, had a low temperature OCV which decreased during heat-treatment, but not as drastically as 246-C. The CdS:In cells were unstable at low temperatures and their poor low light-level response made accurate measurements impossible.

## 7.9 VARIATIONS IN OCV WITH TEMPERATURE AT DIFFERENT WAVELENGTHS

An attempt was made to determine whether various spectral components of the white light contributed differently to the overall variation of the OCV with temperature. In so doing it was hoped to discover both the source of the poor low temperature response of the

FIG.7.14 OCV VERSUS TEMPERATURE, (am O) SUNLIGHT ILLUMINATION

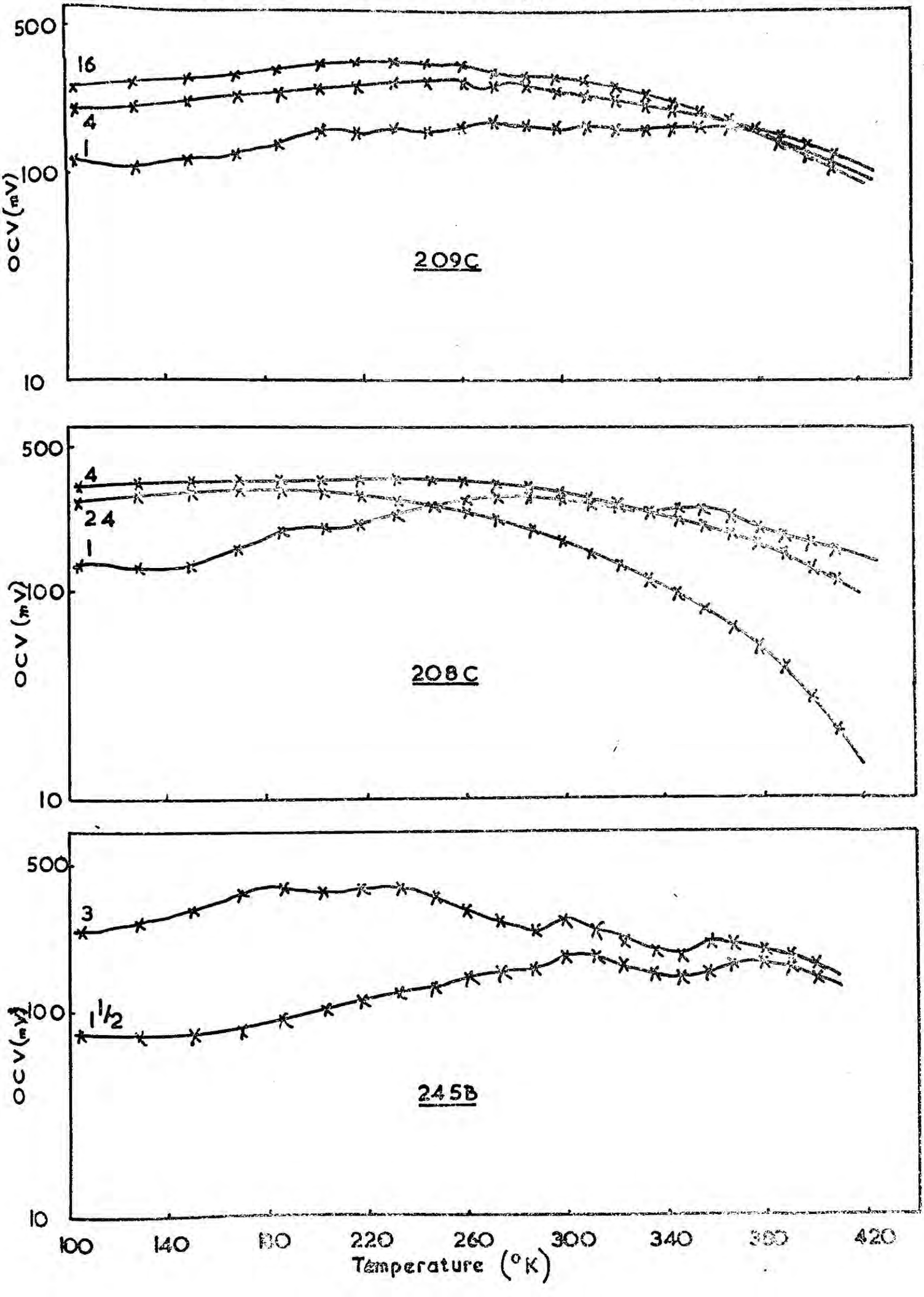

FIG. 7.15 OCV VERSUS TEMPERATURE, amO SUNLIGHT ILLUMINATION

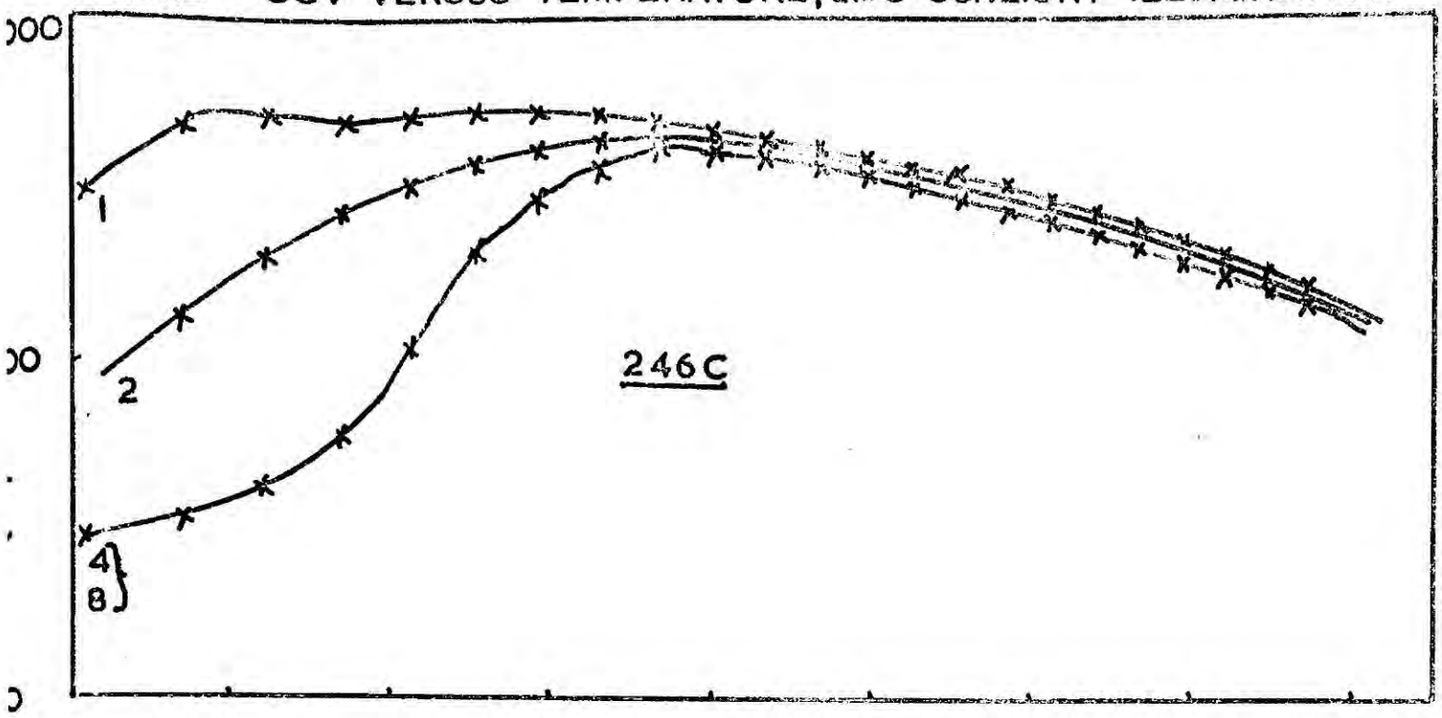


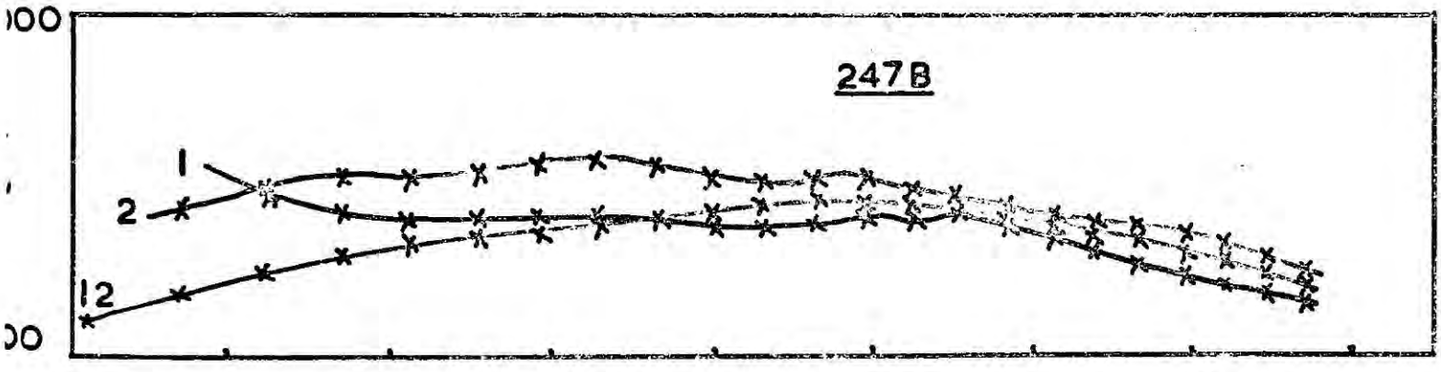


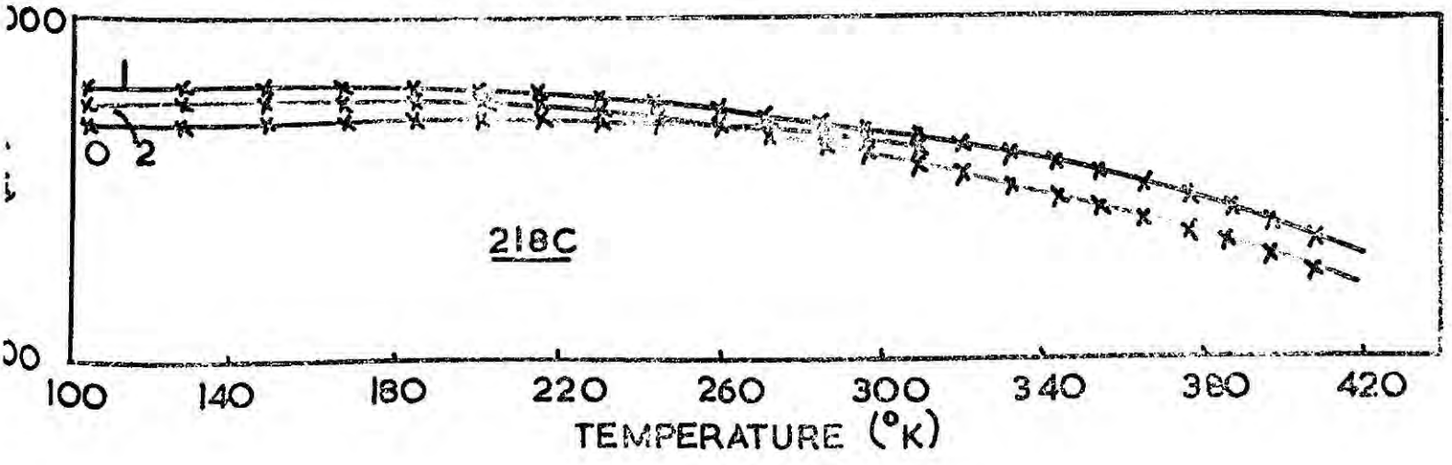

CdS:Cl cells, and the source of the poor high temperature response of all of the cells after lengthy heat-treatment.

First consider Figure 7.16 which shows the OCV excited by light of three different wavelengths as a function of temperature for cell 208-C. Three peaks in the spectral response at approximately 0.90, 0.64 and 0.49 microns have already been shown to account for most of the light usefully absorbed. For this reason light at these three wavelengths was used in this particular experiment. The response of 208-C at 0.90 microns had a maximum at a temperature of 330°K after one minute at 200°C, but this gradually changed during heat-treatment to a minimum, while two adjacent peaks at 230°K and 370°K appeared after 24 minutes at 200°C. Nevertheless after 24 minutes at 200°C the OCV of this device at 370°C under white illumination was falling rapidly with temperature (Figure 7.14). From the lower part of Figure 7.16 it will be seen that the OCV under illumination with both 0.64 and 0.49 micron radiation, the dominant wavelengths after heat-treatment, were falling with temperature.

It is concluded therefore that: (a) the poor high temperature response of this cell to white illumination is due to the decreasing response to 0.64 and 0.49 micron illumination; (b) a quenching effect exists around 0.90 micron, 330°K for the heat-treated cell.

Cell 209-C, also grown with excess sulphur, had a broad minimum at 0.90 micron, 330-370°K, possibly resolvable into two distinct minima.

FIG. 7.16 OCV VERSUS TEMPERATURE, MONOCHROMATIC ILLUMINATION

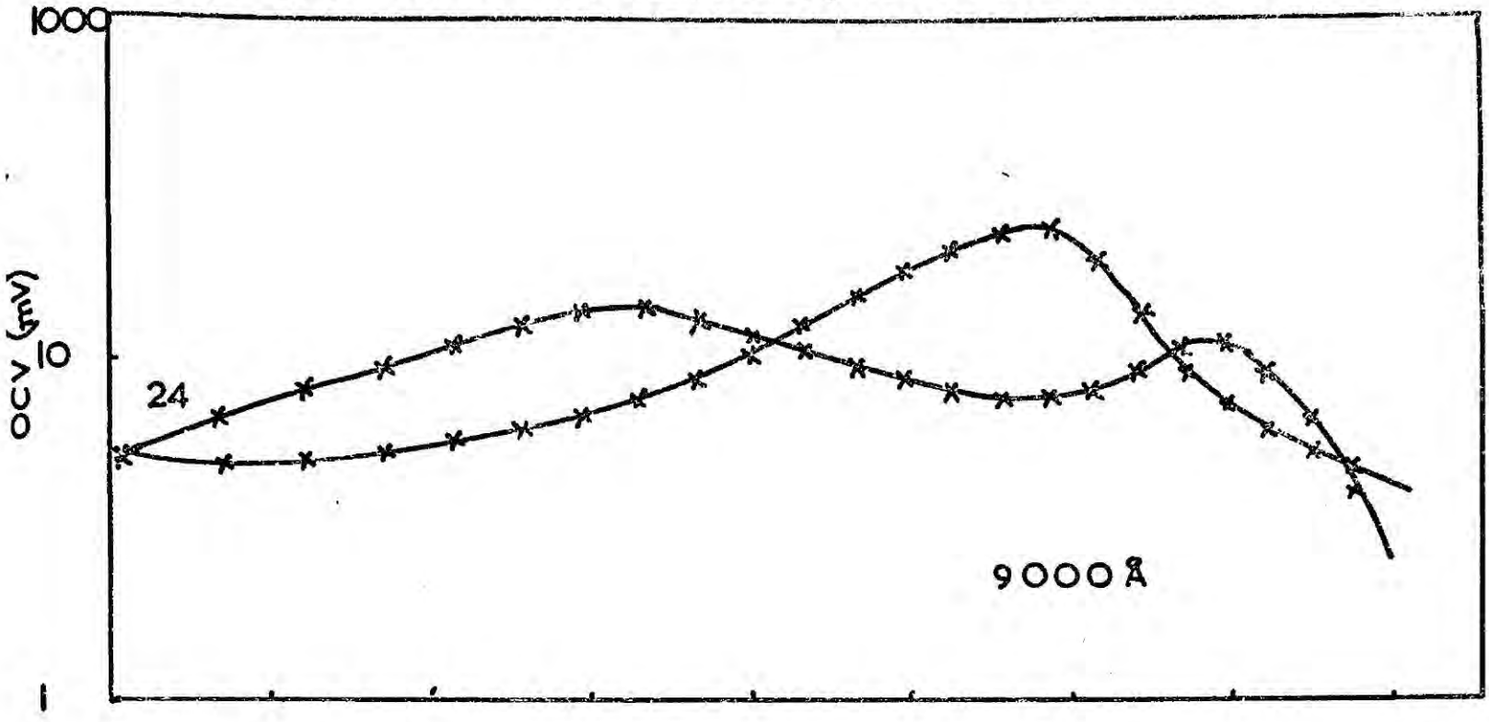


208C

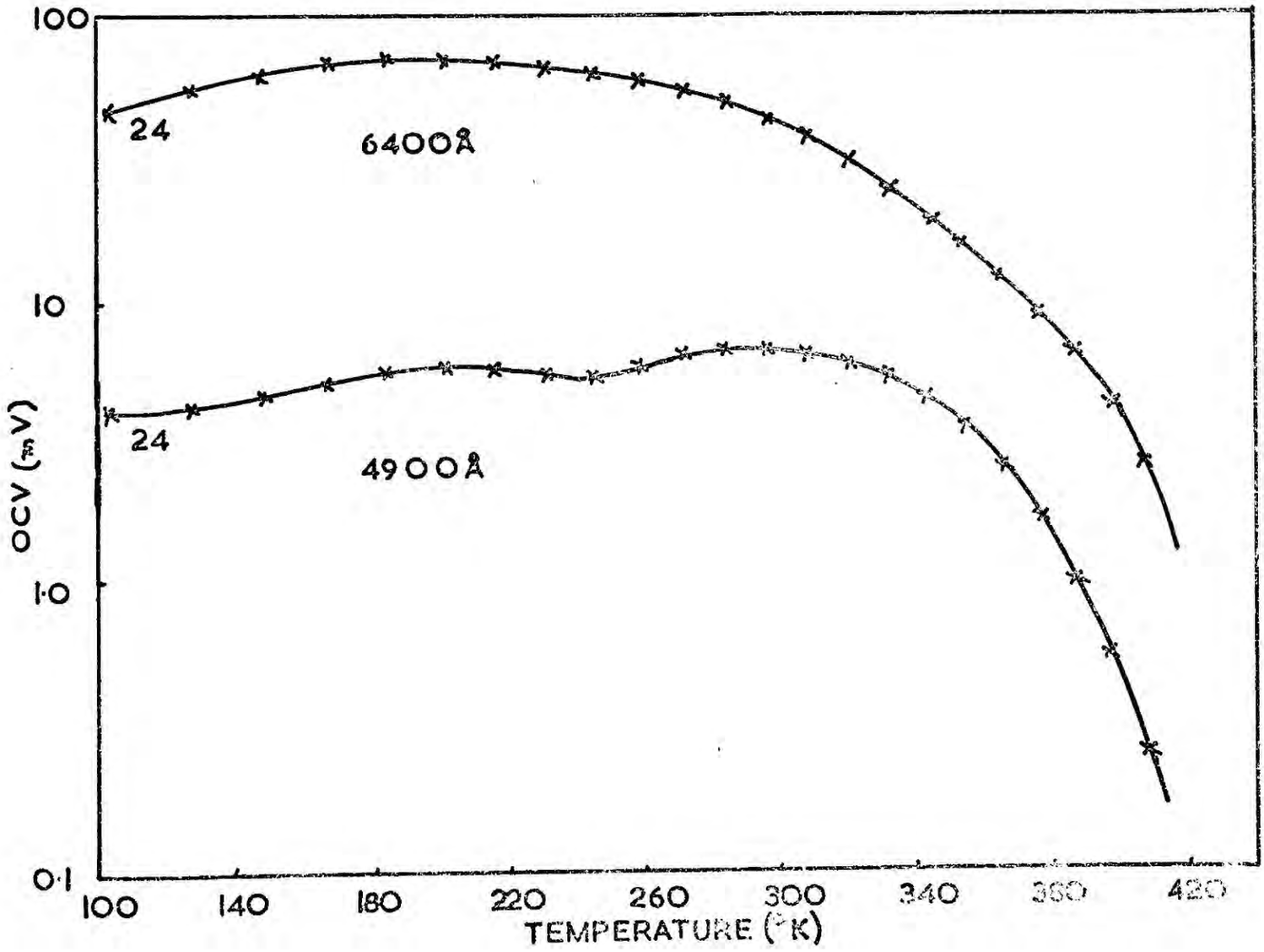

Now consider Figure 7.17. This shows the OCV of cell 246-C as a function of temperature under monochromatic illumination at two stages in the heat-treatment. Two wavelengths have been used, 0.90 and 0.64 micron, and with both of these a large drop in OCV occurred at low temperatures. The OCV excited by white light also displayed this feature (Figure 7.15) but only after several minutes at 200°C. The high OCV of this device at low temperatures in white light after only one minute at 200°C was found to be due to the 0.49 micron component, which for most cells was found to parallel the 0.64 micron response. No definite quenching bands appear for the 0.90 micron illumination but there was a small drop in the 0.64 micron response at 360°K for the heat-treated cell.

The results obtained from the other CdS:Cl cell, 247-B, have evidence of a small broad quenching band near 340°K for the 0.90 micron radiation and a clearer minimum at 330°K for the 0.64 micron radiation.

Results from measurements of the same type on the copper doped cell 218-C are given in Figure 7.18. These exhibit the same broad structureless shape associated with previous curves from this device. A quenching effect was again present for the heat-treated cell, at 0.90 micron, 310°K.

Cell 594-A had minima on both the 0.90 and 0.64 micron curves after prolonged heating. These were at 340°K (0.64 micron) and at 320°K (0.90 micron).

FIG.7.17 OCV VERSUS TEMPERATURE, MONOCHROMATIC ILLUMINATION

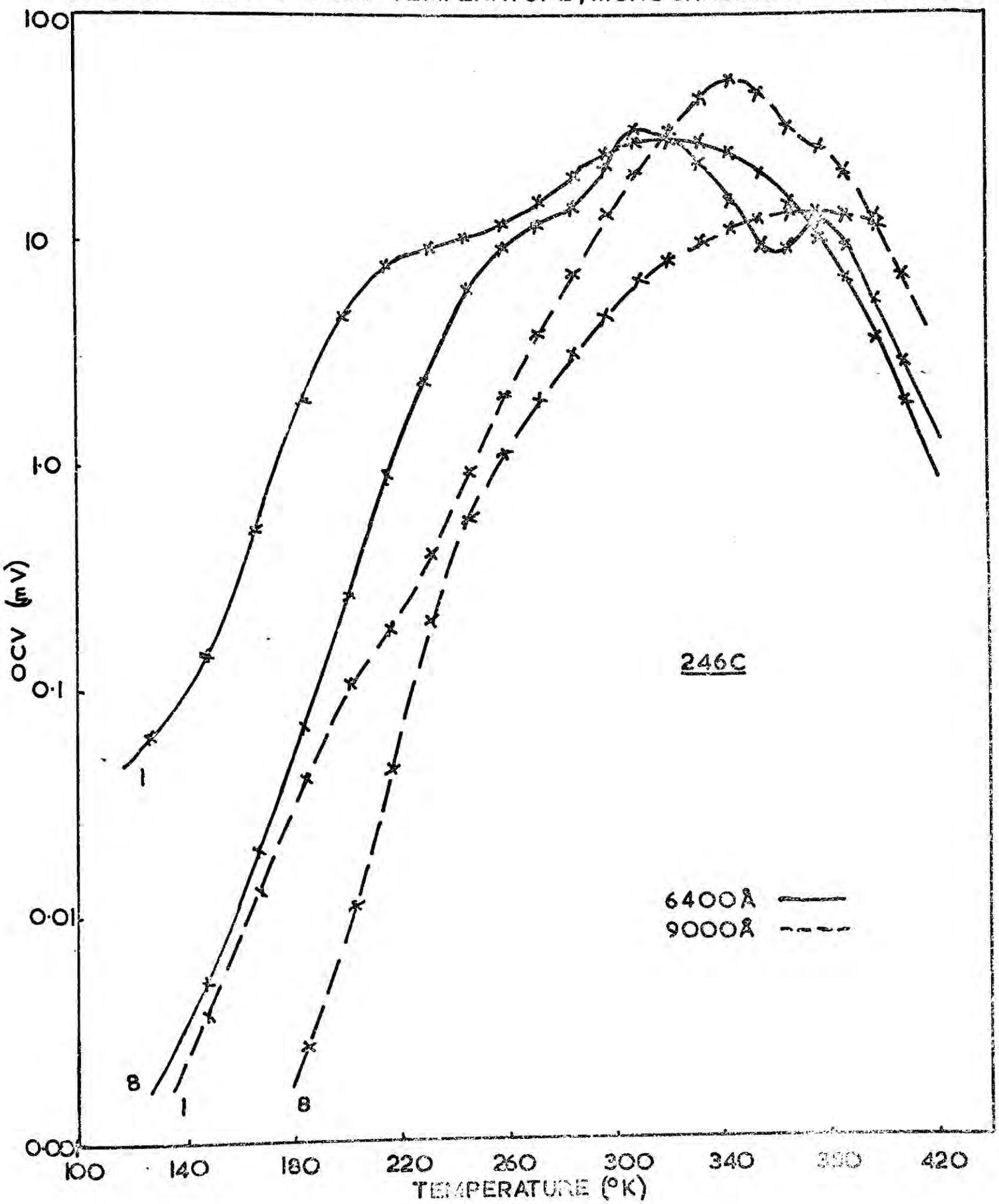

FIG.7.18 OCV VERSUS TEMPERATURE, MONOCHROMATIC ILLUMINATION

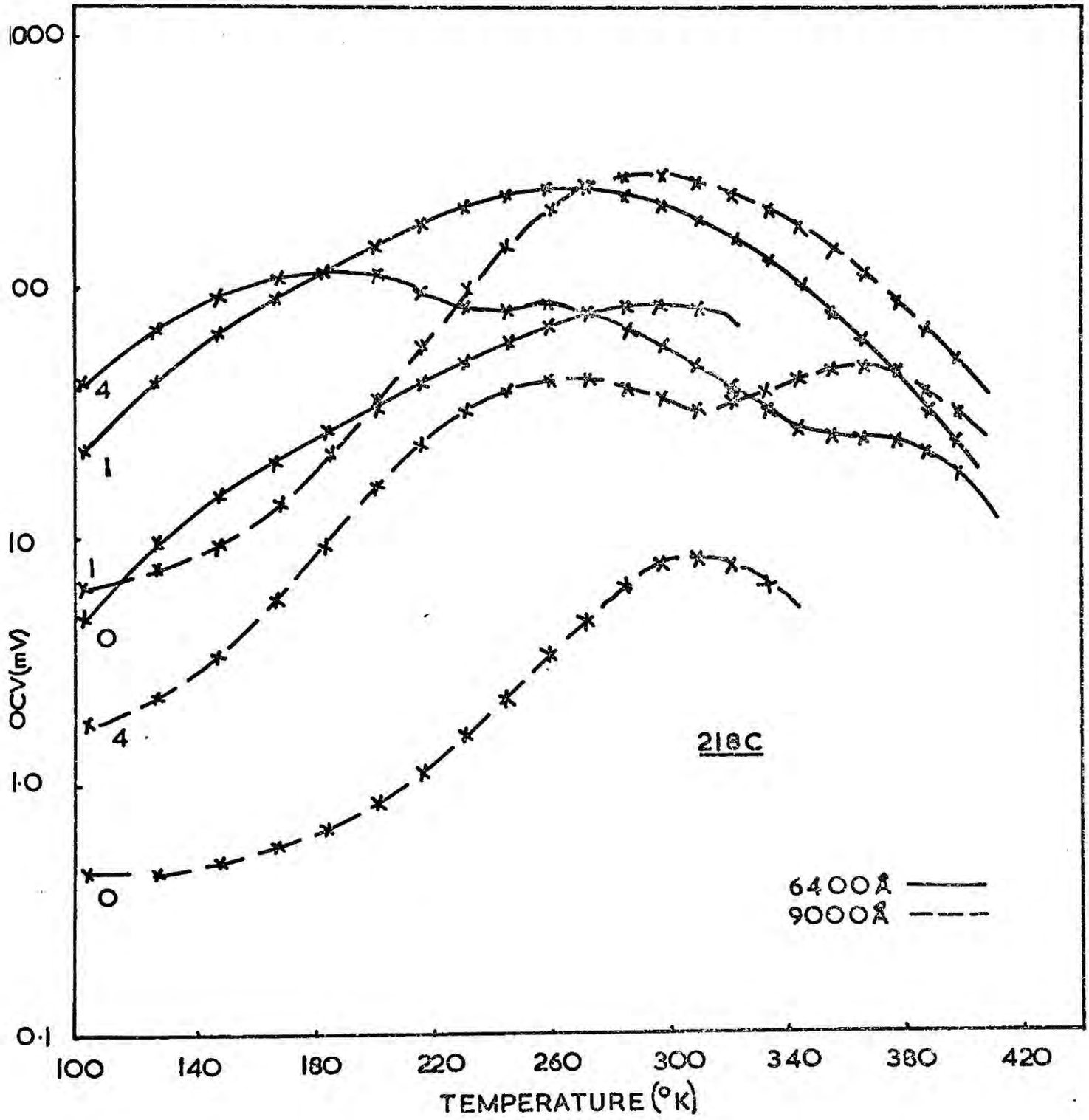

It is possible that some of the structure of these curves is similar to that found in TSC measurements, and which is associated with the presence of traps in the CdS, but TSC experiments on reverse-biased CdS/$Cu_2S$ junctions fabricated from these CdS boules have so far failed to yield any information owing to the relatively high reverse leakage current. This is expected to be lower on perfect single crystal cells, since the boule CdS slices have many structural defects (e.g. grain boundaries) which aid leakage and carrier recombination.

The minima observed in the OCV versus temperature curves are summarised in Table II.

TABLE II

| Cell No. | Dopant | Minima ($^{o}$K) | |
|---|---|---|---|
| | | 0.90 micron | 0.64 micron |
| 208-C | S excess | 330 | — |
| 209-C | S excess | 330-370 | — |
| 218-C | Cu+S excess | 310 | — |
| 246-C | Cl+Cd excess | — | 360 |
| 247-B | Cl+S excess | (340) | 330-340 |
| 594-A | — | 320 | 340 |

## 7.10 JUNCTION CAPACITANCE

Preliminary measurements of conductance and capacitance as a function of the bias voltage have been made using an instrument designed and built by Martin (1970). These have shown the existence of photocapacitance effects (i.e. illumination with white light produced

an increase in junction capacitance), and merit further study to determine if enhancement and quenching effects are present for combinations of wavelength and temperature, similar to those already described. Lindquist and Bube (1970) have published some photocapacitance results, obtained mainly from non-heated devices, and have used the evidence to support their theory of conduction across the junction by tunnelling.

## 7.11 ELECTROLUMINESCENCE

Attempts were made to detect i-r electroluminescence from biased CdS/$Cu_2S$ devices. The detector employed was an EMI 9684-B i-r photomultiplier with S1-type photocathode, mounted in a metal cryostat which enabled the photocathode to be cooled with liquid nitrogen. This reduced the dark current to about 6nA at 1.1kV. The sensitivity was 20A $lm^{-1}$ at room temperature but was reduced by cooling the tube. The long-wavelength response peak was found to be at 6000Å, with a cut-off at about one micron.

No detectable emission was obtained from any of the devices either with forward or reverse bias, both before and after heat-treatment, even when the photomultiplier input was mechanically chopped at 800Hz and the anode was connected to the Barr and Stroud 7921 tuned amplifier. Either the emission was beyond the sensitivity or waveband of the photomultiplier, or the injected carriers recombined non-radiatively at, say, the junction interface states.

## 7.13 SUMMARY

To obtain the maximum OCV from the CdS/$Cu_2S$ photovoltaic cell it has been found necessary to use CdS with a resistivity of a few hundred ohm cm. This can easily be achieved by thin film techniques whether dopants are incorporated into the film or not.

Unfortunately the use of indium as a dopant has been found to yield poor devices with long response times and poor low light intensity response. A possible advantage of a CdS:In/$Cu_2S$ cell is that the response to light intensity is linear. Cells formed on CdS grown in excess sulphur were also poor except in respect of their OCV response to low light intensities which was good. CdS:Cl produced cells with a high OCV, but the dopant had no great effect on the other characteristics. CdS:Cu was more useful as the starting material since it produced a device which had good characteristics before any heat-treatment, coupled with a fast response. Heat-treatment, which is usually necessary to achieve high performance, generally has the effect of slowing the response.

Heat-treatment of the other cells, whilst improving the OCV which could be obtained with low level illumination, also produced temperature quenching effects with 0.90 micron illumination, especially at temperatures slightly above room temperature. CdS:Cl cells showed temperature quenching effects above room temperature with 0.64 micron illumination.

After heat treatment, all devices possessed a slow component of the OCV under excitation with wavelengths greater than 0.49 micron. This either enhanced or quenched the initial rapid response, according to wavelength. The 0.49 and 0.64 micron peaks in the steady-state spectral response became more dominant with extended heat-treatment at 200°C.

No differences in the shapes of the spectral responses were found for any of the cells formed on doped CdS, but the variation of the OCV with temperature was different from one sample to another, and became more complex as the heat-treatment continued. The cell with the smoothest temperature variation was again that prepared on the CdS:Cu base layer.

The treatment given to the surface of the CdS before plating with $Cu_2S$ was found markedly to affect the maximum OCV obtainable from any one boule. Rough surfaces gave poor OCVs, but good SCCs.

The interpretation of these results will be continued in a further chapter.

REFERENCES

W.D. Gill and R.H. Bube (1970), J.A.P. 41, 3731-3738.

P.F. Lindquist and R.H. Bube (1970), Proc. Eighth IEEE Photovoltaic Specialist's Conference.

P.G. Martin (1970), M.Sc. Thesis, Durham University.

# CHAPTER 8 : DISCUSSION OF THE PHOTOVOLTAIC MEASUREMENTS

## 8.1 INTRODUCTION

Several of the results described in the previous chapter require more discussion than was afforded by the brief comments which accompanied their description. It is possible to offer reasonable explanations for much of the behaviour of our CdS-$Cu_2S$ heterojunctions in terms of the 'Clevite' model of the device. (See Section 2.6).

## 8.2 HEAT-TREATMENT

The effect of the heat-treatment was to modify the responses of the cells to a variety of stimuli. Not only were the magnitudes of the OCV and SCC affected, but their spectral response, response time, and their variation with temperature were also affected. When certain dopants were present in the CdS layer, heat-treatment produced less drastic changes in the cell behaviour.

In general terms we can understand all these phenomena as due to the thermally enhanced diffusion of copper from the $Cu_2S$ into the n-CdS to form a compensated layer of high resistivity CdS. As the heating period at 200$^{o}$C was extended this layer grew and its presence became more obvious. The initial stages of the heat-treatment also affected the surface reflectivity of the $Cu_2S$, and it became darker and more matt.

Since the OCV and SCC both increased during the initial stages of heating, there must be either more efficient light absorption or better carrier collection,

together with an increased barrier height. After the height of the barrier had attained its constant value and the OCV was at a maximum, the response to low light levels improved, whilst both the SCC and OCV began to decrease slightly.

## 8.3 i-CdS REGION

It will be remembered that the best cells possessed an OCV before any heat-treatment whatsoever. This means that a potential barrier of some unknown height must exist between the $Cu_2S$ and the CdS before heat-treatment. The intermediate i-CdS layer helps to improve the SCC by photoconductive effects which aid electron transport across the junction region, and at the same time allows larger OCVs to be developed by the potential barrier than would otherwise be possible between $Cu_2S$ and CdS, by reducing the recombination currents. It also prevents tunnelling between $p^+$ and $n^+$ regions which produces instabilities in diode behaviour, as observed in the I(V) characteristics of the unheated cells. Further it is suggested that the poorer cells had defects in the junction region which shorted out the photovoltage, but that subsequent formation of the i-CdS region widened the junction region and removed the short-circuit paths.

The long time constant effects associated with the baked cells are similar to those which exist in high resistivity, photoconductive, CdS which contains traps which are responsible for the slow decay observed in photoconductivity measurements. Several

tens of seconds are required before such traps attain thermal equilibrium after any change in the bias illumination. The quenching and enhancement behaviour of the slow component of the OCV response to monochromatic excitation is typical of the photoconductive effects in CdS which are connected with the capture and release of holes at recombination centres in the CdS.

The increase in OCV for baked cells on exposure to 4900Å radiation is probably due to increased light absorption in the CdS layer. Since the $Cu_2S$ does not appear to be becoming more transparent to illumination with continued heating, then light absorption must be becoming more efficient in the CdS. The only suggested change in the CdS is the increase in width of the insulating layer so that it must be this which is actively involved in the light absorption at 4900Å. It will be remembered however that not all of the cells had a noticeable peak in the spectral response at this wavelength.

## 8.4 DOPANTS

As might be expected from the preceding section, cells formed on CdS which already contained copper needed little heating before optimum performance was obtained. The use of CdS:Cu resulted in good efficient cells without the impaired response time or temperature quenching effects which were characteristic of the heat-treated cells. The CdS:Cu cells are likely to have an extremely thin i-CdS region and its presence is

practically undetectable. It appears from this that an i-CdS layer is not essential for cell operation.

Indium in the CdS layer appears to affect the rate of growth of the i-CdS region, because much longer periods of baking were required to produce the behaviour typical of the other heated cells. In fact it was difficult to achieve high OCVs at low light levels, and a linear response to light intensity was recorded. The CdS:In slices always formed cells with long response times. (Shiozawa et al, 1968, reported that indium doping slowed the rate of growth of i-CdS and thus improved the high temperature stability of these cells).

CdS grown in excess sulphur had similar effects on the properties of the heterojunctions for which it formed the base layer, but to a lesser degree than CdS containing indium. It should be noted that the problem of poor cells formed from sulphur-rich CdS is not encountered in the thin film device since, as will be shown in Chapter 9, the evaporation of CdS leads to cadmium-rich rather than sulphur-rich layers.

Junctions formed on chlorine-doped CdS always had a poor OCV under 4900Å illumination, as had the less-highly doped CdS:In cells. In addition they had more extreme temperature quenching effects than junctions on other CdS crystals.

## 8.5 OCV SPECTRAL RESPONSE

The maxima of the three peaks in the OCV spectral response were located at wavelengths of 4900Å, 6400Å,

9000Å, which correspond to photon energies of 2.53eV, 1.94eV, 1.38eV. The first of these has already been attributed to direct band to band transitions in the CdS. The other two were at first thought to be caused by absorption in the $Cu_2S$ layer which has the two band gaps of 1.8eV (direct) and 1.2eV (indirect). However if that were so it would be difficult to explain why their relative heights should change after heat-treatment, and in particular to find reasons for the increased absorption at 6400Å in the heat-treated cells. This latter effect may be connected with the change in composition of the copper sulphide layer as it undergoes heating and becomes deficient in copper (Section 2.2), which will produce a change in the absorption coefficient and energy gaps. Any such effect however is unlikely to be large. If these two peaks in the spectral response were due to absorption in the copper sulphide layer, then there would be little direct evidence for photo-carrier creation at impurity levels in the CdS. However, we suggest that the 6400Å peak is due predominantly to absorption of photons by centres in the copper-doped CdS, in agreement with Gill et al (1968) who came to a similar conclusion from their experiments on the SCC spectral response of CdS-$Cu_2S$ junctions. It should also be noted that copper doped CdS has a photoconductive maximum at about 6400Å. Thus the suggestion is that an increase in the OCV at this wavelength after baking is associated with the increased number of copper impurities in the CdS, and

only the 9000Å absorption is due to excitation across the indirect gap in $Cu_2S$. (In agreement with these conclusions it should be stated that Bube et al (1962) reported that copper levels exist at about 1.7eV below the conduction band in heavily copper doped CdS).

Corroborating evidence is provided by Nakayama (1969) who found that cells with thick copper sulphide layers had their spectral response centred on 9000Å, whereas cells with thin $Cu_2S$ gave a large response at 6400Å and less at 9000Å.

Thus the observation that the long wavelength spectral response was constant irrespective of CdS impurities is not so surprising since this portion of the spectrum is associated solely with absorption in the $Cu_2S$. Indeed, impurities may provide recombination centres for the photo-electrons passing through the CdS, and so would be a source of inefficiency (Section 1.3.2).

## 8.6 THERMAL QUENCHING OF THE OCV

Finally we must mention the temperature quenching effects observed in heat-treated cells under monochromatic excitation. Similar optical and thermal quenching effects have been observed in the luminescence and photocurrent phenomena of CdS crystals. For example, Burgett and Lin (1970) have attributed the i-r quenching of the cathodo-luminescence of CdS:Cu to doubly ionised copper centres at levels 0.89eV and 1.38-1.55eV above the valence band of CdS. Rushby (1966) has observed i-r quenching of the photocurrent in

sulphur-rich CdS which was produced by levels at about 1.40eV and 0.86eV above the valence band. Optical quenching of the photocapacitance of CdS-$Cu_2S$ junctions has been reported by Lindquist and Bube (1970) which may be caused by energy levels at about 1.4eV and 0.92eV above the valence band of the CdS. Thus two energy levels at about 0.9eV and about 1.4eV are frequently observed in various quenching phenomena in CdS crystals, some of which are intentionally doped with copper. Gill and Bube (1970) have also deduced the presence of two further levels from their investigation of optical quenching of the photocurrent in CdS-$Cu_2S$ junctions. They suggest the existence of two centres at 0.3eV and 1.1eV above the CdS valence band, perhaps due to copper impurities in the CdS. Bube et al (1962) report that somewhat similar levels were found by Avinor (1959), i.e. at 2.13eV below conduction band in copper-doped CdS and at 1.38eV below conduction band in CdS doped with copper plus indium.

Now let us return to the quenching effects observed in the present experiments on the OCV response of the cells to monochromatic illumination. The first of these was the slow optical quenching or enhancement of the OCV response to monochromatic illumination. For wavelengths greater than 0.78 micron quenching took place, and for wavelengths between 0.5 and 0.78 micron enhancement of the initial OCV occurred. The second effect was the thermal quenching of the OCV at certain wavelengths of illumination, as summarised in Table II, Chapter 7.

Enhancement of the OCV at wavelengths between 0.5 and 0.78 micron is associated with optical absorption in the i-CdS as discussed above. There appears to be a slow increase in the photoconductivity of this region when the cell is exposed to the low levels of illumination obtained from the monochromator. The resulting slow growth in the OCV is associated with the low capture cross-section of the shallow and medium depth electron traps, which must be filled before the maximum photocurrent can be attained.

Quenching of the OCV at wavelengths greater than 0.78 micron is probably caused by negative photoconductivity, which is analagous to the i-r quenching observed when two beams of light of the correct wavelength fall simultaneously on a CdS photoconductor. Thus irradiation in this band of wavelengths (0.78 to 1.2 micron) will cause the resistance of the i-CdS to increase as the recombination centres become active and the OCV will fall as the loss mechanisms become more important.

It is difficult to give the exact mechanism for the combined optical and thermal quenching of the monochromatic OCV, but the reduction in the low OCV at 0.90 or 0.64 micron at temperatures only just above room temperature may be connected with thermally assisted filling of copper levels or complexes. It should be noted that the usual thermal quenching of photoconductivity requires temperatures of about $400^{o}K$.

Much remains to be done concerning the important impurities in the CdS region of the junction, but it is interesting to note that the $Cu_2S$ layer has a behaviour which is consistent with the general belief that it is highly degenerate, i.e. heat-treatment has little effect on the characteristics of the $Cu_2S$.

REFERENCES

A. Avinor (1959) Thesis, University of Amsterdam.

R.H. Bube et al (1962), Phys. Rev. 128, 532.

C.B. Burgett and C.C. Lin (1970), J. Phys. Chem. Solids, 31, 1353-1359.

W.D. Gill et al (1968), 7th I.E.E.E. Photovoltaic Specialists' Conference.

W.D. Gill and R.H. Bube (1970), J.A.P. 41, 3731-3738.

P.F. Lindquist and R.H. Bube (1970), 8th I.E.E.E. Photovoltaic Specialists' Conference.

N. Nakayama (1969), Jap. J.A.P. 8, 450-462.

A.N. Rushby (1966), Ph.D. Thesis, Durham University.

L.R. Shiozawa et al (1968), Ninth Q.P.R. Contract AF33(615)-5224.

# CHAPTER 9 :

# EFFECTS OF THE SOURCE COMPOSITION ON THE THIN FILM PROPERTIES

## 9.1 INTRODUCTION

In this chapter it is intended to enlarge on the brief explanations given for some of the experimental observations in the previous chapters, and to provide some theoretical basis for these suggestions wherever possible.

Many of the problems which have arisen out of the experimental results are concerned with the transport properties of the charge carriers in the films. For example, an explanation is required of the origin of the photosensitive behaviour of the films, and the source of the additional conduction electrons in the thicker films. Connected with these phenomena are the roles of impurities, dopants, and non-stoichiometry in the electrical behaviour of the layers.

This chapter is concerned with a theoretical study of the evaporation and condensation kinetics, following a scheme suggested in an IRD & Co. Ltd. report (Syms et al, 1966). These ideas explain why it is important to control both the evaporation rate and the substrate temperature if it is desired to grow CdS or CdSe films with reproducible properties. It is also possible to show from such a study that the evaporation rate (which is controlled by the source temperature) should dominate the substrate temperature in determining the properties of CdSe films and vice versa for CdS films.

## 9.2 EVAPORATION KINETICS

### 9.2.1 The Vapourisation of CdS

Let us examine the processes whereby a source of CdS is vapourised and subsequently condensed on a heated surface.

Somorjai and Jepsen (1964a, b) have studied the evaporation mechanism of CdS single crystals and have suggested that the following four processes occur.

$$CdS\ (solid) \rightleftharpoons Cd\ (surface) + S\ (surface)$$

$$Cd\ (surface) \rightleftharpoons Cd\ (gas)$$

$$2S\ (surface) \rightleftharpoons S_2\ (surface)$$

$$S_2\ (surface) \rightleftharpoons S_2\ (gas)$$

The first of these is the rate-controlling process, and gives rise to a lower evaporation rate than that calculated from vapour pressure data using the Langmuir equation:

$$R = 5.83 \times 10^{-2} P. (M.T)^{-\frac{1}{2}}$$

where R is the evaporation rate in moles $cm^{-2}$ $S^{-1}$, and P is the saturated vapour pressure in torr of an evaporant with molecular weight M at an absolute temperature T.

The experimental value of the evaporation rate differs from this equilibrium value by a factor, a, the evaporation coefficient. 'a' has a value of about 0.1 for the (0001) face of CdS but varies with temperature. The values of a for the other faces of CdS crystals are usually different, but Somorjai and Stemple (1964) suggest that crevices can form on some faces to expose

small c-facets. We shall assume the same value of a for a source formed of crushed flow-crystals as for a uniform c-face. We shall also assume (i) that the evaporation of CdS is congruent, thus providing the same numbers of cadmium and sulphur atoms in the vapour as in the solid, and (ii) that no CdS molecules exist in the vapour with the source temperatures employed.

Figure 9.1 shows the temperature of the large resistance-heated crucible used for the present investigation as a function of the current passed through the element. For these measurements a NiCr/NiAl thermocouple was embedded in the quartz wool baffle and the crucible temperature was raised in steps of about 25°C allowing the temperature to reach equilibrium each time. The background pressure was $8 \times 10^{-6}$ torr. The two deposition rates employed in much of this work, i.e. 2500 Å/minute and 350-400 Å/minute, were found to be produced by crucible mouth temperatures of 725°-740°C and 675°-700°C respectively. In our calculations we shall use the two temperatures of 680°C and 725°C.

Making use of the evaporation rate of a CdS c-face determined by Somorjai and Stemple (1964) which is reproduced in Figure 9.2, the evaporation rates from the crucible used in the present work (surface area 0.8 $cm^2$) can be calculated. The result is:

$3.52 \times 10^{-7}$ moles of CdS $S^{-1}$ at 680°C

$1.00 \times 10^{-6}$ moles of CdS $S^{-1}$ at 725°C

From these values we can find the impingement rates of

FIG. 9.1 CRUCIBLE TEMPERATURE VERSUS FILAMENT CURRENT

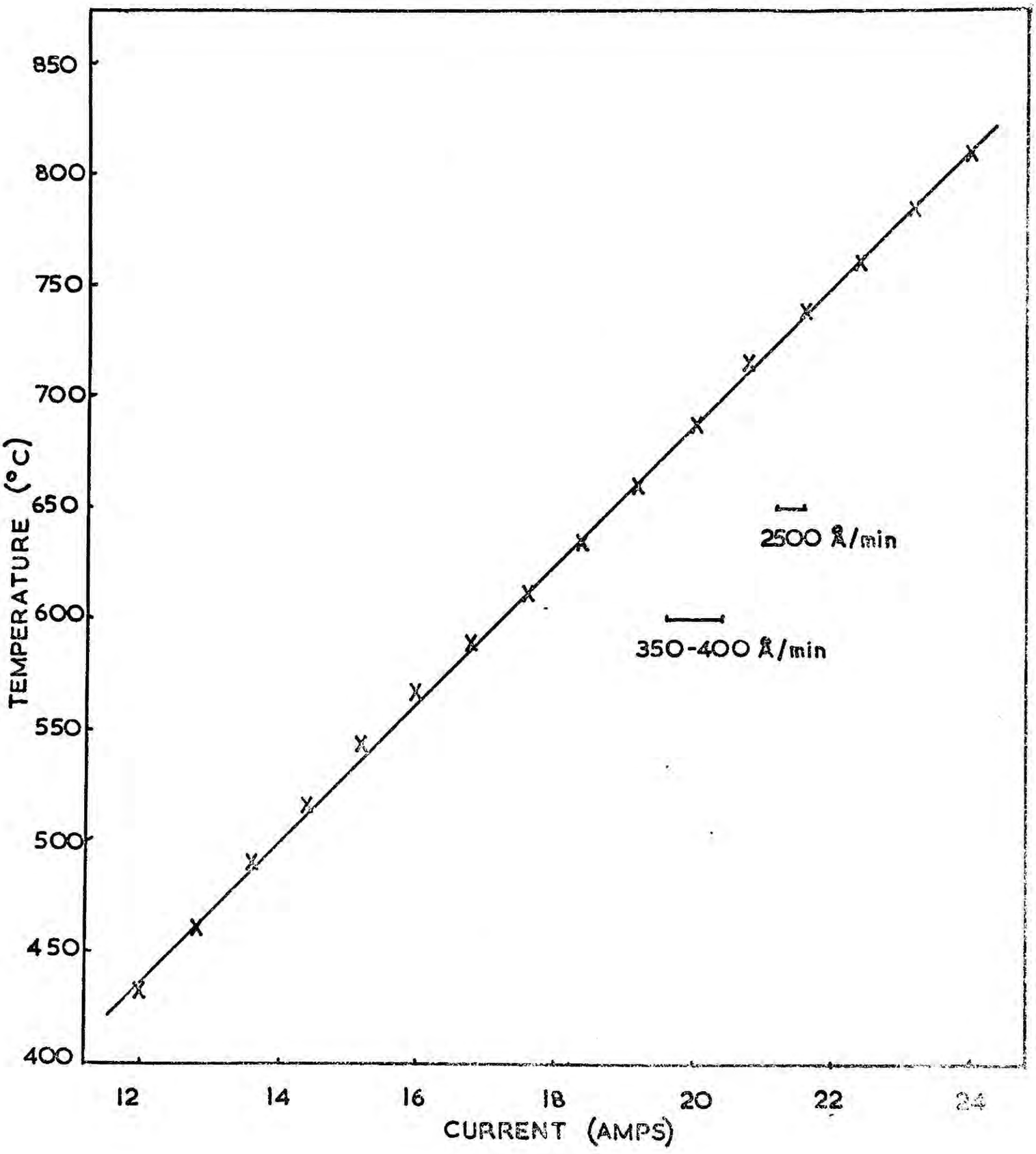

FIG.9.2 EVAPORATION RATE OF CdS C-FACE, AFTER SOMORJAI AND STEMPLE, 1964

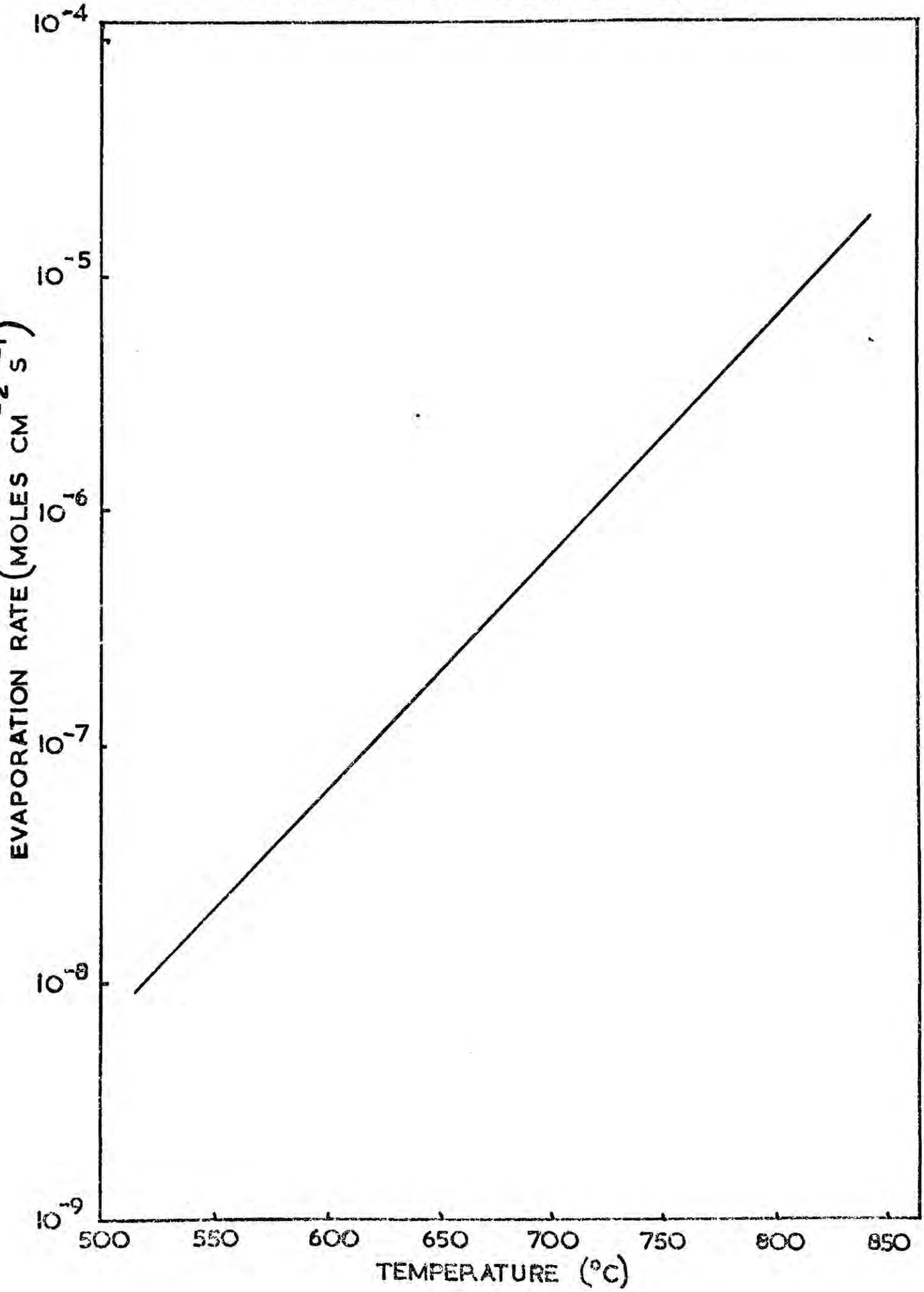

FIG. 9.3 EVAPORATION RATE OF CdS C-FACE (EXTRAPOLATED)

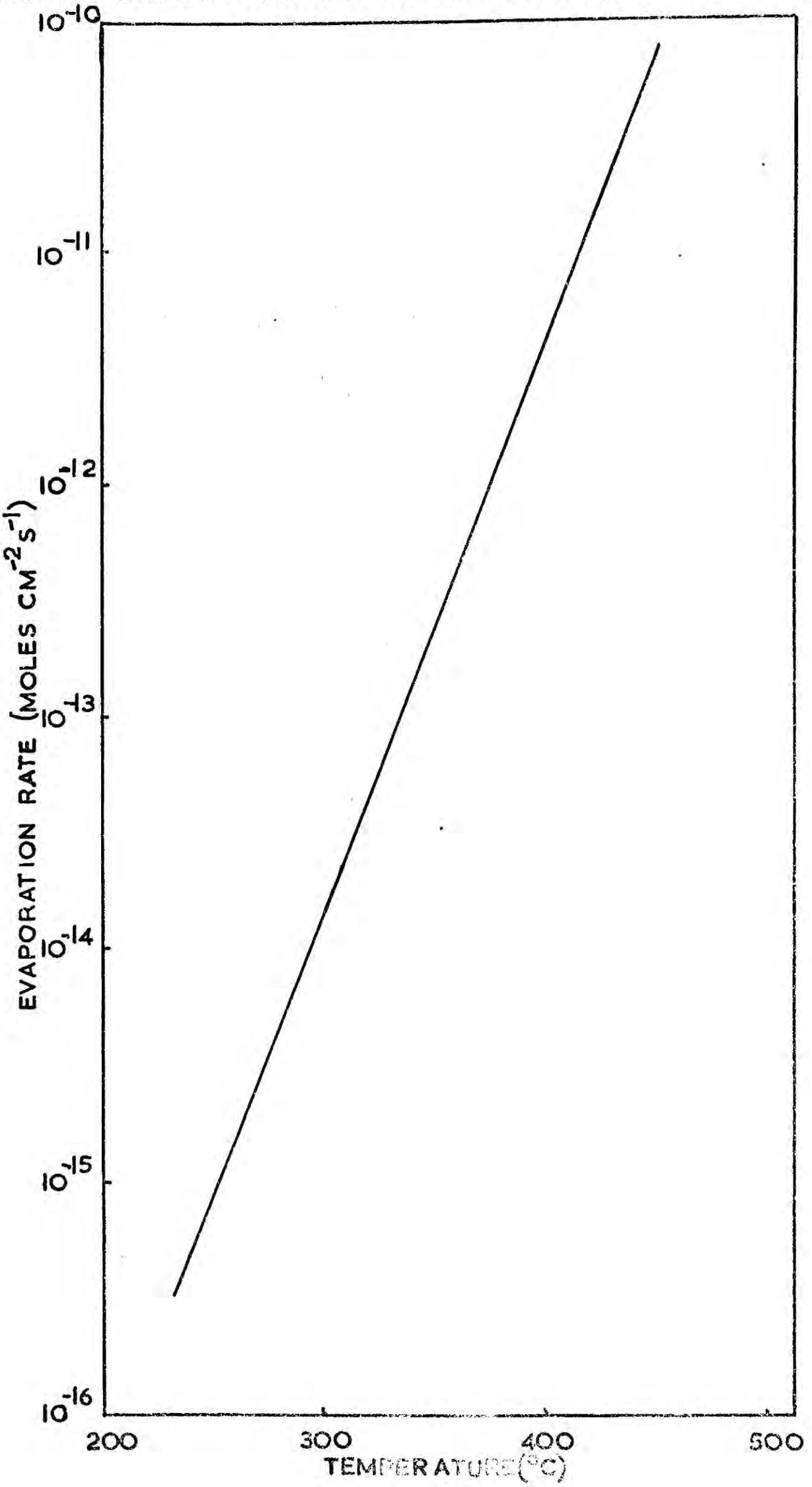

CdS on a small substrate positioned 10 cm directly above the source. It is assumed that the vapour from the crucible follows a cosine distribution law. The quantities of vapour striking the substrate are found to be:

$1.12 \times 10^{-9}$ moles $cm^{-2}$ $S^{-1}$ at 680°C

$3.18 \times 10^{-9}$ moles $cm^{-2}$ $S^{-1}$ at 725°C

(It is interesting to compare these figures with the measured growth rates of 6 Å/S and 42 Å/S: i.e. $2.00 \times 10^{-9}$ moles $cm^{-2}S^{-1}$ and $1.39 \times 10^{-8}$ moles $cm^{-2}S^{-1}$. We shall comment on the apparently low impingement rates calculated from the source temperatures at the end of this section).

The two impingement rates for CdS can be used to obtain the fluxes of cadmium and sulphur vapour at the substrate if we remember the assumption that the evaporation is congruent. However, below about 600°C a complication arises because the stable configuration of sulphur vapour is as $S_8$ molecules, whilst at higher temperatures it is as $S_2$ molecules (Nesmayov, 1963 and Drowart, 1964). Taking this into account the following impingement rates on the substrate were calculated for the two source temperatures chosen:

at 680°C $1.12 \times 10^{-9}$ moles of Cd $cm^{-2}S^{-1}$

$1.12 \times 10^{-9}$ moles of S $cm^{-2}S^{-1}$

$5.60 \times 10^{-10}$ moles of $S_2$ $cm^{-2}S^{-1}$

at 725°C $3.18 \times 10^{-9}$ moles of Cd $cm^{-2}S^{-1}$

$3.18 \times 10^{-9}$ moles of S $cm^{-2}S^{-1}$

$1.59 \times 10^{-9}$ moles of $S_2$ $cm^{-2}S^{-1}$

9.2.2 The significance of the substrate temperature

On reaching the substrate these components may condense, but their subsequent behaviour will depend on the substrate temperature. A thin film will grow initially from nucleation centres by a process which is not well understood, but it is known that for any particular set of conditions there exists a critical temperature above which nucleation will not occur. It seems likely that for CdS, since the critical temperatures for nucleation of cadmium and sulphur are low, nucleation will occur after the recombination of the cadmium and sulphur surface species in a series of reactions which are the reverse of those for evaporation. Film growth then proceeds at such preferential sites as steps and corners in the layer. It will be appreciated that since the four given reactions are reversible, a substrate temperature exists above which no film can grow, i.e. the critical temperature for CdS.

We have already said that at low temperatures the molecular form of sulphur is $S_8$, and it is probable therefore that a competing reaction to that of the formation of CdS(solid) is the formation of $S_8$(surface) from 8S(surface). The $S_8$ surface species will then either condense fully or vapourise according to the substrate temperature. If the re-evaporation rate of sulphur is very high then excess cadmium will be left on the substrate. Eventually with further increase in the substrate temperature, the excess cadmium will also possess a high rate of re-evaporation and only CdS will

be deposited, until a temperature is reached beyond which no deposit can form on the substrate.

This description providesa qualitative explanation of the varying properties of the CdS film produced under various growth conditions. Thus with any one evaporation rate, as the substrate temperature is increased over a series of films these films will have compositions which vary gradually from one to another. At first there will be both excess cadmium and sulphur, then excess cadmium alone, then stoichiometric CdS which eventually becomes increasingly difficult to deposit.

### 9.2.3 Condensation and re-evaporation

It is now proposed to calculate the condensation rates of cadmium, sulphur, and cadmium sulphide for the two chosen source temperatures as a function of the substrate temperature in an attempt to gain some idea of the critical temperature values.

We shall assume that the condensation coefficients of Cd and $S_2$ are unity at all practical substrate temperatures (i.e. all the Cd and $S_2$ vapour impinging on the substrate sticks at least momentarily, regardless of substrate temperature). This of course gives condensation rates for Cd and $S_2$ which are identical to the impingement rates.

Some of the surface cadmium and sulphur then combines to form cadmium sulphide whilst the remainder re-evaporates. At the lower substrate temperatures where sulphur and cadmium can condense separately on the substrate, the rate of formation of CdS is determined by

the sticking rates of cadmium and sulphur, and principally by the sticking rate of $S_2$ since sulphur re-evaporates (as $S_8$) much more easily than cadmium. However at the higher substrate temperatures normally employed (above 150°C) both cadmium and sulphur re-evaporate from the substrate very easily, and the rate of formation of CdS is then determined by some different step in the process. This will be similar to the mechanism which controls the evaporation of CdS, and so we shall suppose that the mechanism of condensation on the substrate is the exact opposite of evaporation and use the product of impingement rate of CdS and evaporation coefficient of CdS as a good approximate to the rate of formation (condensation) of CdS. The use of a condensation coefficient (i.e. in this case the evaporation coefficient) allows for the fact that not all of the Cd and $S_2$ forms CdS, but forms other phases or re-evaporates as well. Thus the rate of condensation of CdS will be obtained from the product of the CdS impingement rate and the temperature dependent evaporation coefficient of CdS given by Somorjai (1964a) and reproduced in Figure 9.4

The next step is to calculate the rate of re-evaporation of Cd, $S_8$, and CdS from the substrate. This will be done for Cd and $S_8$ by using the reported saturated vapour pressure (SVP) curves and employing Langmuir's formula with an evaporation coefficient.

The SVP of Cd (Figure 9.5) is taken from the 'Handbook of Physics and Chemistry' (45th edition)

FIG. 9.4 EVAPORATION COEFFICIENT OF CdS, AFTER SOMORJAI, 1964

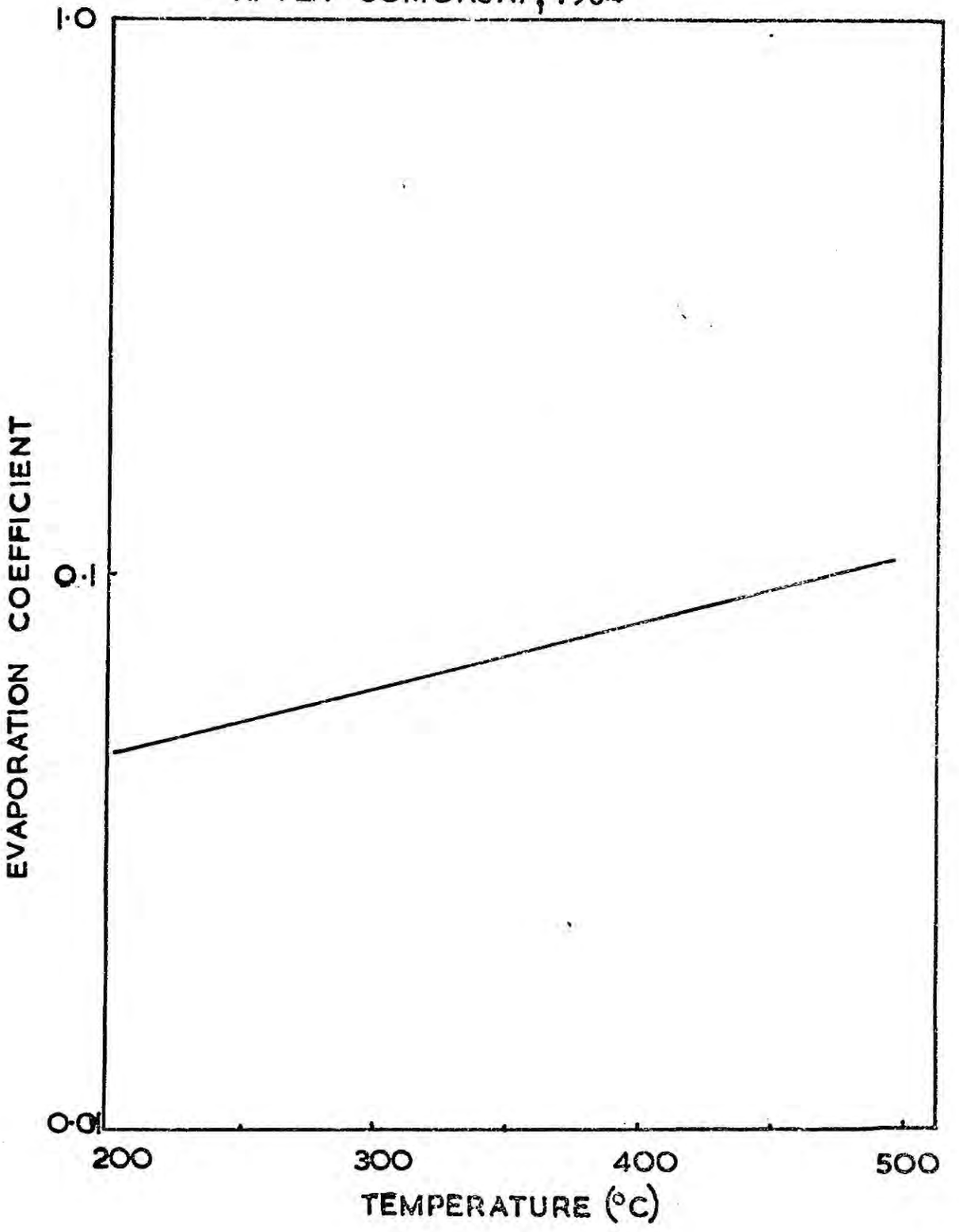

FIG. 9.5 S.V.P. OF Cd AND $S_8$.

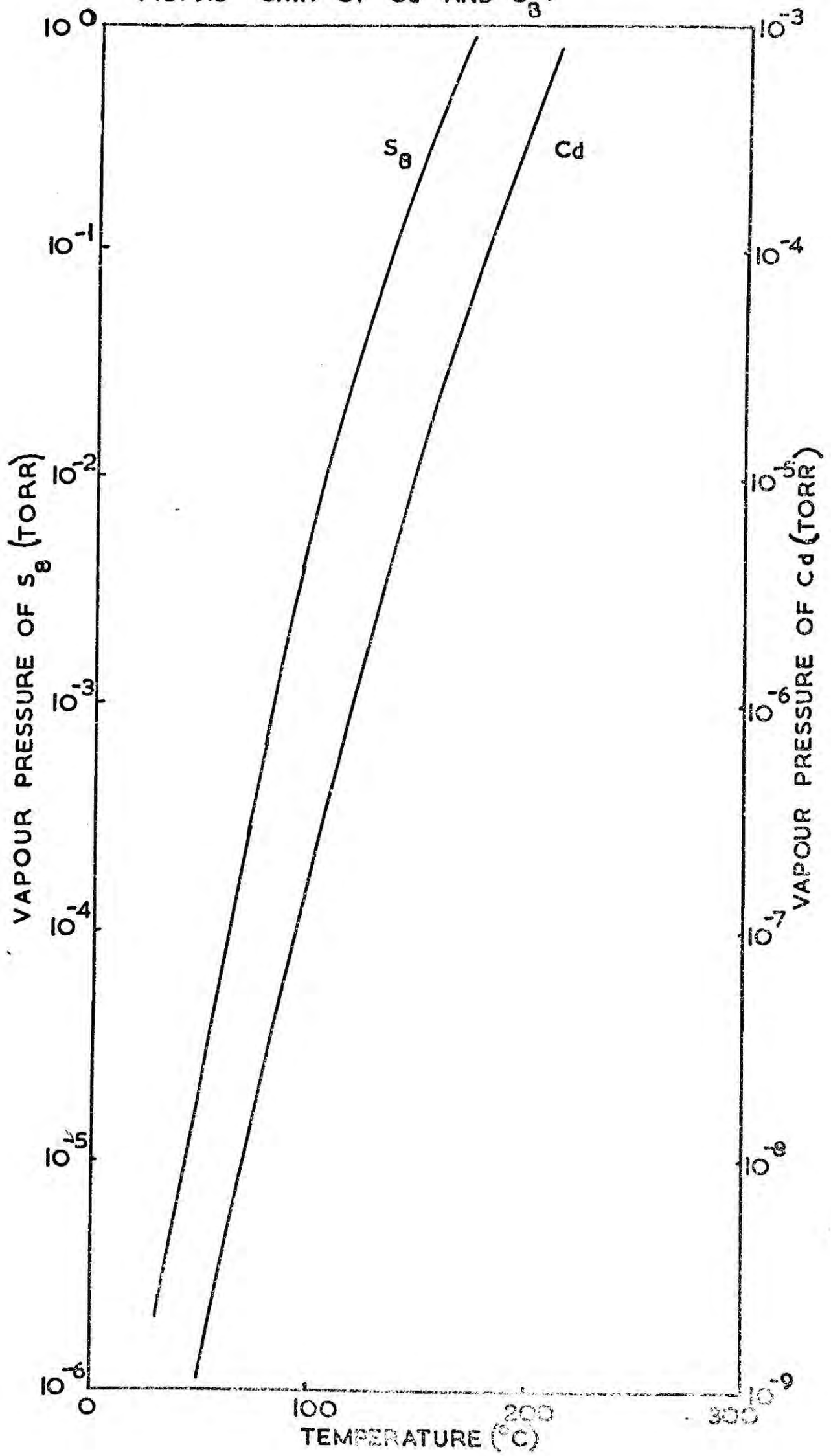

which gives the following formula.

$$\log_{10} P_{Cd}(\text{torr}) = 8.564 - \frac{5693.07}{T^{\circ}K}$$

The evaporation coefficient, as for the condensation coefficient, is taken to be unity.

The SVP of $S_8$ (also Figure 9.5) is from Bradley (1951) who determined the following formula, and also obtained a temperature independent value of 0.73 for the evaporation coefficient.

$$\log_{10} P_{S_8}(\text{torr}) = 9.763 - \frac{5240}{T^{\circ}K}$$

The calculated evaporation rates of Cd and $S_8$ from a heated substrate are given in Figure 9.6.

The evaporation rate of CdS from the substrate is taken from the extrapolated data of Somorjai and Stemple (1964) and reproduced in Figure 9.3.

The final stage in these calculations is to find the actual composition of a film grown on a heated substrate for each of the two selected source temperatures. To do this we shall use the sticking factor which we shall define as the ratio of the evaporation rate from the substrate to the condensation rate on the substrate. The values of this factor for Cd, S, and CdS are given in Figure 9.7. For all values less than unity a deposit will form, and for all values greater than unity no deposit forms.

at a source temperature of 680°C:

( no free S if substrate temp. above 20°C
( no free Cd if substrate temp. above 106°C
( no deposit if substrate temp. above 460°C

FIG. 9.6 EVAPORATION RATES OF Cd AND $S_8$

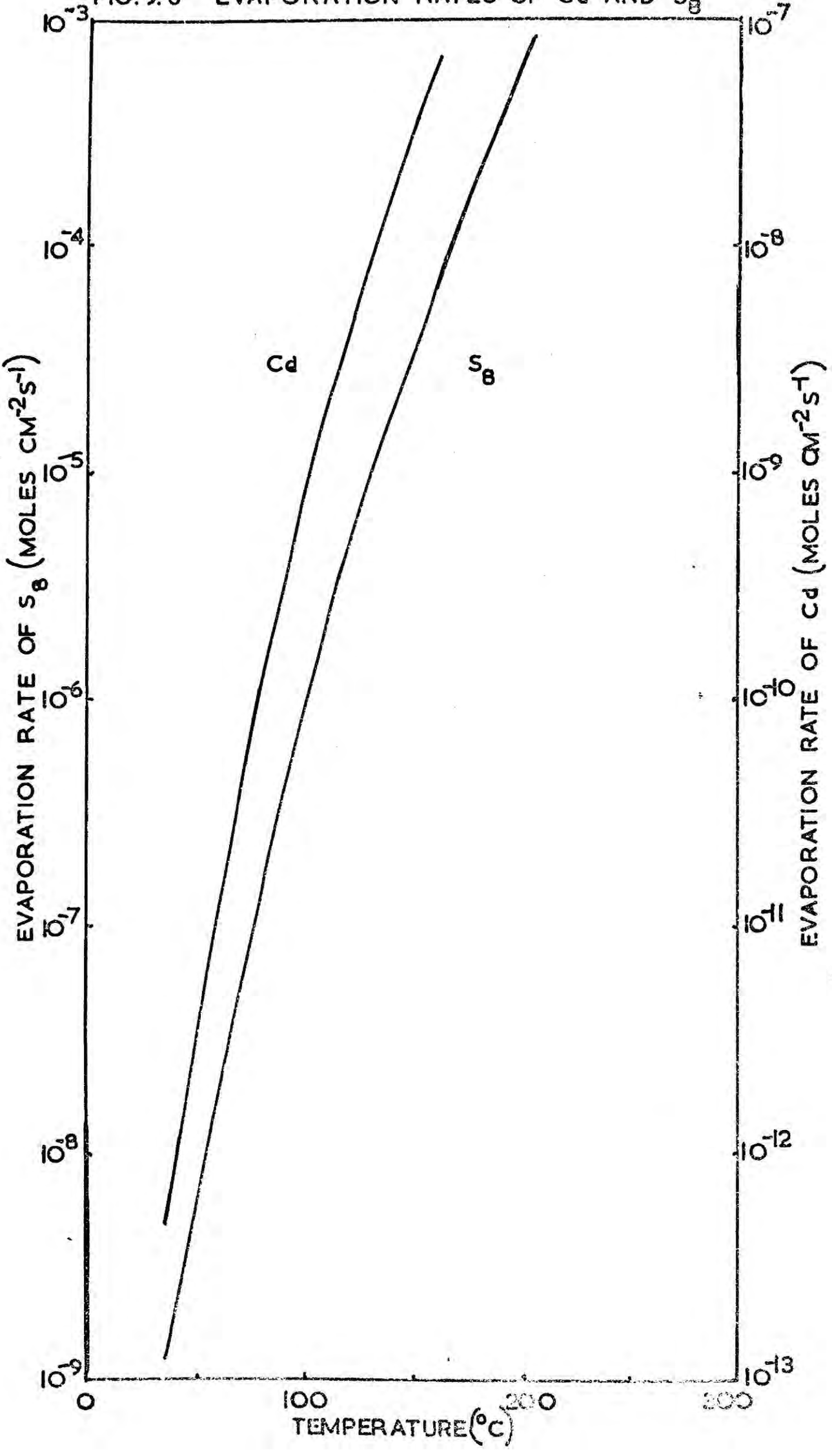

FIG.9.7 STICKING FACTORS FOR Cd, S, CdS

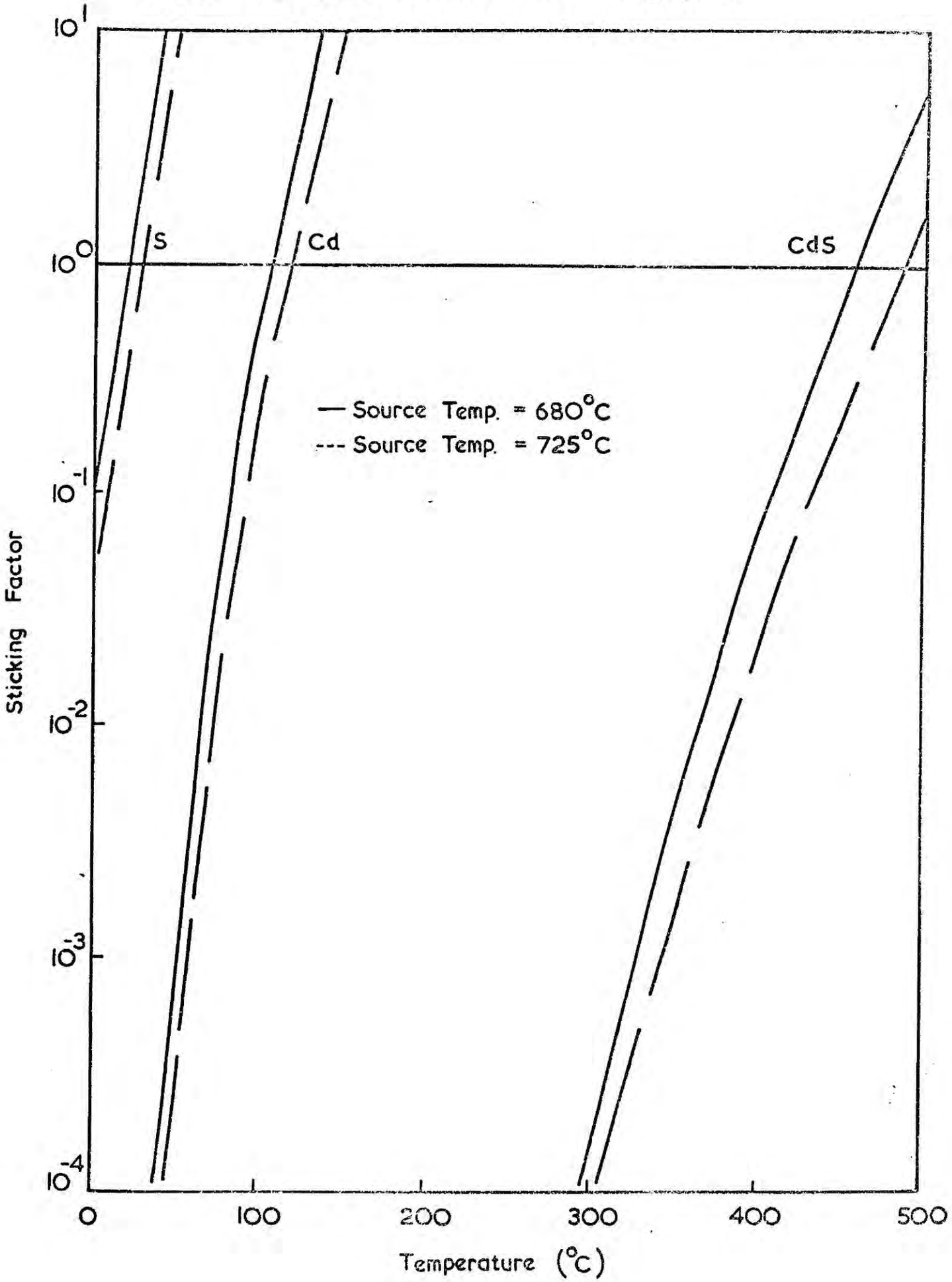

at a source temperature of 725°C

(no free S if substrate temp. above 28°C
(no free Cd if substrate temp. above 117°C
(no deposit if substrate temp. above 490°C

9.2.4 Thin film composition

The above considerations show that there is a gradual change in composition of a series of films prepared over a range of substrate temperatures. This explains the observed changes in colour already remarked upon. At very low substrate temperatures the excess cadmium will give the films a black appearance unless a very low deposition rate is employed (i.e. low source temperature), in which case it is possible to grow a dark yellow film.

Those films containing excess cadmium will also possess low resistivities. At the commonly employed substrate temperature of 220°C no free sulphur or cadmium can normally exist, thus such films will have high resistivities. If very high evaporation rates are employed then excess cadmium can once more be deposited and the films will have low resistivities.

The curves in Figure 9.7 indicate that the change in composition takes place gradually with change in source temperature, but more rapidly with change in substrate temperature.

The final conclusion from this theoretical study is that at the two selected source temperatures no deposit at all forms if the substrate temperature is above about 460°C, and that it becomes increasingly

difficult to form any deposit on a substrate at temperatures above 400°C. These substrate temperatures are higher than those observed experimentally, for no deposit formed above 380°C. Clearly a closer investigation is required of the validity of the assumptions used in the theory.

### 9.2.5 Theoretical Assumptions

It is obvious that the processes of evaporation and condensation are not exactly the inverse of each other. In evaporation all the atoms are initially bound to the surface whereas in condensation an atom may re-evaporate before it can become bound. This will lead to a maximum substrate temperature for film formation which is lower than has been calculated, in agreement with our observations and the evaporation and condensation coefficients of CdS will not be identical.

It has also been shown (Somorjai, 1964b) that illumination of CdS during heating can decrease the evaporation rate, which would again lower the maximum substrate temperature.

It has been assumed that the evaporation coefficient, a, for a CdS microcrystalline source is the same as for a single CdS c-face, but this may not be true. An increased value of 'a' would imply higher impingement rates, which would lead to better agreement between calculated and measured growth rates. (Although Hsaio and Schlechten, 1952, using

a CdS powder source obtained lower values for the SVP than Somorjai did using single crystals, our source was composed of crushed flow crystals which are more like Somorjai's samples than a powder).

The condensation and evaporation coefficients of cadmium were taken to be unity, which is a reasonable assumption for a metal. The condensation coefficient of $S_2$ was taken to be unity since this molecule also has a low vapour pressure at the substrate temperatures used. (It was the species $S_8$ which evaporated from the substrate, and this molecule has a higher vapour pressure than $S_2$).

Further sources of error arise in estimating (a) the effective area of the crucible, which may differ from its physical aperture, and (b) the effective surface temperature.

The degree of dissociation of CdS was assumed to be 100%, but this may not be true, in which case the calculated impingement rates of Cd, $S_2$, and CdS would be different. Caveney (1970) has discussed the work reported by earlier investigators on the SVP and degree of dissociation of CdS. Goldfinger and Jeunehomme (1963) using mass spectroscopic techniques concluded that complete dissociation occurred, but Caveney (1970), and Sen-Gupta (1934), suggest from results obtained by atomic absorption that CdS vapour contains a measurable number of undissociated molecules at 750°C. In addition Caveney suggests that CdS crystals grow from

these CdS molecules and not via the recombination of Cd and $S_2$. If his conclusions are correct then the growth mechanism of CdS thin films may not be that suggested in our calculations, but the qualitative agreement between our theoretical and experimental results strongly supports the existence of a recombination reaction between cadmium and sulphur in the vacuum chamber apparatus.

The actual vapour pressures of cadmium, sulphur and cadmium sulphide above the substrate in our experimental arrangement will differ from those calculated owing to the presence of the hot-wall cylinder. This has the effect of trapping $S_8$ molecules close to the substrate thus ensuring that sulphur is not lost rapidly from the substrate by condensation on the cold surfaces of the apparatus. The result is to produce a stoichiometric CdS film over a larger range of substrate temperatures than would otherwise be possible.

### 9.2.6 Conclusions

Despite the acknowledged sources of error, the theoretical conclusions provide explanations for several of the experimental observations described in Chapter 6 and in the appendix. The dominance of the substrate temperature over the evaporation rate in determining the properties of CdS films is to be expected from the theory since it is primarily this temperature which controls the film composition. The

change in source temperature required to produce a ten-fold increase in deposition rate is only about 40°C which does not have a great effect on the sticking coefficients of the components, as the curves in Figure 9.7 show.

According to the theoretical argument some change in the film properties might be expected as the substrate temperature was increased beyond 120°C because above this temperature only stoichiometric CdS is deposited, whereas below this temperature excess Cd exists in the film. This should lead to increasing resistivity with increasing substrate temperature, as was observed from the films deposited more rapidly.

The films grown at 200Å/minute exhibited the opposite effect of resistivity decreasing with substrate temperature, which cannot be explained by the theory. It is also difficult to suggest why the resistivity increased as the rate was increased (see Section 9.3.1).

In the case of the CdSe thin films, the group VIb component of the compound is more metallic than in CdS, so that the SVP's of the two components are more nearly equal. This gives rise to a much smaller dependence on the substrate temperature than has been found with CdS, and a stoichiometric film of CdSe should be easier to grow on a substrate held near room temperature. Hence the dominant growth parameter for CdSe is not the substrate temperature but is the

evaporation rate, although neither of these would be expected to have such a great effect on the properties of CdSe layers as on the properties of CdS layers. The observed small increases of resistivity with increase in substrate temperature or decrease in rate agree with the conclusions of the theory: both changes would result in slightly less excess Cd being incorporated into the deposit and consequently the resistivity would increase. A theoretical discussion of the evaporation and condensation of CdSe is given by Gunther in Anderson (1966).

## 9.3 TRANSPORT PROPERTIES

### 9.3.1 Film thickness effects

We now turn to a discussion of the electrical properties of the thin films described in Chapter 6 and in the Appendix. Let us first examine the changes in resistivity and Hall mobility with film thickness.

We have already seen that the variation of mobility with thickness (Figure 6.9) is insufficient to explain the decreasing resistivity with increasing thickness (Figure 6.7), which is in fact due to the change in carrier density with thickness (Figure 6.10). This is contrary to certain other reports of a similar phenomenon, where it was possible to invoke an explanation involving mobility changes alone. For instance, Berger et al (1969) showed that the change of resistivity with thickness in their CdSe films was attributable solely to an increase in the size of the microcrystallites

as the film increased in thickness. The effect was manifestly a mobility variation. In the present work, not only did the crystallite size change too slowly with thickness (Figure 5.3), but it also continued to increase at the same rate when the mobility was constant. To explain our results we have successfully used a surface scattering model in contrast with Berger et al (1968) who stated that such a model was invalid and unnecessary because the changes in crystallite size were sufficient to account for the changes in resistivity.

Vergunas et al (1966) suggested that the resistivity of their CdS films was decreasing with thickness because of the increasing fibre axis orientation of the films. This again would affect the mobility and not the carrier density. However in our films the preferential orientation does not appear to change over a wide enough range of thickness to account fully for the results.

The other possible causes of a resistivity which decreases with thickness rely on a change in the film composition as it is growing, although a further suggestion is that a depletion layer forms between the CdS and the substrate. This last possibility can be eliminated since such a layer would not be expected to extend its influence over several microns.

The growing film may change its composition by one of several methods:

(a) the cadmium excess may increase slowly during the evaporation;

(b) the impurity content (e.g. metal filament contamination or source impurities) of the layers may increase as the evaporation proceeds;

(c) a gettering process may take place.

It is not very likely that any gettering effect occurred while the CdS films were growing since the pressure was never observed to fall during the evaporation process, although any such fall might have been masked by source outgassing. However oxygen has the opposite effect to that required since it is known to increase the resistivity of CdS or CdSe crystals and films (see Section A.3.4).

On the other hand it is in our opinion entirely possible that the cadmium content of the films increases during the evaporation. CdS is commonly believed to evaporate congruently, that is, the vapour has the same composition as the source, and there is no reason to oppose this view. It is still possible to obtain a CdS vapour which changes composition with time if the source itself changes composition with time. To explain the observed effect it would therefore be necessary for the source to become more Cd rich with time.

Somorjai and Jepsen (1964) have shown that a source rich in Cd or S has a different evaporation rate from a stoichiometric source, but that the evaporation remains congruent. (The same authors have also shown that the presence of dopants depresses the

evaporation rate in a similar manner, by affecting the outward diffusion of S vacancies).

Now, the solid equilibrium area of the CdS composition versus temperature diagram is of the shape shown in Figure 9.8 (Shiozawa et al, 1968). The $P_{min}$ locus shows the composition which has the lowest vapour pressure at each temperature. The partial pressures of cadmium and sulphur are related by the equilibrium constant of the reaction:

$$2CdS\ (solid) \rightleftharpoons 2Cd\ (gas) + S_2\ (gas)$$

as follows:

$$k = P_{Cd}^2 \cdot P_{S_2}, \quad \text{where } P = P_{Cd} + P_{S_2}$$

The lowest total pressure, $P_{min}$, is obtained when:

$$\frac{\partial P}{\partial P_{Cd}} = \frac{\partial P}{\partial P_{S_2}} = 0$$

(See for example the article by Lorenz in Thomas, 1967). This means that a source heated to 700°C will tend towards point A in composition, i.e. it will become Cd-rich. The time taken to achieve this condition is the crux of the problem. If it takes many minutes then the source will only reach a stable composition towards the end of the evaporation. If the change is more rapid then the swing towards the cadmium-rich CdS will be completed during outgassing.

Further consideration of the phase diagram shows that when vapour from point A, say, strikes the substrate

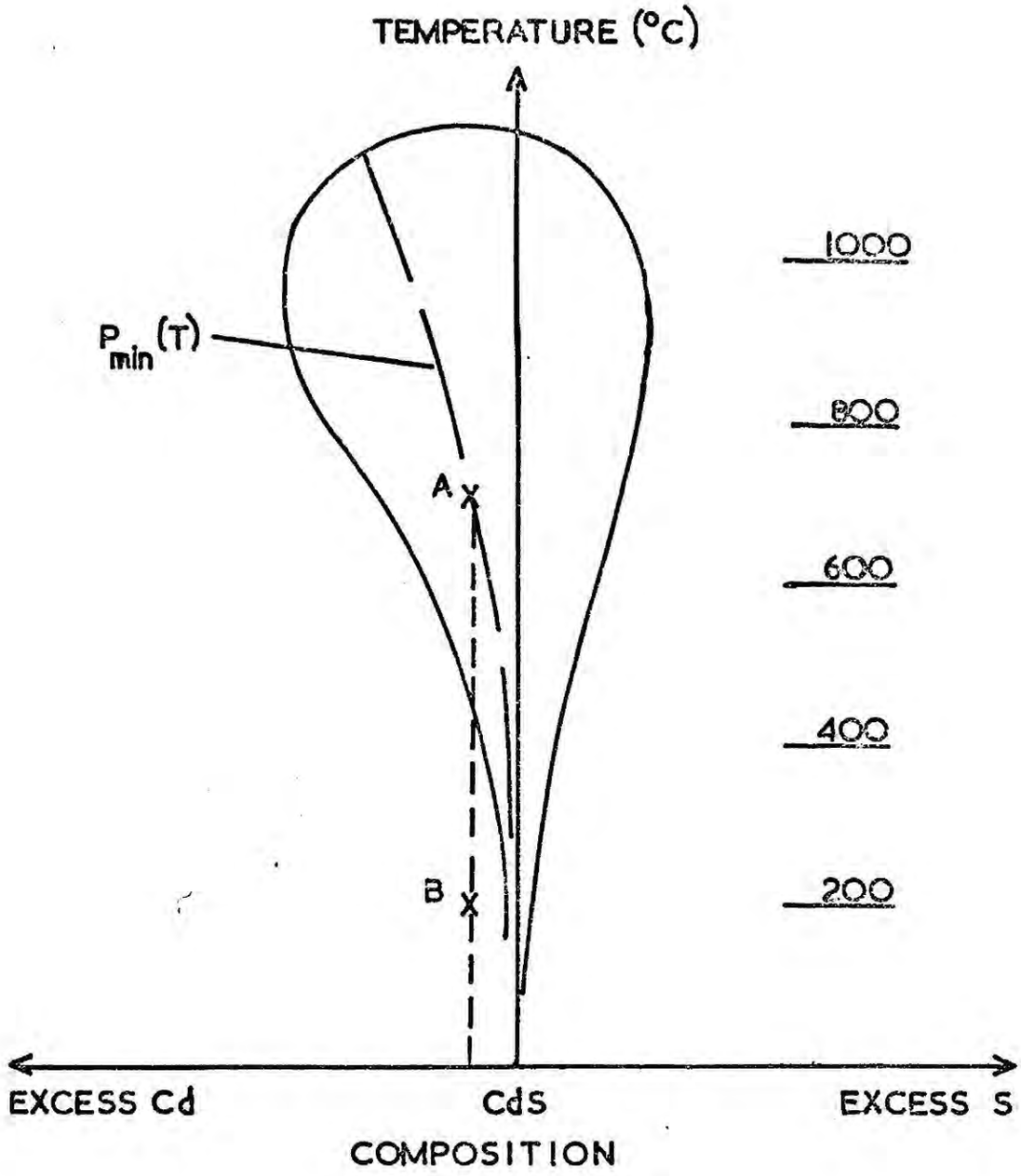


FIG. 9.8 CdS PHASE DIAGRAM

it is cooled to the temperature represented by point B. There will then be more cadmium than can exist in the CdS with sulphur-vacancy compensation so that it must form a second phase or re-evaporate.

Finally there remains the possibility that impurities affect the conductivity of the films ('b' above). The source would be expected to undergo a distillation process during heating if it contained significant proportions of impurity (whether added intentionally or otherwise), and it has already been suggested that the volatile compounds containing Cl are driven off first when they are present, giving rise in some cases to poor film adhesion (see Section 5.2.1). However this would mean that on prolonged heating the source would become increasingly more pureand thicker films should become better with higher resistivities. Alternatively the source filament might give off more metal vapour as the evaporation proceeds. (The temperatures at which Mo, Ta, and W have vapour pressures of $10^{-5}$ torr are 1923°C, 2407°C, and 2554°C, from the 'Handbook of Physics and Chemistry' 45th edition). This problem has not been thoroughly investigated during the course of this work, but it should be noted that the films prepared by electron beam evaporation had higher resistivities than the equivalent films prepared from the resistance-heated source (see Section 6.5.4).

It appears that both changes in stoichiometry and incorporation of impurities are equally likely causes

of the observed decrease in resistivity with film thickness. Either the cadmium content of the films increases as they grow, or the contamination from the source filament increases with the time taken to grow the films. Perhaps both effects occur, but the experimental evidence reported in Chapter 6 supports the view that the cadmium content changes as the films grow thicker. Figure 6.7 shows that the films grown more rapidly have higher resistivities than those grown more slowly with the same thickness. If the shape of the curves in Figure 6.7 was due to impurities from the heater-helix being incorporated into the films, then the higher temperature evaporant would be expected to provide more impurities and hence a lower resistivity. This is the exact opposite of what is observed.

### 9.3.2 Photosensitivity

The source of the photosensitivity observed in all of the films is the next problem to be discussed. The curves of Figure 6.11 show that CdS films with a dark resistivity of around $10^2$ ohm cm (i.e. carrier densities of $10^{16}$ $cm^{-3}$) had photosensitivities of approximately 2. Since illumination of the films produced no noticeable effect on the Hall mobility, this change in resistivity must be mainly due to a change in carrier density. If the photosensitivity is solely the result of photo-created electron-hole pairs, then we have the following expression:

$$\text{Photosensitivity} = \frac{\Delta n_e + n_e}{n_e}$$

This implies that for films with the parameters given above, $\Delta n_e$ is $10^{16} cm^{-3}$.

The average energy per photon for the spectral distribution of the lamp was 1.48eV (Altman, 1969). Since the total energy from the lamp was 75mW $cm^{-2}$ this gave a photon flux of $10^{17}$ $cm^{-2}S^{-1}$ incident on the film. Only a fraction of these photons had energies greater than 2.4eV, and hence the useful photon flux was about $10^{16} cm^{-2}S^{-1}$. If we assume that the quantum efficiency was 100%, that is, each photon created one electron-hole pair, then $10^{16}$ electrons were created per second in the films because the surface area was $1cm^2$. This may be written as $2 \times 10^{20} cm^{-3}S^{-1}$ for a 5000Å thick film. Since the number of photo-created carriers present is given by the product of the generation rate and the carrier life-time to a first approximation, the carriers are deduced to have a life-time of 50 micro-seconds. This is a reasonable value for this parameter and hence it is possible for the photosensitivity in the thin films to be solely due to photo-created carriers. Espevik et al (1971) have come to a similar conclusion for PbS polycrystalline layers and have found that only a small proportion of the photosensitivity of these layers is due to a change in the carrier mobility.

### 9.3.3 Large Hall Mobilities

If, as has been suggested in Section 9.3.1, it is possible for excess cadmium to form a second phase

then this metal may precipitate preferentially at the grain boundaries. Similarly, CdS:In films may also have grain boundaries which are rich in indium if this cannot be taken up in the CdS lattice. Both indium-doped films (Section 6.5.6) and, to a lesser extent, undoped films grown at low substrate temperatures (Section 6.5.5) have higher Hall mobilities than undoped CdS films grown on substrates at 200°C or more.

If the effect of this metal concentrated around the crystallite boundaries is to reduce the height of the potential barriers between the crystallites, then from the Petritz formula for the mobility (Section 6.4.3) the barrier height would need to be reduced from 0.098eV to 0.058eV to obtain a mobility of $20cm^2V^{-1}S^{-1}$, which is typical of our CdS:In films, and to be reduced proportionately less for undoped films deposited at low substrate temperatures.

In order to obtain the same increases by reducing the impurity scattering in the crystallites, the mobility in the crystallites would have to be increased five times (i.e. from 200 to 1000 $cm^2V^{-1}S^{-1}$) for the CdS:In layers. This mobility is far too high for CdS at room temperature, and so any mechanism whereby the metal dopant (i.e. indium) removes impurities from the crystallites must be rejected.

## 9.4 SUMMARY

A model has been proposed which describes the composition of thin films of CdS (and CdSe) as a function

of their preparative conditions. This model provides semi-quantitative explanations for many of the features observed during sample preparation and during the subsequent investigation of the electrical resistivity.

It is suggested that the change of resistivity with film thickness is due either to increasing metal contamination from the crucible heating element, or more probably to an increase in the cadmium content of the samples as the evaporation proceeds. We strongly support the theory of increasing cadmium percentage as the films grow.

The anomalously high Hall mobility of CdS:In films and the high mobility of undoped CdS films grown on cool substrates is probably due to a reduction in the height of the intercrystallite potential barriers, possibly by local excess of metal. The effect of excess Cd in the layers appears to be two-fold: principally an increase in carrier concentration is brought about, but also a reduction in the height of the inter-crystallite barriers occurs.

Finally it has been demonstrated that the observed photosensitivity of the layers may be solely due to the direct generation of free carriers by the illumination.

REFERENCES

M. Altman (1969), "Elements of Solid State Energy Conversion (Van Nostrand).

J.C. Anderson (1966), ed. "The Use of Thin Films in Physical Investigations." (Academic Press).

H. Berger et al (1968), Phys. Stat. Sol. 28, K97.

H. Berger et al (1969), Phys. Stat. Sol. 33, 417-424.

R.S. Bradley (1951), Proc. Roy. Soc. (London) 205A, 553-563.

R.J. Caveney (1970), J. Cryst. Growth, 7, 102-106.

J. Drowart (1964), in "Proc. Int. Symp. on Evap. and Condens. of Solids", Ohio 1962, (Gordon and Breach).

S. Espevik et al (1971), J.A.P. 42, 3513-3529.

P. Goldfinger and M. Jeunehomme (1963), Trans. Faraday Soc. 59, 2851.

C.M. Hsaio and A.W. Schlechten (1952), J. Metals, 4, 65-69.

A.N. Nesmayov (1963), "Vapour Pressure of the Chemical Elements" (Elsevier).

P.K. Sen-Gupta (1934), Proc. Roy. Soc. (London) 143A, 438-454.

L.R. Shiozawa et al (1968), 2nd Quarterly Progress Report, Contract F33 (615)-68-C-1601.

G.A. Somorjai (1964a) in "Proc. Int. Symp. on Evap. and Condens. of Solids", Ohio 1962 (Gordon and Breach).

G.A. Somorjai (1964b), Surface Science, 2, 298-306.

G.A. Somorjai and D.W. Jepsen (1964a), J. Chem. Phys. 41, 1389-1393.

G.A. Somorjai and D.W. Jepsen (1964b), J. Chem. Phys. 41, 1394-1399.

G.A. Somorjai and N.R. Stemple (1964), J.A.P. 35, 3398.

C.H.A. Syms et al (1966), I.R.D. Co.Ltd. Research Report 66-63.

D.G. Thomas (1967) ed. "II-VI Semiconducting Compounds" (1967 Int. Conf.) (W.A. Benjamin Inc).

F.I. Vergunas (1967), Sov. Phys. Crystallog. 11, 420-421.

# CHAPTER 10 : SUMMARY OF CONCLUSIONS

## 10.1 CdS THIN FILMS

In this investigation polycrystalline CdS thin films with reproducible properties have been prepared by vacuum evaporation of the compound. It has also proved possible to understand the relative importance of the substrate temperature, deposition rate and film thickness in controlling the properties of the films by considering the processes of evaporation and condensation of CdS. This involved the equilibrium approach using the CdS phase diagram, and the non-equilibrium approach in which the dissociation of CdS into two species with different sticking coefficients was considered. Thus a film will contain only CdS if the substrate temperature is higher than the critical temperatures for nucleation of cadmium and sulphur. At low substrate temperatures both free sulphur and free cadmium may exist unless very slow evaporation rates (i.e. low source temperatures) are employed.

The equilibrium theory predicts that the CdS source will become rich in cadmium with time, and since CdS evaporates congruently the deposited film will become richer in cadmium as an evaporation proceeds. Experimentally this has been found to have the effect (i) of lowering the resistivity by increasing the carrier density, and (ii) of increasing the Hall mobility slightly by reducing the heights of the intercrystallite potential barriers.

The Hall mobility is dominated by surface scattering phenomena in films less than one micron thick, but with thicker films it is controlled by the inter-crystallite barrier height (about 0.09eV) which is reduced by indium doping or excess cadmium.

Metal impurities from the source heating element can be screened from the substrate by using focussed electron-beam evaporation of CdS. This has been found to yield films with higher resistivities than those produced from resistance-heated sources for comparable evaporation rates. An electron microscopy study of 1000Å thick epitaxial CdS on (100) NaCl substrates has revealed that hexagonal grains exist in those cubic films produced with the resistance-heated source. This is thought to be due to metal contamination from the filament since no such grains were observed in films produced using electron-beam evaporation.

Various other defects in epitaxial CdS including vacancy loops have also been identified by transmission electron microscopy. The planar defect density in electron-beam evaporated films was less than $4 \times 10^{10}$ $cm^{-2}$, but much higher in films prepared using the resistance-heated source. Electron microscopy has also shown the existence of a possible phase transition from cubic to hexagonal CdS in epitaxial films removed from their substrates.

Other structural investigations of polycrystalline CdS films using X-rays and reflection electron microscopy

have shown that a fibre axis orientation exists in these layers, which becomes more pronounced with increases in film thickness or with reductions in the evaporation rate. This change in orientation was insufficient to explain completely the observed dependence of the electrical properties on film thickness. Instead, as stated above, the stoichiometric composition of the film is postulated to change with evaporation time.

The photosensitivity of the layers was found to be essentially a photoconductive effect since there was very little change in the carrier Hall mobility which would have resulted if there had been an optical reduction of the intercrystallite barrier heights.

In conclusion it is important to remember that in order to grow reproducible films it was necessary to use a hot-wall technique together with resublimed CdS as the source material.

## 10.2 CdSe THIN FILMS

Polycrystalline CdSe films with reproducible properties have been prepared empirically by setting the substrate temperature and evaporation rate to predetermined values, but it has also been possible to understand the dominance of source temperature over substrate temperature in determining the properties of the resultant films by studying the evaporation and condensation reactions of CdSe. Although the importance of film thickness was not fully investigated it would seem likely from our results that the Hall mobility is

again determined by surface scattering in thin films, and by intercrystallite barriers, reduced in height by metallic impurities, in thick films.

Electron microscopy has shown the presence of a high density of planar defects in the epitaxial cubic CdSe layers prepared from a resistance-heated source, and has also shown that other defects such as included hexagonal grains, and vacancy loops ($10^6$ $cm^{-2}$), exist in certain orientations in the films.

Electrical studies have shown the existence of a large distribution of traps in the forbidden energy gap, particularly around 0.60eV below the conduction band.

Polycrystalline layers have been heat-treated in air at 350°C with the result of first a reduction and then an increase in the conductivity, due to a combination of recrystallisation, defect annealing, and oxygen sorption. The carrier density rather than the mobility was more affected.

It was essential to use the hot-wall technique, together with resublimed CdSe if high quality reproducible films were to be prepared.

## 10.3 CdS-$Cu_2S$ PHOTOVOLTAIC JUNCTIONS

Despite the fact that the majority of the light is absorbed in the p-$Cu_2S$ top layer, the properties of the n-CdS base region have been found to determine

much of the behaviour of these devices, particularly with heat-treated cells. Copper-doped CdS is the key to understanding many of the experimental phenomena reported in Chapter 7, since copper is seen to diffuse into n-CdS giving a compensated i-CdS region with both photoconductive properties and the ability to absorb light to create free electrons.

It was found that the best cells had a base layer doped with copper and a resistivity of a few hundred ohm cm. Other dopants had various effects on the secondary characteristics of the devices but did not alter the spectral response and were generally not beneficial. CdS:In was found to yield cells with long response times and a linear response to light intensity. CdS grown in excess sulphur or cadmium was found to have different rates of copper diffusion with consequent effects on the cell behaviour, but in general the CdS:S cells were poor. (Thin film CdS in any case contains excess cadmium rather than sulphur).

Baking the cells was essential to achieve a high OCV and a wide absorption spectrum, but this treatment always lengthened the response time, which is probably of no importance for a power generator.

The spectral response was divisible into three bands:

(i) a band centred on 4900Å due to band to band absorption in the CdS;

(ii) a band centred on 6400Å due to absorption at copper centres in the CdS, together with some direct band to band absorption in the $Cu_2S$;

(iii) a band centred on 9000Å due to indirect band to band absorption in the $Cu_2S$.

Optical quenching effects were observed from the i-CdS region and were typical of the photoconductivity quenching phenomena reported in high resistivity CdS.

Finally the surface treatment of the CdS before chemiplating was found to be critical. A highly smooth surface gave high OCVs but low SCCs, and vice versa for a rough surface.

## 10.4 FUTURE WORK

There are many topics which have arisen during the course of this work which are worthy of further attention. It would be interesting to study the relevance of the equilibrium theory versus the non-equilibrium theory of CdS evaporation by performing an evaporation in a totally enclosed container. The distribution of the cadmium, sulphur and CdS along the temperature gradient between source and substrate on the walls of the container should provide some useful information on the role of the 'hot-wall' in the present work.

It would also be useful to extend the study of doped CdS layers either by evaporating doped CdS or CdS plus dopant. This would have relevance in the study of the importance of excess cadmium in evaporated CdS

layers, and indeed, cadmium could be added to the source. Similarly the work on electron-beam evaporation should be extended to investigate the resistivity versus thickness relation to eliminate effects due to the possible presence of metal-filament contamination.

A study of the temperature dependence of the carrier Hall mobility is required to distinguish between scattering by impurities and scattering by intercrystallite barriers. This requires a cryostat with a long warm-up period to enable the off-set voltage between the Hall probes to be balanced at each temperature.

Other possible experiments which could be performed involve the heterojunctions. Some experiments have already been suggested, such as a full study of the surface treatment of the CdS and a study of photo-capacitance. Other work should be carried out on the optical quenching phenomena in high efficiency cells by employing two light sources, but care would have to be taken in the relative intensities used.

Some preliminary work has been done in co-operation with another member of this department (R. Cottam) into the production of CdS thin film piezo-electric transducers for launching ultrasonic waves into GaAs crystals. The transducers prepared have been found to have the advantages of high coupling coefficient, low noise, and good mechanical stability down to liquid helium temperatures. Both longitudinal and transverse

waves have been passed into (100) and (110) GaAs crystals in order to determine the elastic constants of the material by ultrasonic attenuation measurements. The transducers so far deposited have low 'Q' values and therefore can be used over a wide frequency band (e.g. 30 to 800 MHz for a 4 micron thick CdS layer, heat-treated with silver). This work is well worth further effort.

# APPENDIX : CdSe THIN FILMS

## A.1 PREPARATION OF THE FILMS

A.1.1 This work was a continuation of that started by Krysiewicz and Woods (1970) on the evaluation of CdSe thin films for use in thin film transistors of the type described by Shallcross (1963), Wilson and Gutierrez (1965), Weimer (1964). There are many similarities between the two compounds CdS and CdSe, but the successful preparation of thin films of these materials was found to require a different ranking of the preparation parameters.

A.1.2 The apparatus used to prepare the CdSe layers was the conventional 3" diffusion pump system described in Chapter 4, with a few minor differences in the work-chamber fixtures. At first the 'hot-wall' silica cylinder was omitted, but it was soon discovered that reproducible results could not be obtained unless this component was in position, for the early films were anomalously thin and possessed poor electron mobilities. The resistance-heated silica crucible was smaller than that used for the CdS depositions, which placed an upper limit on the CdSe film thickness of one micron. The electron-beam evaporator had yet to be purchased.

As was found later for the CdS films, the type of glass used as a substrate was unimportant, and the same cleaning procedure was employed. Most of the results to be described were obtained from polycrystalline CdSe on amorphous substrates (microscope slides), but a number of additional films were grown epitaxially on (100) and (110) NaCl surfaces.

Indium contacts on top of the CdSe were not always ohmic, having non-linear I(V) characteristics at low bias voltages. Consequently most of the polycrystalline films were grown on glass substrates with predeposited gold contacts, which were found to behave most satisfactorily.

## A.2 STRUCTURAL AND ELECTRICAL PROPERTIES

A.2.1 The structure of these polycrystalline films was not examined in such detail as with the CdS films, but although the importance of the film thickness was therefore not fully appreciated at that time, two standard thicknesses were adopted of 1800 Å and 5000 Å.

By changing the substrate temperature from 100°C to 325°C and the deposition rate from 20 to 1000 Å/minute, it was possible to grow a variety of films with dark resistivities ranging from $1 \times 10^4$ to $3 \times 10^5$ ohm cm. This range of values is smaller than that covered during the CdS investigation. A decrease in resistivity of 40 to 80 times was produced by illuminating these films with 75 mW $cm^2$ of white light. From measurements of the temperature dependence of the resistivity of several films the activation energies for conduction were calculated, following the Petritz polycrystalline film model. The room temperature Hall mobility in the dark was generally larger than for CdS films, with values ranging from 3 to 30 $cm^2 V^{-1} S^{-1}$. An exploratory investigation of TSC, and of the spectral response of the photoconductivity completed the work performed. All of these results will now be discussed more fully.

A.2.2 Figure A.1 shows the dark resistivity obtained from several combinations of deposition rate and substrate temperature for two film thicknesses. It is noticeable that the substrate temperature had little effect on the resistivity although an increase in this variable did produce a small increase in resistivity. The deposition rate was much more effective in producing a resistivity change. Figure A.1 shows that an increase in rate gave rise to a decrease in resistivity, as has also been reported by Wilson and Gutierrez (1965). The opposite effect was reported by Brodie and Lacombe (1967), and by Shallcross (1966) who used substrates at room temperature only.

It is obvious that the properties of CdSe films are more sensitive to changes in the deposition rate than to changes in the substrate temperature. This was particularly apparent for the 1000 Å thick cubic (100) layers grown epitaxially on NaCl substrates. These films will be described more fully later, but attention is drawn to Figure A.2 which shows the "in-plane" resistivities possessed by four of these layers grown at 300°C at rates of 5 to 7 Å/minute. Nearly an order of magnitude change in resistivity was produced, which could not be explained by a straight-forward improvement in epitaxial quality since the film with the lowest number of low angle grain boundaries was that grown at 5.7 Å/minute.

A.2.3 A straight line was again obtained when the log of the photosensitivity was plotted against the log of the dark resistivity (see Figure A.3), but the photosensitivity

FIG. A I Dark Resistivity versus Deposition Conditions of CdSe Polycrystalline Films on Glass

Parameter = Dark Resistivity (ohm cm)

o = Film Thickness of 5000 Å

x = " " " 1800 Å

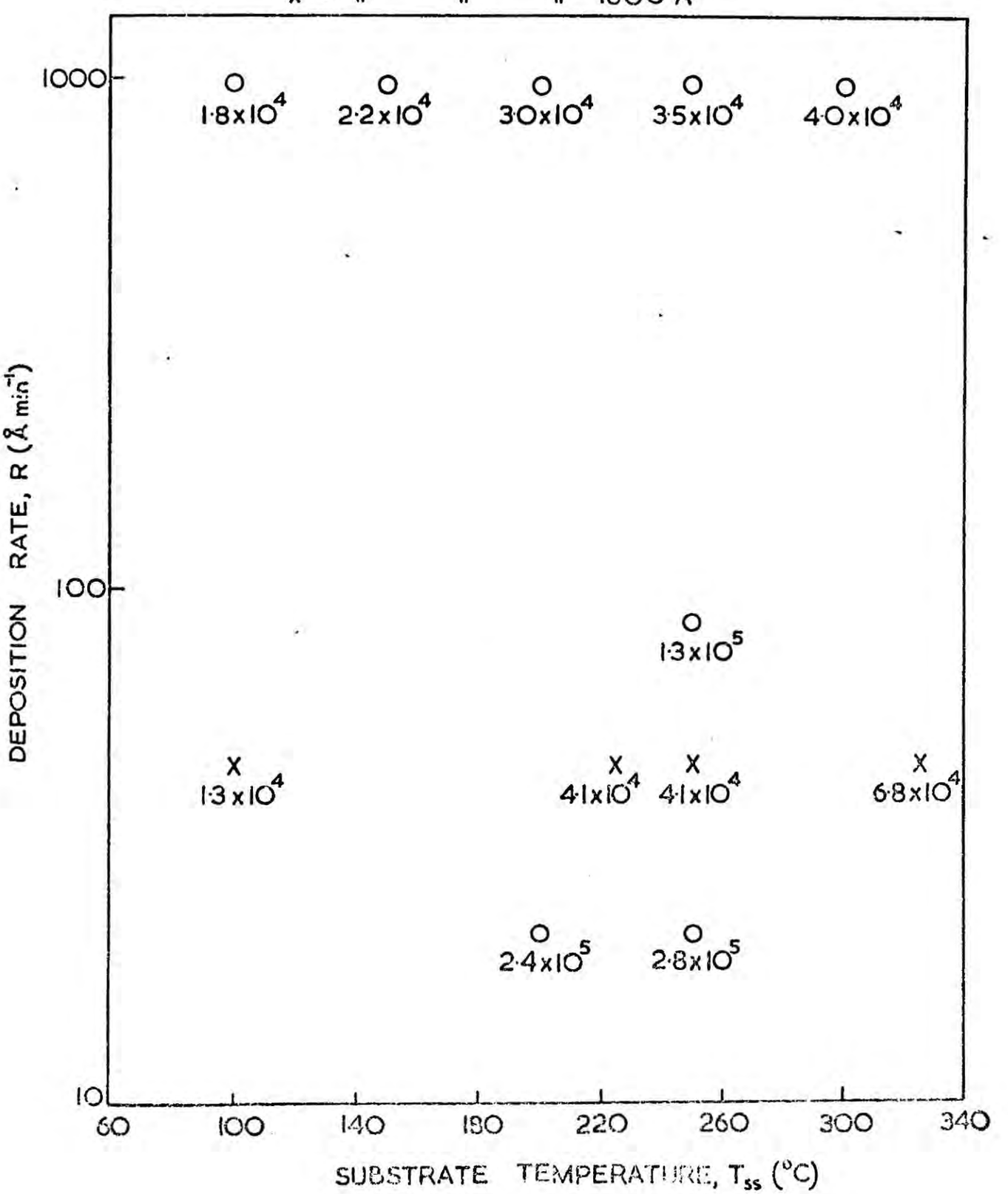

FIG. A 2 Dark Resistivity of CdSe Cubic (100) Thin Films

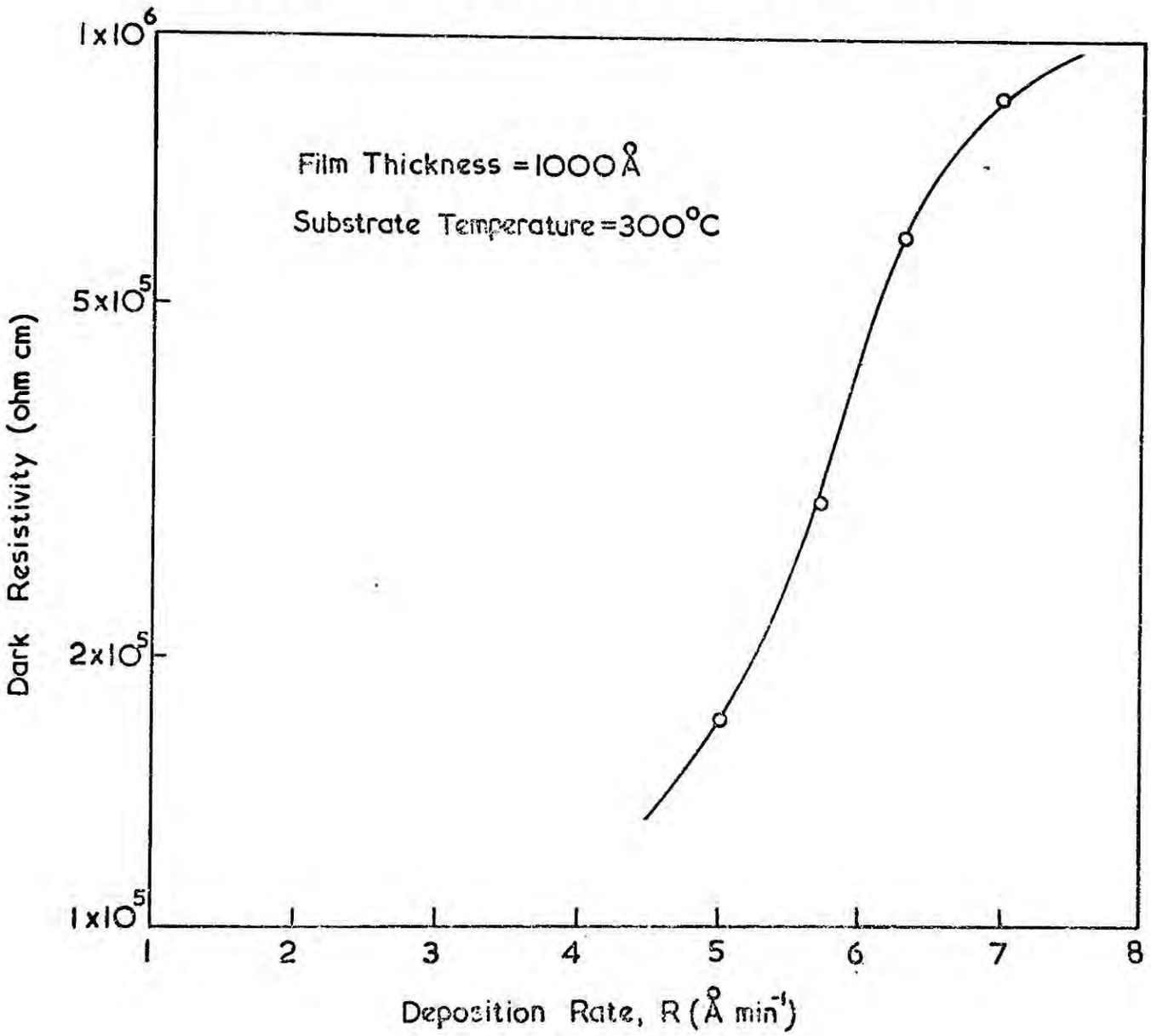

FIG. A 3 Dark Resistivity versus Photosensitivity of CdSe Polycrystalline Films on Glass

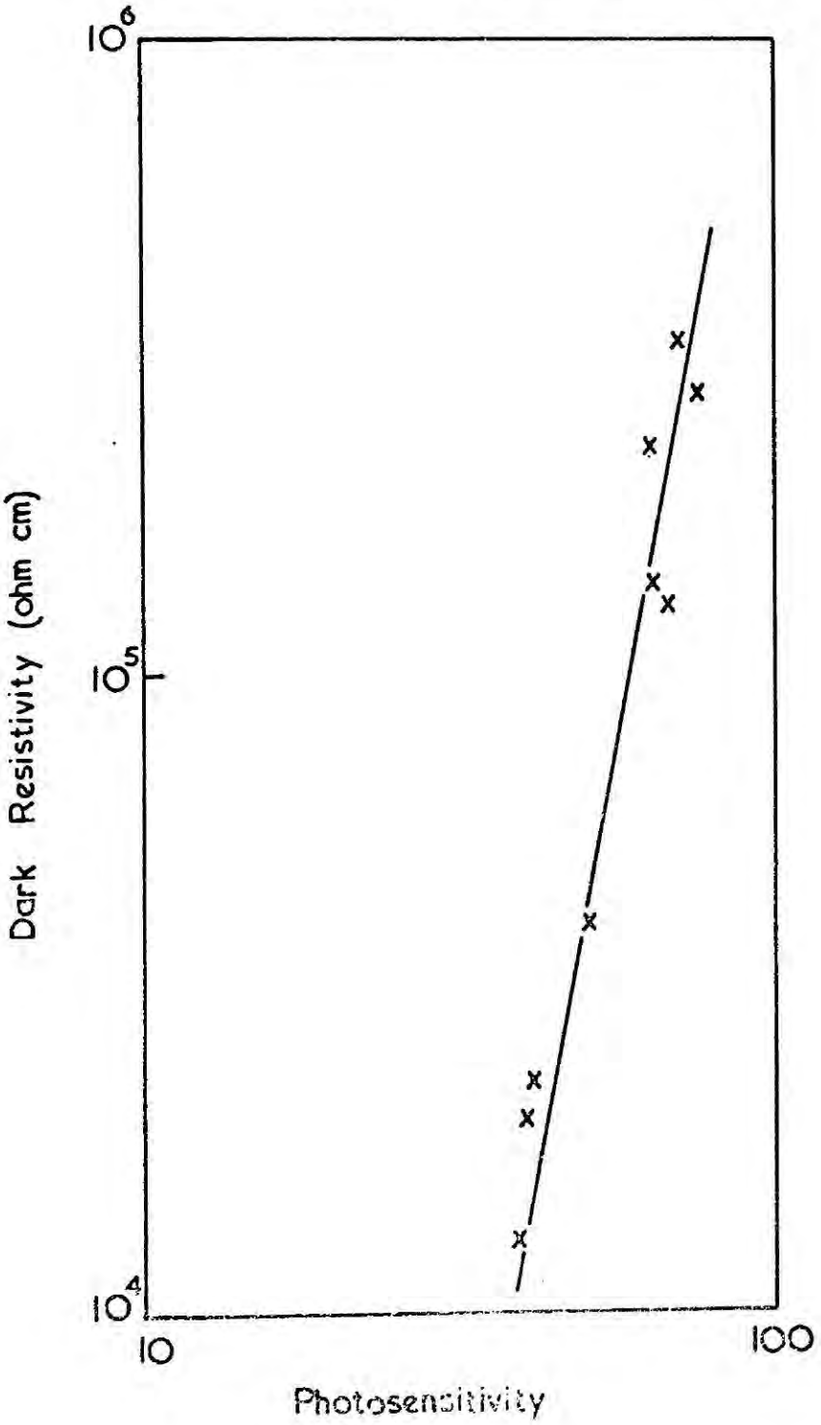

of the CdSe layers was much higher than that of the CdS layers.

Results from only one lot of flow-purified CdSe are shown. This was lot 514 purchased from Derby Luminescents Ltd. A second batch (602) from the same source, also flow-purified, repeatedly failed to give reproducible results, and the films grown from it had uneven matt surfaces. The epitaxial layers grown from this batch of CdSe were invariably poor, with polycrystalline areas and a high defect density.

A.2.4 The Hall mobility was not investigated as a function of the thickness, but for constant thickness and deposition rate the mobility fell with increasing substrate temperature (see Figure A.4). For constant thickness and substrate temperature the mobility rose with deposition rate. It is probable that similar mobility versus thickness curves can be obtained for CdSe films as have been described earlier for CdS, but we were unable to confirm this in the time available.

A.2.5 The photoconductive spectral response, corrected to constant incident energy, is shown in Figure A.5 for a typical film at room temperature and at 100°K. The only structure is a small hump on the band edge absorption near 6000 Å at 100°K, and a corresponding change of slope on the 300°K curve. The increasing photocurrent for wavelengths greater than 1.5 microns indicates that impurity levels may be active in the photosensitivity phenomenon.

FIG. A4 Hall Mobility of CdSe Polycrystalline Films on Glass.

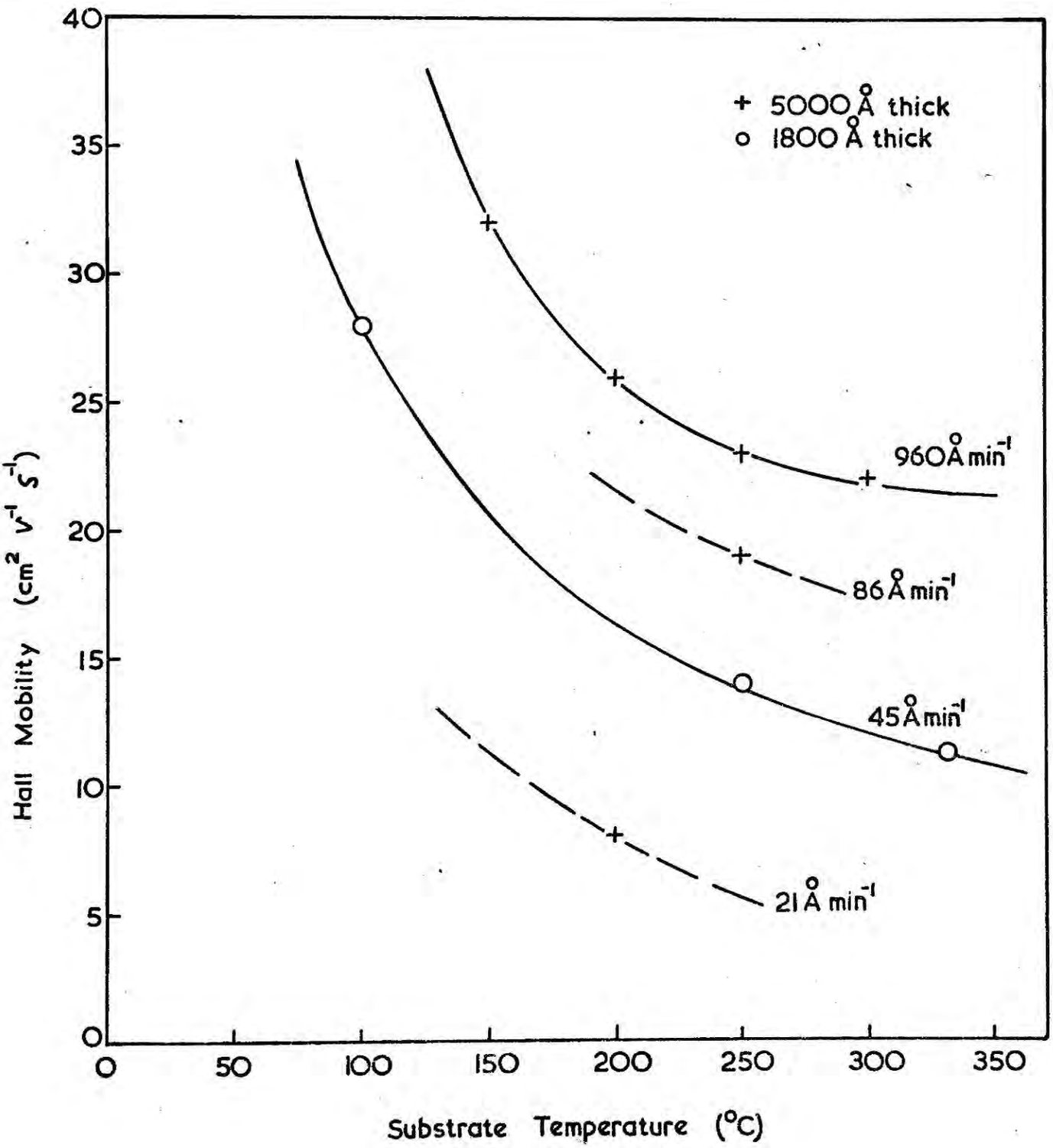

FIG. A5 Spectral Response of Photocurrent in CdSe Polycrystalline Films on Glass (corrected for lamp spectral output)

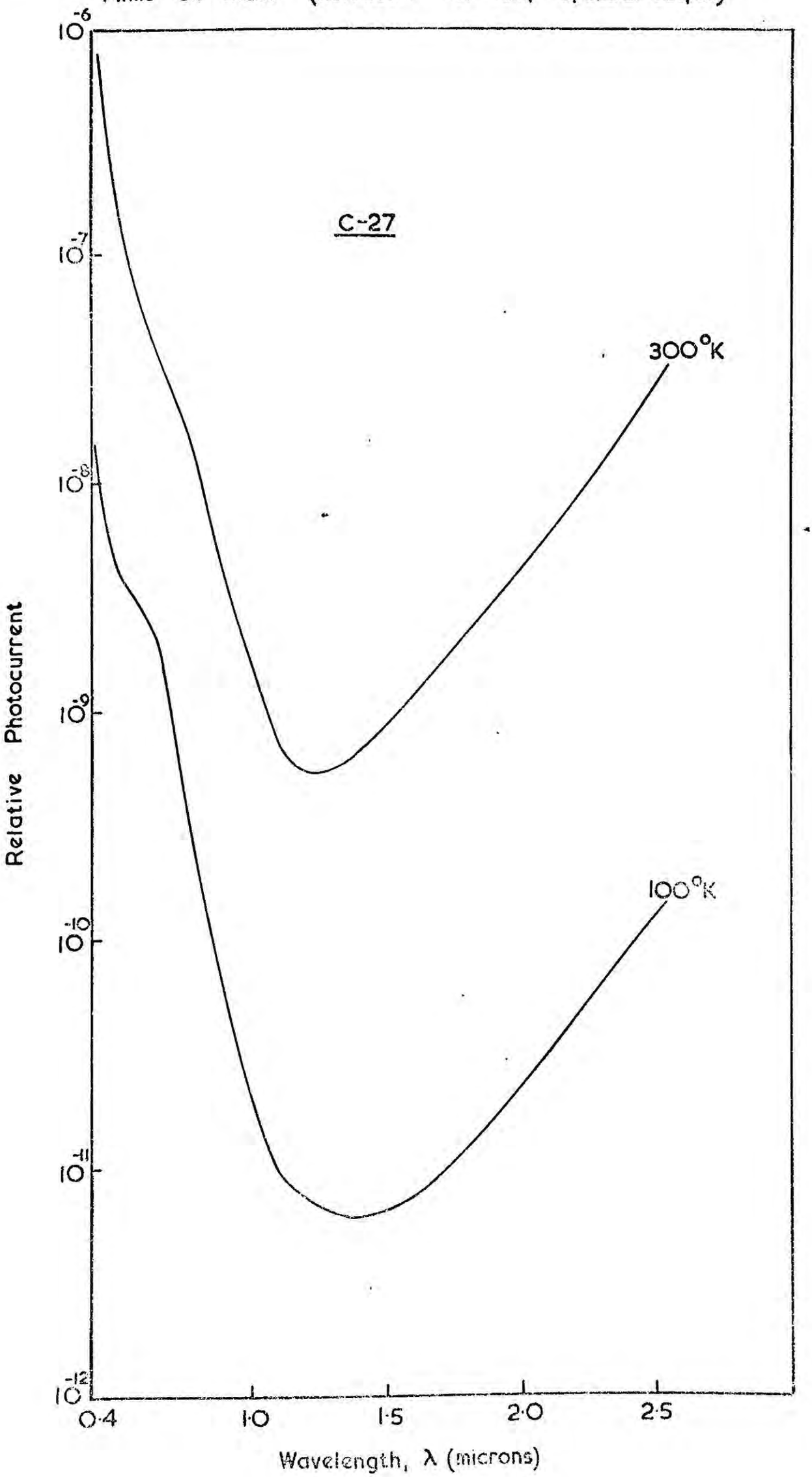

A.2.6 The temperature dependence of the dark resistivity is shown in Figure A.6 for the two films with the most extreme gradients. All of the remaining films, together with those deposited by Krysiewicz and Woods (1970), give results which lie within these two lines. These two 1800 Å thick samples were grown on glass at 45 Å/minute, C-9 at 325°C and C-27 at 100°C. C-27 had an activation energy for conduction of 0.59 eV at low temperatures and 0.35 eV at slightly higher temperatures. This was the only sample with two activation energies. C-9 had an activation energy of 0.28 eV.

In this investigation it was the low resistivity films deposited at low rates (45 Å/minute) on substrates at low temperatures which had the higher activation energies. This is in contrast to the results of Shimizu (1965) who reported that low substrate temperature, low resistivity CdSe films had activation energies of 0.14 eV, and high substrate temperature, high resistivity films had activation energies of about 0.40 eV. Krysiwicz and Woods (1970) used rates of about 1000 Å/minute and found that low substrate temperature, low resistivity films had low activation energies, in agreement with Shimizu.

Under illumination the samples gave high temperature plots which became curved, tending to a lower but indeterminate activation energy than in the dark. At low temperatures the photocarriers appeared to swamp the intrinsic carriers and an approximately horizontal plot resulted.

FIG. A6 Temperature Dependence of Dark Resistivity of Polycrystalline CdSe Films on Glass.

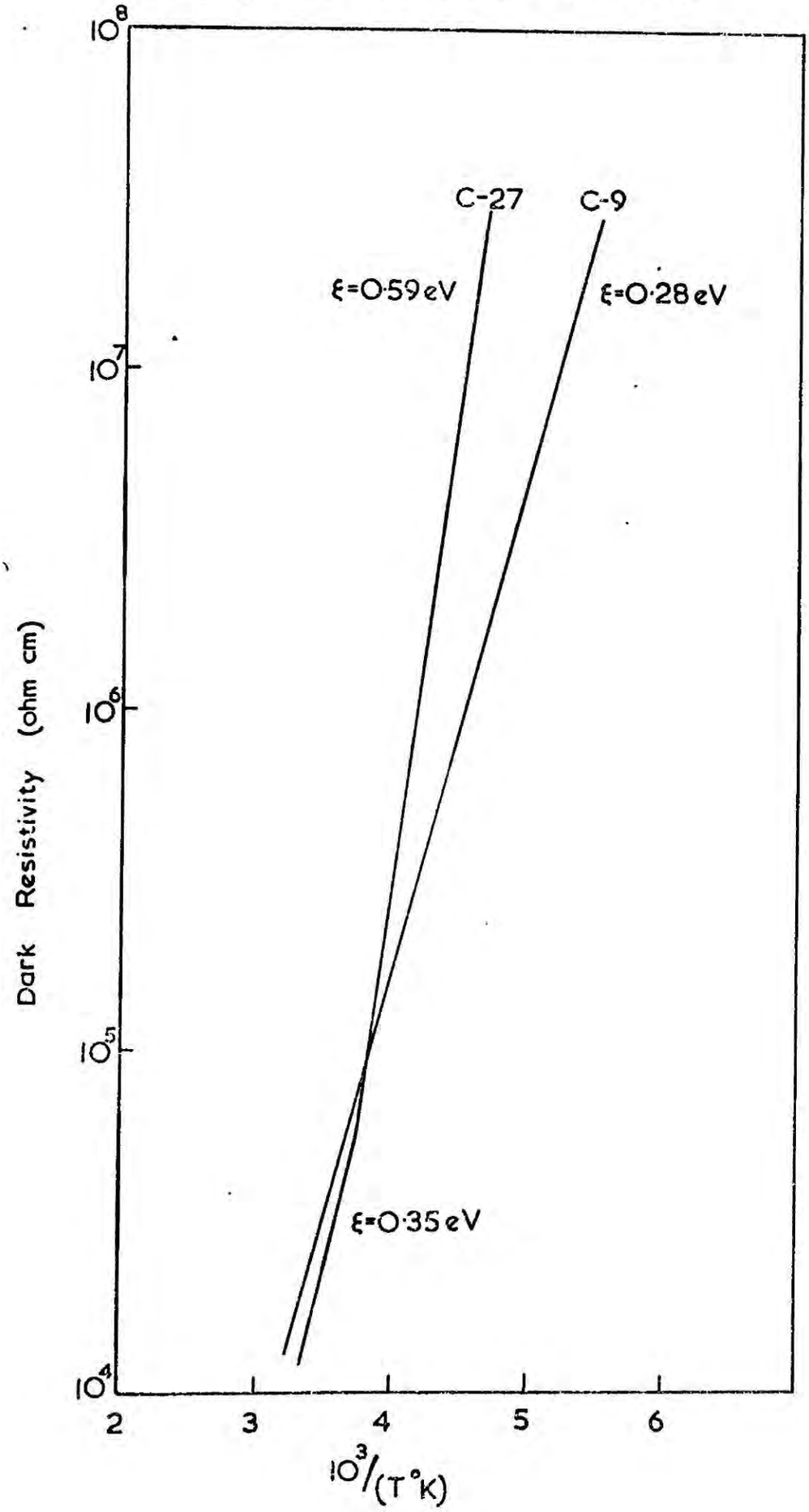

A.2.7 Figure A.7 shows the TSC curve for sample C-27. This is typical of the results obtained from CdSe films in the present investigation in that no clearly defined peaks were obtained. However, C-27 had a small TSC peak at about 280°K, similar in shape to a curve published by Okimura and Sakai (1968) for one of their films, also deposited on a 100°C substrate. Kindleysides and Woods (1970) have observed a TSC peak for CdSe single crystals at 270°K which they attributed to a trap 0.59 eV below the conduction band. Although analysis of TSC peaks requires the shape of the curve to be taken into consideration, the value of 0.59 eV does suggest a correlation between the deep trap and the activation energy for conduction of C-27 (0.59 eV). Okimura and Sakai measured the photocurrent of their films as a function of light intensity and deduced from the breakpoint on the plot of photocurrent versus light intensity that the film possessed a deep trap at 0.60 eV. A deep trap at 0.60 eV in bulk CdSe has also been reported by Bube and Barton (1958).

The shape of the full TSC curves for our CdSe films suggests that there is a very large number of discrete levels within the forbidden energy gap.

## A.3 HEAT-TREATMENT OF THE CdSe FILMS

A.3.1 A popular technique for improving the transport properties of II-VI thin films is to subject them to one of the forms of post-deposition heat-treatment discussed in Chapter 3. Okimura and Sakai (1968) are among those workers who have employed this technique with CdSe

FIG. A7 T.S.C. of CdSe Polycrystalline Film on Glass.

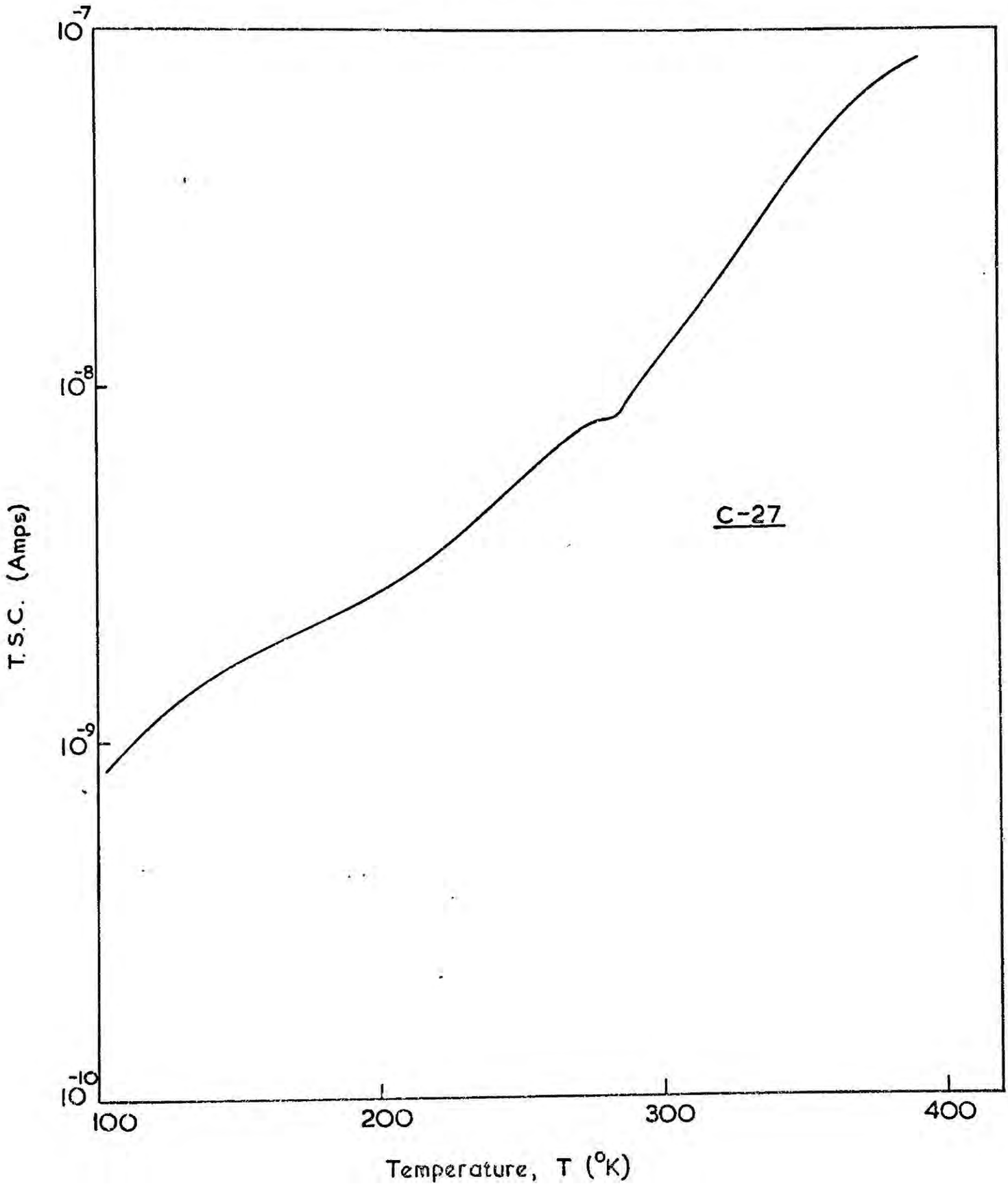

layers, and they have stated that the substrate temperature is less important than the post-deposition heating temperature, if highly photosensitive films are to be obtained.

A.3.2 Some of the films prepared for the present investigation were subjected to successive periods of heat-treatment at 350°C in an open tube furnace. A summary of the dark resistivity changes which were observed is given graphically in Figure A.8 for three 1800 Å thick specimens. The plotted points mark the times at which the samples were removed from the furnace and quenched to room temperature in an air stream, after which their resistivities, photosensitivities and Hall mobilities were determined.

With all the samples examined the dark resistivity followed a smooth curve with duration of heating, reaching a maximum value after about 1¾ hours at 350°C. Only C-10 was observed to suffer an initial fall in resistance.

The photosensitivity followed the dark resistivity and also reached a maximum after 1¾ hours at 350°C, but the Hall mobility was little affected by this treatment. (C-27 for instance had a mobility which increased from 28 to 32 $cm^2V^{-1}S^{-1}$ after three hours at 350°C).

A.3.3 Prolonged heating was observed to produce substantial recrystallisation of the films. Laue back-reflection X-ray photographs became sharper and the originally diffuse rings became more clearly defined, although no spots appeared (see Figure A.9a and b). With sample C-10 the X-ray line-width decreased approximately four times after three hours at 350°C, but accurate

FIG. A.8 EFFECT OF HEAT-TREATMENT ON CdSe THIN FILM RESISTIVITY

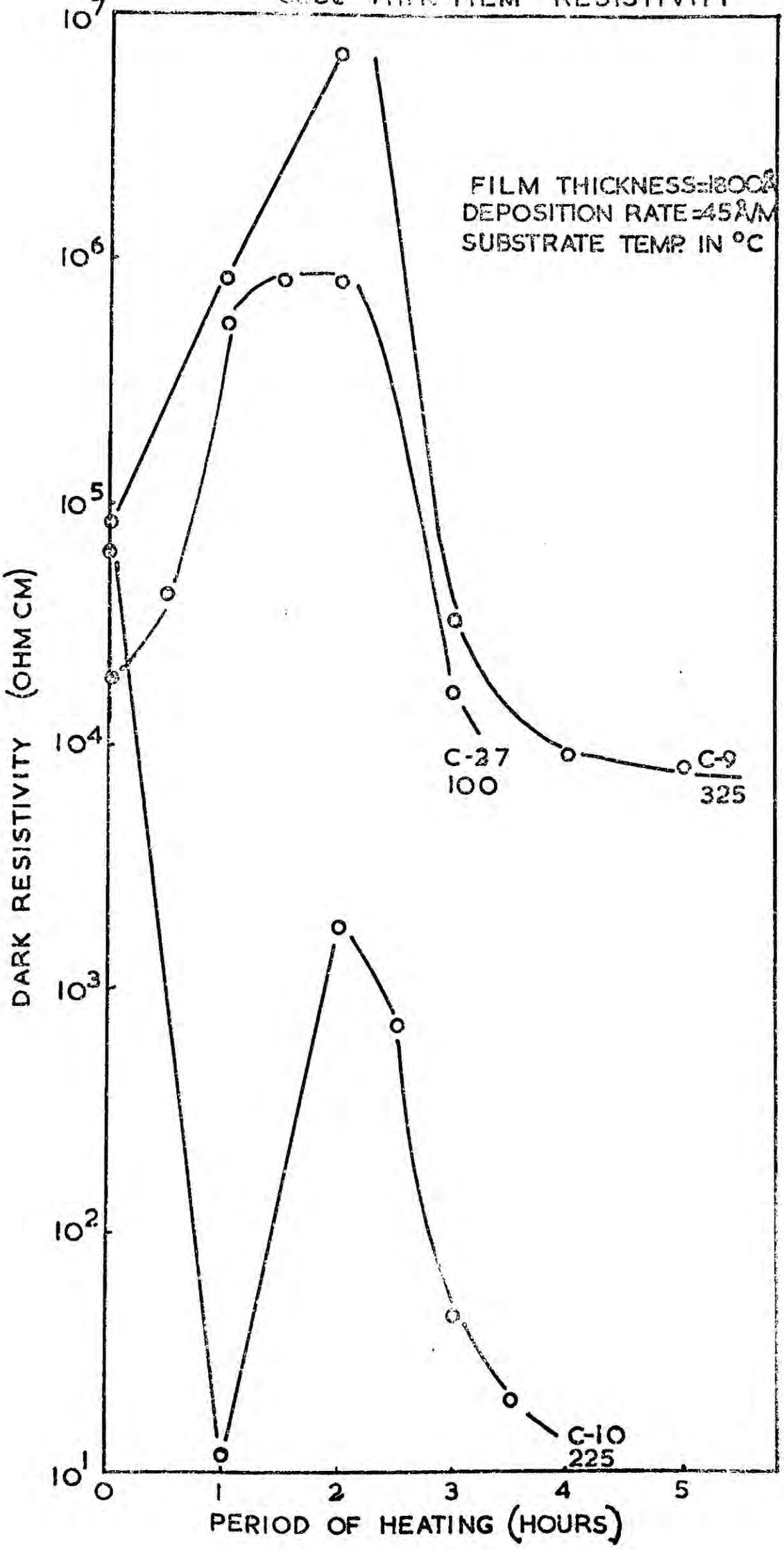

Fig.A.9(a) X-ray Back Reflection - CdSe as Deposited

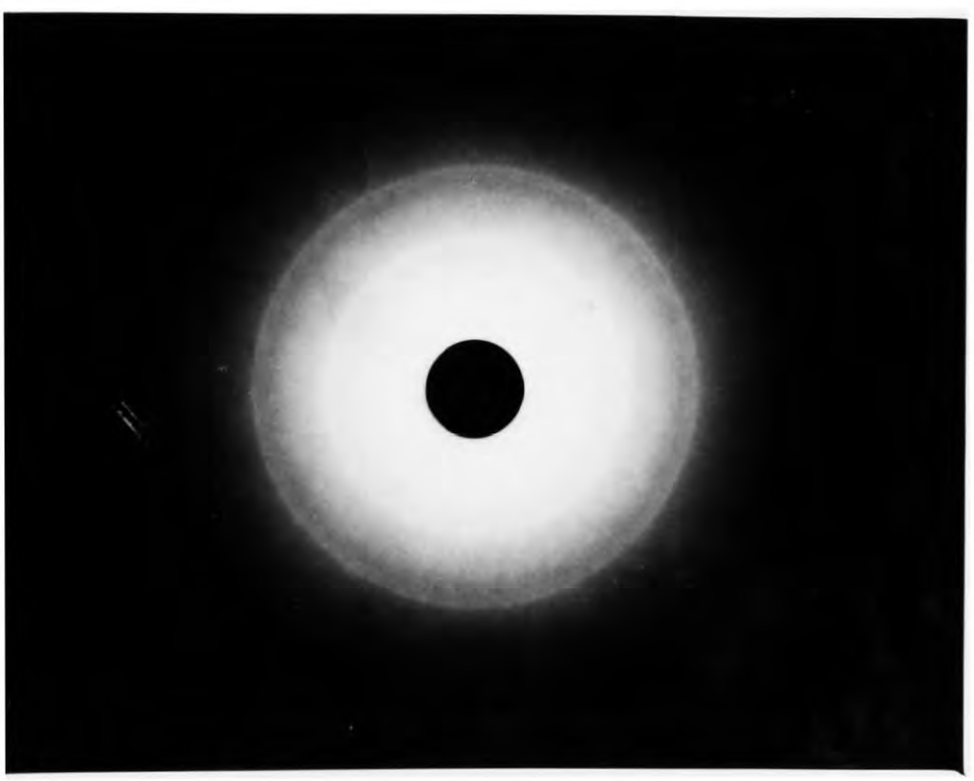

Fig.A.9(b) X-ray Back Reflection - CdSe after Heating

microphotometer traces were impossible to obtain. A similar difficulty had appeared for the CdS films.

None of the films was photoluminescent (even after cooling to liquid nitrogen temperatures) although luminescence might have been expected if the recrystallisation had proceeded far enough.

A.3.4 It is suggested that the changes in electrical properties following heat-treatment were due to a combination of the sorption of oxygen, recrystallisation and the annealing out of defects. Initially the oxygen sorption predominates, and an increase in resistivity is the result. Such an effect has been reported by Bube (1957) and Somorjai (1963) for single crystal and thin film CdSe respectively. Further heating anneals defects and promotes crystal growth which results in a reduction of the number of traps (Okimura and Sakai, 1968) and intercrystallite boundaries, and hence both the free carrier concentration and the mobility begin to rise.

## A.4 EPITAXIAL LAYERS

A.4.1 The amount of published work on epitaxial layers of CdSe is much smaller than that on CdS, and many of the reports omit much important detail. Holt (1966) has reviewed the subject of defects in epitaxial semiconducting films with the sphalerite structure, and included some references to CdSe. Other relevant research includes that of Berger et al (1964) on surface replicas of epitaxial CdSe, Ludeke and Paul (1967) on CdSe grown on (111) $BaF_2$, and Yasuda (1968) on very thin layers of CdSe layers for growth studies.

In this section we shall describe results from a number of sphalerite (100) and (110) CdSe layers grown on NaCl substrates cleaved in air. The dark resistivity of some of the (100) layers has already been shown in Figure A.2 as a function of deposition rate. It should be noted that for these samples the resistivity increased with deposition rate, perhaps due to an unproven increase in defect content. The photosensitivity was slightly higher than would be expected from Figure A.3, since the resistivity versus photosensitivity plot had a shallower slope than the corresponding plot for polycrystalline films.

A.4.2 The films were removed from their substrates in water and examined by transmission electron microscopy. The early (100) electron diffraction patterns were poor, containing many fine extra spots, although polycrystalline rings were not present. It was soon discovered that this was due to the high deposition rates employed (over 60 Å/minute) and when rates of 4-10 Å/minute were substituted the diffraction patterns became much cleaner. A rate of 5 Å/minute and a substrate temperature of 300°C were found to yield the best quality (100) films. (See Figure A.10).

These (100) layers gave split spot diffraction patterns over some of their areas, and it was only possible to determine their origin by use of bright- and dark-field microscopy, and by tilting the specimen, as was described in Chapter 5. However, comparison with the patterns given by Pashley and Stowell (1963) for fcc (100) gold films indicates that some of these extra features were due to included wurtzite grains and not to twinning. Other

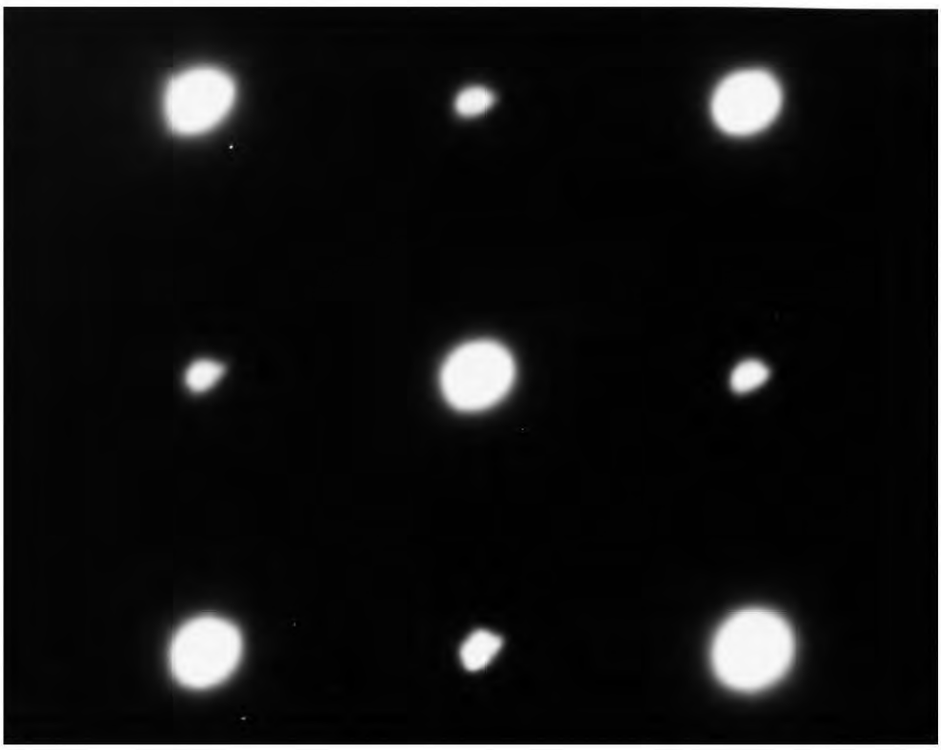

Fig.A.10 (100) Epitaxial CdSe

'splitting patterns' on some micrographs were caused by planar defects in the {111} planes, and these features vanished as the specimen was tilted.

Dislocation lines were observed on one high quality film of (100) orientation, deposited at 7 Å/minute on to NaCl at 300°C, but only after storage on a grid in air for several weeks. This sample had very little spot splitting and no streaking due to planar defects.

A.4.3 A few (110) films were grown on NaCl and showed similar defects to those of the early (100) layers. The poorer films had micrographs containing spot and fringe contrast, and streaks between the diffraction spots in the (111) direction (see Figure A.11). By employing dark-field techniques, and by tilting the specimen, it was apparent that many of the fringe patterns were due to the 'streaky' part of the diffracted beams. These features have generally been attributed to planar defects (see Chapter 5).

Some areas of the same films possessed loops about 300-600 Å long by 150 Å across (about $10^6 cm^{-2}$) (see Figure A.12), similar to those reported by Holt (1971) for CdS deposited on high temperature (111) $BaF_2$ substrates. These are likely to be vacancy clusters.

A.4.4 The streaks due to planar defects were eliminated by paying attention to the cleaning and loading procedure, and by using the optimum growth conditions described above. The CdSe layers still failed to reach the same degree of perfection as that achieved with CdS. This is thought to be due to the poor quality source material and to the absence of a clean evaporation technique such

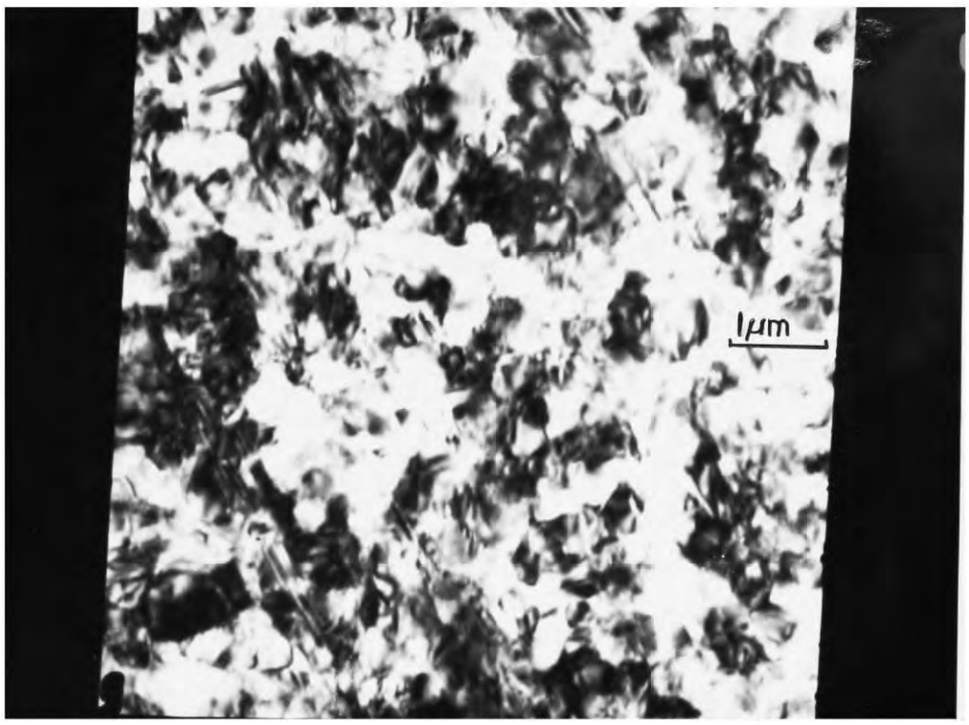


Fig.A.11(a) Selected Area of (110) CdSe

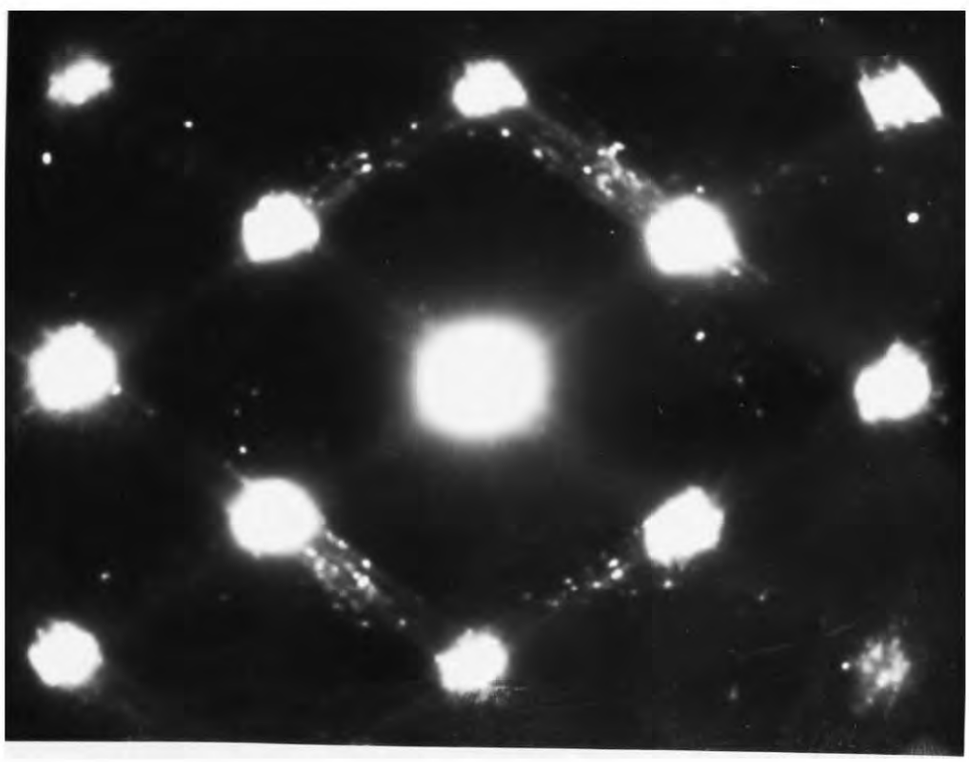

Fig.A.11(b) Diffraction Pattern from (a)

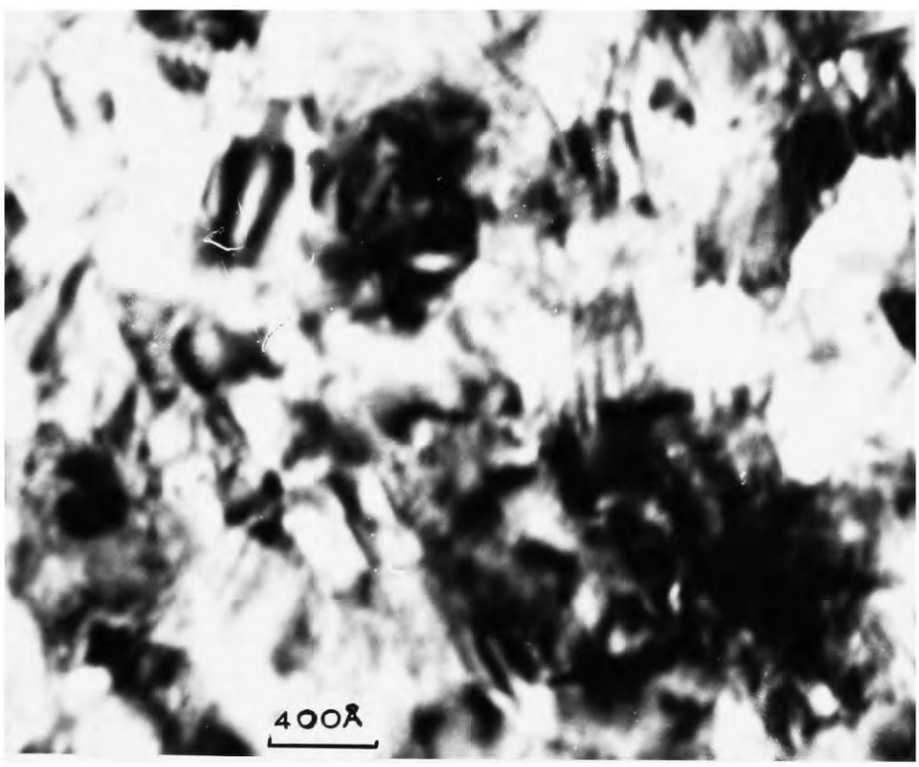


Fig.A.12 Defects in (110) CdSe Film

as electron-beam heating. It was impossible to grow epitaxial layers from untreated CdSe, or from flow crystals which were too finely ground (and so gave non-uniform deposition rates).

## A.5 CONCLUSIONS

This investigation was necessarily incomplete, but several useful results were obtained, with both contrasting and similar effects to those observed later with CdS films.

The conclusions drawn from the measurements are listed below:

### A.5.1 For polycrystalline CdSe films on glass

(a) The hot-wall method is essential for reproducible results from a resistance-heated source.

(b) Resistivity increased with substrate temperature over the range 100°-325°C.

(c) Resistivity decreased with deposition rate over the range 21-960 Å/minute.

(d) The deposition rate dominated in this process.

(e) Hall mobility decreased with substrate temperature over the range 100°-325°C.

(f) Hall mobility increased with rate over the range 21-960 Å/minute.

(g) The resistivity changes with growth conditions are due only partially to changes in electron mobility.

(h) The activation energies for conduction in these films are distributed between the extremes of 0.28 and 0.59 eV (when calculated according to the Petritz theory).

(i) Although the photosensitivity and Hall mobility of these films is greater than in the CdS films, the mobility is one or two orders smaller than in bulk CdSe. This fact together with (h) above indicates the existence of intercrystallite barriers and traps, as has previously been suggested by the measurements of Brodie and Yeh (1968), Van Heek (1968), Jåniche and Berger (1969) and Karpovich and Zvonkov (1969) on CdSe layers.

(j) From TSC measurements on one low substrate temperature film it appears that there is a deep trap at 0.59 eV which has a direct correlation with the activation energy for electrical conduction in that film.

(k) Heat-treatment in air at 350$^{o}$C produced recrystallisation. The resistivity increased initially and then fell after 1¾ hours heating. The Hall mobility was increased slightly by the process. Oxygen is believed to play an important part in changing the transport properties in this manner, but with prolonged heating the changes were dominated by recrystallisation and by the annealing of imperfections.

A.5.2 For epitaxial CdSe on NaCl

(a) The resistivity of cubic (100) CdSe layers was very sensitive to the deposition rate, and decreased at least 50 times under illumination with 75mWcm$^{-2}$ of white light.

(b) The spot splitting observed on diffraction patterns from poorer (100) samples was due to included grains with the wurtzite structure and not to twinning.

(c) If a substrate temperature of 300°C and a deposition rate of 5 Å/minute were employed, then planar defects were eliminated, and no satellite diffraction spots existed.

(d) The source material had to be flow-purified both for good epitaxy and to obtain reproducible polycrystalline layers.

A.5.3 Many suggestions can be made for the direction to aim in future work on CdSe thin films, but the most rewarding would be a deeper investigation of the defects in both polycrystalline and epitaxial layers. This should be performed on electron-beam evaporated films, and should involve the techniques of bright- and dark-field electron microscopy.

To complete the studies on polycrystalline CdSe layers a determination of the importance of film thickness should be undertaken.

A further interesting topic would involve the preparation of mixed CdS/CdSe layers (as reported by Yu and Weng, 1970) to see how the conflict of dominant substrate temperature (CdS) and dominant deposition rate (CdSe) is resolved.

REFERENCES

H. Berger et al (1964), Phys. Stat. Sol. 7, 679.

D.E. Brodie and J. LaCombe (1967), Canad. J. Phys. 45, 1353-1362.

D.E. Brodie and G. Yeh (1968), Canad. J. Phys. 46, 1993.

R.H. Bube (1957), J. Chem. Phys. 27, 496-500.

R.H. Bube and L.A. Barton (1958), J. Chem. Phys. 29, 128.

H.F. van Heek (1968), Solid-State Electron. 11, 459.

D.B. Holt (1966), J. Mat. Sci. 1, 280-295.

G. Jäniche and H. Berger (1969), Proc. Int. Conf. on Thin Films in J. Vac. Sci. Technol. 6, 552-555.

I.A. Karpovich and B.N. Zvonkov (1969), Sov. Phys. Sol. St. 6, 2714.

L. Kindleysides and J. Woods (1970), J. Phys. D. Appl. Phys. 3, 451-461.

J. Krysiewicz and J. Woods (1970) Studia i Materialy, 2, 3-10.

R. Ludeke and W. Paul (1967), Phys. Stat. Sol. 23, 413-418.

H. Okimura and Y. Sakai (1968), Jap. J.A.P., 7, 731.

D.W. Pashley and M.J. Stowell (1963), Phil. Mag. 8, 1605-1632.

F.V. Shallcross (1963), R.C.A. Review 24, 676-687.

F.V. Shallcross (1966), Trans. Met. Soc. AIME, 236, 309-313.

K. Shimizu (1965), Jap. J.A.P. 4, 627-631.

G.A. Somorjai (1963), J. Phys. Chem. Solids, 24, 175-186.

H.F. van Heek (1968) Solid-State Electron, 11, 459.

P.K. Weimer (1964), "Physics of Thin Films" II, 147.

H.L. Wilson and W.A. Gutierrez (1965), J. Elect. Chem.Soc. 112, 85-91.

Y. Yasuda (1968), Jap. J.A.P. 7, 1171.

H.J. Yu and T.H. Weng (1970), Solid-State Electron, 13, 93-94.